MICRO-EXPLOSION PHENOMENON OF TRI-FUEL EMULSION

MUHAMMAD MUKHTAR BIN NOOR AWALLUDIN

اونيـﭭﻮﺭﺳﻴﺘﻲ ﻣﻠﻴـﺴﻴﺎ ﭬﻬـﭭ

UNIVERSITI MALAYSIA PAHANG

DOCTOR OF PHILOSOPHY

UNIVERSITI MALAYSIA PAHANG

UNIVERSITI MALAYSIA PAHANG

DECLARATION OF THESIS AND COPYRIGHT	

Author's Full Name   : MUHAMMAD MUKHTAR BIN NOOR AWALLUDIN

Date of Birth   : 21 AUGUST 1981

Title   : MICRO-EXPLOSION PHENOMENON OF TRI-FUEL
EMULSION

Academic Session   : SEM 2 2019/2020

I declare that this thesis is classified as:

- ☐   CONFIDENTIAL (Contains confidential information under the Official Secret Act 1997)*
- ☐   RESTRICTED (Contains restricted information as specified by the organization where research was done)*
- ☒   OPEN ACCESS I agree that my thesis to be published as online open access (Full Text)

I acknowledge that Universiti Malaysia Pahang reserves the following rights:

1. The Thesis is the Property of Universiti Malaysia Pahang
2. The Library of Universiti Malaysia Pahang has the right to make copies of the thesis for the purpose of research only.
3. The Library has the right to make copies of the thesis for academic exchange.

Certified by:

_____   _____
(Student's Signature)   (Supervisor's Signature)

     DR. FTWI YOHANESS HAGOS

_____   _____
New IC/Passport Number   Name of Supervisor
Date: Date:

NOTE : * If the thesis is CONFIDENTIAL or RESTRICTED, please attach a thesis declaration letter.

SUPERVISOR'S DECLARATION

We hereby declare that we have checked this thesis and in our opinion, this thesis is adequate in terms of scope and quality for the award of the degree of Doctor of Philosophy.

_____

(Supervisor's Signature)

Full Name   : DR. FTWI YOHANESS HAGOS

Position   : SENIOR LECTURER

Date   :

_____

(Co-supervisor's Signature)

Full Name   : TS. DR. MUHAMAD MAT NOOR

Position   : SENIOR LECTURER

Date   :

STUDENT'S DECLARATION

I hereby declare that the work in this thesis is based on my original work except for quotations and citations which have been duly acknowledged. I also declare that it has not been previously or concurrently submitted for any other degree at Universiti Malaysia Pahang or any other institutions.

_____
(Student's Signature)

Full Name   : MUHAMMAD MUKHTAR BIN NOOR AWALLUDIN

ID Number   : PMM16009

Date   :

MICRO-EXPLOSION PHENOMENON OF TRI-FUEL EMULSION

MUHAMMAD MUKHTAR BIN NOOR AWALLUDIN

Thesis submitted in fulfilment of the requirements
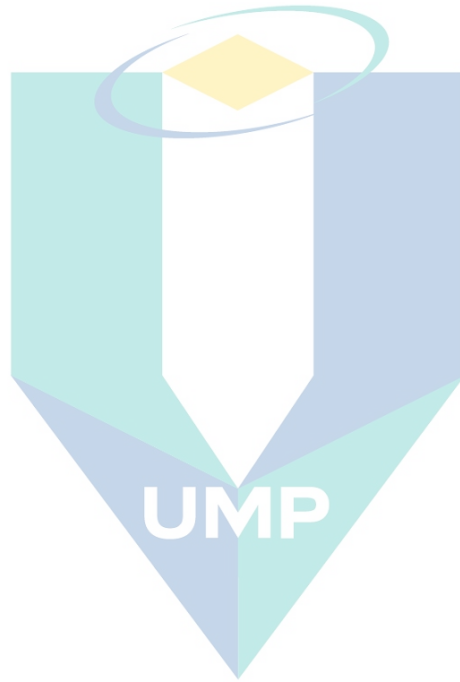for the award of the degree of
Doctor of Philosophy

College of Engineering
UNIVERSITI MALAYSIA PAHANG

SEPTEMBER 2020

DEDICATION

Special dedication goes to my field supervisor, Prof. *Dr A.* Rashid *A. Aziz from Centre for Automotive Research and Electric Mobility (*CAREM*) in the Universiti Teknologi Petronas (UTP). Without his support and facility provision, the research milestone might not be achieved.*

ACKNOWLEDGEMENTS

ABSTRAK

Enjin mampatan-pencucuhan mempunyai bahagian penting dalam industri pengangkutan dan banyak industri utama lain kerana kemampuan untuk menanggung nisbah mampatan yang tinggi, ketahanan tinggi dan dengan kos yang efektif. Walaupun ada usaha untuk menghasilkan fenomena *micro-explosion*, atas tujuan untuk mengurangkan zarah partikel dan NO$_x$ secara serentak, fenomena tersebut belum disiasat dalam suntikan semburan bertekanan tinggi dan suasana seperti dalam enjin. Dalam kajian ini, *Tri-fuel emulsion* dengan tiga campuran bahan bakar terdiri daripada diesel, etanol dan biodiesel yang dipercayai mampu memberi kelebihan sebagai atomisasi sekunder yang dikenali sebagai fenomena *micro-explosion* yang boleh dihasilkan menggunakan pengemulsi ultrasonik. Kaedah reka bentuk faktorial dua peringkat digunakan dengan platform *Design of Experiment* untuk menganalisis kesan faktor kawalan pengemulsikan ultrasonik dan nisbah kandungan etanol dan biodiesel ke dalam *Tri-fuel emulsion* pada sifat fizikokimia yang diperolehi. Ciri fizikokimia termasuk *density*, *viscosity*, *surface tension* dan *average droplet size*. Bukti menunjukkan bahawa fenomena *micro-explosion* berlaku pada titisan semburan yang disuntik dari sistem suntikan bahan api dari *common rail* bertekanan tinggi. Ia dikenal pasti dengan menggunakan teknik *shadowgraph* dengan bantuan kamera berkelajuan tinggi di bawah suhu tinggi dalam *optical constant volume combustion chamber*. Enjin silinder tunggal telah digunakan untuk mendapatkan ciri-ciri pembakaran *Tri-fuel emulsion*. *Ignition delay, heat release rate,* dan *in-cylinder pressure* telah diperoleh dan dianalisis. Dari kajian pencirian bahan bakar, hasilnya menunjukkan bahawa *density* telah dipengaruhi oleh kandungan etanol (interaksi tunggal) dengan *P-Value* ialah 0.0023. Sementara itu, tahap *viscosity* dipengaruhi oleh interaksi etanol dan nisbah biodiesel (dengan *P-value* < 0.0001). Tetapan *cycle* memainkan peranan penting untuk mengimbangi interaksi itu. Selain itu, paras *surface tension* bergantung kepada ketetapan *cycle* dan kandungan etanol. Penurunan tahap *surface tension* bergantung kepada peningkatan *cycle* dan tahap etanol. Walaubagaimanapun, tetapan *cycle* tinggi mengurangkan kekakuan cerun yang mewakili penurunan *surface tension* dengan P-value 0.0383. Sementara itu, amplitud memainkan peranan penting dalam memanipulasi kesan biodiesel pada peningkatan atau penurunan tahap *surface tension*. Purate saiz titisan juga dicetuskan oleh tetapan penetapan amplitud kepada peratusan biodiesel dalam *Tri-fuel emulsion*. Apabila pecahan biodiesel tinggi digabungkan dengan tetapan amplitud yang rendah, saiz titisan purata meningkat secara mendadak sebanyak 80%. Penetapan amplitud yang rendah sambil mengurangkan tetapan kitaran menyebabkan saiz meningkat secara dramatik sebanyak 372%. Fenomena *micro-explosion* dengan intensiti berkadar rendah dikenali sebagai *puffing* ditemui berlaku pada titisan tunggal dari semburan suntikan bahan api. *Puffing* dianggap sebagai letusan tunggal dan boleh juga berganda. Kesan fenomena pada titisan boleh diteliti melalui *centricity, diameter, spread axial distance and surface area plot*. Kesan fenomena *micro-explosion* pada titisan membuka pintu di antara tempoh yang sangat singkat peluang untuk menjalani proses evaporasi , penguapan dan bercampur dengan udara untuk berlaku. Dari ciri semburan, sudut semburan dan penyebaran semburan menunjukkan peningkatan. Keputusan ciri-ciri pembakaran purata memberikan hasil yang positif apabila enjin berjalan tanpa beban. Kadar pelepasan haba, suhu dalam silinder dan tekanan silinder emulsi tri-bahan api semasa tempoh penangguhan penyalaan melebihi diesel. Puncak kadar elepasan haba, dan tekanan silinder emulsi tri-bahan api telah meningkat berbanding dengan diesel.

ABSTRACT

Compression Ignition engine has a significant share in transportation and many major industries because of the ability to withstand high compression ratio, reliable and cost-effective. While effort is there to generate micro-explosion for the simultaneous reduction of particulate matter and NO_x, the phenomenon has not been investigated in the high pressure spray injection and engine light atmosphere. In this study, tri-fuel emulsions consist of diesel, ethanol and biodiesel which is believed to be capable of secondary atomization advantage known as micro-explosion phenomenon were prepared using an ultrasonic emulsifier. The two-level factorial design method was employed with Design of Experiment platform to analyze the effect of ultrasonic emulsification control factors and the formulation ratio of ethanol and biodiesel into tri-fuel emulsion on the obtained physicochemical properties. Physicochemical properties include density, viscosity, surface tension and average droplet size. Evidence that micro-explosion had occurred on a spray droplet injected from the high-pressure common rail fuel injection system was identified using shadowgraph technique with the aid of high-speed camera under high temperature in the optical constant volume combustion chamber. The single-cylinder engine was set up to attain tri-fuel emulsions combustion characteristics. Ignition delay, heat release rate, and in-cylinder pressure were obtained and analyzed. From the fuel characterization study, the result revealed that density was influenced significantly by the ethanol content (single interaction) with the P-Value of 0.0023. Meanwhile, the viscosity level was influenced strongly (with the P-value < 0.0001) by the ethanol interaction with biodiesel ratio. Cycle setting plays a significant role to balance that interaction. Moreover, surface tension level was significantly dependent on cycle setting and ethanol content with P-value 0.0383. Surface tension decrease as ethanol level was increased. However, high cycle setting reduces the slope stiffness representing the decrease of the surface tension. Meanwhile, amplitude plays a significant role in manipulating biodiesel effect on the increase or decrease of the surface tension. Average droplet size also was triggered by amplitude setting prompt to biodiesel percentage in Tri-fuel emulsion. When high biodiesel fraction was combined with low amplitude setting, the average droplet size increased dramatically by 80%. Low amplitude setting while reducing the cycle setting causes the size to increase dramatically by 372%. Low-intensity micro-explosion phenomenon known as puffing occurred on a single droplet from a fuel injection spray. Puffing was regarded as single and double side puffing. The impact on droplet was appreciated via centricity, diameter, spread axial distance and surface area plot. The impact of micro-explosion phenomenon on single droplet opens up the door in between short period for the opportunity to atomize, evaporate and mix with air to take place. From spray characteristics, spray spread characteristics shows improvement of all tri-fuel emulsions as compared to diesel by 38.75% overall average enhancement. Average combustion characteristics result offered a positive outcome when the engine was running with no load. The heat release rate and in-cylinder pressure of tri-fuel emulsion during the ignition delay period exceed diesel. The peak of heat release rate and in-cylinder pressure of tri-fuel emulsion were improved compared to diesel.

iv

TABLE OF CONTENT

LIST OF TABLES

LIST OF FIGURES

xii

LIST OF SYMBOLS

μ	Dynamic Viscosity
τ	Shear Stress
γ	Surface tension
Φ	Local equivalent ratio
ρ	Density
μ	Viscosity

LIST OF ABBREVIATIONS

AC	Alternating Current
ANOVA	Analysis of Variance
ASTM	American Society for Testing Material
BDC	Bottom Dead Center
BTDC	Before Top Dead Center
CAREM	Center for Automotive Research and Electric Mobility
CA	Crank Angle
CI	Compression Ignition
CMD	Command
CNC	Computer Numerical Control
CO	Carbon Monoxide
CO_2	Carbon Dioxide
COV	Coefficient of Variation
DEF	Diesel Exhaust Fluid
DFI	Ducted Fuel Injection
DLS	Dynamic Light Scattering
DOC	Diesel Oxidation Catalyst
DoE	Design of Experiment
EDR	Extreme Dynamic Range
EGR	Exhaust Gas Recirculation
HRR	Heat Release Rate
HC	Hydrocarbon
IMEP	Indicated Mean Effective Pressure
K	Kelvin
LSC	Loop Start Count
NO	Nitric Oxide
NO_2	Nitrogen Dioxide
NO_x	Nitrogen Oxide
O_2	Oxygen
OFAT	One Factor At Time
PM	Particulate Matter

RPM	Revolution Per Minute
SCR	Selective Catalytic Reduction
SI	Spark Ignition
SLR	Single-lens reflex
SOI	Start of Injection
TDC	Top dead centre
THC	Total hydrocarbon
TIFF	Tagged Image File Format
UMP	Universiti Malaysia Pahang
UTP	Universiti Teknologi Petronas

LIST OF APPENDICES

CHAPTER 1

INTRODUCTION

1.1   Research Background

Fossil fuel demand continues to rise (Martins et al., 2019; Tran, 2019; Vinet et al., 2010). It is expected that between 2020 and 2030, the irreversible decline of global fossil fuel production per capita is forecasted (Nehring, 2009). Meanwhile, there are less than 44 years of oil remaining with primary oil fields now already started demonstrating production decreasing (Leopold et al., 2016). Furthermore, BP 2017 statistics have revealed a decreasing pattern on world oil production and with a slight increase in reserve. Nevertheless, the calculated figure suggested that the reserve is sufficient for 50.6 years of current production (Vinet, 2010). According to ExxonMobil, through 2040, diesel demand is expected to account for at least 70% of all transportation fuel growth.

One of the prominent fossil fuel is diesel used in compression ignition (CI) engine. Perceptively controversial, however, the engine is versatile and has been in many major applications because of the durability. However, the engine emission is the main limitation which challenging its existence. The concentration of gas emission in the city is identified. Especially in the urban area, the air quality problem is found to be concentrated (Dunmore et al., 2015). Partly, exhaust emission from CI engine is the contributor to air pollution (Agarwal et al., 2015). Nonetheless, CI engine is still remain as the affordable option considering running with diesel fuel is much more efficient and cheaper than running with petrol fuel.

The gases that contribute the most from the combustion of the CI engine includes unburned hydrocarbon (HC), Nitrogen oxide (NO_x), carbon monoxide (CO) and carbon dioxide (CO_2). CO is a colourless gas with the same density as air formed because of the incomplete combustion process. It could replace oxygen in the blood. Theoretically, CO_2 and water are converted from the combustion of diesel fuel. However, due to impurity and imperfection of combustion, CO is produced and react with oxygen and producing CO_2. An excessive amount of CO_2 in the long term may affect global climate change.

CO$_2$ excessive emission comes from fossil fuel combustion (Höök et al., 2013). The increase in CO$_2$ and NO$_x$ are a lethal combination. NO$_x$ actually poisoners and have been linked by the health organization to a serious respiratory condition. Originally, mitigation from a petrol engine to the diesel engine is because of CO$_2$ reduction. This seems like a solution at first but actually not. To counter this, emission regulation implemented strict emission standard and continuously pressuring engine manufacturer to act upon the issue. By the year 2021, heavily regulated, the expectation of NO$_x$ emission will be set to become 1/10th of today limit (Santini et al., 2016).

Traffic congestion is one of the root cause of air pollution. Moreover, there is an increasing concern that the CI engine as one of the significant emission sources with immense air pollution contributor to one extent. Exposure to the diesel engine emission is a potential risk associated with a health problem such as the risk of brain damage, increased of cardiovascular illness, lung cancer and heart diseases (Costello et al., 2018). Although individual transport vehicles with diesel fuel-powered may seem like minor suspects at one glance. Nevertheless, the statistic on pollution watch revealed otherwise.

World demand for transport fuel alone accounts for 60% of world oil consumption with a market share of a vehicle with a diesel engine in some of the European countries have exceeded 60% (Hegab et al., 2017). Particularly, heavy engine class and passenger vehicle run on diesel correspondingly accountable due to the expected demand increase by 85% between 2010 and 2040 (Hegab, 2017). Consequently, a heavy-duty diesel engine shared the highest portion of NO$_x$ to the scenario (Kim et al., 2017). Agricultural and construction sector widely attached to the heavy-duty application of diesel power machinery. Subsequently, the demand for diesel is higher as compared to gasoline due to the wider scope of diesel engine application, unlike gasoline engine which is only for transportation (Abu-Hamdeh et al., 2015).

The source of biofuel is widely available and potentially has a lot to offer. Unfortunately, it has not been fully utilized specifically as a source of energy for the engine. Malaysia for example with large feedstock source such as palm oil promote value to remove biofuel technology barrier associated with the energy source for the CI engine. Palm oil as potential feedstock has been reviewed elsewhere (Mohd Hafizil Mat Yasin et al., 2017). Lately, the Malaysian Palm Oil Board (MPOB) is seen in full swing to improve the palm oil industry. On the light of that, mix approach with biodiesel, bioethanol and

diesel received interest. Several mitigation strategies that have already been the topic of research interest such as water in diesel, fuel additive as well as bi-fuel indirectly inspired the idea of tri-fuel and has begun to appear in the literature.

Unlike diesel, bioethanol has no serious market in diesel engine fuel for the transportation sector. The second generation of ethanol use biomass which can boost rural economy unlike the primary generation of ethanol from starch content such as cone, sugar cane or many more which competes with the food source. The discouragement is understandable since while the number of people dying on food hunger in someplace increases, to utilize the source for fuel production does not make sense, not recommended and a non-ethical. Moreover, since the limit factor is viscosity and oxygen content, NO_x emission will be expected to be higher with beyond 20% biodiesel input.

With less than 20% biodiesel, the performance is almost on par with conventional diesel but to go beyond, the performance may decline. The same is true with ethanol-diesel blend optimization benchmark up to 15%. Together as the tri-fuel application, the replacement can be possible to achieve up to 30% (S. A. Shahir et al., 2014).

Using tri-fuel in comparison to pure diesel, engine performance and emission shows positive outcome (Klajn et al., 2020; K. Rajesh et al., 2019). Meanwhile, blend properties limit of tri-fuel is reported within of the diesel standard (Pradelle et al., 2019a). Research also suggest tri-fuel blend having the same oxygen concentration yield promising emission with engine load (Ghadikolaei et al., 2018). Meanwhile, secondary atomization process known as micro-explosion phenomenon is one of the essential factor among others that are overlooked but contributed to the result (Avulapati et al., 2019). The rapid disintegration of fuel droplet via micro-explosion facilitates the speed of fuel air mixing process and subsequently promote combustion process to initiate rapidly.

1.2 Problem Statement

Fundamentally, the knowledge of the micro-explosion phenomenon to date has not been fully explored due to accessibility and technology constraint. The lack of understanding on the phenomenon could invite the tone of disbelief among scholar to the probable occurrence of the event in the CI engine (W. Fu et al., 2006). Meanwhile, evidence in the literature has pointed out to tri-fuel with the discovery of the improved burning output (Krishna et al., 2019; Venu et al., 2018). Extensive research on tri-fuel

study without realizing the existing of the phenomenon which could occurs a few milliseconds prior to combustion until recently (Avulapati, 2019). In addition, there is still exist some ambiguity as to can micro-explosion phenomenon can really occur with tri-fuel emulsion in CI engine (Corral-Gómez et al., 2019). Micro-explosion phenomenon manifestation under high pressure common rail injection is unknown. Furthermore, considering micro-explosion as secondary atomization mechanism, finely atomized droplet is expected to affect the spray. The micro-explosion phenomenon should also be acknowledged from the macroscopic perspective as spray. Thus, the detailed spray characteristics of tri-fuel emulsion is needed to analyze the impact of the micro-explosion phenomenon on droplets. In addition, the chain reaction of spray behaviour and ignition characteristics are essential to justify the discovery of the unique tri-fuel combustion outcome reported in the previous research.

To the best of author knowledge, study about micro-explosion with tri-fuel emulsion in the spray jet at high pressure and under high temperature resembling real engine is still limited. Methodologically vague, single droplet suspended or hanging techniques is a common but intrusive approach due to the interference of micro-size thermocouple or wire (Avulapati et al., 2016). Hence, is not suitable for the study of the micro-explosion phenomenon. In addition, Leiden frost and hot plate techniques are also not suitable considering the size of the droplet is too large. Furthermore, the detailed impact of the micro-explosion on a single droplet deformation and the spread as its impact on the spray formation are yet to be explored despite it has a direct contribution to the combustion (A. Ismael et al., 2018). It was reported that using tri-fuel, the spray behaviour was altered, however the cause and effect were generally pointed out at the physicochemical properties solely and no acknowledge to the significant hidden occurrence of micro-explosion phenomenon (Hulwan et al., 2011; Mofijur et al., 2016). Overlook phenomenon which partly responsible for the reported unique combustion characteristics in the previous studies. In response to the state problem, the study is deliberately aiming to prepare tri-fuel emulsions, investigate the micro-explosion phenomenon via macroscopic and microscopic approach and analyse the combustion characteristics.

4

1.3 Significant of the study

The study emphasized the role of biofuels as one of the Tri-fuel emulsion content. The study not only towards convincing diesel engine manufacturer to consider biofuels but also in the long run, holistically parallel with the total fossil fuel dependency concern. The finding of this study will enable one to prepare tri-fuel emulsion effectively and aware of the interaction between the formulation ratio and emulsification setting in preparing the fuel. The created model can be used to prepare the fuel with a specific desire of physicochemical properties. The in-depth understanding of the important phenomenon will be used as evidence to substantiate combustion characteristics which can address excessive HC and NO_x emission. Ethanol, volatile compound as tri-fuel emulsion component should enhance the micro-explosion and with the adequate level latent heat of evaporation, excessive NO_x formation issue can be addressed simultaneously. The research will demonstrate that with tri-fuel emulsion, fuel atomization can be improved which leads to better combustion characteristics. Consequently, not just to make tri-fuel applicable in the existing CI engine with little or no engine modification but also to make it more efficient than singular conventional diesel fuel. The study will reveal the combustion characteristics of the fuel with the secondary atomization attribute.

1.4 Research question

This research seeks to address the following question:

i. What is the effect of emulsifying settings and formulation ratio on the physicochemical properties of tri-fuel emulsions?

ii. What type of micro-explosion occur with tri-fuel emulsions and how it will affect droplet and spray?

iii. If micro-explosion happens, how will it affect combustion characteristics?

1.5   Research Objective

The research objectives are derived as follow.

i.   To synthesize the effect of formulation ratio and emulsification parameters on selected physicochemical properties of the Tri-fuel emulsion.

ii.   To investigate the presence and sequence of micro-explosion with selected tri-fuel emulsion conducted in a constant volume chamber.

iii. To assess the effect of the micro-explosion phenomenon on spray characteristics conducted in a constant volume chamber.

iv.   To evaluate the effect of micro-explosion on the tri-fuel emulsion combustion characteristics in the compression ignition engine.

1.6   Research Scope

The scope of the study includes:

i.   The preparation of tri-fuel emulsion using ultrasonic emulsification and properties acquisition.

ii.   The physical insight of micro-explosion phenomenon dynamic behaviour that can be obtained by experiment.

iii. The investigation of secondary atomization known as micro-explosion with tri-fuel emulsion in the optically accessible constant volume chamber that almost meet the combustion chamber environment.

iv.   Engine test to obtain combustion characteristics.

6

1.7   Thesis outline

The thesis comprises of five chapters. The next chapter is an opportunity to look again at the literature in depth. The purpose is to reveal, evaluate, defines and describe the research gap in detail. The literature review is structured by start-off broadly and then taper-off gradually to the specific research gap. The third chapter is concerned with the methodology used for this study. After the introduction of fuel source, the methodological approach for fuel characterization was elaborated in detail. Next, the experimental configuration for the investigation of the micro-explosion phenomenon is been explained. Finally, the experimental configuration for obtaining combustion characteristic was described. The fourth chapter presents the findings of the research. The finding was divided into four major sections, characterization, droplet, spray and combustion. Finally, the conclusion drawn and answering research question with a list of future work recommendation are presented in Chapter 5 along with the shortcoming and limitation.
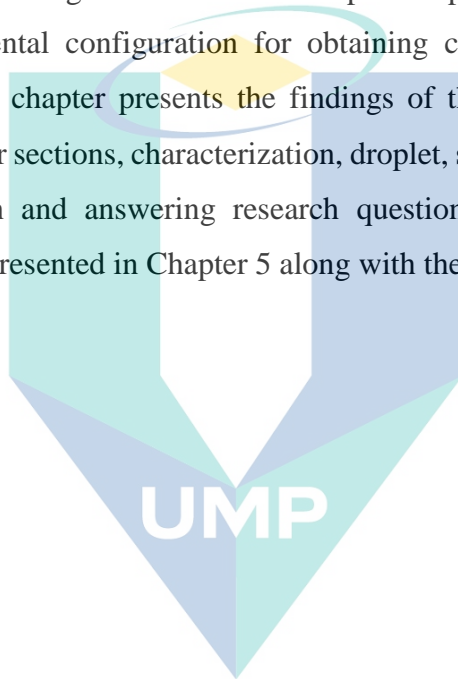
CHAPTER 2

LITERATURE REVIEW

2.1   Introduction

Compression ignition (CI) and spark ignition (SI) are the two-famous widely accepted engines in the automotive industry. Among the two, diesel engine under compression ignition category dominant in the heavy-duty class vehicle because of the advantages to run under high compression ratio with high thermal efficiency and cost-saving (Klett et al., 2017). The origin of diesel engine cycle was proposed by Rudolf Diesel in 1890, patented in 1892 and granted three years later. The need for increasing efficiency has put diesel engine with compression ignition concept a forefront compared to petrol engine (Reitz et al., 2015). The technology of engines in both CI and SI engines has advanced over time since their emergence as power train for automotive vehicles. CI engine has evolved overtime to become efficient to the extent that the SI engine can no longer cope thermodynamically. A diesel engine is proven to be capable of delivering higher torque at low revolution per minute (RPM) power.

The four-stroke CI engine consists of intake (induction), compression, power, and exhaust strokes. During the induction stroke, the intake valve is open for air intake into the cylinder. There is no restriction of air intake in CI engine during the intake stroke. Both the valves closed in the compression stroke and the piston is pushed up to the top dead centre (TDC) to compress the air within the clearance volume. In CI engine, it is not the spark plug that ignites the fuel but rather only by the compressed air that turns hot enough to the level above the fuel ignition temperature. Just a few crank angles before the piston reach the top dead centre, fuel is injected into the cylinder. Hence, spontaneous ignition occurs in the cylinder causing power stroke to initiate. The power stroke is when the combustion pushes the piston down to bottom dead centre (BDC) and the crankshaft converted the heat energy into mechanical work. Exhaust stroke follows that with the crankshaft turned and push the piston back up exhale the emission out from the cylinder via open exhaust valve.

Fundamentally, there are three basic conditions necessary to obtain normal combustion in CI engine which are the fuel, sufficient oxygen, and compressed hot air. Increase in pressure and temperature change are the common key monitors for the desirable combustion characteristic. Mechanism of combustion process includes ignition delay period, flame propagation period, direct combustion period and post-combustion period. Ignition delay is the period between the time fuel is injected until the fuel starts to ignite. Air and fuel mixing take place within this duration although, in reality, it is not possible to achieve 100% mixing efficiency. High-pressure injection in the form of mist from the nozzle into the hot cylinder undergone this preparation period before combustion can be initiated. It is desirable that the ignition delay period to be kept as short as possible because it may affect the next cycle of the combustion process.

Meanwhile, the flame propagation period refers to the time when the flame is spreading to the fuel injected. The ignition creates heat while rising the cylinder temperature and pressure even higher. These promote much faster evaporation and mixing of air and fuel compared to during the ignition delay period. As a result, the flame spread to all other parts of the cylinder that is filled with mixed air and fuel that are created during the ignition delay period. If the ignition delay is too long, the in-cylinder pressure will become either too high or too low. Meanwhile, the period flame is spreading until the time the fuel injection is over is called direct combustion period. Here is when instant fuel-burning occurs without delay as the fuel get injected. The pressure level is at the highest level after the top dead centre. Finally, the post-combustion period is the time between the stop of the injection and the end of combustion. Here is when the leftover unburned fuel continues burning as the fuel injection already stop before slowly end. Pressure and temperature can be seen in a drop pattern at this point.

Diesel is is a fossil-based fuel that is used in the compression ignition engines. Under the petroleum refining process, fractional distillation has been used typically to separate hydrocarbon into numbers of fractions. One of that fraction is diesel fuel with boiling point approximately between 250 to 350°C. Diesel fuel is suitable for CI engine not only because of low volatility nature but also because it will easily self-combust when it reaches a specific temperature as a result of high compression. Diesel fuel can withstand high compression or in other words, an ability to tolerate high pressure.

Physicochemical properties of diesel are shown in Table A1.1. The measure of knock tendency of diesel can be observed from the cetane number value that is based on its paraffinic content. Diesel cetane number which measures the fuel ignition characteristics range from a quarter to half from the total range of 100. In term of density and viscosity, diesel is greater than gasoline. Viscosity effect is on the fuel atomization during injection as much as surface tension. Meanwhile, the density effect is on the amount of fuel that enters the engine. The pattern of density and viscosity of diesel behaviour subject to variation temperature and pressure are illustrated in Figure 2.1.

<div align="center">(a)   (b)</div>
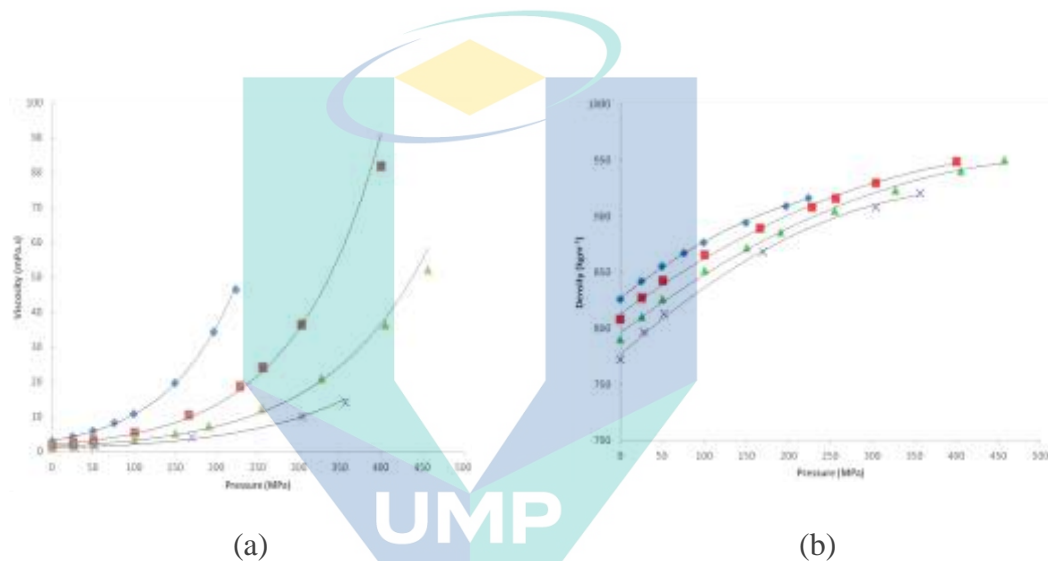
Figure 2.1   Variation of diesel viscosity (a) and density (b) readings subject to variation in temperature and pressure
Source: Schaschke et al., (2013)

To reach full combustion, diesel consumes a lot of oxygen. Longer chain of carbohydrate molecules in the diesel demand for a large number of oxygen molecules per each molecule for complete combustion. Unfortunately, diesel contains zero oxygen contain to support the oxygen consumption requirement. Although it is possible to include oxygen atom in the diesel via specific chemistry method, however, it could reduce the fuel energy density. Therefore, another fuel with oxygen content is needed to address the research gap.

Diesel has high auto-ignition temperature and able to avoid pre-ignition tendency caused by the residual heat in a relatively high hot combustion chamber. The amount of heat released during the combustion of a unit mass can affect engine emission and refers

to as calorific value. The calorific value or the amount of energy in diesel has got potential for efficient combustion. Consequently, inefficient combustion could cause unwanted exhaust emission. Therefore, another fuel with high calorific value or an approach to counter the reduction of calorific value is needed to fill the research gap.

2.2   Current improvement strategy

Efforts to reduce harmful emissions sometimes lead to a reduction in the performance of the engine. These efforts are generally classified as pre- and post-combustion treatments.

Table 2.1   The various post-combustion treatment approach

No	Approach	Source
1	Exhaust gas recirculation	(Ravi Kumar, 2017)
2	Selective catalytic reduction (Using Diesel exhaust fluid)	(de França et al., 2019)
3	Catalytic converter	(Ghodke et al., 2017)
4	Diesel particulate filter	(Patil et al., 2017)
5	Ducted fuel injection	(Gehmlich et al., 2018; Mueller et al., 2017)
6	Diesel oxidation catalyst	(Caliskan et al., 2017)
7	Catalyst lean trap/ Lean NO_x trap	(Y. Li et al., 2017)
8	deNOx Zeolite coated converter	(Karthe et al., 2016)

2.2.1   Post-combustion and pre-combustion treatment

Post-combustion treatment is about cleaning diesel engine unwanted exhaust emission. Selective Catalytic Reduction (SCR) is one of the approach installed in the exhaust system and it works in conjunction with Diesel exhaust fluid (DEF). Current post-treatment mitigation has been reviewed comprehensively elsewhere (Praveena et al., 2018). Table 2.1 shows the various post-combustion treatment research currently ongoing. All the mentioned treatment strategy contains its own merit and specific limitation. The approach, however, did not thoroughly analyse the root cause of the issue. Merely, the approaches are more towards adaptation and compensation to the unresolved

11

issue. Moreover, some of the approaches even require major engine modification or wide-ranging of add-on mechanism.

Table 2.2   The various pre-combustion treatment under non fuel based approach

No	Approach	Source
1	Piston geometry modification	(Lalvani et al., 2015)
2	Combustion chamber modification	(Sener et al., 2020)
3	Diesel injection timing (DIT) strategy	(Sener, 2020)
4	Fuel injection design (Auto thermal)	(Pasel et al., 2020)
	Common rail solenoid injector	(Ghaedi et al., 2020)
5	Turbocharger variable nozzle	(E et al., 2019)
6	Low temperature combustion (LTC) strategy	(Pachiannan et al., 2019)
7	Homogeneous Charge Compression Ignition (HCCI)	(Calam et al., 2019)

Table 2.3   The various pre-combustion treatment under fuel based approach

No	Approach	Source
1	Diesel-alcohol	(Ağbulut et al., 2020)
2	Diesel-water emulsion	(Hasannuddin et al., 2018)
3	Diesel-biodiesel	(Elsanusi et al., 2017)
4	Diesel-biodiesel-alcohol	(Ağbulut et al., 2019)
5	Nano material additive	(EL-Seesy et al., 2019)
	Oxygenated fuel	(Nabi et al., 2020)
6	Biofuels	(Unglert et al., 2020)
7	Low temperature combustion (LTC)	(Pachiannan, 2019)

Pre-combustion treatment refers to an approach to combat undesired engine emission at the level before the combustion stage. Pre-combustion treatment can be non-fuel-based treatment or a fuel-based treatment. Table 2.2 and Table 2.3 shows the various post-combustion treatment research currently ongoing under non-fuel based and fuel based respectively. This is not an exhaustive listing. The focus of this work is on the pre-

combustion treatment, specifically on the fuel based approach. The concept of multi-component mixing fuel is under a fuel-based approach which has been an area of interest recently. Mainly with diesel as the base fuel, the mixing fuel strategy has been tried to be presented combined diesel with biofuels, additive, Nano particle or even water.

2.3   Biofuel as fuel-based treatment

Biofuel is the term used to indicate a source of the fuel that is coming from a biomass source base. Biomass is a biological material harvested from forestry, agriculture residual or any organic crops to produce energy. Apart from producing electricity through the burning of biomass, converting biomass into combustible biofuel is a useful exertion from the biotechnology field of discipline. With common feedstock such as forest residue, typically woodchip undergo thermal chemical conversion processing.

The first generation of biofuel is made out of direct food crops. Because of limited agricultural resources, sharing food resources with fuel production have been a debate. The risky link between biofuel and food security has been taken seriously despite the need for renewable fuel. Thus, second-generation biofuel was introduced comes from non-food category and renewable resource. It is from cellulosic material. Some of the commonly known cellulosic material is like grass, wood and non-editable part of the plan. The material requires special pre-treatment process before it can extend to the fermentation process practised in the first-generation biofuel production. Sound management of harvest and the return of biomass back to earth is called sustainable renewable energy. Close loop of biomass lifecycle is what the world needs with biofuel as the source of sustainable renewable energy. It has been a growing concern that use of biomass faster than growing it will result in survival competition apart from expected excessive CO_2 in the atmosphere

The third generation of biofuel is produced from lipid production of algae. This is the most advanced technology to date which use food waste, fat or vegetable oil waste to produce biofuel. A lot of research in this area now. Biofuel from new generation feedstock study and impact to current and the future engine has been reviewed elsewhere (Bergthorson et al., 2015). The potential benefit of utilizing biofuel is reducing the dependency on crude oil, engine cleaner emission and hopefully better performance.

13

The pressing need for fossil fuel replacement and energy security indirectly shape the biofuel demand and supply scenario. To date, the biofuel market trend is growing steadily as stated in the market research report published by the Global Industry Analysts Inc. The United State, Asia Pacific and Latin America are the top three biofuel market reported with promising growth demand. Government support and global strategic campaign for environmentally friendly alternative motivate biofuel demand worldwide. The growing popularity is currently witnessing on the second-generation biofuel. A developing nation with high feedstock capacity receives motivation. Innovative technology provides biofuel producer competitive advantage. Finally, the most important motivation is the encouraging fuel blending mandate to drive research towards higher biofuel formulation ratio into conventional fossil fuel.

2.3.1 Alcohol

As a fuel, non-aromatic hydrocarbon compound or known as aliphatic alcohol include ethanol, methanol, propanol and butanol. Those four alcohol types are well known to be suitable as alcohol fuel because chemically, they can be synthesized. The first generation of ethanol is made from the food supply chain material through the fermentation process. Sugars are fermented to ethanol before distilled into its final liquid form. Fermentation is a metabolic process occurs in micro bacteria or fungi. Metabolic process means life-sustaining chemical transformation. Ethanol fermentation occurs in yeast and some bacteria. Ethanol is converted from acetaldehyde. Acetaldehyde is converted from Pyruvate acid and Pyruvate molecules are converted from glucose molecules. Bio-based ethanol is produced from food crops typically corn, sugarcane and soybean. To sum up, glucose is converted into two molecules of ethanol and two molecules of carbon dioxide.

The second generation of ethanol production such as Cellulosic ethanol undergoes a biochemical conversion process. Pre-treatment, hydrolysis, fermentation and purification. Another method is via thermochemical conversion. There are many advantages of ethanol and one if it is the exergy contributor. Exergy analysis is a tool to indicate the system sustainability and ethanol is known to increase exegetic engine efficiency (Paul et al., 2017).

Alcohol has potential as fuel too but it is not advisable as standalone in the CI engine. Table A2.1 shows the fuel properties of different alcohols potentially available for CI engine applications. Alcohol is not like water that leads to corrosion and facilitates microbiological growth (Nour et al., 2017). Alcohol as stand-alone fuel can cause additional wear on all kind of different part within the engine. Specifically, at the cylinder liner at the top of the bore, mid bore and piston top ring gap. Apart from that the weight loss of the cam follower and cam lobe. From the fuel economic standpoint, because alcohol has a low energy density, it is hard to obtain credit on mileage saving with alcohol stand-alone in the engine. In other words, it is not practical.

Two vital engine emission level is known as NO_x and soot rise and reduce interchangeably. Alcohol potential benefit to this is the latent heat of evaporation. Alcohol present in the cylinder is believed could cause an environment temperature drop. This heat absorption and a temperature drop of the combustion cylinder involved latent heat of vaporization. The latent heat of vaporization energy reflects the temperature of the environment. The enthalpy of the system that is provided to the vapour during the process that occurs at a constant temperature cool off the system. Thus, the cooling effect takes place after high-temperature combustion takes place. High latent heat of vaporization reduces combustion temperature (Lapuerta et al., 2009). It cools down the temperature in the combustion chamber which contribute to the reduction of NO_x (Qi et al., 2010). Alcohol has latent heat of evaporation four times stronger than gasoline on a stoichiometric basis (Morganti et al., 2018). Despite the advantage, the latent heat of evaporation may also increase the ignition delay period. Hence, it is critical to find a balance factor to compensate for the time lost by increasing the speed via improving the fuel atomization.

The different substance has a different boiling point. Boiling point depends on the vapour pressure and atmospheric pressure at the equilibrium state. Equilibrium state means that the vapour pressure is equal to the atmospheric pressure which then boiling takes place. Alcohol is famous with volatility. Volatility means the boiling point is lower. Therefore, it is much closer to get vapour pressure reading to reach atmospheric pressure. Volatility effect of alcohol is on the ignition time. Ethanol is more volatile than water with a boiling point of 78.5°C, slightly lower than the boiling point of water at 99.85°C (Gan et al., 2012). In addition, the latent heat of evaporation of ethanol is four times higher

15

than gasoline on a stoichiometric basis (Morganti, 2018). It could reduce the gas temperature and endorse the cooling down of the cylinder walls.

Butanol is four-carbon chain alcohol produced from a bio-based feedstock while in contrast, ethanol is a two-carbon chain type of alcohol (Rao, Karmakar, et al., 2017). Several studies have proposed butanol as a substitute for ethanol in tri-fuel. The proposal to convert or to supplement ethanol as the primary biofuel with butanol has several advantages such as excellent blending ability, additional energy content and low water absorbent (Dürre, 2007). It is also acknowledged that butanol can be prepared from almost all of the agricultural plant waste wood bases, which possess higher energy density and lower volatility in comparison to ethanol (Trindade et al., 2017). However, the production of butanol is considered to be costly, while as the production grows progressively, the price of butanol remains high with the limited market due to lack of investment (Zverlov et al., 2006).

Despite the price fell below ethanol due to the oil price drop after 2015 (Pereira et al., 2018), the development of technology for scaling up the production process is still at a low development stage. Costly production and non-economical method made butanol behind ethanol. In addition, bio-butanol is more difficult to produce compared with ethanol (Mehta et al., 2012). Butanol is less toxic but volatility is not so much compared with ethanol. From properties comparison, in most cases, ethanol value is in between methanol and butanol (Fayyazbakhsh et al., 2017; Srinivasnaik et al., 2015). This moderation is important to balance the effect.

Furthermore, the rapid growth of the vapour bubble is observed in ethanol is more in comparison to butanol (Rao, Syam, et al., 2017), which is imperative for micro-explosion manifestation. Potentially higher thermal efficiency could be achieved for ethanol blend with biodiesel attributed to the high peak pressure in comparison to butanol blend with biodiesel (H. Liu et al., 2011). Although the expected decrease of soot formation and the reduction in fuel consumption appears promising, further investigation is required to explore the full operating range of the engine with various blend ratios of butanol, prior to utilization of butanol as a substitute to ethanol. In the meantime, ethanol remains the best candidate as part of the emulsion component with diesel.

Methanol is another candidate of alcohol that can be utilized in tri-fuel. It has a similar physical appearance and high volatility reading as ethanol. Like ethanol, it has a cooling effect that could lead to reduced NO_x (Qi, 2010). Based on the property comparison of the alcohols, the property of methanol is in between of ethanol and butanol (Srinivasnaik, 2015). However, ethanol has higher energy consumption saving in comparison to methanol. Due to the considerably high risk of methanol toxicity and its poisonous nature, utilizing methanol as a component in tri-fuel is not a promising option. Despite physically, methanol and ethanol are look-alikes, combust individually, ethanol and methanol presented unique combustion characteristics. In addition, ethanol is miscible with water while methanol is not. Furthermore, it has been investigated, ethanol has got higher chances of miscibility with diesel in comparison to methanol (Rakopoulos et al., 2011).

Ethanol or methanol as an additive to diesel has been investigated from combustion and emission perspective (Datta et al., 2016; Ghadikolaei, 2016; Tutak, 2014; Tutak et al., 2015; Yilmaz, 2012). Synthesize from the study of two fuel combination suggested that, ethanol effect was opposite than methanol when mixing into diesel. If the objective is for CO and HC reduction, then methanol is the best-suggested alcohol. However, if NO emission reduction is what to accomplish, then ethanol is the alternative. Choosing methanol over ethanol is sometimes due to oxygen content. Nevertheless, this is relevant for dual fuel mixing strategy that is alcohol and diesel. Instead, the centre of the argument is on the reduction of cetane number which commonly associated with the quality of the combustion. Alcohol with a low cetane number is expected to have poor self-ignite ability (R. Li et al., 2014; Rakopoulos, 2011). Methanol is however toxic. It is under a low cetane number category which is not ideal for high compression ratio engine application.

Meanwhile, propanol has never been examined as a potential tri-fuel candidate in CI engine. This is because propanol is known to be challenging and expensive alcohol to produce. Similarly, pentanol contains similar properties to butanol and acetone-butanol-ethanol (ABE), an intermediate product during the fermentation process of butanol production. Its solubility and stability in tri-fuel were less debated (Campos-Fernández et al., 2012; H. Wu et al., 2015). Overall, the suitability of ABE and pentanol as an

17

acceptable replacement or at least compliment for diesel in tri-fuel mixing is not promising.

2.3.2 Biodiesel

Many studies are conducted on biodiesel from different origins since the late 1990s. Production of biodiesel is through the transesterification of vegetable oils by alcohols (methanol or ethanol) in the presence of a catalyst (Atabani et al., 2012; Issariyakul et al., 2014). The raw materials can be any vegetable oils from both edible and non-edible categories (Anwar et al., 2018; M. Rahman et al., 2017). Different countries have different preferences based on the climate and availability of stock. Four main categories of sources of raw material for biodiesel namely edible vegetable oil, non-edible vegetable oil, recycle oil and animal fat (Kumar et al., 2013). It was found that the location and origin of vegetable oil feedstock are greatly linked to the regional climate. For instance, feedstock in India with Jatropha oil and Karanja oil, the United States with soybean oil, Canada, and Europe with Rapeseed oil and Malaysia and the South East Asia region with coconut oil and palm oil (Issariyakul, 2014; Mohd Hafizil Mat Yasin, 2017).

The feedstock is mixed with a certain type of alcohol and a catalyst, which triggers the chemical reaction. A processing unit is needed to mix all the ingredients thoroughly under controlled pressure and heat. Glycerin, a harmless bioproduct, is produced due to the chemical reaction, which is a common ingredient in soap production. Transesterification is utilized to produce biodiesel whereby the glycerin is separated from the vegetable oil or fat leaving methyl ester as biodiesel (E. M. Shahid et al., 2011). In some cases, ethanol can be used rather than methanol, hence the term ethyl ester instead of methyl ester as biodiesel.

Despite being at mature stages in terms of research, the transportation sector has been struggling to accommodate biodiesel fuels. Therefore, countries are solely dependent on fossil fuels despite the availability and capability of producing biodiesel fuel (Naylor et al., 2017). In the South East Asia context, palm oil is still the primary raw source for biodiesel production and one of the biggest feedstock in the world.

Today, the future of Palm oil feedstock currently under pressure by the European Union proposed palm oil ban campaign due to mass deforestation issue (Rulli et al., 2019; Wilman, 2019). The phase-out attempt on one of the major biodiesel feedstock not only

obstruction to the bio-fuel campaign but also an add-on to the current state of struggling with demand fluctuations and lack of proper marketing of biodiesel from the automotive industry. However, researchers continuously strive to demonstrate the merits of biodiesel, and the production of second-generation fuel such as Fischer–Tropsch, hydrotreated vegetable oils, waste cooking oils and fats are increasing.

It goes by many names, biodiesel of palm oil origin is the most feasible biodiesel in Malaysia and easy to extract. Recently, palm oil plantation has been accused poses a massive threat to the environment such as killing endangered wildlife, create pollution through massive forest burning that contributes to CO_2 emission and destroying acres of forestry land. Burning the forest for clear land for plantation. Second, to Indonesia, the high percentage of deforestation in Malaysia as a result of committing to palm oil plantation has been used as evidence to the labelled palm oil industry as one of the biggest environmental offenders.

In term of trade, Palm oil has been condemned and labelled destroying animal habitat. Palm oil biodiesel is being boycotted with the basis that palm oil feedstock dissipating virgin forest. Mongering and false information, boycotters failed to acknowledge forest ratio in which almost 50% of Malaysia still remains a reserved protected forest. Not even those countries that pledge palm oil propaganda mostly competing with the palm oil industry do not practice such massive green reserved. For example, western countries with massive crops plantation such as soybeans are seen grown in western country dissipating a lot more land. In other words, most of the campaign is apparently contain systematic business agendas, not more than simply to compete and kill the palm oil market.

Biodiesel has the potential to substitute diesel not only due to the availability but also due to the advantages such as lower peak rate of heat release, shorter ignition delay, higher ignition temperature and higher in-cylinder pressure (Mahmudul et al., 2017). Furthermore, enriching the level of oxygen during combustion is one of the approaches for obtaining complete combustion. Unlike diesel, biodiesel contains oxygen and thus, indirectly supply additional oxygen to the combustion zone effectively for efficient combustion. However, the approach shows unfavourable consequence on emission in comparison to diesel fuel (Alptekin, 2017; Hoekman et al., 2012; V. K. Shahir et al., 2015; Song et al., 2016). Moreover, the use of biodiesel generally results in 10% more

19

fuel consumption and 10% lower thermal efficiency in comparison to fossil-based diesel fuel (E. Shahid et al., 2011). Other impediments of biodiesel include high viscosity, low volatility, high vaporization temperature, high ash content, difficult ignition control and low calorific value (Singh et al., 2014).

Several limitations have been reported related to the utilization of biodiesel as a stand-alone fuel for the CI engine. One of the major disadvantages is the higher viscosity in comparison to diesel fuel (Yu Liu et al., 2015). Higher density and viscosity have a negative impact on the engine, specifically on the internal nozzle flow of the injection system (Salvador et al., 2017). Furthermore, the effect of viscosity is related to the physical mixing process in the combustion chamber, specifically on the atomization of the fuel after the injection. The consequence of the properties could be lack of proper fuel atomization upon injection into the combustion chamber. Evidently, high viscosity leads to low injection velocity, promotes less momentum and short penetration, resulting in high resistance to breaking up (Ghurri et al., 2012). The breakup resistance may lead to combustion inconsistency, which promotes emission of undesirable particles.

The utilization of biodiesel is yet to be acknowledged globally (Sorate et al., 2015). Current biodiesel blending with diesel of more than 5% is not accepted by many of the engine manufacturers (Sadhik Basha et al., 2011). However, that statement is more towards recommendation rather than restriction with no assurance that biodiesel may not reduce the performance of the existing commercial engine. Despite numerous publications have indirectly supported the claim that biodiesel is not suitable as a stand-alone fuel in CI engine, researchers are still prone to the idea of mixing biodiesel with diesel along with other bio-fuel such as alcohol not only as property enhancer (Gautam et al., 2016) but also as a stabilizer and co-solvent or natural surfactant (Han et al., 2016; Thangavelu et al., 2016).

Biodiesel is biodegradable, safe to handle, easy to transport and works in its pure form in the engine. However, biodiesel is doing more harm than good in CI engine as stand-alone. Biodiesel is not recommended to be used as stand-alone in CI engine is because of biodiesel limitation. Impediment of biodiesel includes high viscosity, low volatility, high vaporization temperature, high ash content, difficult ignition control and low calorific value (Singh, 2014). In addition, biodiesel with ester double bond is also not recommended due to promoting excessive NO_x emission (He, 2016).

20

Different biodiesel origin, with different characteristics of emission, has been reviewed elsewhere (He, 2016). This is the reason, research attempt to include additive to improve biodiesel weaknesses has been done (Rashedul et al., 2014). Another disadvantage of using biodiesel as stand-alone is that standard operating parameters like fuel injection timing and pressure set by the manufacture are meant for diesel and are not suitable for biodiesel as stand-alone in the engine. Hence, adjusting fuel injection timing and pressure is necessary to obtain the desired emission subject to biodiesel from difference origin (Mohamed Shameer et al., 2017).

Although biodiesel challenge with compatibility on the automotive system is tough (Sorate, 2015), there are many advantages of biodiesel and one of it is the high oxygen content. With the source of oxygen to enrich the oxygen contained in the chamber to facilitate better combustion. Apart from fuel and energy, the oxidizing agent is one of the most important elements for combustion to take place. Oxygen is one of the most prevalent oxidizers. When oxygen is not enough due to insufficient time for the oxygen released in the chamber to spread, oxygen content in the fuel is an extra advantage.

In comparison, biodiesel from any feedstock has not much significant difference in density value. However, some researcher had claimed that jatropha biodiesel is more viscous than palm oil biodiesel which can degrade the spray characteristics, emitted higher CO and HC (S. M. A. Rahman et al., 2014), side by side comparison conclude no significant difference and the review of Biodiesel from different feedstock has been presented elsewhere (Ramkumar et al., 2016; Wan Ghazali et al., 2015). Physicochemical properties of biodiesel are presented in Table A3.1.

In comparison with diesel, biodiesel contains density value at least 0.4 g/m^3 greater than diesel and the range could exceed diesel maximum value. Likewise, biodiesel is extensively more viscous than diesel and could reach 3.0 cSt more than diesel max viscosity level. Biodiesel maximum acceptable value can be referred from ASTM D6751 and ASTM D7467 (Ali et al., 2016). At high temperature, viscosity reading of biodiesel and diesel are almost similar. Nevertheless, at low temperature, the viscosity difference is great. Typically, biodiesel has slightly higher kinematic viscosity level in comparison with diesel. Too viscous could damage the fuel pump. Too low may incur lubrication issue.

Biodiesel is assigned a cetane number higher than diesel. The lower heating value of biodiesel is within the range of diesel value. The surface tension of biodiesel is relatively higher than diesel which could cause large droplet size. As a result, the droplet has difficulties in atomization during the fuel injection takes place. Range of calorific value of biodiesel starts smaller than diesel and has a similar maximum value. Auto-ignition of biodiesel is higher than diesel. Unlike diesel, biodiesel is by default an oxygen carrier fuel. Oxygen content did not affect the energy density.

2.4   Water-in-diesel emulsion

The motivation of water-in-diesel approach includes micro-explosion phenomenon as secondary atomization mechanism (Hagos et al., 2011; Moussa et al., 2018). Apart from that, the cooling effect of water on the combustion to quickly after combustion to avoid the region of excessive NO_x formation. Nevertheless, water-in-diesel approach over-focus on NO_x reduction and tend to overlook the effectiveness of PM. However, the issue with water-in-diesel is the fast phase separation rate like diesel-alcohol blend. As a result, a complete independent injection system under electronic control is strictly required to address the issue apart from available commercial surfactant. In addition, the commercial surfactant is not playing any significant part during the combustion process. Consequently, the release of other produced unwanted chemical substance in the emission as a result of unknown chemical reaction in the combustion chamber will come into the picture. Furthermore, the inclination of water to contact with the cylinder wall or other components could lead to corrosion and major engine problem. Frequent replenishment is also needed thus; water generation equipment should be in place.

2.5   Diesel-biodiesel blend and diesel-alcohol blend

Diesel-biodiesel blend already in the market with low biodiesel concentration due to manufacturer warranty coverage. The formulation ratio is growing towards biodiesel utilization (Abu-Hamdeh, 2015; Datta et al., 2014). However, as the ratio of biodiesel is increasing, drawback kicks in. Increasing oxygen content through biodiesel resulted in increasing the combustion temperature. Consequently, increasing the NO_x formation. Furthermore, extensive properties degrading with a serious increase in reading exceeding the acceptable standard level for viscosity and surface tension. High viscosity and surface

tension level for diesel-biodiesel blend could not only cause the fuel injection system failure but also produce undesirable spray characteristics. Consequent to such heavy and large size droplet, combustion characteristics, performance and emission are not even on par with conventional diesel fuel.

Diesel-alcohol blend also has some drawback. The blend experience physicochemical properties degrading opposite to diesel-biodiesel blend. Density, viscosity, surface tension and calorific value decrease substantially below the acceptable standard level (Han, 2016; HANSEN, 2005). In addition, apart from the too volatile and the incapability of alcohol to provide lubrication, diesel and alcohol are immiscible by nature. At least ratios of up to 1.5% (by vol.) emulsifying agent is a must for diesel-alcohol blend stability or otherwise immediate phase separation issue coincided. The opposite setback of the diesel-alcohol blend gives the impression that it is almost opposite to diesel-biodiesel blend. Complementary limitation of both approaches motivates tri-fuel (diesel-alcohol-biodiesel) approach to close the research gap. Alcohol as an additive to diesel-biodiesel blend has been experimented and offer enhanced emission characteristics but require further investigation (K. Rajesh, 2019).

2.6   Tri-fuel (Diesel-alcohol-biodiesel)

2.6.1   Overview

The tri-fuel mixing strategy that has been developed over the past 10 years is believed could be implemented without engine retrofitting. The term 'Tri-fuel' is used here to represent a combination of the composition of fuels up to three components through proper mixing or simply blending, and macro or micro-emulsification. Various studies have investigated tri-fuel, and there have been different terminologies in the literature to designate the mixture. Tri-fuel, comprising diesel, biodiesel, and alcohol, which are blended at specific proportions offer a promising alternative for the unmodified diesel engine (Mofijur, 2016).

Technical utilization of tri-fuels is believed to replace up to approximately 20 to 30% of the diesel fuel (S. A. Shahir, 2014). According to the literature analysis, the focus of the study has been more to the engine performance and emission and less attention on the droplet or spray studies until recently (Corral-Gómez, 2019). Currently, it is inadequate to link the compositions mixing parameters such as formulation ratio and

23

preparation technique with the engine combustion performance. However, claims have been reported regarding the improvement in engine performance and emission enhancement (Labeckas et al., 2014; Mahmudul et al., 2016) through tri-fuel physicochemical properties attribute solely (Hussan et al., 2013).

Recent studies indicated that there could be other contributing factors that are yet to be explored in order to improve engine performance or emissions apart from just tri-fuel mixture properties attribute. Several studies believed that by means of the correct percentage composition and setting, secondary atomization could occur through the micro-explosion phenomenon (Avulapati, 2016; Boggavarapu et al., 2019; Han, 2016; Venu, 2018). Physics of puffing and micro-explosion of the tri-fuel emulsions have been investigated however inadequate evidence is presented to suggest that the occurrence is similar in the engine.
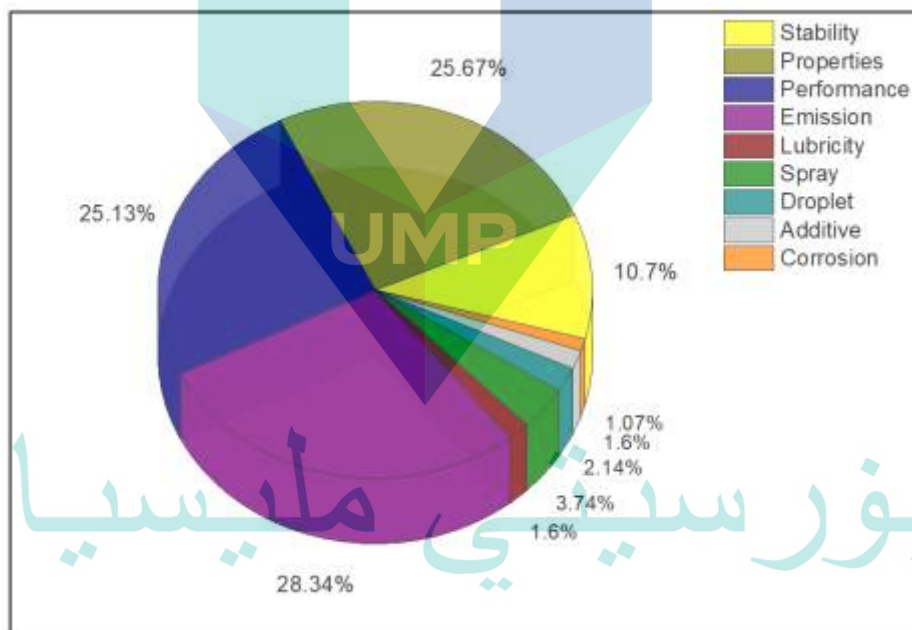
Figure 2.2   Tri-fuel research from 2003 to 2018

Figure 2.2 illustrates the limited research on the droplet and spray studies. Intriguingly, puffing and micro-explosion are believed could occur with tri-fuel composition. Whether it occurs under real combustion environment is yet to be established and requires further investigations. Furthermore, the chain reaction of values from the quality of tri-fuel properties to engine performance and emission was found to be speculative due to the disregarded values of Tri-fuel's hidden embedded feature on

24

atomization enhancement. Moreover, the micro-explosion phenomenon investigated in previous studies are under atmospheric conditions and the real combustion environment demand connectivity. In other words, to bridge the idea that tri-fuel blended or emulsified could improve engine combustion by secondary atomization traits needs substantial evidence.

2.6.2 Preparation technique

A fuel emulsion is a combination of two or more substances in the same phase. By definition, an emulsion is a specially prepared mixture with sufficient agitation of such substance in the presence of an emulsifying agent to achieve a homogeneous dispersant of droplet micro-bubble. In the case of two liquids being incapable of forming a homogenized mixture, an unstable milk-alike solution known as emulsion will be obtained. Through the incorporation of a surfactant and the appropriate procedure, the immiscible mixture can be expected to be thermodynamically stable.

Tri-fuels can be prepared by applying a shear force, which breaks up the surface tension of the fluids in the mixture and forms an emulsified fuel in the presence of a surfactant. The characteristics of tri-fuels may vary when different tools and mixing techniques are applied. Popular tools are currently being utilized to induce the shearing force in the preparation of tri-fuels include high-speed blender (Hagos, 2006), magnetic stirrers (Avulapati, 2016, 2019; Khoobbakht et al., 2016; S. Rajesh et al., 2011; Sharanappa et al., 2017; Venu, 2018; Venu et al., 2017) and mechanical homogenizers (Aydın et al., 2017; Júnior et al., 2018; Tan et al., 2017) for average macro droplet. Unconventional agitation such as ultrasonic homogenizers (Venu, 2018) is for obtaining average micro size droplet. The investigation of the agitation effect on the distribution size and uniformity of the dispersed droplet are receiving attention.

Tri-fuel emulsified fuel can be categorized based on the size of the dispersed droplet. Its size ranging from 1 mm to less than 1 µm (Fenouillot et al., 2009). Macro-emulsion describes a fluid with droplets more than approximately 0.1 µm in diameter, while a micro-emulsion is when the droplets are in the range of between 100 and 1000 Nm (Avulapati, 2016). Photomicrographs of tri-fuel droplet microstructure are presented in Figure 2.3. Ethanol appears as large circular droplet size while the biodiesel appears as dispersed tiny droplet size. The three-phase dispersed microstructure diameter to be in

25

the range of 50 to 250 µm (Tan, 2017). The similar finding can be seen in other publication with smaller scale (Fernando et al., 2004). The distribution size of the dispersed droplet matters because it can be used to improve the prediction of droplets behaviour before and after the injection. Moreover, it is an advantage to understand the effect of droplet size on the probability of micro-explosion occurrence.
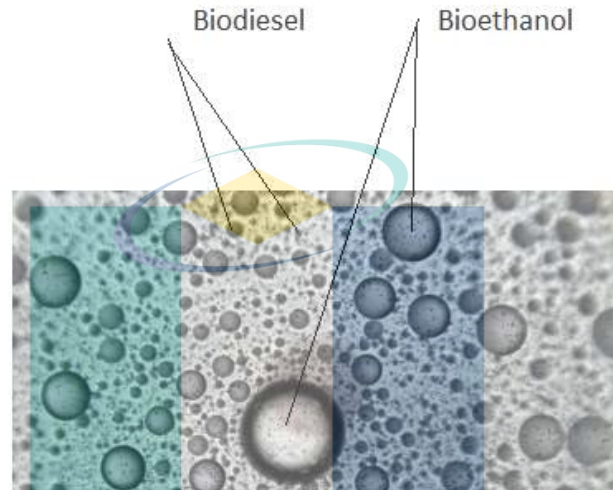
Figure 2.3   Photomicrographs of tri-fuel category showing the components of the typical emulsion
Source: (Tan, (2017)

It was found that most of the related detail effect of various mixing technique was not discussed with tri-fuel but broadly in other fields such as oil-water system, drug and food processing (Farzad et al., 2018; Juttulapa et al., 2017). Moreover, the effect of stirring has been considerably discussed in biodiesel production for yield and conversion (Al Basir et al., 2015; Marinho et al., 2018; Mashkour et al., 2017). The stirring speed is known to build the inertia for gathering the droplets and facilitate the coalescence. In addition, it provides shears to elongate droplets breakup. Thus, a higher RPM in the function of time should magnify the rupture mechanism, hence influence the droplet size distribution (W. Wang et al., 2014). With conventional agitation involving mechanical part, impeller shaft blade design govern the rate effect (Abidin et al., 2013; Afshar Ghotli et al., 2017).

Thus far, various methods have been experimented on tri-fuel including ratio blending, sequential blending, hybrid blending, side stream blending (Jamrozik et al., 2017; Mahmudul, 2016; Mahmudul et al., 2018), and splash blending (Venu, 2018;

Yilmaz et al., 2017). In-line blending technique is similar to side stream blending except that in-line blending technique is more suitable for 50/50 mixing or no base fuel in the blend. In-tank blending is normally being used with splash blending technique or another non-conventional agitation tool such as ultrasonic vibration apparatus for further refine result (Yasin et al., 2014). Inline mixing process setup, however, requires a smart control system. Notice from the study example of simply mix, tri-fuel mixing were done without even physical blade or emulsifier (Barabás et al., 2010; López et al., 2015). Among all, splash blending technique was found to be the most widely used approach (Joshi et al., 2007; H. Liu et al., 2016; Yilmaz, 2017).

Droplet deformation to the extend breakup into a uniform smaller size is desirable for stability and suggested by increasing stirring time and intensity (G. Chen et al., 2005). The induced by dispersed fuel component, resistance by surface tension and internal viscosity are the expected factors that demand systematic comparison among techniques which has less been discussed with tri-fuel. For example, the effect of stirring time and the intensity of mixing involving tri-fuel were still limited (C.-Y. Lin et al., 2006). The distinction between tri-fuel prepared with conventional and non-conventional agitation require attention. Distribution of rapid agglomerations among droplets is significantly noticeable when using conventional agitation whereas a lot more uniform distribution of dispersed droplet is observed with non-conventional agitation tool. The agglomeration is not necessarily undesirable although it is believed to increase the size of the droplets and this eventually promote fast phase separation.

Microphotograph of tri-fuel may have appeared to be comparable to the oil-water system. However, cautious interpretation is advised considering alcohol sensitivity to air contact is a lot more aggressive than water. Due to alcohol high volatility and sensitivity influence on the timescale of vaporization, the morphology structure formation can be expected to be dissimilar. Agglomeration development overtime as commonly observed on the water in diesel micro-structure behaviour may not be observed in tri-fuel that is prepared using non-conventional agitation such as ultrasonic agitator. The amount of force and energy applied in the process have not been evaluated, considering that it could significantly affect the solubility and stability of the mixture. Moreover, with non-conventional agitation tool like an ultrasonic emulsifier, the process may generate heat and could affect the fuel quantity in the mixture (Guo et al., 2013; Hielscher, 2005; C.-Y.

Lin, 2006). Therefore, the rate of evaporation due to air contact should be taken into account in the quest to produce effective tri-fuel. Direct contact with open-air could cause rapid phase separation of ethanol and diesel mixtures (Jin et al., 2019; Park et al., 2009).

Furthermore, the effect of equipment on tri-fuel dispersed phase from morphology perspective could be an important subject of interest but yet neglected. Thus far, microstructure before and after the injection has been merely assumed to be identical. It was not identified or confirm whether the identity of tri-fuel microstructure before and after going through the fuel injector nozzle would be identical. The persuasive argument valid for the discussion could be the interaction between the nozzle wall and the cavitation film, which influenced by the tri-fuel dynamic flow. Considering the sudden pressure from advance injector rail pressure on the liquid injected, the cavitation film may occur due to the act of pushing the fluid faster than its reaction time (Badock et al., 1999). Whether the high-velocity surface contact interaction between the nozzle hole walls with tri-fuel modified the microstructure of either emulsified or blended tri-fuel requires further research. Moreover, the relation of the quality of blend in term of the morphology, properties and stability with the occurrence of micro-explosion still remains unknown. Last but not least, droplet distribution status before and after the injection received no affirmation and merely assumed to be identical.

2.6.3 Surfactant

The mixing of tri-fuels can be stabilized normally by the utilization of an additive known as emulsifier or surfactant in order to prevent phase separation. The surfactant should be able to act as a binding agent between two or more immiscible substances in an emulsion and is a necessary ingredient with useful properties. Hydrophobic surfactant such as Span 80 and hydrophilic surfactant such as tween 80 were commonly employed in the fuel mixing research. However research suggested that biodiesel acts as an amphiphilic component in tri-fuel and forms an aggregate of molecules with polar and nonpolar tail subject to their diesel or ethanol orientation (Fernando, 2004). Amphiphilic terminology refers to hydrophilic or water liking polar and hydrophobic or fat liking polar. Therefore, it is fundamental to note that in this case, authors were not referring to the conventional hydrophilic definition on water inclination tendency but instead are referring to water alike loving polar.

Among the polarity groups, the top polar compound known is water, while alcohol is also known to be on the list, and to some extent, alcohol can be classified as a polar solvent (Tse et al., 2015). This can be demonstrated in cases where ethanol is miscible with water. Hence, alcohol can be treated as water (polar). From this understanding, researchers posit the ability of biodiesel as a surfactant. However, it was a strong statement to put forward that biodiesel can be used as an amphiphilic in the ethanol-diesel blend. In other words, to some degree, the statement somewhat significant in symbolizing biodiesel as a surfactant.

Moreover, surfactants must accumulate at interfaces with a hydrophobic portion orienting towards the hydrophobic phase and a hydrophilic portion at hydrophilic phase. Thus, in this case, the term hydrophobic does not refer to water liking but refers to alcohol inclination. This interpretation was supported by tri-fuel composition homogeneity (Kwanchareon et al., 2007). The stability result substantiates the question of whether biodiesel is suitable to be utilized as a natural surfactant in tri-fuels. Most of the studies regarding tri-fuels do not provide brief descriptions and offer no proper clarifications for the utilization of biodiesel as a surfactant.

2.6.4 Formulation ratio

There is an argument in the literature on the best ratio of constituent fuels recommended for tri-fuel emulsion and blending category. Figure 2.4 shows a plot of the recommended ratio from the literature with various motives such as comparing with diesel standard, physicochemical properties alteration, exergy, combustion, performance, emission and production perspective. To improve emission, it is recommended between 4% to 5% maximum ethanol content while biodiesel content at 2.5% the lowest and maximum 50% subject the engine load (Aydın, 2017; S. Rajesh, 2011). 11% biodiesel and 5% ethanol are the only ratio that meets the standard diesel requirements.

Moreover, hydrous ethanol content should not reach more than 1% in the blend, or else, the strong polarity of water could negatively influence the phase separation (Cheenkachorn et al., 2010). Through regression analysis, it is recommended that ratio of 0.6% ethanol 9.4% biodiesel and 90% diesel be the optimum blend considering viscosity as a function of palm oil methyl ester to ethanol (Hussan, 2013). As a primary component

in tri-fuel, the ratio of ethanol and biodiesel should be greater than 1:1 in order to obtain a stable micro-emulsion (S. Fernando et al., 2005).
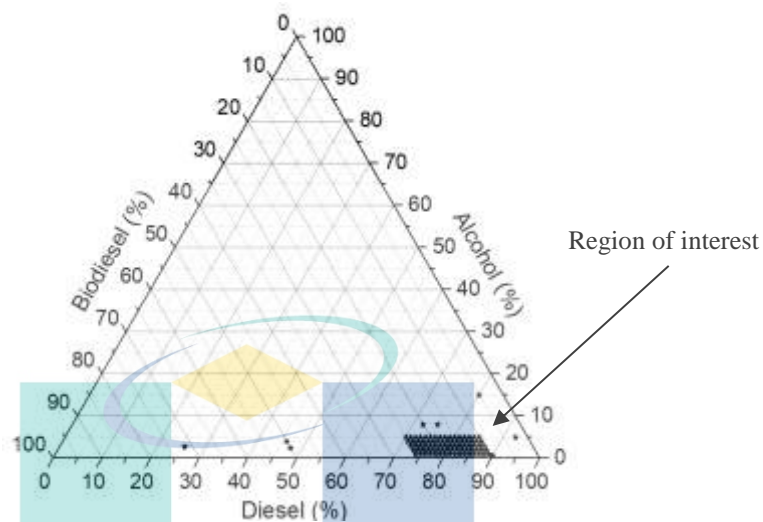
Figure 2.4   Recommended ratio with various motives

Source: Barabas et al., (2011); Cheenkachorn, (2010); Kwanchareon, (2007); LI et al., (2011); S. Rajesh et al., (2018); Sarkar et al., (2018); Zöldy, (2011)

5% ethanol and 25% biodiesel is the best ratio for the commercial production stage. In addition, the recommended portion of biodiesel in the tri-fuel emulsion is based on the ethanol content. It is recommended that biodiesel must be at least twice the content of ethanol in order to fulfil the lubricity properties, kinematic viscosity and cetane number requirement for standard diesel (Zöldy, 2011). In these regards, it is noteworthy that the undesirable safety-related properties of ethanol could be controlled with the aid of biodiesel. Nevertheless, the high flash point temperatures of tri-fuels due to the existence of ethanol may require additional consideration in the context of production, transportation, and distribution.

The maximum acceptable concentration for ethanol is 5% while 10 to 25% as the ideal amount for biodiesel in tri-fuel on a passenger automobile. Acceptable miscibility and stability are the keys to the recommendation (Barabas, 2011). The recommendation, however, can be argued as over-ambitious, as the outcome did not reflect the recommended ratio. In addition, with this ratio, engine efficiency will be degraded and causes an increase in fuel consumption. For passenger car, 5% maximum ethanol and maximum 25% biodiesel are recommended (Barabas, 2011; Mehta, 2012).

Interestingly, the tri-fuel composition was found to be stable under below freezing temperature range when oxygen content increased up to 25.72%. Based on the engine performance and emission tests under cold climate region, the optimal oxygen content in tri-fuel was recommended to be between 15% to 19% (Sendzikiene et al., 2006). To release optimum oxygen molecules for efficient combustion, the recommendation ratio is alcohol 8% while biodiesel at 20% (Sarkar, 2018).

For biodiesel as base fuel, simulation studies suggested 2.72% ethanol with 71.58% biodiesel and 2.41% ethanol with 50% biodiesel as the two optimum ratios to obtain adequate engine power, improve emission and cost-effective under several engine modes (LI, 2011). This is being emphasized recently that the mixing ratio involving oxygenated fuel should be limited to the stability of the combustion and the rise of pressure rate (Zheng et al., 2016).

To induce micro-explosion, it has been suggested that increase alcohol and biodiesel content enlarge the gap volatility and boiling point. The bigger the volatility gap, it affect the starting time of micro-explosion positively (Y Liu et al., 2010). However, with alcohol under 10%, micro-explosion is hard to detect (Y Liu, 2010). 10–40% ethanol favour micro-explosion while more than that, puffing may take over (Avulapati, 2016; Botero et al., 2012; Venu, 2018).

What is not yet clear is the effect of various formulation ratio on tri-fuel physicochemical properties such as density, viscosity or surface tension. It is still unclear of adding biodiesel how much could it compensate the ethanol possible hard influence on physicochemical properties. It is also unknown among the two, which component will have hard tendency effect on the physicochemical properties of tri-fuel.

2.7   Physicochemical properties of tri-fuel

Ethanol percentage is known with the pattern effect to tri-fuel viscosity and density. With biodiesel content at a constant rate, the higher the ethanol, the density and the viscosity degrading (Noorollahi et al., 2018). On the contrary, some of the tri-fuel properties obtained disconcerted the expected pattern (Alptekin, 2017; Sharanappa, 2017; Tan, 2017). The pressing doubt leave the floor open to the misconception. Not only the ethanol and biodiesel interaction but also the mixing method effects essentially associated

to rationalize the collective tri-fuel physicochemical properties obtained so far. Table A4.1 presented the collective tri-fuel physicochemical properties.

2.8   Micro-explosion and the secondary atomization process

The term secondary atomization is to describe a re-atomization occurrence which happens after the droplet goes through the first stage of atomization known as the primary atomization process. Recently, there is a growing body of literature that recognizes the advantage of secondary atomization with tri-fuel (Avulapati, 2016; Hagos et al., 2017; Han, 2016). That secondary atomization process scholars refer to is known as micro-explosion phenomenon (Alptekin, 2017; Avulapati, 2019; Boggavarapu, 2019; Corral-Gómez, 2019; Venu, 2017; Zhan et al., 2018). Given the diversified application of compression ignition engine, it is not surprising that micro-explosion has been the subject of research since 1960. Ivanov was the first to discover and observe micro-explosion for emulsified fuel between 1957 to 1965 (W. Fu, 2006). It was, in fact, a major area of interest within the water-in-diesel emulsion literature.

The term secondary atomization has also been used to describe as subsequent droplet fragmentation process. This is a further disintegration process occur at the distance of which the micro-explosion took place subjectively. The accidental or side effect of the droplet hit one another is also referred with the similar term; secondary atomization. It is not accurate to refer to it as the cause of micro-explosion occurrence though. Rather, it is an interactive process between droplets. On certain condition, favourable oscillation is due to the instability of the droplet.

Micro-explosion phenomenon is defined as the rapid disintegration of an emulsion droplet caused by explosive boiling of embedded liquid sub-droplets with a lower boiling point (Boggavarapu, 2019; Mehta et al., 2015). The disintegration is not gradual but simply a breakup process. It is a sudden bursting of liquid in droplet form which encapsulated dispersed component with high volatility compound (Annamalai et al., 2016). The dispersed bit with volatile compound reaches the superheated stage sooner than continuous layer while expands in sudden period faster than the other one. Vapour expansion breakup that is created causes a spontaneous explosion (Khan et al., 2014; Vellaiyan et al., 2016). The term micro-explosion is also defined as instantaneous violent vaporization process (Yang et al., 2013).

Puffing is defined as a partial breakup or low-intensity micro-explosion of a droplet (Avulapati, 2019). It can change the shape of the sphere droplet (Watanabe et al., 2010). Even when the droplet is opaque, puffing can occur (Watanabe, 2010). It is believed that puffing always occurs prior to micro-explosion (Rao, 2017), Some argue that puffing is the cause of the micro-explosion phenomenon due to the coalescence of droplet satellite originate from the puffing. This could be accepted in some cases since puffing frequency is a function of parent droplet and higher droplet size produces higher puffing frequency (Yahaya Khan et al., 2017). Thus, alteration in the droplet structure is expected due to the puffing phenomenon. Moreover, the quantified liquid penetration was considered as a confirmation of the secondary atomization (H. Wu, 2015).

The micro-explosion phenomenon is expected to dislocate smaller droplets, to tear the droplet apart and at the same time accidentally disturbing the neighbour droplet. The disorder is created by the explosion to distribute or spread tiny pieces of a droplet in the form of mist to all direction. The distinguishing feature of such disorder is partly secondary atomization. The event complements the effort of the injector as primary atomizer. In addition, the micro-explosion phenomenon can also be described as disruption (Mehta et al., 2014). The sudden fragmentation of droplet causes unsteady burning process (Ocampo-Barrera et al., 2001). The unsteadiness triggered sudden interruption of phase transition within the combustion. However, the interruption is welcomed because it promotes gasification. In the case of bigger size droplet, micro-explosion induced by coalescence of a smaller droplet (Yahaya Khan, 2017).

The micro-explosion phenomenon behaviour captured within the flame is also unclear. Nevertheless, the event normally been over-simplified within a complex flame and notably as a bright flash. Very rapid combustion is expected as a result of vapour flash flame. At times, flame spreading also could be interpreted as a micro-explosion phenomenon. Because micro-explosion sometimes creates spontaneous ignition, the bright spark within combustion is at times theme to micro-explosion phenomenon. Furthermore, the micro-explosion phenomenon starting time is more subject to volume percentage and droplet diameter rather than affected by a variety of high ambient temperature (Jeong et al., 2008). The micro-explosion phenomenon occurs before ignition begin (Ocampo-Barrera, 2001).

Micro-explosion phenomenon is also known as sudden fragmentation of a droplet that causes unsteady burning (Ocampo-Barrera, 2001). The unsteadiness is caused by the sudden interruption of phase transition within combustion, while micro-explosion occasionally generates spontaneous ignition. As mostly seen in experiments, the event of micro-explosion is often seen as a bright spark within combustion. The micro-explosion affects the brightness and local shape of the flame (Y. H. Li, 2011). In addition, a study micro-explosion occurred before ignition started (Ocampo-Barrera, 2001). In other fuel mixing study, micro-explosion phenomenon is predicted to occur so long as a mixture of fuel with multiple reading of boiling point (G. Fu et al., 2012; Kubota et al., 1988). Increasing alcohol and biodiesel in tri-fuel is an effective way to induce micro-explosion occurrence as a result of increasing the volatilities and boiling point among components (Botero, 2012; Y Liu, 2010).

Boiling is the term that is important to the study of the micro-explosion phenomenon. When the kinetic energy of the majority of molecules has enough energy to overcome the mutual attraction between them, then it is boiling. Boiling will not occur before nucleation initiated somewhere. Merely it is the expansion of initiate of the nucleation. Because it happens within the liquid phase, the vapour pressure has to be high enough or same as atmospheric pressure. Low atmospheric pressure means a lower boiling point for the liquid is required. The level for the vapour pressure inside the bubble to achieve will be much less hence bubble expansion occurs or rise up. High atmospheric pressure means a high boiling point is required.

Micro-explosion phenomenon is occurring because of different boiling temperature (Senthil Kumar et al., 2014). At least 50/50 boiling point difference between fuel component is a pre-requisite condition to micro-explosion phenomenon plus a period of droplet residence time (H. Wu, 2015). Furthermore, for the phenomenon to occur, internal droplet temperature needs to exceed homogeneous nucleus temperature which formed an internal bubble ready for the explosion (Ocampo-Barrera, 2001). When heat is transferred to the low boiling point liquid covered with high boiling point liquid, micro-explosion occurred because the low boiling point liquid becomes unstable towards the superheated state (Liang et al., 2013; Subramanian, 2011).

The stages or sequent of micro-explosion phenomenon evolved subject to a different level of elevated temperature charge. The significant difference between one

stage to another is the micro-explosion strength and droplet size (G.-B. Chen et al., 2017). Surface micro-explosion is the first stage to appear at the initial period of the heating process. Since the heat is in contact with the surface of the droplet primarily before penetrating deeper, the compound with low boiling temperature on the surface experience the heat and initiate nucleation at the droplet surface. Nucleation spread and minor micro-explosion intensity follow and reshape the droplet. Micro-explosion causes the small droplet to erupt and some fuel component with low boiling point evaporate and escape. These happen before the heated exceed 250°C.

Next stage, homogeneous nucleation and aggressive evaporation rate start. Due to the accumulation of inner pressure of the droplet, droplet swell developed and become noticeable before eventually burst. Micro-explosion phenomenon with a high level of intensity continues until the temperature reaches approximately 450°C. Before the phenomenon end, a series of low-intensity micro-explosion occur due to the release of acid content. In short, minor micro-explosion occur at around 200°C, droplet swelling from 250°C above and high strength micro-explosion at superheating temperature 350°C above before comes back to the lower intensity at 450°C. Combustion should expect to occur between 500°C and 550°C. In comparison, the third stage is much stronger than the first stage while the second stage with the highest intensity of the micro-explosion phenomenon (G.-B. Chen, 2017).

The addition of water concentration and low oxygen content may improve the effectiveness of the micro-explosion phenomenon but at the same time delay the occurrence. The effectiveness is expected because water has got unique high specific volume change upon converting to gas from a liquid state. As a result, a much greater rate of bubble expansion generated during the micro-explosion phenomenon. The delay is because of the effect of period extension due to water vapour domination at the droplet surface temperature. Ethanol, on the other hand, accelerates the onset of the phenomenon but water increases the shattering effectiveness of micro-explosion (Shaddix et al., 1998).

The boiling point of ethanol is around 78°C (D. Li et al., 2005; Shudo et al., 2009), in comparison to diesel which is between 210 to 235°C (Geng et al., 2017) and biodiesel which is in the range of 347 to 357°C (Yuan et al., 2005). As the base fuel boiling point increase, the rate of micro-explosion increase (Toshikazu Kadota et al., 2007). Boiling is a form of vaporization at high speed. It is strongly influenced by atmospheric pressure.

35

Because molecules in the surrounding air got more space to move about and with enough energy due to free space, they move freely in all direction. The behaviour of the molecules in the surrounding air will tend to move towards low energy state which will be in this case the droplet. As a result, the molecule in the air accidentally pushing down or hit on the group of molecules from the liquid at the surface droplet. The act creates pressure towards the surface of the droplet which is called atmospheric pressure.

Meanwhile, molecules that are energized trying to push upward and collide with the molecules from the air which then reduce the vapour pressure from the liquid. The vapour pressure is the upward pushing attempt from the liquid. Since the vapour pressure is not equivalent to the atmospheric pressure, hence no boiling is expected to occur. According to the theory, the boiling point is when the vapour pressure is equivalent to the environment atmospheric pressure. The molecules in the liquid require additional energy to escape due to low vapour pressure in the liquid. Or, a little bit more time to overcome the obstacle of pressure hit on the surface created by the molecules in the surrounding air.

Boiling formation from within the liquid is the coexistence of the vapour phase and liquid phase together. It is a delayed evaporation process with progressive gas molecules motion within the liquid interface. This paradox occurs when one substance in the liquid phase while another in the gas phase within the confine of the liquid phase. Superheating is the key to premature bubble formation.

When the molecules in the middle part of the droplet received enough heat transferred and obtain enough to push upward, the molecules leave some useful empty space which then allowing the space to be utilized by other energetic molecules to move within the empty space. As space becomes bigger and bigger, the vapour pressure within the space reaches the equilibrium rate as outside atmospheric pressure, the bubble is then formed from within the droplet among the crowded molecules. Because the formation is very rapid and the size of the bubble rapidly grow to exceed the size of the droplet itself, the micro-explosion occurs from the inside out. Increasing vapour pressure or decreasing vapour pressure is one of the approaches to reach the boiling point. The boiling point level is also subject to how strong is the molecules in the liquid attracted to one another or referring intermolecular forces. The stronger the attraction, the higher the boiling point. In other words, more difficult to boil with vapour pressure in the liquid is a lot less

36

compared to the atmospheric pressure. To convey the energy from the outside to the inner core of the droplet is where the radiation as heat transfer mode comes in the picture.

A normal boiling formation that one normally observed with the heating source from the bottom, the bubble floats up or coming from the bottom to the top because the vapour at the bottom reaches the same level as atmospheric pressure. The evaporation initiates from the bottom and forms a bubble. The molecules that have already turn into gas will tend to push out of the bubble towards the other molecules in the liquid phase. If the vapour pressure inside the bubble can push just as hard as liquid molecules push, the bubble will float up as what normally observed. However, the complexity of the droplet breakup process caused by the micro-explosion phenomenon is still not yet fully understand. There has been little knowledge of boiling theories involving droplet without any solid surface contact or wall heat flux.

Thermal history shows a slight decrease in droplet temperature in the event of the micro-explosion phenomenon (Mura et al., 2012). Occur at a certain temperature and stronger at proper ambient temperature (Sheng et al., 1994). The micro-explosion phenomenon is not only suggested to occur as long as the mixture of fuel contains components of different boiling point values but also likely to occur at a certain specific temperature and increases at some selected appropriate values of temperature (G. Fu, 2012; Yu Liu, 2015). The temperature recorded for micro-explosion was found to be between 131.85°C to 449.85°C (Han, 2016) and higher temperatures did not necessarily assist in increasing the probability of micro-explosion occurrence (D. Wu et al., 2012). However, it was noted that the required superheat temperature was between 50K to 80K for micro-explosion and between 20K to 50K for puffing depending on the properties of the emulsified fuel (Watanabe et al., 2008).

Temperature can be thought of as average kinetic energy. Average because in the droplet, molecules are there with different pre-stored kinetic energy. When temperature increase, molecules in the liquid energized at different rates. Imagine some are trapped due to unfavourable position within the molecules but with higher energy while some at the surface blocking the other molecules with higher kinetic energy. Not to mention molecules with weaker energy and trapped. In other words, not all molecules going fast and not all going slow. The distribution of molecules with a variety in energy level is there. The unfavourable states require time or more heat transfer to overcome the

conflicting issues among molecules at the specific time. Ambient temperature too high could stop micro-explosion due to the insufficient time for the droplet to create bubble nucleation (Yu Liu, 2015). It is also believed that excellent vaporization could stop the micro-explosion phenomenon. Hence it safe to say that the micro-explosion phenomenon could be utilized when evaporation is slow.

Critical pressure level might advance the onset of micro explosion (Zeng et al., 2007). On the other hand, when pressure is significantly high, it probably will postpone the onset. Pressure increases the boiling point of heavier fuel (W. B. Fu et al., 2002). Imagine the boiling point of the outer layer increasing higher. This effect could be assisting and even at the same time refusing the event. Once get into compression cycle, under higher air pressure, more partial pressure oxygen is expected to increase combustion. Since fuel exerts pressure in all directions. Pressure builds up in the combustion promote the start of the micro-explosion phenomenon (C. H. Wang et al., 1985). Increasing ambient pressure helps reduce the delay in the micro-explosion phenomenon onset. High ambient pressure is conducive to the impact caused by the micro-explosion phenomenon because it causes the boiling point of different fuel component gap to become huge (D. Wu, 2012). Previous studies also mentioned specific optimum pressure which could hinder droplet disruption (Cho et al., 1991). Dynamic instability which promotes micro-explosion at normal ambient pressure is somehow suppressed at high pressure (Cho, 1991).

Micro-explosion is also believed to be due to the vapour pressure difference between the interior and exterior droplets (Annamalai, 2016; Han, 2016). Micro-explosion is an attributed of dispersed embedded fuel component, as it reaches the superheated stage earlier than the base fuel. As a result, it creates a vapour expansion breakup that causes a spontaneous explosion (Vellaiyan, 2016). Under the thermodynamic metastable condition, bubble nucleation of alcohol (dispersed fluid) initiates while other components (continuous fluid) remain in liquid form. The bubble expands until it overcomes the surface tension of the surrounding fluid (continuous fluid). The formation of bubbles due to inner nucleation in the droplet may interfere with the initiating process (Watanabe et al., 2013). The term nucleation is defined as autogenous initiation of bubble formation (Jones et al., 1999).

With ethanol-based emulsion, accumulated superheating could results in nucleation of ethanol that is covered by the base fuel, while the bubbling of ethanol generates pressure build-up (Gan, 2012). With ethanol, vapour bubble growth is fast (Rao, 2017). As a result, micro-explosion occur and would reduce the lifespan of the droplet which then facilitates the transformation phase speed from liquid to gas form (Zeng, 2007). It is important to take note that the droplet lifetime cut is much depending on the initial size of the droplet and how strong the micro-explosion. Hence, nucleation of multi-component fuel is probably the pre-requisite for the occurrence of micro-explosion (Zeng et al., 2001).
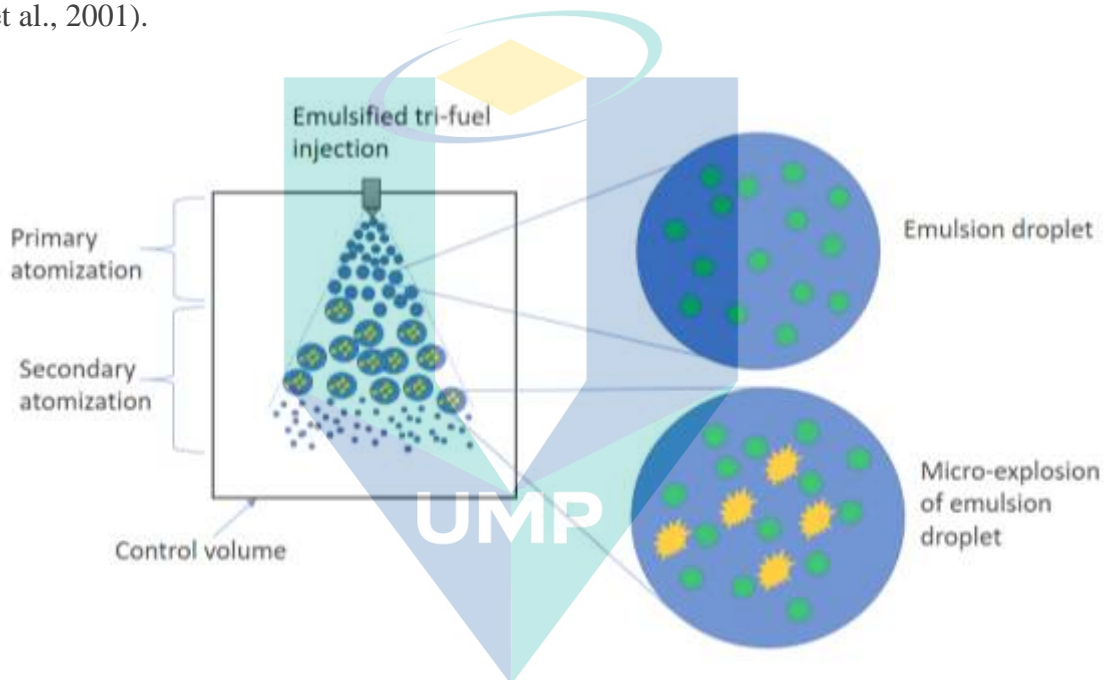
Figure 2.5   Micro-explosion phenomenon of tri-fuel emulsion

Micro-explosion is due to fuel component volatility differences. Apart from increasing volatility difference, increasing ambient temperature defines the starting time of the micro-explosion phenomenon in the spray (Y Liu, 2010). Temperature-dependent and wide volatility differential in multi-component fuel such as tri-fuel promotes competition to change phase. Thus, encourage violent vaporization from inner droplet composition to burst out (Botero, 2012). Variations of volatility among fuel components, which may directly contribute towards micro-explosion phenomenon, have been highlighted in tri-fuel related studies. Fundamentals of the micro-explosion phenomenon have been illustrated in Figure 2.5.

Enhancing micro-explosion can be done by adding less high-volatile liquid (Y Liu, 2010). Micro-explosion phenomenon was hard to be detected with alcohol less than

10% in tri-fuel (Y Liu, 2010). Suggested constant alcohol and increase biodiesel content is the step to see micro-explosion phenomenon to take place at low ambient temperature (Y Liu, 2010).

2.8.1 Droplet size and phase separation

Droplet size in many studies varies greatly depends on the visualization setup and available technology. Typically, droplet size is measured in microns and 1/1000 mm is equal to a micron. For comparison, the diameter of hair is typically around 100 microns. Micro-explosion tends to occur in big droplet size than small droplet size due to unbalance to be kept is easier than the smaller one (H-Z.Sheng, Z-P.Zhang, 1990). Small droplet size also weakens the strength of the micro-explosion phenomenon due to the low residual content of particle dispersed with insufficient energy for bursting (Vellaiyan, 2016). Moreover, the small-diameter droplet with a uniform distribution offers less help in the manifestation of micro-explosion (Khan, 2014). The dispersed liquid specifically as sub droplet covered by the base liquid in the droplet. The size distribution of the disperse capsule in the droplet is important to the micro-explosion occurrence (Mura, 2012). Minimum requirement size is twice the size of a dispersed droplet or more (W. B. Fu, 2002). A specific range of droplet diameter that can contribute to the micro-explosion phenomenon (D. Wu, 2012). Too small, the droplet may evaporate rapidly and skip micro-explosion. The size of the droplet will determine the micro-explosion intensity level (W. B. Fu, 2002). Apart from that, the inner capsule in a droplet with bigger size has got more energy to burst than the small size. Therefore, micro-explosion can present itself. In term of speed, bigger size droplet accelerates much faster than the small one. This argument is based on the fact that the weight of the droplet had a hard time to overcome the air resistant.

The micro-explosion phenomenon is believed to be a stochastic event. Nevertheless, two important points to pay attention to for the manifestation of micro-explosion phenomenon which could be adapted in tri-fuel studies are phase separation process and dispersed droplet size distribution (Mura, 2012). Therefore, the investigation of the micro-explosion phenomenon should highlight the droplet size to be between 0.4 to 1 µm for macro-emulsified fuel. Micro-emulsified fuel has droplet sizes between 0.4

to 0.1 µm while values less than 0.1 µm are for the nano-size category (Ismael et al., 2016). The recent tri-fuel study incorporated relatively large droplets in the range of 1000 µm to 1500 µm (Avulapati, 2016), which are relatively larger in comparison to the droplet size in the real combustion environment. It is important to state that larger size indicates a larger weight. Hence, considering the tri-fuel research, it is noticeable that fewer studies of micro-explosion have been conducted on droplet sizes ranging from 20 to 30 µm (Yu Liu, 2015).

Studies of micro-explosion with an emulsion of large droplets have shown that phase separation occurs prior to micro-explosion. The base fuel that wraps the dispersed phase decrease with time, while inner content remains constant (Toshikazu Kadota, 2007). This is a finding that raises the question as to whether the stability of the tri-fuel emulsion is actually essential, or a simple blending is actually sufficient for practical use in the engine. In contrary, research also suggested that element of emulsion instability encourage the occurrence of micro-explosion phenomenon (Califano et al., 2014). This led to discussions regarding the utilization of mixing fuel as homogeneous emulsions are important or simple blending is sufficient. The dilemma is that stable emulsion is required for stable engine combustion, However, homogeneity was reported to be stopping the micro-explosion phenomenon. The phase separation condition is much preferable during the post-injection period while stability is needed at the pre-injection stage. Nevertheless, it is some good news and a prospect to trust on micro-explosion phenomenon for compensating tri-fuel stability shortfall on stability issue. Furthermore, phase separation is commonly expected regardless of emulsion category due to improper mixing procedure, long storage or ambient condition.

Droplet shape is subject to the surface tension of the components which prompting continuous self-correction on shape towards a sphere. A droplet can be in any shape one can think of as it got shot out from the injector nozzle. However, the surface area of droplet normally tends to go sphere because the act of surface tension. The interconnected force between one molecule to other at the surface of the droplet prone towards the highest surface area. A sphere is apparently the regular shape which micro-explosion phenomenon is prone to encounter.

41

2.9 Benefits of micro-explosion

2.9.1 Improve air-fuel mix

The air-fuel mix process can be addressed by improving the liquid jet atomization and the micro-explosion phenomenon could contribute to this (Y Liu, 2010). It is a positive root which led to enhancement in mixing and flame propagation (Liang, 2013; Nazha et al., 1998). Because droplet size dramatically decreases due to the micro-explosion phenomenon, the particle becomes easy to gain contact with air and improve mixing for complete combustion (Hasannuddin, Wira, Sarah, Wan Syaidatul Aqma, et al., 2016). Furthermore, micro-explosion enhances the breakup and the air entrainment thus, producing vigorous and fast evaporation process (Boggavarapu, 2019). As a result, the air-fuel mixing and combustion reaction is improved. It is inconsistency with the effect of the micro-explosion phenomenon found in other emulsion studies (Bidita et al., 2016). Consequently, the premixed combustion process and heat release rate (HRR) could be enhanced by refining the air-fuel mix process. Ultimately, it should contribute to the overall reduction of burning time and fuel consumption (Venu, 2017).

2.9.2 Ignition delay

Ignition delay in compression ignition engine is defined as a fleeting moment between the initiation of fuel injection and ignition. Practically, no fuel can instantly start the combustion when fuel injection is initiated. Instead, there is a concise period between initiation of spray injection and the mixture preparation before combustion. Within that ignition delay stage, there are two more important sub-stages to be noted. The first sub-stage is the pre-ignition delay or evaporation stage, which is a transformation form of fuel from liquid to gas. The second sub-stage is the actual mixing of fuel vapour with air. The air-fuel mixing stage depends on several circumstances such as mixing fuel properties, injection setting, combustion chamber temperature, pressure and previous residual combustion products.

Considering the fact that it is almost impossible to obtain 100% perfect burning result, it can be assumed that there will be remnants of incomplete combustion which will have a negative impact on the combustion process of the subsequent cycle. Theoretically, the process in the ignition delay period after a physical mixture change, the period of mixing is expected to pause while interaction starts. However, the mixing period

continues since the remnants are still present, even after the ignition. Physical changes continue although the interaction period occurred. Therefore, one of the effective methods to enhance the performance and emission of the CI engine hidden in the ignition delay phase. In other words, enhancement in fuel-burning efficiency could be obtained by alteration of the period before initial combustion. Since the interaction between the in-cylinder gas and the spray injected fuel is pretty complex (Kraft, 2014), the attempt of systematically optimizing the mixing of air and fuel by breaking down the fuel into tiny droplets is now justifiably vital.

Similar to diesel, tri-fuel should aim for accelerated phase transformation from liquid to vapour as soon as the fuel is injected in order to facilitate rapid combustion. The delay period prior to combustion needs to be reduced as much as possible in order to accelerate the combustion. As a function of crank angle, approximately values more than 5° crank angle (CA) after the start of injection has not been utilized since the initiation of premixed combustion and by default delayed. Hence, the ignition delay before the pre-mixed combustion stage can be optimized with the aid of the micro-explosion phenomenon as a potentially reliable secondary atomization process.

As the fuel is injected into the cylinder, the droplets are relatively large and hence the evaporation period is rather long. As the engine speed increases, the crank angle duration that is required for evaporation of injected fuel reduces, demanding rapid evaporation. The micro-explosion directly affects the PM formation by breaking up the fuel so that a small amount of unutilized and unburned fuel can be employed. When a breakup occurs, the phenomenon allows a small amount of fuel, which would otherwise be wasted due to lack of evaporation, to be further utilized. Utilizing the unexploited portion of fuel by means of micro-explosion again offers a solution to the expected increase in combustion pressure as well as the heat or combustion temperature. Apart from mass satellite droplet formation and mass droplet loss, the reduction of average droplet size fluctuate the evaporation phase and tuned down the temperature fast (Han, 2016).

2.9.3   Compensate for low calorific value

In comparison to diesel fuel, the biodiesel and ethanol fractions in tri-fuel have lower calorific value (Shi et al., 2005). The calorific value of different tri-fuel emulsion

43

composition can be expected to decrease as diesel volume percentage increases. Nonetheless, the degradation can be compensated by the micro-explosion behaviour, which could enhance the engine performance with the reflection of higher thermal efficiency reading. This can be explained from the relationship that exists between combustion efficiency and the micro-explosion phenomenon from the previous study (Ithnin et al., 2014).

2.9.4 Heat sink

It is believed that micro-explosion can combat high flame temperature and shorten the burning time (Bidita et al., 2014). This can also be explained from the effect as the bigger coverage heat sink, reduce burning temperature and time due to micro-explosion (Bidita, 2016). The term heat sink refers to a substance or mechanism which can absorb excessive heat. Micro-explosion phenomenon has often been linked to such term in combination with the latent heat of evaporation. The micro-explosion may offset the "heat sink" cooling effect of latent heat of evaporation. (Fahd et al., 2013).

2.9.5 Latent heat

Latent heat exchange is the energy exchange in the phase change between liquid and vapour states without temperature increment. The exchange is an advantage in emission reduction effort. The phase transition from a liquid phase to gas involves additional hidden energy in transit or heat called latent heat. The energy is used to break the bond of molecules in the liquid phase. Therefore, the temperature remains constant at that point. The high value of latent heat vaporization is an advantage. When the arrangement of molecules in liquid contains high thermal energy, the substance in the molecules absorbs energy from its environment and the environment temperature drop down a bit. Unless energy input is increased, the temperature at least remains constant and no temperature increment can be detected. Latent heat is equal to the heat absorb or release over the mass. Sensible heat is giving ways to latent heat to absorb energy, hence temperature could not climb up. The temperature remains unchanged because the energy is being used to change the liquid into the vapour state.

The term latent is use when the heat did not change the temperature but changing the state or physical phase of the composition. Total energy to change liquid into a gas is called latent heat of evaporation. Latent heat is undetected by the thermometer. Hence the

term latent means invincible. This hidden potential heat is waiting to be released and appear with the physical state but not as temperature raise. The action supplied through latent heat also touches about liquid expansion. It is important to highlight that energy is not lost in latent heat transfer but absorbed.

The rapid drop of localizes temperature due to the effect of alcohol latent heat of evaporation discharge thermal penalty consistent with the reduction of global flame temperature (Yatsufusa et al., 2009). However, higher latent heat exchange means more energy is required for the next cycle (Bedford et al., 2000). This may cause a longer ignition delay.

Little research has been done to investigate the effect of micro-explosion in competition with the effect of latent heat of evaporation. The latent heat of evaporation act as a "heat sink" enhance by the micro-explosion that reduces the combustion duration and temperature (Bidita, 2016) resulting in a reduction in the NO_x formation (Sadhik Basha et al., 2014). During the micro-explosion, latent heat may stop or delay the increment of droplet temperature but distorted the increment environment temperature. When the droplet is exposed to the high-temperature combustion cylinder, heat is absorbing into the liquid and the result is that the cylinder temperature drops while the droplet temperature remains constant. Micro-explosion as secondary atomization process can offset the cooling effect with the possibility of fast-burning (Fahd, 2013). In addition, evidence from thermal history shows a slight decrease in droplet temperature in the event of the micro-explosion phenomenon (Mura, 2012).

2.9.6 Improve emission and less carbon deposit

Complete combustion can be achieved with the help of micro-explosion phenomenon and that is the key to the soot and HC emission reduction (T. Kadota et al., 2002). The side effect, NO_x excessive emission due to the high temperature can be tackled by the latent heat of evaporation effect. Micro-explosion also causes CO_2, NO_x and smoke reduction (Bidita, 2016; Seifi et al., 2016). In other words, reduce HC and NO_x altogether. Furthermore, effective micro-explosion phenomenon contributes to less carbon deposit in the engine (Hasannuddin, Wira, Sarah, Ahmad, et al., 2016). Less carbon deposit means engine durability improvement. Durability test such as surface microstructure

45

analysis on engine component concluded that tri-fuel is possible for CI engine (Armas et al., 2011).

2.10   Micro-explosion theory

2.10.1 Mechanism

Unless large droplet exists in the droplet, coalescence among dispersed droplet is a must for micro-explosion to occur (Califano, 2014). Collision, coalescence, merging, join or stretching may occur in the event of micro-explosion. The collision occurs before, during and after micro-explosion occur. The probable outcome would be the bigger droplet may swallow the smaller droplet. The smaller droplet bounces back and reduces the bigger droplet velocity. Other circumstances, the small one changes shape and wrap the big one. The small one penetrates the big one. Bouncing not necessarily break the droplet. The bouncing distorted a slightly. The droplet boundary will be ruptured. Reflexive separation due to collision may create a birth of droplet embryo. In any collision, there is a conservation of linear momentum depending on the type of collision.

Typically, when one or two droplets collide, energy loss is expected. But not the case when the collision is elastic. Where the collision causes no increase or decrease in energy. Elastic collision refers to droplet flying apart due to collision and remain separated after the collision with no energy lost what so ever. This is not the case when a micro-explosion phenomenon occurs. Near to elastic collision with two droplet collapse and remain two with some mass evaporated and energy lost as heat and sound. The collision of two or more droplets and sticking together become one mass after the crash are called non-elastic collision. Sometimes, the collision resulted in a larger body created. Non-elastic collision is when the energy is a loss. Imperfect inelastic collision conserved almost total momentum but not the kinetic energy.

Micro-explosion phenomenon generates momentum (T. Kadota, 2002; Toshikazu Kadota, 2007; Y.-S. Lin et al., 2010; H. Liu, 2011). In a collision, momentum is conserved. But micro-explosion is believed to be like a collision in reverse. When micro-explosion happens, broken droplets are expected to spread to a random direction. Whether to a negative or positive direction, upward or downward with a variety of angle. Momentum is a vector quantity with magnitude and direction as the velocity. Or simply mass by its velocity. When droplet undergoes micro-explosion phenomenon, an impulse

46

is supplied by the explosion which in turn change the droplet momentum. It is true that droplet has momentum before and after the micro-explosion. Dealing with a short time interval and irregular force during the shot made dealing with impulse and momentum rather physics. The absence of complex external force is needed to explore the outcome of micro-explosion phenomenon to the droplets.

Droplet in motion can have more momentum by the increase of mass and velocity. Fuel injection pressure increases the momentum of the droplet (Adam et al., 2007, 2009). Furthermore, mixing fuel has got higher momentum due to bigger mean size distribution (Lee et al., 2005). High momentum means higher acceleration to overcome ambient gas drag (Lee, 2005). In other words, with the large-size droplet, the momentum is bigger and easier to counter air resistance in comparison with a small droplet (Ghurri, 2012; Kumar, 2013). The small droplet has a large momentum loss in the atomization process (Park, 2009). Mass increase momentum (Palash et al., 2013) while increasing the vapour density can create additional momentum (Bedford, 2000). In contrast, low density induced deceleration droplet momentum (Park et al., 2014).

2.10.2 Liquid distortion

The liquid is in distorted due to the motion as it got injected and due to impact because of micro-explosion phenomenon. Within the various stage of breakup due to the micro-explosion phenomenon, liquid in droplet form actually distorted. A study specifically devoted to investigating the various stage of splashing liquid drop acknowledge the existing of the liquid in distortion state (Harlow et al., 1967). The distortion caused by the micro-explosion phenomenon could affect the neighbour droplets. Liquid distortion as a result of the occurrence of micro-explosion on a single droplet in motion is less discussed. The distortion due to the motion could facilitate the manifestation of micro-explosion phenomenon occurrence. The distortion could even actually be stopping the micro-explosion phenomenon remains as a research gap.

2.10.3 Gravity influence

Gravity is a constant pull downward on Y-axis direction and always present as much as 9.8 m/s². Gravitational force does not depend on the mass of the droplet. In other words, bigger droplet does not fall faster than the small droplet. Set aside the discussion on pressure or momentum interference, the gravity accelerates each one of the droplets

47

downward equally. Gravity is also a common source of potential energy for the droplet. However, little is known on the effect of less intense micro-explosion phenomenon for example on a single droplet in motion. Puffing burst towards different axis direction may or may not affect other droplets. Micro-explosion phenomenon is capable of strong ejaculation of fragments torn droplet tip to several millimetres away from the main spray tip and angle of dispersion (Y Liu, 2010). This strong breakup jetting in various direction and the direction is random (Gan, 2012). Puffing that occurs in the same direction as gravity force may increase the spray penetration remains hypothetical. The research gap may warrant serious consideration to investigate. Could be the spray formation got effected by such event remain as speculative.

2.10.4 Fuel atomization

By definition, under the condition of diesel engine fuel injection system, fuel atomization is a process of breaking up liquid fuel into finer droplet from a larger size to smaller ones. It is one of the important steps in the chain of droplet physical process transformation leading to chemical energy release initiation in the vapour phase. The injection originated from the injector orifice into a combustion cylinder offer few split seconds for review before combustion takes place under compression cycle. The word atomization here does not represent actual atom, but merely a droplet disintegration process which unfortunately can only be controlled to a certain extent.

The quality of the fuel atomization can be observed, measured and analysed strictly under a certain limited ideal state. Limited condition because it is difficult to analyse the atomization phenomenon in the actual exercise combustion environment. Therefore, the assumption is being made and study is conducted on the subject with simplification parameters in a customized environment. In other words, one step at a time study in the absence of certain critical parameters such as high pressure, high temperature or enclosed gaseous environment.

The process reduction of size as the droplet is in falling downstream motion shot out from the atomizer has got something to do with the pressure differential at the nozzle which altered droplet dynamism into kinetic energy as droplet jet. Normally, the region at which atomization occurs is not only happening close to the nozzle orifice but also along the way down before combustion begins. However, it is actually an

oversimplification to think that way. As the droplet jetted out, gas and liquid interaction occur.

The term atomization is an important part in spray study covering multi-industrial practice such as humidification, spray painting, crop spraying and combustion with similar meaning, spray breakup dynamic process. In particular, the process is a concern with liquid dispersal into a fine droplet. Generally, atomization can be classified as conversion process based on three-mode; surface, mixed and bulk fluid or from five existing liquid form class; jet, film, sheet, prompt and discrete partial (Lightfoot, 2009).

Emulsion or micro-emulsion method can improve viscosity and atomization (Melo-Espinosa et al., 2015). Two distinctions but complimenting each other perspectives categorized under the fuel atomization studies are macroscopic and microscopic perspective. Macroscopic perspective paid attention to the development stage (Rhim et al., 2001) and the feature of the spray. The value is on breakup length and the quality of the spray by analysing the shape geometry, area, volume coverage and the penetration distance along with the velocity. Spay formation has been widely discussed in the literature with a variety of atomization mechanism and parameters.

A by-product of atomization is droplet size. Because spray contains droplet, discussion on spray formation cannot be ignored but the detail mostly beyond the scope of this study. Nevertheless, it is worth to acknowledge some of the basic spray patterns. Common spray pattern characteristics related such as full cone, flat fan, solid stream and misting or fog alike. Important characteristics of spray include spray flow rate, spray size, angle, pattern and impact reach.

An atomizer is referring to a fuel injector with a nozzle designed with one small opening or more for the liquid to jet flow stream discharge in the combustion cylinder. There are many atomizers developed practically use in the industry and some still under ongoing research and development. A widely known form of atomizer mechanism been developed to date for industrial application are twin fluid type, rotary or electrostatic categories. However, in typical diesel engine today, high-pressure intermittent atomizer with one or more micro-sized orifice is normally practical.

The purpose of improving the atomization process is to speed up the transformation from a liquid phase to vapour form or gas because only then the diesel can

be combusted effectively and efficiently. The drive is to shorten the time for achieving the complete evaporation charge. At least to cut downtime as much as possible and shorten the ignition delay period. The attempt is critical to achieving a higher rate of evaporation rate can be individual droplet or the distribution of droplet as a result of atomization. Droplet size distribution whether it is going to be narrow or wide is subject to the application requirement. However, in CI engine, failure in transforming the liquid to gas, combustion will be delayed or not happen at all. Wasted fuel is the expected and undesirable outcome is inevitable. Individually, the smaller droplet will have a higher surface area to volume ratio, hence increase the vaporization rate. Proper atomization and wide droplet distribution exhibit vaporization rate in a group which contribute to better combustion. To go deeper on the vaporization rate, it is important though to look at the fundamental of vaporization element which is mass and heat exchange rate between liquid mass and gas medium increase as the interfacial area increase.

Although it is almost impossible to study in detail at the location of the individual droplet within a spray, nonetheless there are many works had been dedicated in this field. Beginning, mid and end stages of primary breakup region (Movahednejad et al., 2010). Micro-explosion phenomenon can be found close to the outer layer and the head of the spray (Sheng, 1994). In a breakup droplet study, Rayleigh was among the pioneer who develops the idealization theory behind liquid jet before Weber extends the study with air resistance interaction and viscosity influence. The extension study demonstrates that as viscosity increase, the optimum wavelength breakup increase. Hence, minimizing the optimum wavelength breakup recommended doing well in the atomization process. Weber number refers to a jet formation with non-critical low viscosity while droplet formation by jetting referred to as Rayleigh breakup (van Hoeve et al., 2010).

The dynamic of droplet atomization is subject to the relative velocity between the surrounding air and jet flow. Rayleigh theory on breakup mechanism is under low-velocity motion. Another category is twisted or the term "sinuous" often use to describe the appearance of the liquid breakup motion. Thirdly, the birth of satellite droplet as a result of disintegration due to small shockwave interference caused by an interaction between air resistance and fluid on the jet surface area.

The physical process of fuel atomization is depending on the type of fuel, discharge velocity, ambient condition and certainly the design of the injector. Without

50

further nod towards exploration on complex physical alteration such as perforation extension or design modification approach on any engine part, the literature review concentrates more on the mechanism relative to the type of fuel and its attribute towards atomization process subject to various pressure discharge velocity.

What influence atomization apart from the design of the injector nozzle and pressure setting is the physicochemical properties of the fuel itself. Some of the most influential properties mentioned in the literature were surface tension, viscosity and density. The mentioned properties are relevant to the study of the fuel atomization mechanism including the micro-explosion phenomenon.

Fall out zone is the area where the bit and pieces of droplet fall after the micro-explosion. Little research has been done to investigate the effect of micro-explosion or puffing of tri-fuel emulsion. Because the micro-explosion is known to be unstable in nature, the explosion will cause the breakup tiny droplet to go into the various possibility of direction erratically. Confinement droplet within a group of droplet that experience micro-explosion phenomenon blasted the surrounded droplet which in return collide with each other and set apart. This is believed in certain case limit the strength of the micro-explosion. But on the other hand, puff the surrounding droplet into fine size. The confinement of the encapsulated volatile compound leads to accelerate explosion. Researchers are excited to improve the explosion, predict and control.

Proposed strength of micro-explosion is violent due to energy storage within the nucleation bubble build up. The bigger the initial diameter, the stronger the explosion (W. B. Fu, 2002; Ithnin, 2014). Not only the onset but also the strength of the micro-explosion phenomenon is the root cause of inconsistency (Ithnin, 2014). This can be witnessed via the lift-off a length of flame increase a couple of millimetre out of the spray boundary (Ghojel et al., 2010). It was believed that viscosity and level of content of dispersed droplet are the cause for the strength of the micro-explosion phenomenon (G.-B. Chen, 2017) apart from the temperature effect. If the temperature is not enough, only a few droplet capsules in the droplet will be boiled. If the temperature is sufficient, all capsules in the droplet will explode and this causes the strength of the micro-explosion to be either strong or not (H-Z.Sheng, Z-P.Zhang, 1990).

51

2.10.5 Spray Characteristics

Spray characteristics is one form of macroscopic study of droplet in a group. High density significantly increase spray penetration because of the increase in the mass flow rate. Consequently, it increases the jet momentum. In contrary, low surface tension and low viscosity decrease the spray penetration and increase the spray cone angle (Corral-Gómez, 2019). Recent research on secondary atomization with tri-fuels have perused various approaches other than via spray including gravity influence free falling droplet (Botero, 2012) and suspended or hanging droplet techniques (Avulapati, 2016, 2019; Han, 2016; Y Liu, 2010; Yu Liu, 2015).

Suspended droplet technique is an intrusive approach which is mainly affected by the contact between the sample and instrument. On the other hand, the Leiden frost droplet method as a less intrusive approach avoids interaction between the measurement and sample. A homogenous process with no physical contact that could lead to perturbation associated with the heating mechanism, while the suspended droplet method has direct physical contact with the droplet, which in turn may or may not compromise the measurements. The influence of the instrument ambiguously lead to inhomogeneous nucleation.
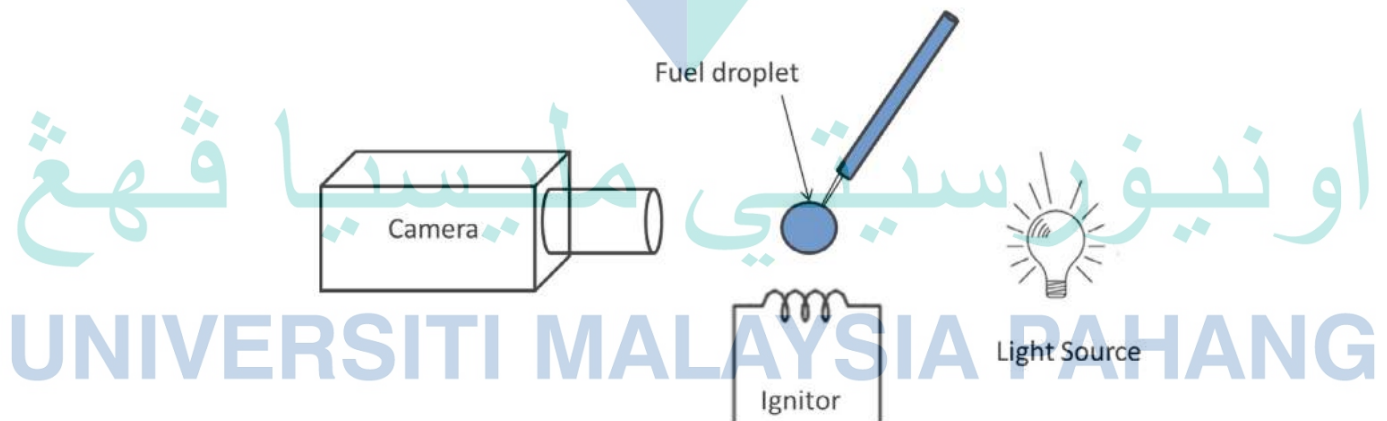
Figure 2.6   Schematic representation of experimental setup for micro-explosion phenomenon study with 2 mm distance between ignitor and hanging droplet
Source: Avulapati, (2016)

The foundation point on the distinction other than spray approaches has its ground to justify but not to overlook the interference of thermocouple wire. Commonly, the thermocouple gauge or wire between 70 µm to 150 µm should not be omitted (Avulapati,

2016; Mura et al., 2014). The experiment that was carried out using the suspended technique by which the droplet was attached to a thermocouple can be argued. As can be seen in Figure 2.6, the heat source could be a direct ignition mechanism, especially when located too close to the samples. Such setup may somehow resemble SI engine principle more than compression ignition principle.

In a study of a free-falling droplet with gravity influence, recognized micro-explosion phenomenon could occur while the droplet is in motion state (Botero, 2012). Spray study should be the focus because the study reveals the macroscopic view of the status of the spray injected. It is about visualizing and analysing the characteristic of injected multi droplets fuel in-group. Common characteristics of the spray to be paid attention to are the spray cone angle, spray spread and the spray penetration. The practical aspect of the spray is the external part of it on a sequence of spray injected. The spray cone is typically used to acknowledge the fuel atomization improvement. Higher spray cone angle signifies a positive fuel atomization process. In other words, the desire small droplet size distribution is achieved. Spray dispersion is the compliment to the spray cone study. Spray spread or radial distance is another perspective of looking at the spray characteristics improvement. No change or improvement on the spray cone does not necessarily imply poor fuel atomization outcome.

Research suggests that ethanol reduce mean droplet size, reduce spray momentum, affected spray tip penetration and cone angle (Park, 2009). Although finding showed viscosity level under standard limit diesel value, the poor quality spray is expected (Cheenkachorn, 2010). Nevertheless, complimentary ethanol and biodiesel on density give just nice spray momentum (S. A. Shahir, 2014). Circumstantial evidence suggests that the micro-explosion phenomenon shortened spray penetration (Y Liu, 2010; Yu Liu, 2015). However, this is not necessarily always the case. The characteristic affected by the environmental temperature and pressure display unique results. Adam et al. 2007 study droplet evaporation and spray with shadowgraph photography technique (Adam, 2007, 2009). In the spray boundary region, what happens at high-density droplet region in the transitional is difficult to observe (Adam, 2009). 10µm droplet diameter is the common size at all time that can be observed (Adam, 2007). A black gaseous occurrence that obstructed downstream of the spray is suspected to be a micro-explosion phenomenon (Y Liu, 2010).

The fuel droplet atomization process from the characteristics of the spray is significantly influenced by the fuel component surface tension (D. Li, 2005). Since alcohol has low surface tension, biodiesel should be expected to compensate and complement interfacial tension between diesel and alcohol. Macroscopically, micro-explosion can be detected when the downstream of spray jet become divergent and fragmentary (Y Liu, 2010). The spray jet penetration length appears shorter than conventional diesel fuel when micro-explosion occur while in contrast puffing exhibit longer spray penetration (Yu Liu, 2015). However, it can be argued, that higher ambient pressure could also be slowing down the spray penetration at the secondary breakup stage/ region (Zhan, 2018). Furthermore, too high ambient temperature could also mean insufficient time for the phenomenon to initiate hence no micro-explosion is expected. As evidence, the sudden drop spray penetration can be detected at a temperature of 800 K and 900 K but not at 1,000 K and 1200 K (Y Liu, 2010). In addition, micro-explosion causes the gaseous region in the spray, located at the outer region, both side of the spray and the spray tip. It also causes strong ejaculation of fragment droplet from the tip several mm which then expand the spray spread and dispersion angle which causes abnormal spray behaviour with irregularity shape accompanied by gaseous region (Y Liu, 2010).

2.11   Concluding remark

Diesel as conventional single fuel for CI engine has some limitation. The limitation is on the emission. The higher the combustion temperature is the higher level of NO_x is formed. The formation mechanism for PM is the incomplete combustion process. Current improvement strategy includes post-combustion and pre-combustion treatment with bio-fuels based. Ethanol remains the best candidate as part of the emulsion component with diesel. Biodiesel of palm oil origin is the most feasible biodiesel in Malaysia and easy to extract. Mixing diesel with ethanol and biodiesel is one of the approaches of interest. The opposite setback of the diesel-alcohol blend gives the impression that it is almost opposite to diesel-biodiesel blend. Complementary limitation of both approaches motivates tri-fuel (diesel-alcohol-biodiesel) approach to close the gap. Unconventional agitation could solve conventional agitation limitation in obtaining stability. Biodiesel could be the natural surfactant for tri-fuel or at least delay phase separation. Recommended formulation ratio is the 15% limit for alcohol and 15% limit

for biodiesel or otherwise allow the risk of engine failure and compromise fuel quality from physicochemical properties standpoint.

Combustion, performance and emission could be expected to improve with tri-fuel emulsion. Tri-fuel with micro-explosion phenomenon benefits include air-fuel mixing improvement, ignition delay period alteration, compensation of low calorific value, heat sink, latent heat effect and emission improved. The theory behind the micro-explosion phenomenon is summaries as follow: -

i.   Collision, coalescence, merging, join or stretching may occur in the event of micro-explosion.

ii. Liquid could possibly distort due to the motion as it got injected and due to micro-explosion phenomenon.

iii. Low-intensity micro-explosion such as puffing that occur in the same direction as gravity force may increase the spray penetration is still hypothetical.

iv. Micro-explosion phenomenon should assist the fuel atomization process and speed up the transformation from a liquid phase to vapour form or gas because only then the fuel can be combusted effectively and efficiently.

v.   Micro-explosion is a sudden release of energy.

vi. When the micro-explosion take place, the droplet deformed or distribute to become smaller pieces in motion and that motion is the kinetic energy.

Experimental procedure to investigate the occurrence of micro-explosion phenomenon includes free-falling droplet, low-pressure spray injection, low-temperature source and intrusive approach. All these approaches are debatable. Suspended droplet technique is an intrusive approach which is mainly affected by the contact between the sample and instrument. Furthermore, the examination environment does not represent the real combustion process in the engine with a non-evaporative condition. On some cases, the heating source is resembling SI engine rather than a CI engine. Table 2.4 shows research gap summary to be addressed.

Table 2.4   Research gap summary

No	Research gap	Category
1	No biodiesel from palm oil feedstock	Material
2	No pure diesel	Material
3	Ethanol as preferable alcohol	Material
4	No ratio of ethanol echo by biodiesel	Ratio
5	No unconventional agitation	Mixing technique
6	Unknown effect of ultrasonic emulsification	Mixing technique
7	Micro-explosion on spray jet not yet investigated	Approach
8	Spray characteristics not available	Approach
9	Droplet size too big	Approach
10	Frame rate too big	Setting
11	No single hole spray injection	Setting
12	No high pressure injection	Setting
13	No high temperature environment	Setting
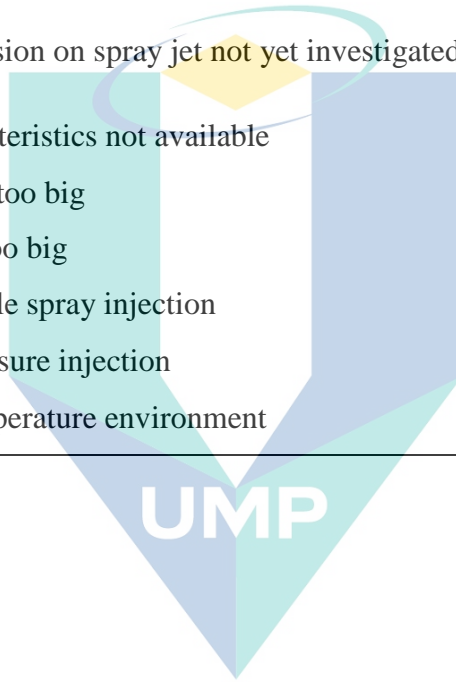
METHODOLOGY

3.1   Introduction

The methodology is essentially divided into four main parts as seen in Figure 3.1. The first part deals with the tri-fuel emulsion characterization. The study was about investigating the effect of some important control factors on the physicochemical properties of the tri-fuel emulsion. The control factors include formulation ratio and emulsifying setting. The second and third parts were about investigating the possibility of micro-explosion phenomenon occurrence as the fuel is injected into the combustion chamber. Research method for the second part was a visualization approach. The method combines both qualitative and quantitative components.

The section presents the detail of droplet visualization technique selected. By employing the mixing of qualitative and quantitative modes of enquiry, the attempt was to explore in detail the micro-explosion phenomenon under the condition as close as possible resemble the real CI engine combustion environment. The second part about the microscopic representation of micro-explosion phenomenon that was observed was used to make sense of the third part which was about the macroscopic depiction of the spray. In other words, the logic of the experiment was to investigate the possibility that affects the macroscopic presentation of the spray. The fourth part was the investigation of physical delay part of the ignition delay in the combustion of the tri-fuel emulsion. The engine test was conducted with a single-cylinder engine setup.
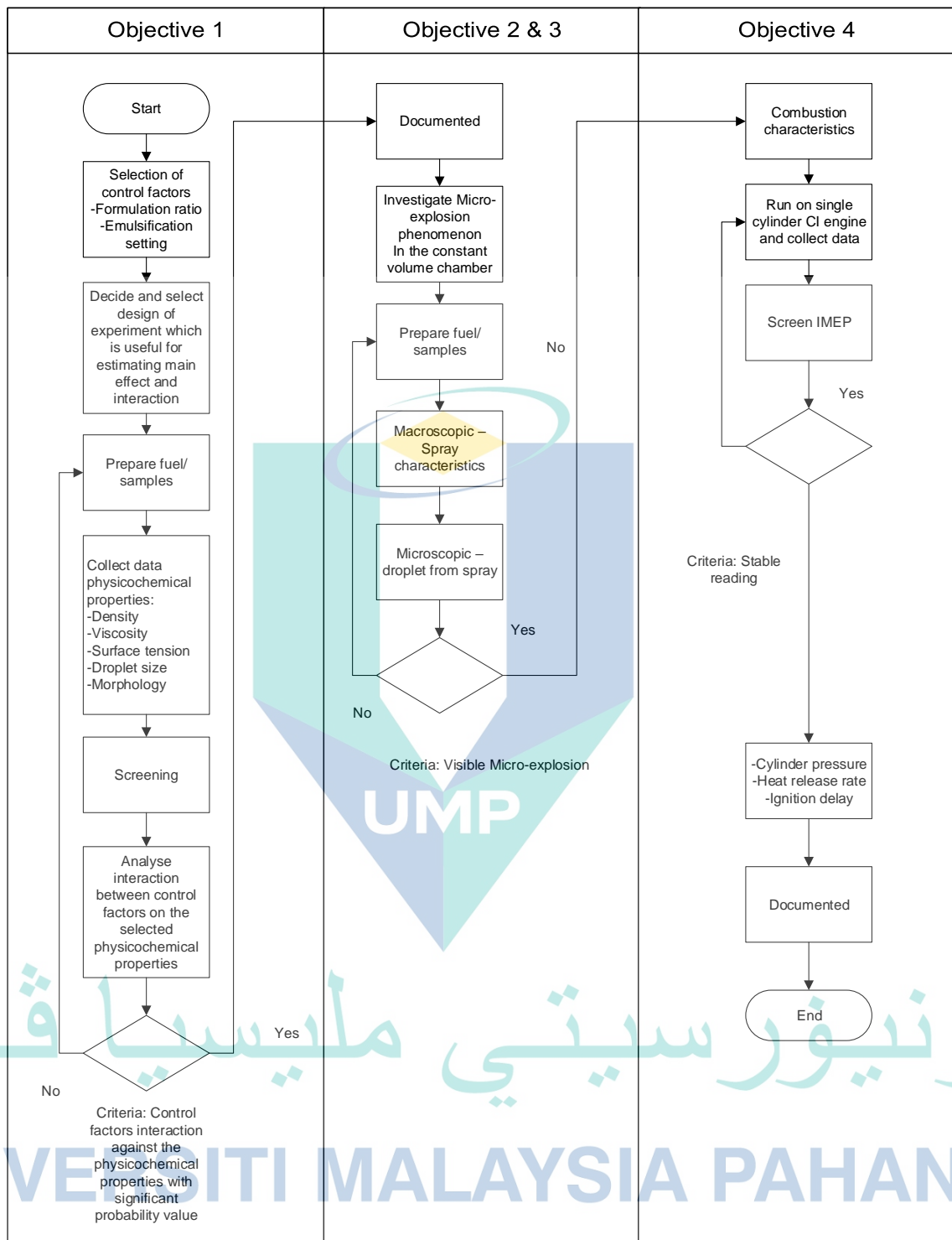
Figure 3.1   Research flowchart

3.2   Materials

The raw materials used in the current study are fossil-based diesel, biodiesel and ethanol. Biodiesel from palm oil feedstock was chosen considering the wide feasibility. Ethanol was chosen as one of the Tri-fuel components considering the highest level latent

58

heat of evaporation among the rest of the alcohol family. Distillate diesel fuel without additive was obtained from an available supplier in Kuantan, Pahang, Malaysia meeting the specifications of Malaysia standards (SIRIM) and Euro 2M standards. Table 3.1 shows the detail technical specification of pure diesel.

Table 3.1   Pure diesel technical specification

Properties	Experimented Value	Unit	Test Method
Density	0.815	g/m^3	ASTM D4052
Viscosity	3.48	cP	ASTM D7042
Surface Tension	22.796	mN/m	ASTM D971
Calorific Value	48.832	MJ/kg	ASTM D240

The biodiesel used in the study is chosen to be the most feasible Biodiesel in Malaysia derived from palm oil origin (Palm Oil Methyl Esters). Biodiesel (B100) that satisfies the international standard was obtained from the manufacturer, FGV Biotechnologies Sdn Bhd. Table 3.2 shows palm oil methyl ester specification while Table 3.3 shows the technical specification of absolute ethanol. Apart from the physicochemical properties, biodiesel is chosen as natural surfactant.

Table 3.2   Biodiesel (Palm oil methyl ester) technical specification

Properties	Experimented Value	Unit	Test Method
Density	0.866	g/m^3	ASTM D4052
Viscosity	5.55	cP	ASTM D7042
Surface Tension	29.623	mN/m	ASTM D971
Calorific Value	42.885	MJ/kg	ASTM D240

Table 3.3   Ethanol (absolute) technical specification

Properties	Experimented Value	Unit	Test Method
Density	0.781	g/m^3	ASTM D4052
Viscosity	1.43	cP	ASTM D7042
Surface Tension	22.27	mN/m	ASTM D971
Calorific Value	30.501	MJ/kg	ASTM D240

3.3 Methodology for fuel characterization study

The purpose of the experiment was to understand the effect of formulation ratio along with emulsifying setting on a number of tri-fuel emulsion physicochemical properties relevant to the study of fuel injection, spray and atomization. The physicochemical properties considered in the study for the first objective will be density, viscosity, surface tension, average droplet size and micro-structure.

3.3.1 Physicochemical Properties Characterization

3.3.1.1 Density test

The density of all samples was measured at 20°C ± 1 using a portable density/specific gravity meter model DA-130N with supplied sampling nozzle vertical to the ground. The measuring method of the tool is resonant frequency oscillation, which was specified in ASTM D777, the standard test method of density by portable density meter. The measuring range capability of the density meter is from 0.0000 to 2.0000 g/cm^3 with a resolution 0.0001 g/cm^3 and accuracy ± 0.001 g/cm^3. After the emulsification procedure took place, the samples were allowed to cool down to 20°C in a mini-refrigerator before measurement procedure took place. To avoid ethanol content in tri-fuel emulsion from evaporation, the prepared samples were contained in a tightly closed plastic screw cap glass laboratory bottle. The procedure was repeated three times with average value obtained as the final reading to minimize the effect of systematic errors.

3.3.1.2 Viscosity test

Viscosity is a measure of the resistance of a fluid to the deformation produced by shear stress. Brookfield, DV-III Ultra Programmable Rheometer was used for the viscosity test. Software used was Brookfield Rheocalc V3.3 Build 49-1. Properties tested was in accordance with the petroleum standard ASTM D445 (Suhaimi et al., 2018). Dynamic viscosity was measured according to Equation 3.1;

$$\mu = \tau \times \frac{dy}{dc} \qquad\qquad 3.1$$

where,

μ = dynamic viscosity of fluid (N s/m^2),

τ = shear stress in the fluid,

c = unit velocity (m/s),

y = unit distance between layers (m),

dc/dy = shear rate (s^{-1}).

Viscosity reading was taken under laminar condition (only directed by the shearing force) and average reading was taken within the detected equivalent range of 10% to 100% torque reading for any combination of spindle speed rotation. The temperature of each sample was recorded at initial stage spindle rotation starts at 40°C ± 1. The experiment was executed immediately after each preparation of the sample with at least three repetitions. Maximum acceptable value of diesel standard viscosity according to ASTM D7467 is 4.1 cSt (Ali, 2016). Table 3.4 shows the primary program setting used for the viscosity test. Results from the original unit were converted to the unit of centipoise (cP) for analysis.

Table 3.4   Primary insert program setting for Rheometer

Primary setting	Parameter set	Description
Set Speed	10	Run the Rheometer at the specified speed
Loop start count	25	Mark the start of the loop
Wait for time	15	Remain at the steps until the specified time interval has elapsed
Speed increment (+/-)	10	Increment or decrement the current speed by the specified value

3.3.1.3   Surface tension test

For surface tension test, Tension meter, Data Physics/ DCAT 9T software was used. Method of surface tension measurement that was chosen was Wilhelmy thin plate and ring method test was used for countercheck result validity. Wilhelmy equation was applied as expressed by Equation 3.2. As shown in Figure 3.2 (a), the stage moved down the plate down towards the surface of the liquid until the meniscus connects with it. The Tensiometer measured the force acting on the plate due to its wetting. The force (F) needed to detach it from the surface of the liquid is expressed as Equation 3.3 where cos θ was equal to 1 considering as the plate was wet completely to achieve 0.1% accuracy. Surface tension acts on both sides of the plate, hence multiplying by two was needed. The same goes to the ring method as shown in Figure 3.2 (b), where the surface tension was multiplied by two because it acts on the inside and outside circumference of the ring. The ring inner and outer radii were assumed equal considering the ring was precisely thin manufactured for the equipment. The total force needed to detach the ring (Total weight) is expressed in Equation 3.4. Humidity and room temperature were controlled at 50% and 25°C ± 1, respectively. The experiment was executed immediately after each preparation of the sample with three repetitions. Properties tested was in accordance with the petroleum standard ASTM D971.

(a) Plate method   (b) Ring method
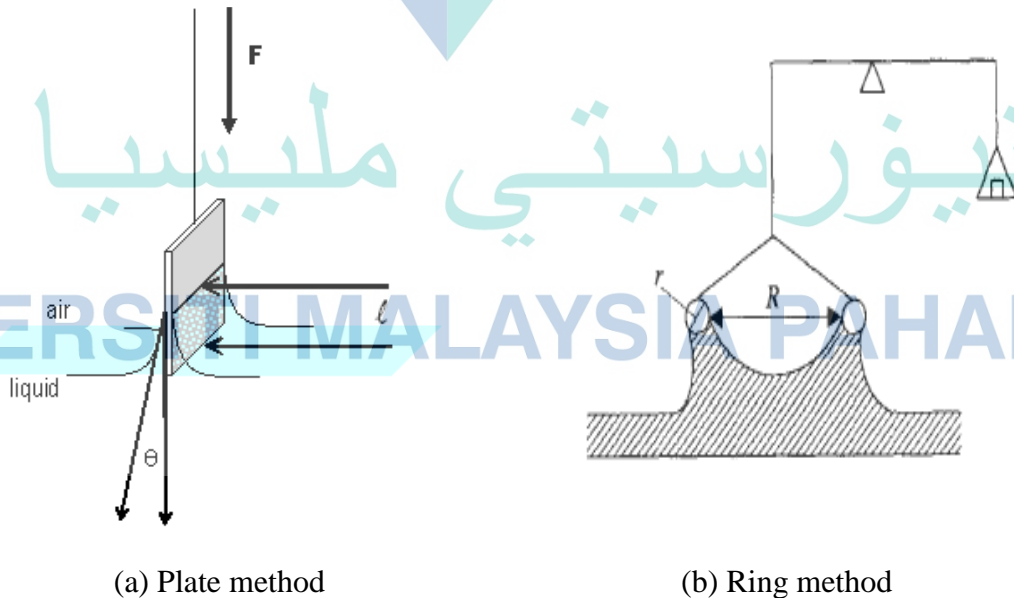
Figure 3.2   Surface tension measurement with (a) plate methods and (b) ring method

$$\gamma = \frac{F}{l\cos(\theta)} \qquad\qquad 3.2$$

where,

γ = Surface tension,

l = Wetted parameter,

F = Force is the total weight of the plate minus the plate weight,

θ = The contact angle between the liquid phase and the plate.

$$F = W_{Total} = W_{plate} + 2l\cos\theta \qquad\qquad 3.3$$

where,

F = Force,

W_{Total} = Total Weight,

W_{plate} = Plate weight,

l = Wetted parameter,

θ = The contact angle between the liquid phase and the plate.

$$F = W_{Total} = W_{Radius} + 4\pi R\gamma = 2l\gamma \qquad\qquad 3.4$$

Surface tension is the tensile force acting on a liquid surface of the fuel. At the surface, the bond is extra tight due to the stretching between molecules. Compared to the surface and the inner area, the bond strength is unbalanced and yield stronger tension. The area at the surface is reducing due to the tendency of the attraction force known as surface tension.

3.3.1.4   Average droplet size test

Average droplet size can be obtained with a Zetasizer machine (Guo, 2013; Guo et al., 2011). Hence, the measurement to obtain the average droplet size of the twenty samples was done using the Zetasizer Nano S90. It is determined by measuring the Brownian motion of the droplet in the sample. By definition, Brownian motion is the random movement of a particle in the liquid as a result of surrounding bombardment motion of other particles around (Sales et al., 2014). Hence, by measuring the movement speed of the particle undergoing Brownian motion, the droplet size can be determined via dynamic light scattering (DLS) system (Fischer et al., 2016). Stokes-Einstein equation defined that relationship between the speed of the Brownian motion and the particle size at a uniform temperature. Since DLS technique takes advantage of Brownian motion, the experiment cannot be conducted with unstable temperature or warm fresh made tri-fuel emulsion due to the rapid motion of Brownian caused by the warm temperature (Bhattacharjee, 2016). Nevertheless, within 24 hours prior to preparation, all the samples were measured with samples temperature at $25°C \pm 1$. At such a stable temperature, the basic principle of DLS can be applied. In principle, slow Brownian motion means large particle while rapid Brownian motion means smaller the droplets.

High-density glass covet was used instead of disposable low-density plastic covet as the standard container. This was to avoid possible low-density plastic covet material to encounter surface degradation due to a chemical reaction with tri-fuel emulsion which consequently may affect the scattering light. The disposable micropipette was used to carefully pour the sample into the high-density glass covet. Size measurement dedicated by the machine is 0.3 nm to 10 microns. The detector in Zetasizer ZS90 is installed at an angle of 90° to the path of incident light as shown in Figure 3.3. Thus, it receives more scattered light compared to backscattering set-up where the angle is usually between 173° and 175°.
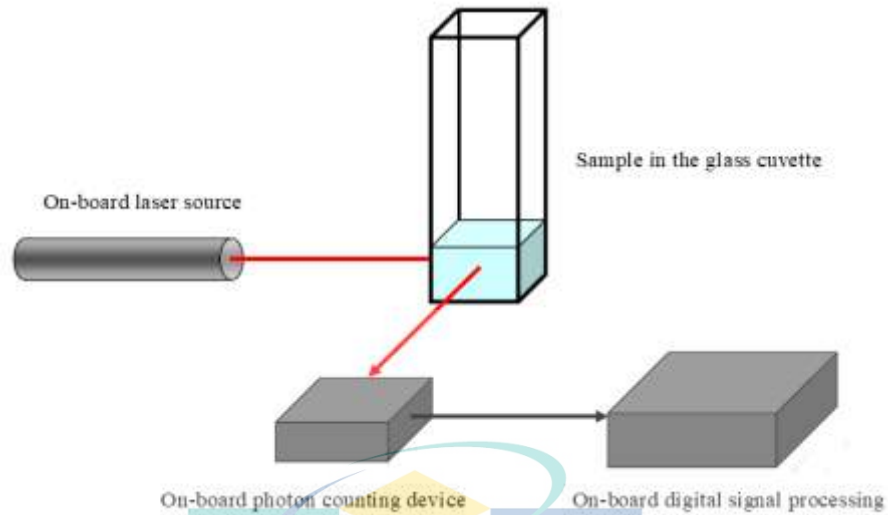
Figure 3.3   Component for Dynamic Light Scattering technique
Source: Malvern instruments, (1999)

3.3.1.5   Morphology

Qualitative analysis on micro-structural configuration and feature of the tri-fuel emulsion was executed with a digital microscope. The method was adopted and modified from the previous study (Mehta, 2012; Tan, 2017). The experiment was relying on the interaction of samples with a visible light coming from below the sample stage as the probe. A two-dimensional image was captured and the process by open-source image processing software available called ImageJ and Motic. The morphology study compliment the Average Droplet size distribution mentioned in the previous section.

The human eye is limited in many respects and hence, the use of a digital microscope could assist in the analysis. The scale that corresponds to the visibility of the sample for analysis can be macrostructure, mesostructured, microstructure and nanostructure. The study is restricted to cover the scale of microstructure. Characteristics feature detection concern was homogeneity or inhomogeneity prone, geometrical formation, droplet size, dispersed droplet within the capsulation, capsulation boundary region, interaction behaviour between droplets capsulated such as collision sequence, any dislocation substructure and droplet size distribution. Digital microscope brand Dolomite Calestron was employed with 5X,10X and 40X objective lens and the total magnification of the images was up to 400X. Samples were observed immediately after prepared within less than 1 hour. The microstructural observation was further investigated after the tri-

65

fuel emulsion has passed through the fuel injector. After injection, Microscope (BX51, Olympus, Model U_LHOOL-3, Tokyo, Japan) was used with 50X magnification and 10 µm depth of field. Software for droplet counting was done by using Motic software.

3.3.2 Design of Experiment (DoE)

In order for the data collection be conducted systematically, a Design of Experiment (DoE) was chosen because of the flexible and quality approach (Barad, 2018). Researchers have utilized numbers of powerful statistical tool for quality control purposes (Khoobbakht, 2016; Yusri et al., 2017). Design expert software version 7 was used as the platform for the application of design of experiment approach utilizing 2-level factorial design. A 2-level factorial design is useful for estimating main effects and interaction which may not be revealed by the traditional one factor at time (OFAT) approach to achieving at least 80% quality level. Method of analysis was adapted from a previous study (Anderson et al., 2018; Trizano-Hermosilla et al., 2016).

The interaction between the independent variable or factors on specific dependent variable or response was analysed with statistical technique. A total of twenty samples were prepared for the physicochemical properties interested and generated randomly by the software. The randomized order was for the purpose of protecting against any lurking factors such as time, temperature, humidity or the like. Out of the twenty samples, four samples were the middle range setting for all factors and replicated four times to provide sufficient information on possible curvature in the system. This is an indicator should RSM to come into play for any optimization approach in the future.

More to consider than simply the main effect of each control factors. That is, the effect of the control factor on the response may not be the same at all level of the other control factors. The effect of one control factor may depend on the level of the other control factor. Four sets of important factors were chosen in sample preparation for this study. Factors from the formulation ratio were the percentage of biodiesel and ethanol in which diesel as the base was considered to be the remaining percentage ratio formulation. To be specific, diesel was used as the base-fuel which complement the variation setting of biodiesel and ethanol with a total combination of 100%.

Meanwhile, emulsification time, cycle and amplitude were the emulsification control factors nominated for the experiment. All samples were prepared using Hielscher

Ultrasonic Processor UP400S Emulsifier. A cycle setting is a pulse control mode to switch on or off the ultrasonic processor. The difference to 1.0 second is the pause time. The experiment was carried out in two sections by varying power applying time. For the low cycle, the power was triggered for 0.1 seconds out of 1.0 second and paused for 0.9 seconds. For the high cycle, the power triggering time is maintained for 0.9 seconds while paused for 0.1 seconds. The ultrasonic output is the rotary amplitude regulator. **Error! R eference source not found.** shows the finalized emulsifier setting and formulation ratio while **Error! Reference source not found.** shows samples with decided control factors w ith the coded factors.

Table 3.5   Finalized emulsification setting and formulation ratio

Acronym	Formulation	Setting	Range
-	Diesel	-	70-90%
A	Ethanol	-	5% - 15%
B	Biodiesel	-	5% - 15%
C	-	Amplitude	30% - 60%
D	-	Cycle	0.4 – 0.6/s
-	-	Time	5 min

The emulsification time was decided based on the temperature level corresponding to the ethanol evaporation tendency and flashpoint. The emulsification setting such as amplitude and cycle setting limit were decided based on the limit of temperature acceptable that corresponds to ethanol evaporation limit. Since one of the main hurdle when dealing with tri-fuel emulsion is the sensitivity of ethanol to the rise of temperature, the limit was set considering evaporation tendency with open cap, time and specific rise of temperature. Because ultrasonic emulsifier may generate heat and could affect the fuel quality (Hielscher, 2005) apart from below the flashpoint level, the temperature range was decided within the acceptable evaporation rate. The outcome of the conducted preliminary experiment was used as the setting range benchmark for the cycle and amplitude setting of the primary emulsion. The pattern has indicated that the sensitivity of ethanol evaporation loss subject to the temperature change was aggressive approximately over 40ºC. Hence, preparation of the sample for the primary experiment was decided to be conducted not exceeding 40ºC with real-time temperature monitoring.

An emulsification duration of five minutes was fixed for all samples with various amplitude and cycle setting which has satisfied the temperature limitation.

Table 3.6   Samples with decided control factors

Sample	Ethanol (A)	Coded Factor	Biodiesel (B)	Coded Factor	Amplitude (C)	Coded Factor	Cycle (D)	Coded Factor
1	5	-1	5	-1	30	-1	0.4	-1
2	15	1	5	-1	30	-1	0.4	-1
3	5	-1	15	1	30	-1	0.4	-1
4	15	1	15	1	30	-1	0.4	-1
5	5	-1	5	-1	60	1	0.4	-1
6	15	1	5	-1	60	1	0.4	-1
7	5	-1	15	1	60	1	0.4	-1
8	15	1	15	1	60	1	0.4	-1
9	10	0	10	0	45	0	0.5	0
10	10	0	10	0	45	0	0.5	0
11	10	0	10	0	45	0	0.5	0
12	10	0	10	0	45	0	0.5	0
13	5	-1	5	-1	30	-1	0.6	1
14	15	1	5	-1	30	-1	0.6	1
15	5	-1	15	1	30	-1	0.6	1
16	15	1	15	1	30	-1	0.6	1
17	5	-1	5	-1	60	1	0.6	1
18	15	1	5	-1	60	1	0.6	1
19	5	-1	15	1	60	1	0.6	1
20	15	1	15	1	60	1	0.6	1

For all experiments the test was conducted under control ambient temperature between 24 to 26°C and humidity recorded was between 50 to 60%. Temperature increment of samples due to emulsification was recorded every minute and must not exceed 40°C. Level of ethanol concentration in all samples prepared was measured and verified with alcohol hydrometer and portable density/ specific gravity meter DA-130N utilizing configuration mode of measuring alcohol concentration calculated from the density at the measurement temperature.

Responses analysed with two-level factorial approach were dynamic viscosity, density, surface tension and average droplet size. As far as the selection process of factorial design, no hard-to-change (HTC) factors were selected. Hence, the study did not consider the split point design. Twenty samples were prepared for each response in the fuel characterization study. Analysis of variance (ANOVA) was employed from the build-in tool in the design expert software. Three selected samples out of the twenty samples were chosen for the investigation of the micro-explosion phenomenon and the combustion characteristics study. The selected samples were S9, S17 and S20.

3.4   Experimental configuration for micro-explosion investigation

The experimental work was conducted in the Center for Automotive Research and Electric Mobility (CAREM) at Universiti Teknologi Petronas (UTP). The method was adopted and modified from the previous studies (Armas, 2011; Avulapati, 2016, 2019; Corral-Gómez, 2019; Y Liu, 2010; Yu Liu, 2015; Tanaka et al., 2006). Limitation of the previous study was that the droplet is subjected to contact on a solid surface. The droplet distortion and disintegration were observed in the previous studies due to contact on the hot surface and secondary atomization were not purely generated. Hence, the setup for the second objective of the study as shown in Figure 3.4 was adopted taking the limitations of the previous studies. The setup is composed of four main components as follow: -

   i.   Optical accessible constant volume chamber and heater

   ii.   Droplet generator/ Fuel injection system,

   iii.   Temperature/ pressure monitoring and control system

   iv.   high-speed camera with LED lighting.
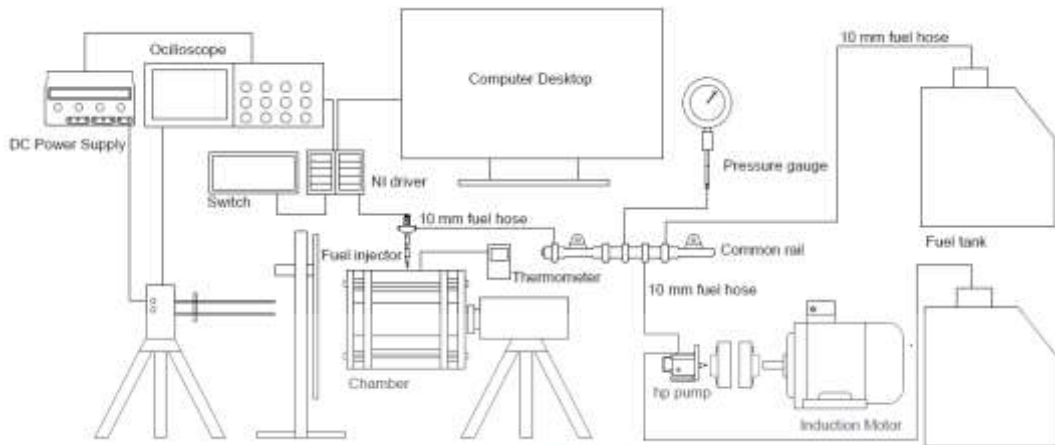
Figure 3.4   Schematics of Micro-explosion study setup

3.4.1   Optical accessible constant volume chamber

Optical accessible constant volume chamber was customized, designed and fabricated in a cylindrical shape with two-channel optical accessible windows using computer numerical control (CNC) lathe and milling machines. Two of which were used for camera view and lighting source access. Two narrow holes were drilled on the side of the cylindrical chamber for the fuel injection and for the real-time temperature measuring thermocouple. Stainless steel was used as the core material considering the high melting point around 1,510°C. The cylindrical shape chamber is assembled with easy to move viewport shutter both side for high-temperature resistance glass installation.

Figure 3.5 shows disassemble optical accessible constant volume chamber consist of flange, heating element and mounting bolts. The optical heat resistance glass was made of fused silica material with high melting temperature, approximately at 1,650°C and low thermal expansion. It was isolated from the metal flange through a heat resistant washer made of Teflon and fibreglass. The combination of Teflon and fibreglass as washer safeguards the optical glass from the excessive force exerted by the fastening of the screws. Fibreglass was used considering the high resistance capability with a melting point of 1,121°C. Flanges with each have five sets of mounting bolt serves as the optical glass attachment. Figure 3.6 shows schematic drawing of the cylinder in the optical constant volume chamber with the measurement. Figure 3.7 shows the complete assembled constant volume chamber with the installed fuel injector.

70

Figure 3.5   Disassemble optical accessible constant volume chamber
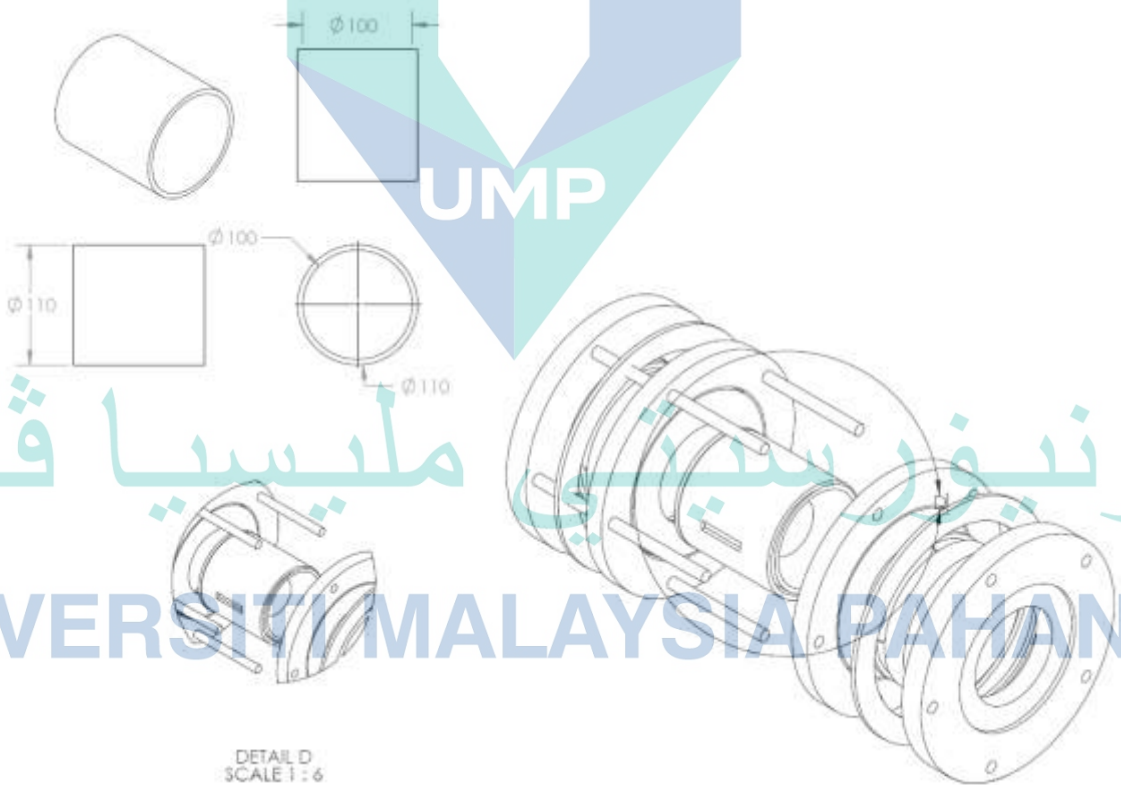
Figure 3.6   Schematic drawing and dimension constant volume chamber

A customized heater was manufactured by VITAR. It was made of ceramic especially band heater designed in lightweight for uniform heat transfer to the chamber. The model is 07/17 IBAA78 with the capability of receiving 240 V and 1,700 W. The temperature was set for 650°C.
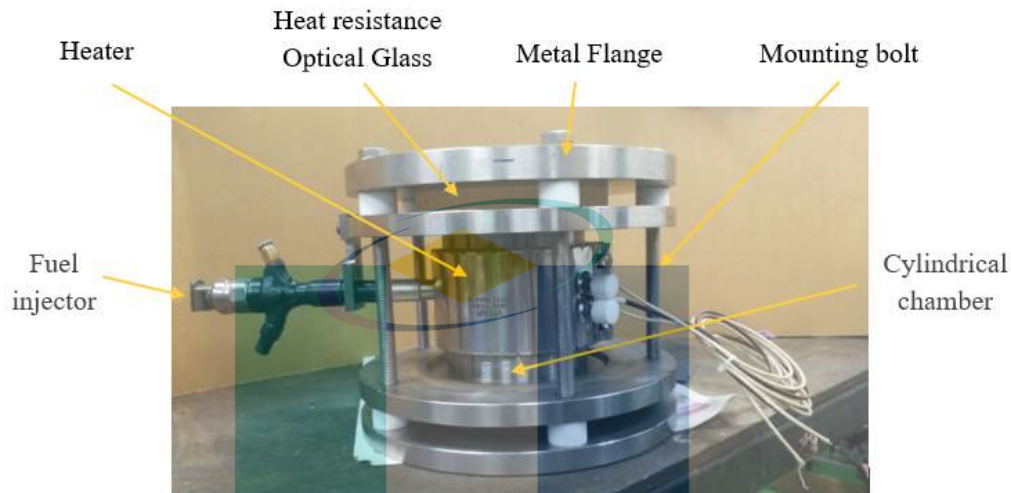
Figure 3.7　　Assembled constant volume chamber with the installed fuel injector.

3.4.2　Droplet generation/ fuel injection system

Droplet is generated from a direct high-pressure common rail fuel injection system. The fuel injection system was consisting of induction motor, fuel pump, common rail accumulator and fuel injector. Fuel pump with allowable maximum pressure 2,000 Bar was connected to the induction motor. The fuel pump was for charging the fuel rail to generate high-pressure fuel. Common rail accumulator was connected to the fuel pump. The high-pressure fuel generated from the fuel pump was fed to the common rail accumulator via the high-pressure delivery host.

Meanwhile, a low-pressure fuel supply host was connected to the fuel tank. Fuel return or excess from the high-pressure fuel pump, rail accumulator and injector were relieved back to the second fuel tank. A high-pressure fuel injector with six-hole nozzle and orifice diameter of 0.2 mm each were used to inject the fuel into the optical accessible constant volume chamber. The fuel injection pressure was set to 500 bar. The injector has undergone minor modification from six holes to a single hole. The injector is position at the top of the chamber with approximately 45° incline position to allow nozzle hole to point out straight down for spray penetration proportion to gravity force. Figure 3.8 shows

the tip of the injector inside the chamber. Injector trigger has been set with three-second delays from the click start button.
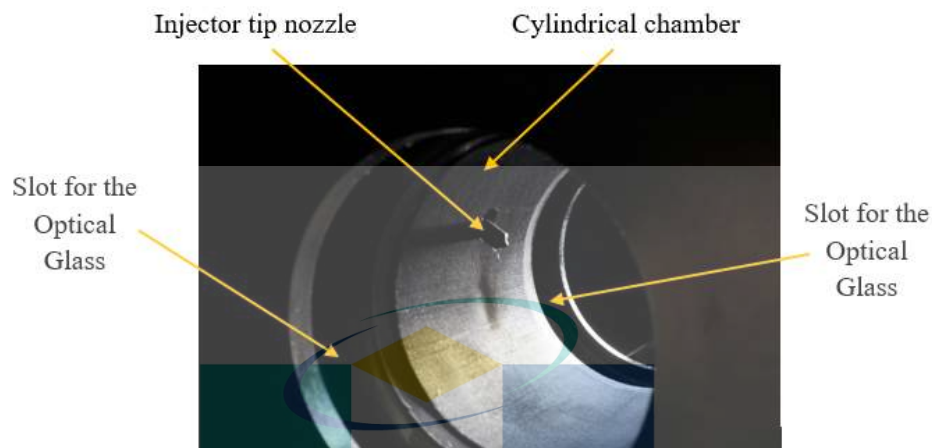
Figure 3.8   Tip of the injector inside the chamber

3.4.3   Temperature/ pressure monitoring and control

The pressure transducer and pressure gauge were connected to the common rail accumulator and controlled manually. The pressure sensor was installed on the accumulator common rail with the purpose to control the fuel injection pressure level. The transducer was installed to convert the physical quantity of the pressure detected into an electrical signal. Pressure relief valve with pressure relief passage was installed at the end of the common rail accumulator to control and limit the overbuild up the pressure in the system for safety purposes.

Considering the reliability, availability and affordable, thermocouple type K (Nickel-Alumel/ Nickel-Chromium) was chosen and installed to monitor the external chamber temperature. Maximum continuous temperature limit thermocouple type K can handle is $1,100^{\circ}$C with accuracy $\pm 2.2^{\circ}$C or $\pm 0.75\%$ and special limit of error around $\pm 1.1^{\circ}$C or $\pm 0.4\%$. The second and similar specification thermocouple was inserted from the fuel injector hole access into the chamber to record the inner chamber temperature before the actual injection. The investigation of micro-explosion phenomenon and spray characteristics will be done at a temperature of 650°C.

3.4.4 High-speed camera setup

Video camera trigger was done manually prompt to injection pressure accumulated in the common rail reach the desired reading level. Figure 3.9 shows the high-speed camera brand Phantom Miro 310/311LC. It has the capability of frame rates up to 650,000 frames per second (fps). However, the speed was compensated by the need to change the trade of time resolution with the sensitivity to the light. For a macroscopic approach, full spray view was visualized using Phantom Miro 310/311LC mounted with AF Micro NIKKOR lens 60 mm f/2.8D. For a strong backlight source, Multi LED LT-V8-15 Tokyo, Japan was used. Software control was Phantom Multicam with 1 µs minimum exposure. White paper sheet was used as backlighting filter. For the microscopic view, the same setup was employed with AF Micro NIKKOR lens was replaced by long-distance microscope Infinity-K2 coupled with a zoom lens or known as Objective-CF1 as seen in Figure 3.9.

The number of define pixel to capture an image is defined as resolution. For spray study, the resolution setting was set to 128 x 400 pixels at 30,000 fps. For the microscopic study, the resolution was set to 256 x 128 with sample rate at 45, 491 frames per second. Extreme Dynamic Range (EDR) mode is a unique feature of the recent high-speed camera model. The purpose of the feature is to allow each pixel in the frame to receive one or two short exposure time for detected overexposed pixel or slightly longer exposure for the pixel that received normal lights level. The EDR exposure time is set to 0 µs.

With a single-lens reflex camera (SLR), the mirror is positioned in front of the shutter, flip-up, away from the shutter, temporary block viewfinder, shutter move away, exposing light, shutter closed followed by the mirror. In order to overcome the shutter delay, video recording was chosen considering it as the best option. Global shutter is needed to get a better shot of scientific analysis because of the very fast-moving object. Unlike a mechanical shutter that captured each line of pixel one line at a time. In a single image, each pixel is captured gradually or not at the same exact time spot. Thus, the global shutter is the best option. Every single pixel is taken at the same spot of time.

The high-speed camera is equipped with a global electronic shutter with minimum exposure of 1 µs. A long exposure gives a bright static image but any motion, the image will be blurred. Short exposure is ideal for motion. Since the motion is very fast, the best practice is to have very bright support light for high shutter speed setting. This is because

the exposure duration to light is very short, hence limited light will be captured. As a result, the darker image appeared. In this study, auto exposure was enabled with 0 µs frame delay. For a macroscopic approach, exposure (shutter) time was set between 30 to 40 µs with 0 µs frame delay. For the microscopic approach, exposure was set to 2.02 µs and an auto-exposure was enabled and locked at the trigger.

Phantom Miro 310/311LC operates in 12 bits' mode, hence, the acquisition was set to 12 bits per colour for both approaches. The camera is positioned approximately 50 cm from the centre of the chamber as seen in Figure 3.9. Via the shadowgraph technique, the focus was at the centre of the tip of the injector installed in the optical constant volume chamber with the backlight and filter opposite to the camera focus as seen in Figure 3.10. A manual adjustment was done from the injector tip by using adjustable focus located at the lens to obtain sharp images. The optical scale was 0.24 mm/pixel. Similarly, the camera position was adjusted manually to get a sharp view of the image. For both approaches, the recording format was raw CINE. The high-speed camera was powered by using an AC power adapter connected to the computer. Fully spread, stable Tripod with independent extensible leg and spreader was employed to hold and secure the position of the camera. Other mobile mounting was not necessary. To avoid unnecessary camera shaking or an accidental movement due to the manual finger pressing button located at the camera, a remote button trigger was installed.

Figure 3.9   High-speed camera brand Phantom Miro 310/311LC.
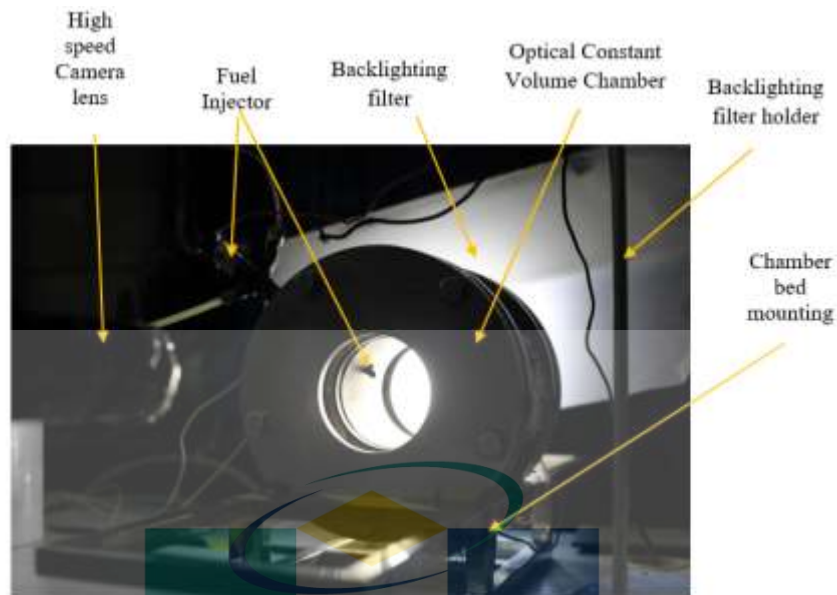
Figure 3.10   Shadowgraph technique setup backlight with filter opposite to the camera focus

Underexposure will cause the image too dark while overexposure will cause the image too bright. To avoid such cases while avoiding damaging the camera, auto exposure brackets mode was enabled. For droplet study calibration, a ruler is inserted at the fuel injector mount hole located at the side of a cylindrical constant volume chamber. The ruler was carefully inserted at the centre of the hole that matches the centre of the fuel injector. For the macroscopic view calibration, the camera was focally aimed at the ruler as seen in Figure 3.11 For the microscopic view calibration, a similar practice was exercised as seen in Figure 3.12. The camera was the first zoom and aim at the injector aiming for texture detail of the nozzle tip. The camera carefully zoomed in and out to focus and reveal the surface roughness nozzle tip. Once the detail is observed, the high-speed camera was carefully tilted up or down and pan left or right to systematically locate the region of the target. It was a close up shot and is suitable for revealing detail.
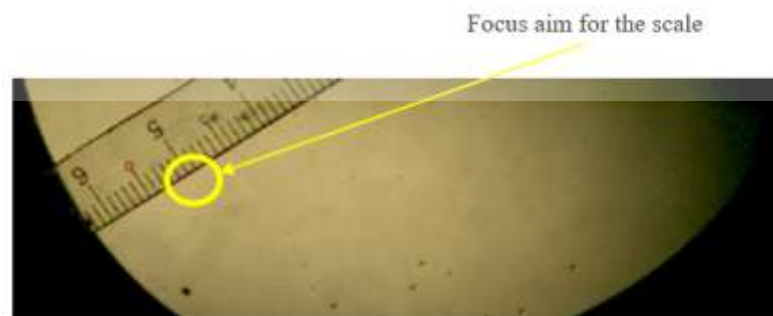
Figure 3.11   Calibration for spray study to measure the pixel.
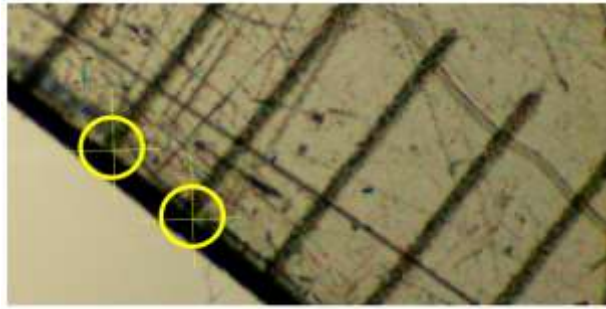
Figure 3.12   Focus and calibration for droplet study before zoom in to measure the pixel.

3.5   Analysing the spray and the micro-explosion phenomenon

The method was adopted from previous studies (Corral-Gómez, 2019; Tang et al., 2017; Zhan, 2018). Figure 3.13 shows the selected definition of spray cone angle and spray penetration adapted from the previous study (Tang, 2017). C. Tang et al (2017) measure spray cone by first of all dividing the spray penetration into half and connect the two end spray point of that half. Figure 3.14 shows the adapted definition of spray spread defined from the measure radial distance.
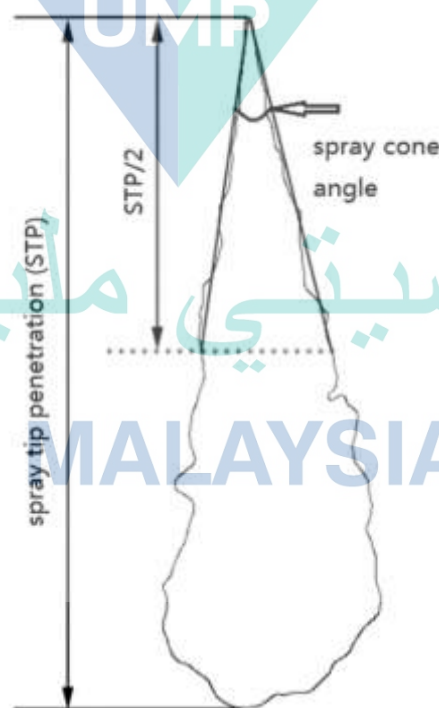
Figure 3.13   Definition of spray cone and the spray penetration
Source: Tang, (2017)

77
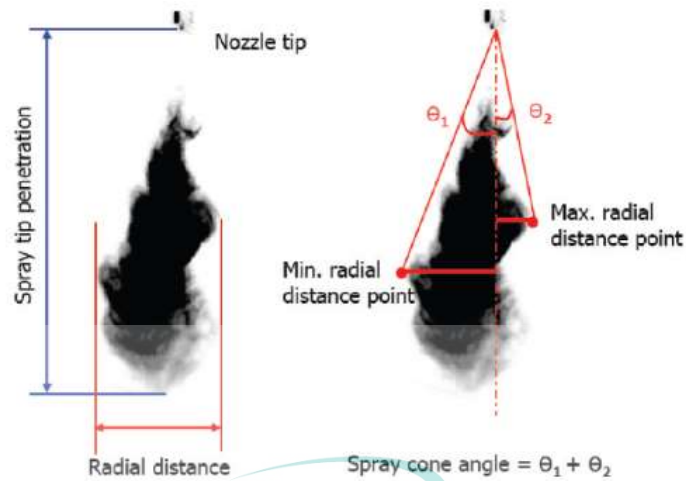
Figure 3.14   Spray tip penetration and radial distance (mm) and (b) spray cone angle (degrees)

Source: S. H. Park, (2009)

In order to capture the specific event of micro-explosion phenomenon on a single droplet, the camera focus was specifically positioned on a few millimetres after the spray nozzle tip. Instead of targeting only at the left or right side of the spray, the targeted area focuses from the tip of the orifice to further down. The method was adopted from the previous study (A. Ismael, 2018). Meanwhile, to capture the spray characteristics, the camera was positioned horizontally straight line from the spray at a distance of approximately 40 cm from the optical accessible chamber.

3.5.1   Image processing and data analysis technique

Visual motion-captured were exploited in various settings. Visual description of an event was presented with common ground found in all the three selected samples of tri-fuel emulsion. The fascination of the captured event was breakdown into an up-close and personal noted observation. The speed of the droplet breaks up caused by the micro-explosion was expected to be very fast. It could have never been possible to notice and watch with the naked eye without high frame rate capacity of the high-speed camera. The set of a still image is presented to detect static and dynamic feature of micro-explosion phenomenon of tri-fuel emulsion droplet under high-pressure injection in the constant volume chamber at high temperature. In addition, the geometry of the droplet was quantified and plotted. Quantitative analysis procedure involved extracted image from video format and process it as an individual frame with image processing software.

After identifying and selecting the desired frame from the recorded video, The processing of the video was performed by first, converted the video from CINE format to individual sequence static image in Tagged Image File Format (TIFFs). TIFFs save the date in a lossless format. In other words, the data can be saved as 8 or 16 bits over itself repeatedly without losing any single image quality along the road. In comparison to JPEG, TIFFs can store more information with greater quality. Furthermore, TIFFs require no conversion like RAW files. With TIFF format, each of the image frames was processed. Some of the TIFF images require conversion into JPEG format before processing can take place. Then, the image is cropped, sharpened, removed the noise and processed before measurement can be done. Since no image is perfect or absolute noise-free, native noise reduction tool was applied with edge-preserving. Noise reduction filters have three settings; strength, preserve details and reduce colour noise. All the images were processed by using a freely available open-source software called ImageJ.

The image enhancement process is to improve the quality of the image with the help of spatial and frequency domain. Here the type of images that can be converted to digital form. Binary or black and white with an only two-pixel value which is 0 and 1. Grey (0 to 255) and coloured (RGB). one element equal to eight bits. Derived from the spray image using the software, the image was processed for analysis. The processes include edge detection, split colour channel, sharpening, binary, histogram and colour balance. The following step was followed to obtain the data via the build-in ImageJ measuring tool. A similar method was adopted and repeated with a single droplet analysis. The image was derived from the countless selected droplet that undergoes a micro-explosion phenomenon.

Resolution is a dimension of which we can measure how many pixels are on the screen. An image is actually a matric. Grey level is a value of that pixel. Pixel is measured with a special image captured of known measurement such as a ruler. Once calibrated, the pixel can be used to measure the droplet image. Quantification of snapshot concern with calibration for pixel measurement. The pixel aspect ratio was set to 1.0 with known distance as per scale on the ruler; 1 mm. For spray study, the set scale was 4.4638 pixel/mm $\pm$ 0.2 pixels/mm while for droplet study the set scale was 37.0539 pixel/mm $\pm$ 2 pixels/mm. With the calibrated scale of the pixel setup in place, droplet surface area and axial distance subject to axial direction X or Y of burst out droplet could be measured

easily using the processed image. Point to note is that axial distance Y refers to the same direction as the gravity pull. The measured droplet diameter could then be used to calculate the droplet centricity. Spherical status of a droplet can be represented by the droplet centricity which is the ratio of shortest to the longest measured axial distance (droplet diameter) adapted from the previous study (Ghaemi et al., 2008).

3.6   An experimental method for combustion characteristic investigation

3.6.1   Engine setup

The experimental work was conducted in the Faculty of Mechanical Engineering, Universiti Malaysia Pahang using a single-cylinder water-cooled horizontal positioned 4-stroked diesel engine. The detail specification of the engine is provided in Table 3.7.

Table 3.7   Engine specification

Description	Specification
Engine Model	YANMAR TF120
Engine Type	Horizontal diesel 4 stroke cycle
Fuel Injection type	Direct injection
No of Cylinder	1
Bore x Stroke	92 mm x 96 mm
Injection timing	17º Before Top Dead Center
Displacement (L)	638 cc
Compression ratio	17.7:1
Rated power	9.0 kW at 2,400 RPM
Rated Torque	43.35 N.m at 1,800 RPM

The setup used was a four-stroke single-cylinder diesel engine model YANMAR TF120. The schematic diagram of the simplify experimental setup is shown in Figure 3.15.
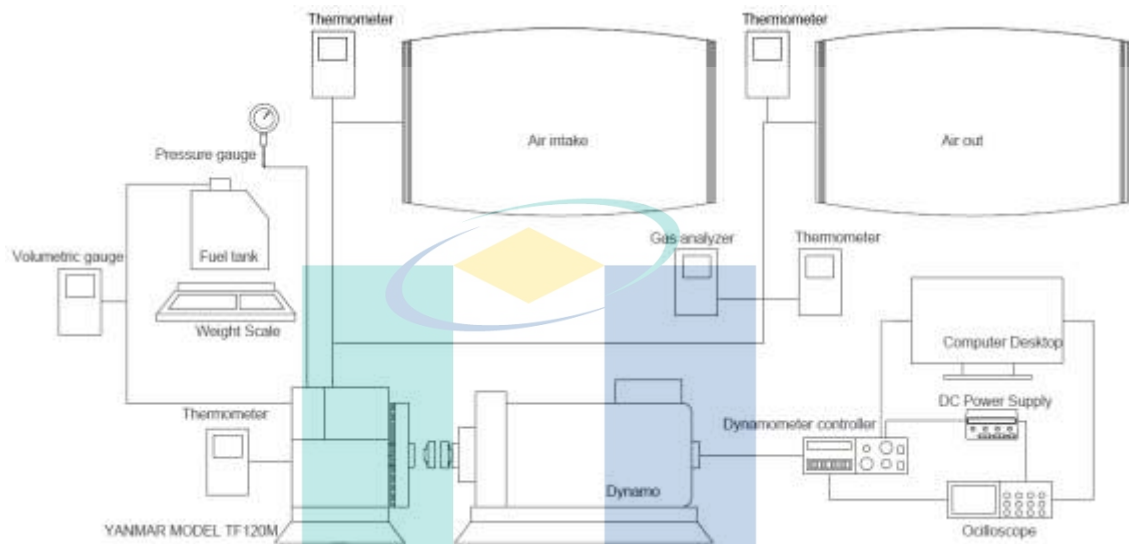
Figure 3.15   Experimental setup for the investigation of the combustion characteristics

3.6.2   Instrumentation and measurement used in the engine

The engine was coupled with eddy current dynamometer model BD-15KW from Focus Applied Technologies with maximum electric power capacity up to 15kW. S-type load cell force sensor (Zemic H3-C3-500 Kg-3B) was installed to measure engine brake torque. Hall Effect proximity sensor (AOTORO SC12-20 k proximity sensor, type PNP-NO, M12 4-24VDC, and 20 mA) was installed to locate the selected pattern crank trigger sensor plate installed on the dynamo that presenting the position of the top dead centre (TDC). TDC is when the piston at the highest position on the compression stroke. Therefore, the sensor is one of the most important sensors for engine management specifically to determine engine speed and position. There is countless different sort of sensor and crank trigger sensor plate in the market. Type of sensor used and the pattern of the trigger sensor plate was configured within the software. Trigger type, trigger signal and home signal are the common setting in the trigger configuration tab in the software that requires standard professional calibration procedure. DEWESoft X2 software was used as a combustion analyser tool to record resolution at every 0.1º CA.

The Optrand fibre optic-based pressure transducer model Auto-PSI C82294-Q was installed to obtain the in-cylinder pressure reading. The cylinder pressure sensor was mounted directly to the combustion chamber ranges up to 3,000 psi, and sensitivity of approximately 2.63 mV/psi. For analogue to digital signal conversion, data acquisition system was needed. Data acquisition system brand DEWESoft DAQ model SIRIUSi-HS was used. The technology picked up, converted and amplified analogue signals from the pressure transducer sensor and proximity sensor. The system is compatible with Windows and allow simple USB and Ethercat cable connection.

3.6.3 Combustion data analysis

The parameter of interest in the combustion analysis includes HRR and in-cylinder pressure. IMEP was used as meant to HRR was derived from the in-cylinder pressure captured data. HRR was calculated using Equation 3.5 derived using the first law of thermodynamics for an open system.

$$\frac{dQ}{d\theta} = \frac{ratio}{ratio-1} p \frac{dV}{d\theta} + \frac{1}{ratio-1} + V \frac{dp}{d\theta} \qquad 3.5$$

Where,

$\frac{dQ}{d\theta}$ = heat release rate of change with regards to the crank angle change,

θ = crank angle,

$\frac{dp}{d\theta}$ = rate of pressure change in with regards to crank angle,

$ratio$ = ratio of the specific heat as cp/cv,

V = Volume at any crank angle position.

Indicated Mean effective pressure (IMEP) which is independent of the engine size and cylinder number was used as a relative selection of performance cycle. IMEP was calculated from the pressure reading collected via the pressure sensor using Equation 3.6. Procedure for selecting the cycle which represents the average cycle is as described.

$$IMEP = \frac{\Delta\theta}{V_d} \sum_{i=n1}^{n2} p(i)\frac{dv(i)}{d\theta}$$ 3.6

where,

$IMEP$ = Indicated mean effective pressure,

$p(i)$ = In-cylinder pressure at a crank angle I,

$v(i)$ = In-cylinder volume at a crank angle i. n1 and n2 representing two successive BDC crank angle position.

The results are defined as the average of three recorded tests run with 200 cycles each. In other words, each sample with an average of 600 cycles per load. Selection of cycle for combustion characteristic processing was done by first extracting all data to excel files. From the first 200 cycles from the first test, the IMEP average was obtained. IMEP average was calculated using Equation 3.7. Then, Coefficient of variation (COV) IMEP was calculated from the average IMEP as per Equation 3.8 and expressed in percentage. The equation is defined as the ratio of the standard deviation of IMEP to the average of IMEP. The standard deviation of IMEP was calculated using Equation 3.9. Next, from the 200 cycles, the one closest to 0 value was selected. The process for all three tests (600 cycles) for each sample was repeated. The test with the smallest COV IMEP was selected and from that selection of test, one of the cycle within that test with the value closest to the average IMEP was selected. The same procedure was repeated for other samples. The same selected cycle in each sample for the next combustion characteristic test was used.

$$IMEP_{Average} = \frac{1}{n} \sum_{i}^{n} p(i)IMEP_i$$ 3.7

where:

n = The recorded number of power cycle.

$$IMEP_{COV} = \frac{IMEP_\sigma}{IMEP_{Average}} \times 100\%$$ 3.8

$$IMEP_{\sigma} = \sqrt{\frac{\sum\limits_{i=n}^{n}(IMEP_{Average} - IMEP_i)^2}{n-1}}$$

<div align="right">3.9</div>

Ignition delay period was derived from the HRR diagram. The delay period was presented from the point of the fuel is injected.

3.6.4 Procedure and setting

All of the experiments were conducted in the evening with varied ambient temperature ± 33°C and 37°C respectively. The relative humidity level ranged from 80% to 90%. The fuel line was flush out every time the fuel is changed. The engine was left running for a warm-up period at idle speed and zero engine load condition before each actual experiment was executed. The start of fuel injection was fixed at 17°C before top dead center (BTDC). Load setting was set to 0, 25%, 50%, 75%, 100% representing 0 Nm, 7 Nm, 14 Nm, 21 Nm, 28 Nm respectively. The engine speed was set to constant 1800 RPM ± 2. The selection of the speed was based on the optimum brake thermal efficiency suggested in the literature.

CHAPTER 4

RESULTS AND DISCUSSION

4.1   Introduction

Considering the research consist of three phases with a marginally broad and wide range of results, only those that are most relevant to the research questions are presented in this chapter chronologically. As discussed in the methodology section, the properties taken into consideration in the study are density, viscosity, surface tension and average droplet size. These parameters have a direct impact on the spray and micro-explosion phenomenon. The section is organized as the effect of control factors such as percentage content of biodiesel and ethanol as well as amplitude and cycle from the ultrasonic emulsification setting. It is a good idea to recall from the previous chapter, table 3.1 for the samples number with decided control factors for clear interpretation of the results presented here onward.

4.2   Physicochemical Properties Characterization of Tri-fuels

4.2.1   The effect of control factor on density

The rationale behind investigating the influence of all the factors on density is because density is one of the main factors that affect the flow characteristic inside the injector nozzle and consequently influence the momentum of the fuel injection spray (Park et al., 2010). If the density of the fuel is decreased too much, the quality of the fuel may not be in favour of the existing engine setting. Peak injection rate will be expected to be deterred by the low-density effect. Consequently, delay the dynamic injection timing at least 1°CA. Another effect to be expected would be on the stoichiometric ratio. Since the decrease in density means lower fuel mass with the same volume, thus, fuel-air mixture setting needs to be re-adjusted to achieve desire burning efficiency. Following a standard method, as discussed in the methodology section 3.3.1, density reading of twenty samples was taken and analysed statistically The final equation in terms of coded factors is shown in Equation 4.1.

$$\rho = 0.81 - 0.006218A \qquad\qquad 4.1$$

The final equation in terms of actual factors is shown in Equation 4.2.

$$\rho = 0.82438 - 0.0012436A \qquad\qquad 4.2$$

It was found that ethanol (A) influence the most to the change in density by 1.54%. Choosing effects to model, Figure 4.1 shows compute effect for model selection via the half-normal plot. Control factor A under the half-normal plot, the furthest factor to the right was obvious. Diagnostic plots as displayed in Figure 4.2 also yield random scatter and no trend. The actual measured value distance with the estimated value is called residual. No outlier is detected to exceed the upper and lower limit. Upper and lower red lines are similar to 95% confidence control limits on a run chart. In this case, none of the points stands out and within the red control limit.
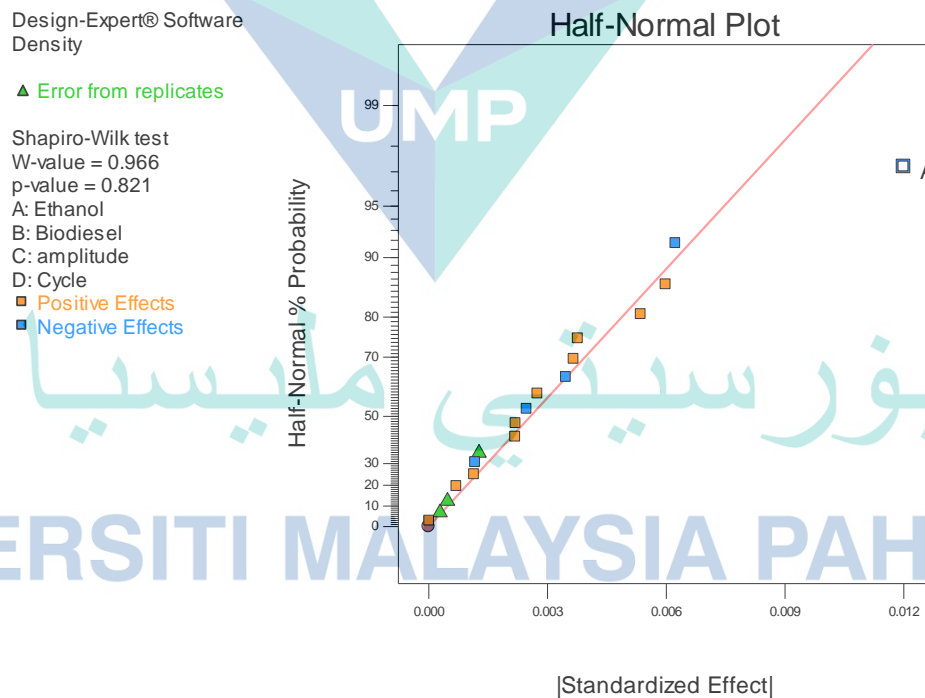
Figure 4.1   Compute effect for model selection via a half-normal plot to analyse the effect of control factor on density
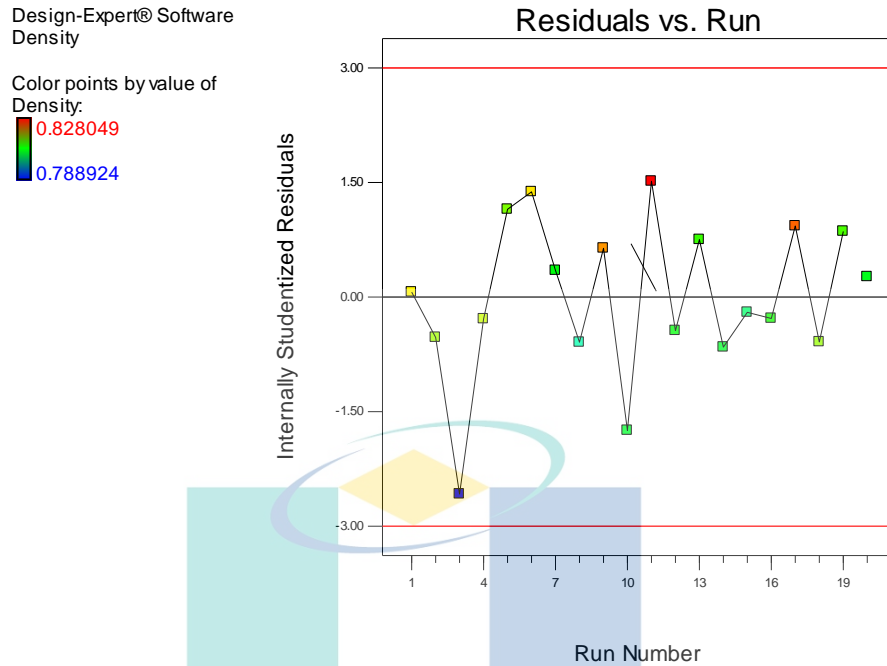
Figure 4.2   Residual plot for density model diagnostic procedure

From the ANOVA result presented in Table 4.1, the selected model was found to be highly significant with the P-Value of 0.0023 (< 0.05). The F-tests for lack of fit was found to be not significant with the value of 0.3774 (> 0.05). The Model F-value of 12.76 has also suggested that the model is significant. Values of "Prob > F" less than 0.05 indicates that the model terms are significant. In this case, A was found to be a significant model term. Values greater than 0.1 indicate that the model terms are not significant. If there are many insignificant model terms (not counting those required to support hierarchy), normally, model reduction may improve the model. But in this case, no modification was made to improve the model. The "Curvature F-value" indicates the no present of curvature. Hence, it is not necessary to proceed for higher quality analysis such as Respond Surface Method (RSM) (Whitcomb, 2004). Non-significant lack of fit is good or desirable.

While R-squared provides an estimate of the relationship strength between the model and the response variable, the low value here does not mean that the model has a bad fit. From Table 4.2, the "Pred R-Squared" of 0.2229 is in reasonable agreement with the "Adj R-Squared" of 0.3951. The difference is less than 0.2. "Adeq Precision" measures the signal to noise ratio. A ratio greater than 4 is desirable. The ratio of 4.611 indicates an adequate signal.

Table 4.1   ANOVA for the selected factorial model (Partial sum of the square – Type III) for response 1 (Density)

Source	Sum of Square	df	Mean Square	F-Value	P-Value Prob>F	Remark
Model	0.0006187	1	0.0006187	12.76	0.0023	significant
A-Ethanol	0.0006187	1	0.0006187	12.76	0.0023	
Curvature	0.000003681	1	0.000003681	0.076	0.7862	not significant
Residual	0.0008243	17	0.00004849			
Lack of Fit	0.0007298	14	0.00005213	1.65	0.3774	not significant
Pure Error	0.00009458	3	0.00003153			
Cor Total	0.001447	19				

Table 4.2   Density model fit statistics between the observed and the predicted values

Responses	Results
R-Squared	0.4287
Adj R-Squared	0.3951
Pred R-Squared	0.2229
Adeq Precision	4.611
Std. Dev.	0.006963
Mean	0.81
C.V. %	0.86
PRESS	0.001121

Figure 4.3 shows a single factor interaction with the response density. 95% confidence bands along the length of the primary slope lines are presented. The factor was found not involved in any interaction with other factors. It was found that the higher the ethanol content, density value response with decreasing pattern. Furthermore, the effect of detection was under the negative effect category. It means, increasing control factor of ethanol resulting in decreasing response density. In other words, more ethanol is added to yield lower density reading. Nevertheless, the decreasing level was considered

minor likely due to biodiesel that compensates the dominancy of ethanol. The counterbalance of these two opposite effects makes tri-fuel emulsion competitor with possible alteration to the current commercial diesel. In the previous work, the range of density in the mixing of diesel and biodiesel without ethanol were all above the density value of diesel (Ali, 2016). But in this study, the presence of ethanol counterbalances the the effect to a very comfortable level far from the maximum acceptable value of diesel standard ASTM D7467 and biodiesel maximum acceptable value ASTM D6751.
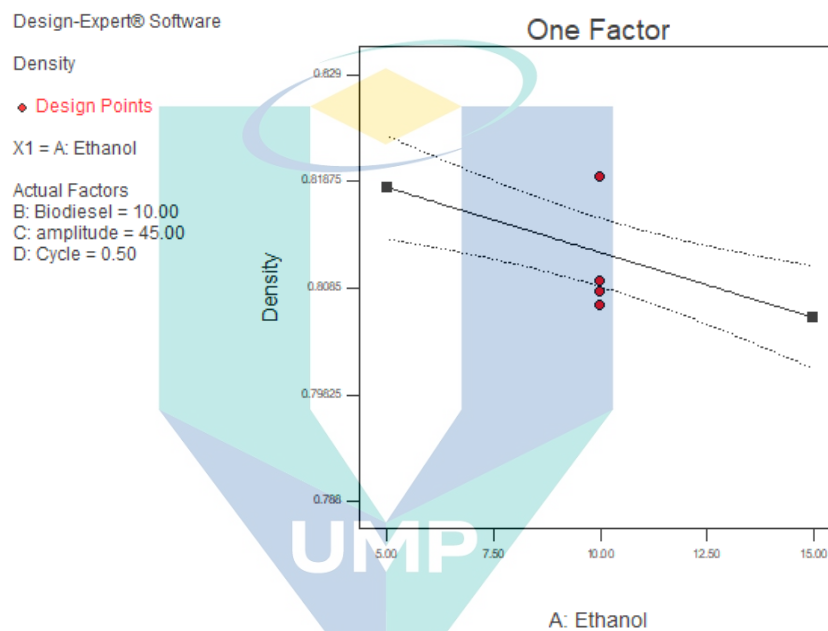
Figure 4.3   A single interaction between ethanol and density.

Density is relevant for affecting the mechanism of fuel atomization. Fuel with high density tends to generate smaller droplet size while low density tends to generate bigger droplet size. The result is comparable to the previous study (Hussan, 2013).

4.2.2   The effect of the control factor on viscosity

Following a standard method, as discussed in the methodology section 3.3.1, viscosity reading of twenty samples was taken and analysed statistically. Choosing effects to model, Figure 4.4 shows compute effects for model selection via half-normal probability plot to select model starts from the biggest effect which was the point furthest to the right. Interaction AD and BD were added after manual regression to preserve hierarchy. It was commonly known that the t-value scale provides a more accurate measure of relative effects. Despite factor interaction AD and BD fall below the t-value

scale, AD and BD were not left off because they were actually involved in other significant interaction.

To convert between coded and actual models, the hierarchy must be supported. Otherwise, the coded model provides a different prediction than the actual model. Lack of linear term by excluding non-significant factors and neglecting the hierarchy could lead one to an incorrect conclusion. Hence, it was not a mistake or botched factor argument consistent with Stat-Ease Consultation. Consequently, it depends on the other factors with which it interacts. Diagnostic plots in Figure 4.5 also yield acceptable random scatter and no trend. No outlier is detected to exceed the upper and lower limit. Upper and lower red lines are similar to 95% confidence control limits on a run chart. In this case, none of the points stands out and within the red control limit.

Table 4.3   ANOVA for the selected factorial model (Partial sum of the square – Type III) for response 2 (Viscosity) with hierarchical terms added after manual regression (AD and BD)

Source	Sum of Square	df	Mean Square	F-Value	P-Value Prob>F	Remark
Model	0.45	7	0.064	182.79	< 0.0001	significant
A-Ethanol	0.39	1	0.39	1107.16	< 0.0001	
B-Biodiesel	0.025	1	0.025	70.87	< 0.0001	
D-Cycle	0.012	1	0.012	33.02	0.0001	
AB	0.009506	1	0.009506	27.16	0.0003	
AD	0.001056	1	0.001056	3.02	0.1102	
BD	0.0007563	1	0.0007563	2.16	0.1696	
ABD	0.013	1	0.013	36.16	< 0.0001	
Curvature	0.021	1	0.021	59.43	< 0.0001	significant
Residual	0.003850	11	0.0003500			
Lack of Fit	0.003250	8	0.0004063	2.03	0.3026	not significant
Pure Error	0.0006	3	0.000200			
Cor Total	0.47	19				
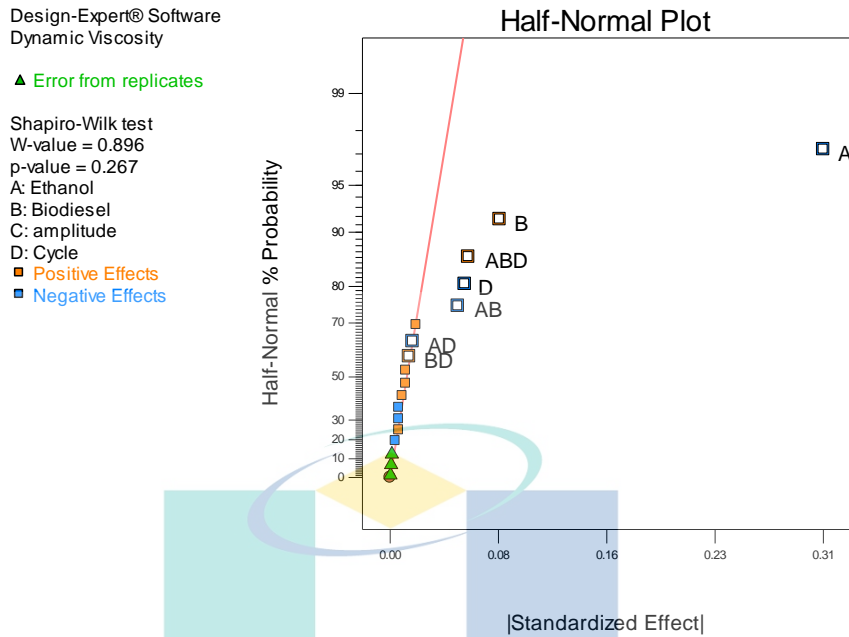
Figure 4.4   Compute effect for model selection via the half-normal plot method to analyse the effect of control factor on viscosity
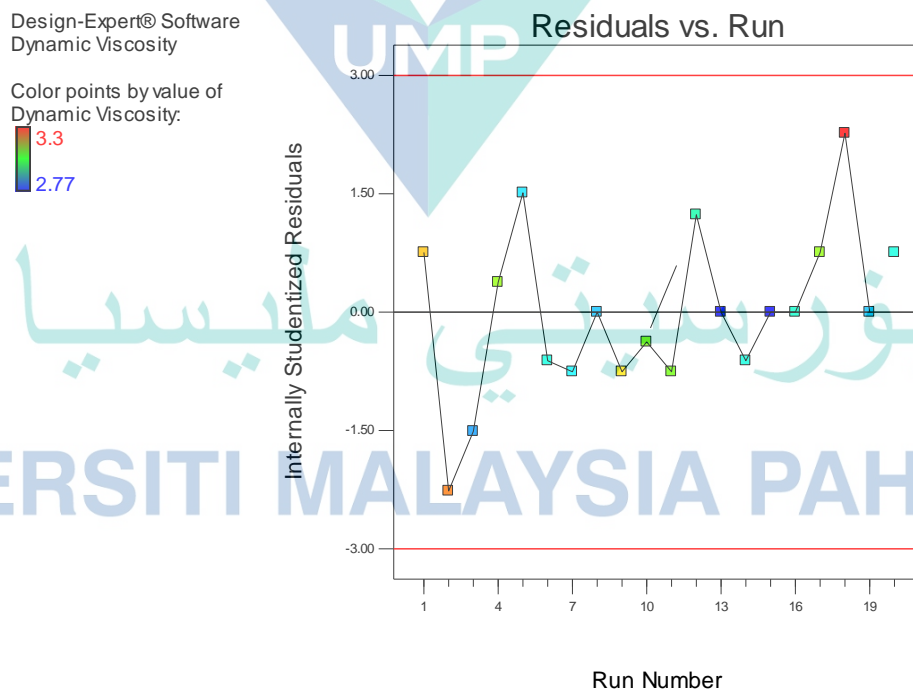
Figure 4.5   Residual plot for viscosity model diagnostic procedure

From Table 4.3, the Model F-value of 182.79 implies the model is significant. Values of "Prob > F" less than 0.05 indicate model terms are significant. In this case, A, B, D, AB, ABD are significant model terms. Values greater than 0.1 indicate the model terms are not significant. If there are many insignificant model terms (not counting those required to support hierarchy), model reduction may improve the model. The "Curvature F-value" of 59.43 implies there is significant curvature (as measured by the difference between the average of the centre points and the average of the factorial points) in the design space. "Curvature F-value" this large offer option should one choose to investigate further for greater detail interaction between control factor and response using the RSM method. Non-significant lack of fit is good as the fit model is desirable.

From Table 4.4, the "Pred R-Squared" of 0.9689 is in reasonable agreement with the "Adj R-Squared" of 0.9861. The difference is less than 0.2. "Adeq Precision" measures the signal to noise ratio. A ratio greater than 4 is desirable. The ratio of 39.841 indicates an adequate signal. The final equation in terms of coded factors is presented in Equation 4.3.

Table 4.4   Viscosity model fit statistics between the observed and the predicted values

Responses	Results
R-Squared	0.9915
Adj R-Squared	0.9861
Pred R-Squared	0.9689
Adeq Precision	39.841
Std. Dev.	0.019
Mean	2.99
C.V. %	0.62
PRESS	0.014

$$\mu = 3.01 - 0.16A + 0.039B - 0.027D - 0.024AB - 0.00813AD + 0.00688BD + 0.028ABD$$

4.3

The final equation in terms of actual factors is depicted in Equation 4.4 as follow:

$$\mu = 2.705 + 0.043A + 0.067B + 0.88125D - 0.00660AB - 0.12875AD$$
$$-0.09875BD + 0.01125ABD \qquad 4.4$$

Figure 4.6 shows biodiesel and ethanol interaction with constant small cycle setting regardless of amplitude variation. Formulation of low ethanol with high biodiesel content yield highest viscosity reading; 3.27 cP. Viscosity drop as a result of both low ethanol and biodiesel content by 5.48%. Meanwhile, with both high ethanol and biodiesel content, viscosity drop by 12.23%. Furthermore, with high ethanol content and low biodiesel exhibit drops of viscosity by 6.12%. This shows that ethanol was dominant in the influence of viscosity change and compensated by biodiesel effect. When the cycle is set lower, the proportionality of the interaction behaviour changes. Especially, when the ethanol ratio just approximately above 12.50%, at one point, the viscosity level is the same for both 5% and 15% biodiesel ratio. After the crossing point, the decreasing level of the viscosity for low biodiesel content is lower compared to high biodiesel content. The twist was not as dramatic as it seems. However, the switch response worth to mention to indicate the effect of the cycle setting.
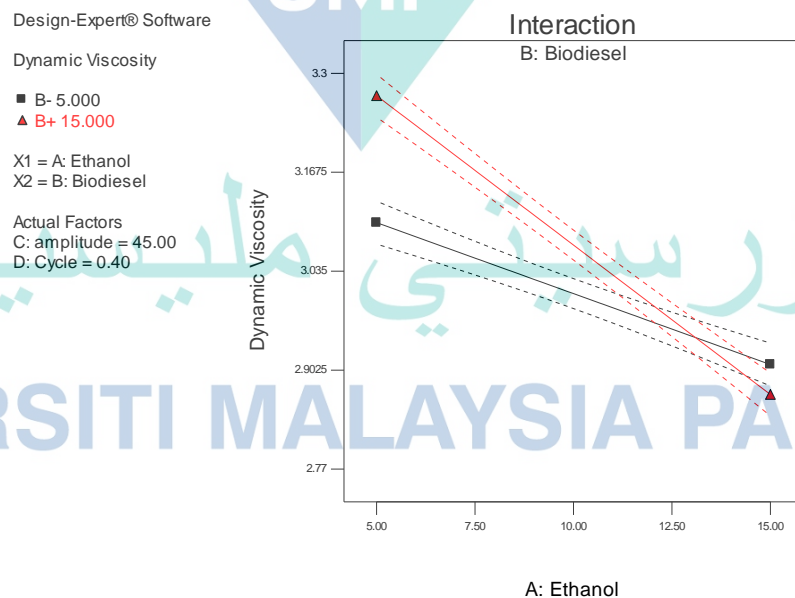
Figure 4.6   Control factors interaction for viscosity where Biodiesel-ethanol interaction on viscosity with constant small cycle (0.4) setting regardless of amplitude variation

Figure 4.7 shows biodiesel-ethanol interaction with high cycle setting regardless of high or low amplitude setting. Low ethanol setting accompanied by the high percentage of biodiesel yield highest viscosity reading; 3.19 cP. Meanwhile, when both ethanol and biodiesel at low proportion, as expected viscosity was found lower by 2.73%. With both high ethanol and biodiesel content, viscosity drop by 10.03%. Furthermore, as expected with high ethanol and low biodiesel content, the viscosity drops by 10.78%.
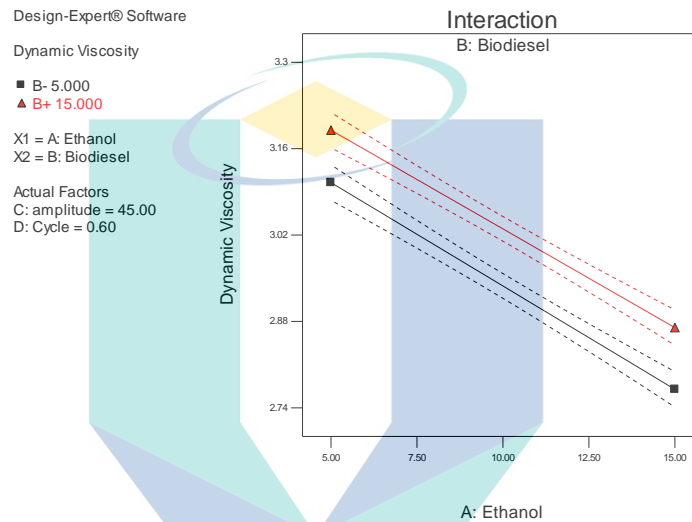
Figure 4.7　Control factors interaction for viscosity where Biodiesel-ethanol interaction on viscosity with higher cycle (0.6) setting regardless of high or low amplitude setting.
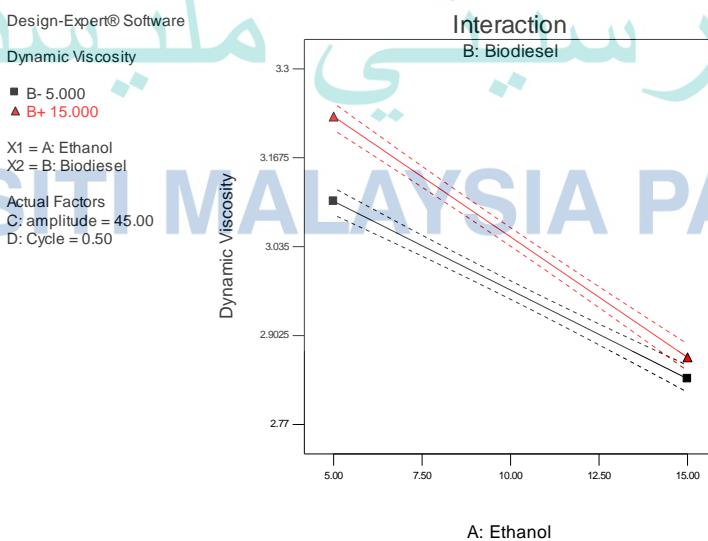
Figure 4.8　Control factors interaction for viscosity where Biodiesel–ethanol interaction on viscosity with cycle middle range (0.5) setting regardless of high or low amplitude setting

94

Figure 4.8 shows biodiesel and ethanol interaction with cycle middle range setting regardless of high or low amplitude setting. The pattern is almost similar to Figure 4.6 but with no cross point. With both high ethanol and biodiesel content, viscosity drop by 11.14%. With high ethanol and low biodiesel content, the drop was 8.46%.
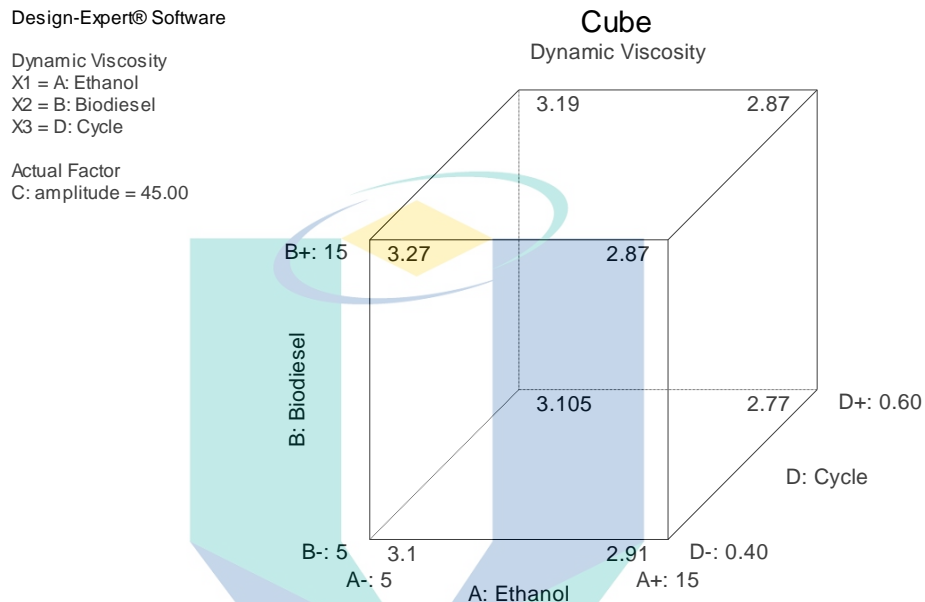
Figure 4.9   Cube display of control factors (Biodiesel–ethanol) interaction on viscosity

Cube plot is displayed as Figure 4.9 while the 3D representation of interaction is displayed in Figure 4.10. Both figures demonstrated ethanol, biodiesel, and cycle interactions when cycle and amplitude were in the middle of their range. Ethanol, biodiesel, and cycle settings were combined in order to affect the viscosity of the tri-fuel emulsion. The cube plot indicates that the lowest viscosity reading was when ethanol content and cycle setting were set at a high level and biodiesel ratio was set at a low level. The viscous condition occurs when biodiesel content was high, while the rest were set low.

As stated earlier in the case of density results, viscosity also plays an important role in the fuel atomization process. Viscosity is as relevant as the density for affecting the mechanism of fuel atomization. Fuel with high viscosity tends to generate larger droplet size while fuel with low viscosity reading leads to smaller droplet size. Affecting the droplet size distribution means affecting the macroscopic spray pattern. As a result of high viscosity, the distance breakup will be longer. Consequently, it will be hard to

95

achieve desirable wave formation and breakup distance rate will be expected to be at a low rate. Ultimately, the quality of the atomization will be deteriorated. Nevertheless, regardless of amplitude setting change, the cycle setting which indicates the time of emulsification process influence the gravity of the effect especially when biodiesel content is less than ethanol in tri-fuel. In other words, as ethanol is added, with low biodiesel content but with high cycle setting, the viscosity trend will be expected to be parallel with the effect of high biodiesel content as ethanol is added. Such cause and effect indicate the significant effect of the cycle setting and time taken for fuel preparation.
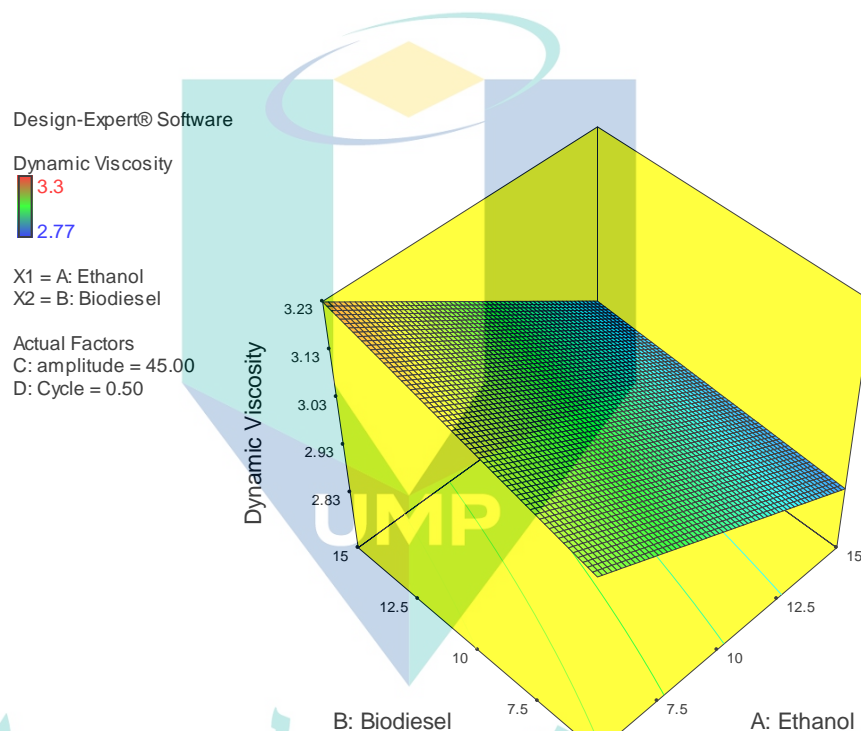
Figure 4.10   3D surface presentation of Control factors (Biodiesel–ethanol) interaction on viscosity

Compare to previous research, the result shows consistency and no discrepancy (Hussan, 2013; Pradelle, 2019a). This finding is important because the knowledge of emulsification time promotes tri-fuel emulsion with low percentage biodiesel as ethanol is added indicates the level of effect variation. The finding is useful because this will be one of the foundations to reason with ethanol and biodiesel counter degrading effect which could be used as a baseline to meet the suitable formulation ratio for CI engine. The decrease level of viscosity reading due to the ethanol effect can be compensated by the level of biodiesel content. Likewise, biodiesel addition that causing the fuel to be viscous could be reduced with the addition of ethanol level.

4.2.3 The effect of control factor on surface tension

The surface tension also affects the atomization process of the fuel in the combustion chamber (Ejim et al., 2010). Following a standard method, as discussed in the methodology section 3.3.1, the reading of surface tension reading of twenty samples was taken and the results were analysed statistically.

Choosing effects to model, Figure 4.11 shows compute effects for model selection via half-normal probability plot to select model starts from the biggest effect which was the point furthest to the right. Despite factor B and C fall below the t-value scale and were not left off because they were actually involved in other significant interaction. To convert between coded and actual models, the hierarchy must be supported. Otherwise, the coded model provides a different prediction than the actual model. Lack of linear term by excluding non-significant factors and neglecting the hierarchy could lead one to an incorrect conclusion. Hence, it was not a mistake or botched factor argument consistent with Stat-Ease Consultation. Consequently, it depends on the other factors with which it interacts.
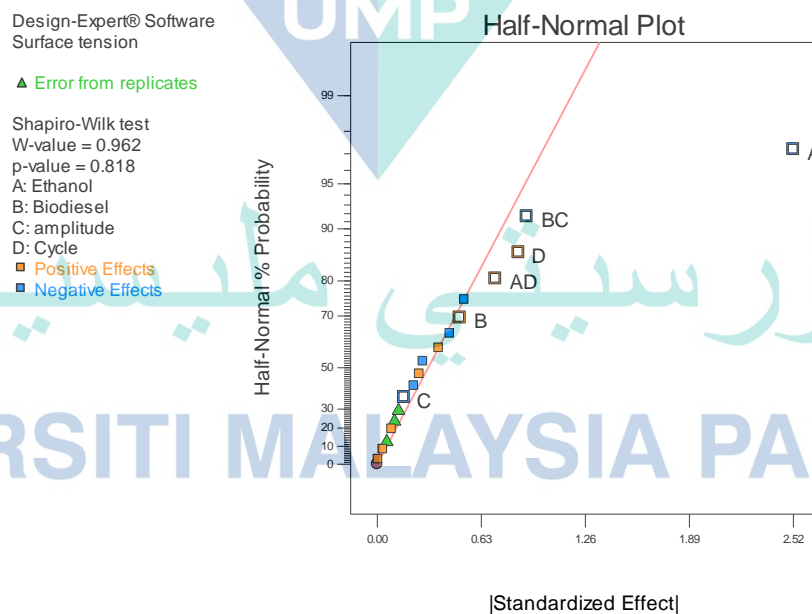
Figure 4.11   Compute effect for model selection via Half-Normal plot to analyse the effect of control factor on surface tension

Diagnostic plots in Figure 4.12 yield random scatter and no trend. No outlier is detected to exceed the upper and lower limit. Upper and lower red lines are similar to 95% confidence control limits on a run chart. In this case, none of the points stands out and within the red control limit.
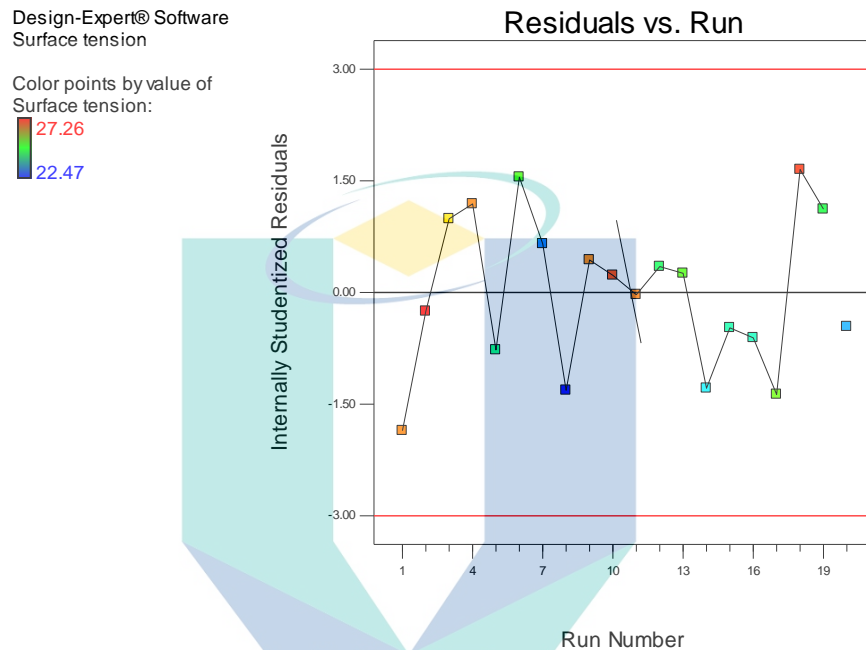
Figure 4.12   Residual plot for surface tension model diagnostic procedure

From Table 4.5, the Model F-value of 15.31 implies the model was significant. Values of "Prob > F" less than 0.05 indicate model terms are significant. In this case, A, D, AD, BC are significant model terms. Values greater than 0.1 indicate the model terms are not significant. The "Curvature F-value" of 10.04 implies there is significant curvature (as measured by the difference between the average of the centre points and the average of the factorial points) in the design space. Non-significant lack of fit is good and desirable.

From Table 4.6, the "Pred R-Squared" of 0.6802 was in reasonable agreement with the "Adj R-Squared" of 0.8267. "Adeq Precision" measures the signal to noise ratio. A ratio greater than 4 is desirable. The ratio of 12.289 indicates an adequate signal. The final equation in terms of coded factors is presented as Equation 4.5 as follow:

$$\gamma = 25.4 - 1.26A + 0.25B - 0.081C + 0.43D + 0.36AD - 0.45BC$$

4.5

The final equation in terms of actual factors is presented as Equation 4.6 as follow:

$$\gamma = 26.38750 - 0.60925A + 0.32150B + 0.05492C - 2.87500D$$
$$+0.71500AD - 0.00603333BC$$

4.6

Table 4.5   Anova for the selected factorial model (partial sum of the square – type iii) for response 3 (surface tension) with hierarchical terms added after manual regression (b and c)

Source	Sum of Square	df	Mean Square	F-Value	P-Value Prob>F	Remark
Model	34.70	6	5.78	15.31	< 0.0001	significant
A-Ethanol	25.35	1	25.35	67.10	< 0.0001	
B-Biodiesel	1.00	1	1.00	2.65	0.1297	
C-amplitude	0.11	1	0.11	0.28	0.6066	
D-Cycle	2.92	1	2.92	7.74	0.0166	
AD	2.04	1	2.04	5.41	0.0383	
BC	3.28	1	3.28	8.67	0.0123	
Curvature	3.79	1	3.79	10.04	0.0081	significant
Residual	4.53	12	0.38			
Lack of Fit	3.24	9	0.36	0.84	0.6335	not significant
Pure Error	1.29	3	0.43			
Cor Total	43.03	19				

Figure 4.13 shows the interaction of ethanol proportion and cycle setting with biodiesel and amplitude at the mid setting. High and low cycle setting interact with low ethanol content yield similar highest surface tension results; ± 25 mN/m. High ethanol content was resultant with surface tension drop by 6.74% with high cycle setting and 12.15% drop with low cycle setting. This proves that cycle setting plays its role in maintaining the reading inclination from dropping further by the ethanol effect. Figure 4.14 shows the interaction of amplitude and biodiesel on the surface tension when cycle and ethanol content at mid-range. The low percentage of biodiesel with high amplitude setting has yielded surface tension higher by 3% compared to low biodiesel content with

99

low amplitude setting. The surface tension is seen responding oppositely when biodiesel at high proportion, regardless of amplitude was set at high or low setting.

Table 4.6   Surface tension model fit statistics between the observed and the predicted values.

Responses	Results
R-Squared	0.8844
Adj R-Squared	0.8267
Pred R-Squared	0.6802
Adeq Precision	12.289
Std. Dev.	0.61
Mean	25.19
C.V. %	2.44
PRESS	12.55
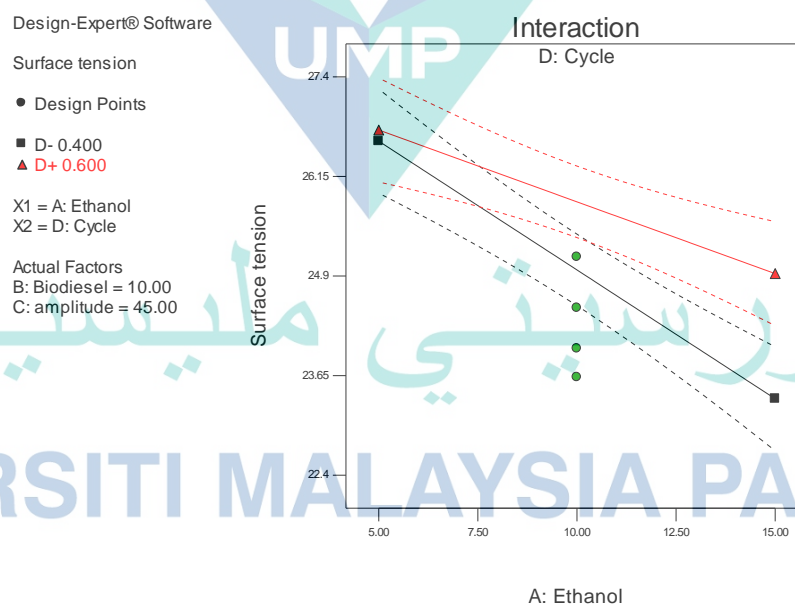
Figure 4.13   Two factors interaction on surface tension with ethanol proportion and cycle setting with biodiesel and amplitude at the mid setting

100
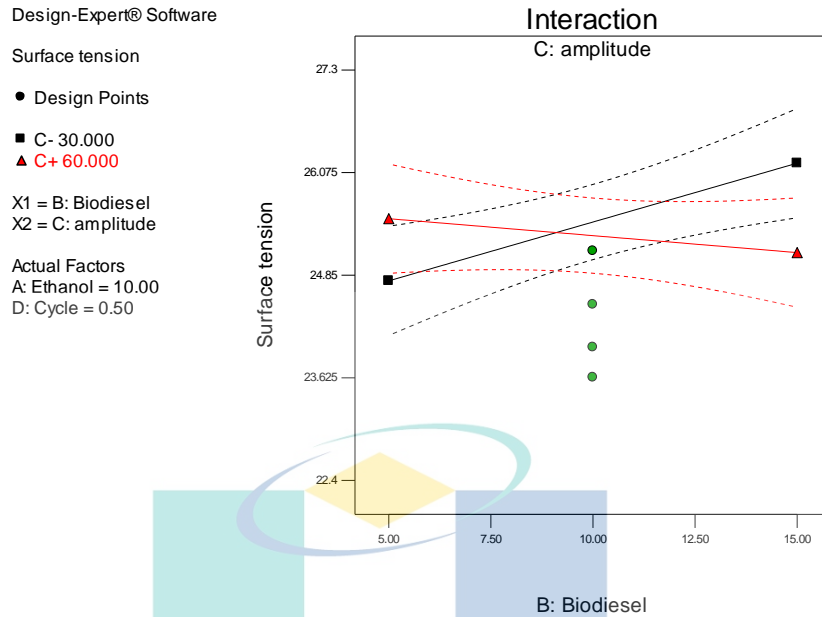
Figure 4.14   Two factors interaction on surface tension by amplitude and biodiesel on surface tension when cycle and ethanol content at mid setting

Surface tension is fuel important properties that are relevant for affecting the mechanism of fuel atomization. Fuel with high surface tension tends to generate larger droplet size while low surface tension leads to smaller droplet size. It resists the act of disruption or irregularity that occur on the liquid surface. In addition, low surface tension liquid could evaporate at a higher rate in comparison to the surface with the strong surface tension liquid (Park, 2010). Biodiesel is one of the tri-fuel emulsion components which could increase surface tension consistent with a previous study (Mehta, 2012). Since the surface tension is an intermolecular attraction between the fuel molecules, it can be assumed that the structure of a droplet is formed due to the surface tension. While it is simple to change the shape of a droplet, cohesive forces of the surface layer act with pulling force. A cohesive force is an attractive force between molecules of the same substance under the category of short-range forces and its magnitude decreases as the distance increases. An adhesive force, on the other hand, is the attraction force between molecules with different physical structure; which could occur between liquid and air or liquid and nozzle hole/tip surface. Theoretically, a sphere of influence with equal pulling force from all directions acts on the liquid molecules. An increase in temperature increases the kinetic energy of liquid molecules and subsequently decreases the cohesive forces through the reduction of the sphere of influence of a molecule, which ultimately reduces the surface tension. Furthermore, when liquid is subjected to unconventional

101

agitation such as ultrasonic capability generate heat, molecules receive kinetic energy through that heat. The molecules then exhibit rapid movements, and at some point, particles overcome the pulling forces between the molecules and turn some of the liquid into gas.

Interaction between cycle setting and ethanol percentage on the decrease of the surface tension was statistically significant. From the interaction between ethanol and cycle setting, with moderate amplitude setting and biodiesel content, surface tension decrease as ethanol is increase. Point to note was that cycle setting deescalates the decreasing effect. In other words, high cycle setting deescalate the decrease of the surface tension as more ethanol content is added. Intensify emulsification mode determine the outcome of the surface tension subject to biodiesel percentage. In other words, amplitude and cycle should be utilized to control the surface tension level. With the optimum setting, effective atomization process can be achieved. The finding affects the understanding of the research problem. Biodiesel and amplitude setting interact in opposite effect to the surface tension.

The result of biodiesel influence to the surface tension was as expected compared to previous research (Pradelle, 2019a), however, the amplitude effect combined with biodiesel affect yield contrasting outcome. In other words, the amplitude setting lessens the upsurge of surface tension rise to the extent cross-section interaction was detected. In other words, amplitude plays a significant role in manipulating biodiesel effect on the increase or decrease of the surface tension. In comparison with low biodiesel content, surface tension response oppositely to the high content of biodiesel regardless of amplitude setting. The finding is useful because biodiesel can be utilized effectively with the aid of ultrasonic emulsification method.

4.2.4 The effect of control factor on average droplet size

The average droplet size is influential in the micro-explosion phenomenon and in the general fuel atomization process. It is mainly influenced by the physical properties of the fuel. On tri-fuel emulsion, the emulsion formulation techniques and their associated parameters have a major role in the physicochemical properties of the emulsion. Following a standard method, as discussed in the methodology section 3.3.1, average droplet size reading of twenty samples was taken and analysed statistically.

Choosing effects to model, Figure 4.15 shows compute effects for model selection via half-normal probability plot to select model starts from the biggest effect which was the point furthest to the right. B and BD were added after manual regression to preserve hierarchy. It was commonly known that the t-value scale provides a more accurate measure of relative effects. Despite factor interaction B and BD fall below the t-value scale, they did not click off because they were actually involved in other significant interaction.
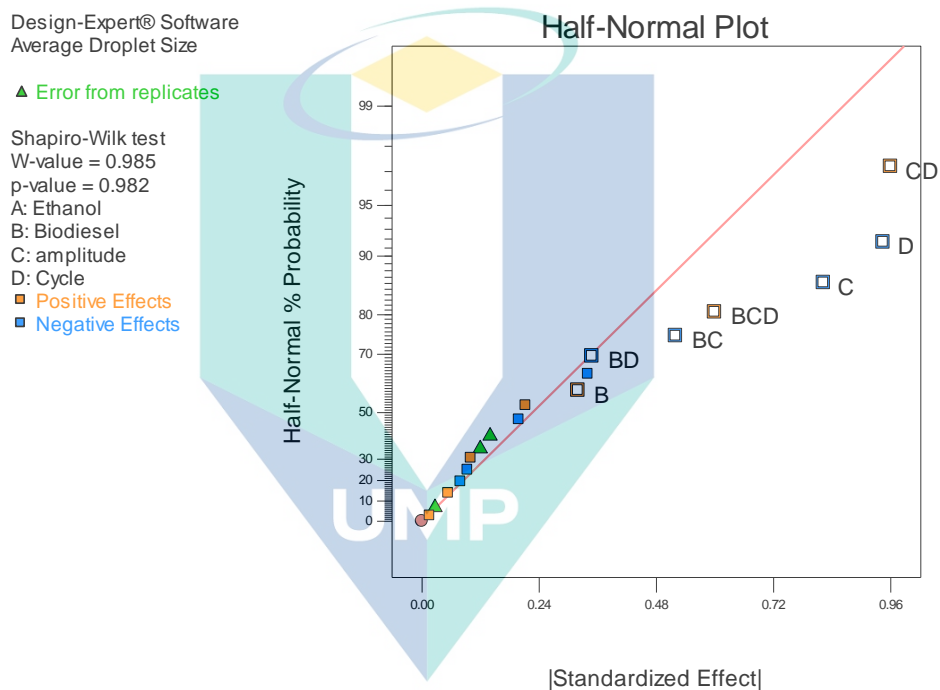
Figure 4.15   Compute effect for model selection via the half-normal plot method to analyse the effect of control factor on average droplet size

To convert between coded and actual models, the hierarchy must be supported. Otherwise, the coded model provides a different prediction than the actual model. Lack of linear term by excluding non-significant factors and neglecting the hierarchy could lead one to an incorrect conclusion. Hence, it was not a mistake or botched factor argument consistent with Stat-Ease Consultation. Consequently, it depends on the other factors with which it interacts. Figure 4.16 also shows acceptable diagnostic plots with random scatter and no trend. No outlier is detected to exceed the upper and lower limit. Upper and lower red lines are similar to 95% confidence control limits on a run chart. In this case, none of the points stands out and within the red control limit.
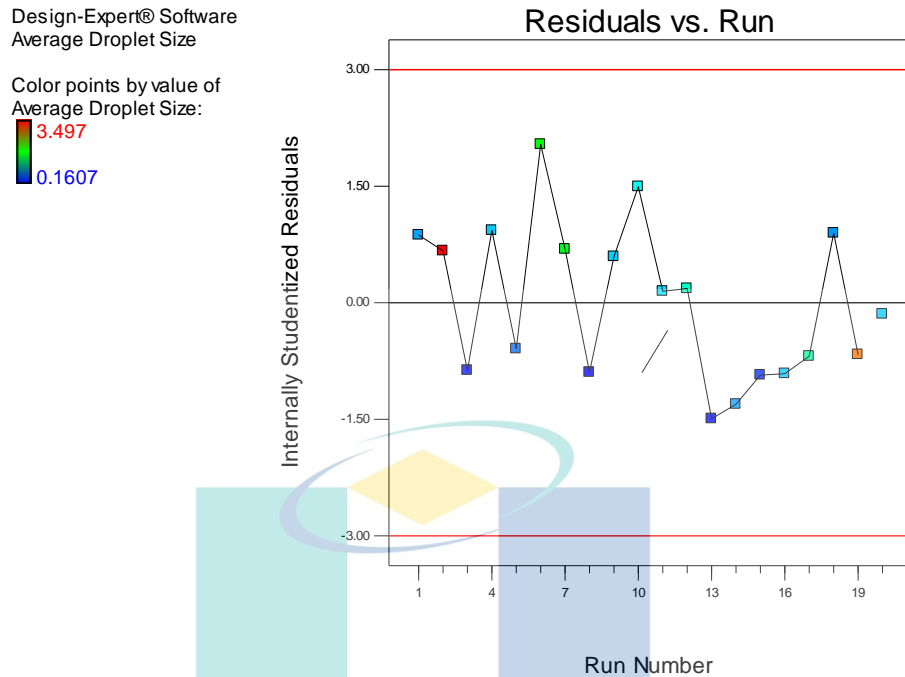
Figure 4.16   Residual analysis plot for the model diagnostic procedure

From Table 4.7, the Model F-value of 12.45 implies the model is significant. Values of "Prob > F" less than 0.05 indicate model terms are significant. In this case, C, D, BC, CD, BCD are significant model terms. Values greater than 0.1 indicate the model terms are not significant. The "Curvature F-value" of 0.09 implies the curvature (as measured by the difference between the average of the centre points and the average of the factorial points) in the design space is not significant. Therefore, proceeding to the RSM method is not necessary. Non-significant lack of fit is good and desirable.

From Table 4.8, the "Pred R-Squared" of 0.6661 was in reasonable agreement with the "Adj R-Squared" of 0.8167. "Adeq Precision" measures the signal to noise ratio. A ratio greater than 4 is desirable. The ratio of 11.044 indicates an adequate signal. The final equation in terms of coded factors is presented as in Equation 4.7. This is the equation that relates the listed input factors to the average droplet size.

$$D_{Average} = 1.05 + 0.16B - 0.41C - 0.47D - 0.26BC - 0.17BD + 0.48CD + 0.30BCD$$

4.7

The final equation in terms of actual factors is presented as in Equation 4.8.

$$D_{Average} = -0.763925 + 1.261885B + 0.047082C + 2.345125D$$
$$-0.023460BC - 2.147875BD - 0.079717CD + 0.039988BCD$$

4.8

Table 4.7　　　ANOVA for the selected factorial model (Partial sum of the square – Type III) for response 4 (Average droplet size) with hierarchical terms added after manual regression (B and BD)

Source	Sum of Square	df	Mean Square	F-Value	P-Value Prob>F	Remark
Model	13.39	7	1.91	12.45	0.0002	Significant
B-Biodiesel	0.41	1	0.41	2.67	0.1308	
C-amplitude	2.71	1	2.71	17.64	0.0015	
D-Cycle	3.57	1	3.57	23.27	0.0005	
BC	1.08	1	1.08	7.04	0.0225	
BD	0.49	1	0.49	3.16	0.1030	
CD	3.69	1	3.69	24.03	0.0005	
BCD	1.44	1	1.44	9.37	0.0108	
Curvature	0.013	1	0.013	0.087	0.7735	not significant
Residual	1.69	11	0.15			
Lack of Fit	0.91	8	0.11	0.44	0.8415	not significant
Pure Error	0.78	3	0.26			
Cor Total	15.09	19				

105

Table 4.8   Average droplet size model fit statistics between the observed and the predicted values.

Responses	Results
R-Squared	0.8880
Adj R-Squared	0.8167
Pred R-Squared	0.6661
Adeq Precision	11.044
Std. Dev.	0.39
Mean	1.07
C.V. %	36.74
PRESS	5.03

Figure 4.17 shows the interaction between amplitude and biodiesel with respect to the middle setting of cycle and ethanol content. Shifting the ethanol level high or low make no difference to the interaction. Low biodiesel content combines with high amplitude setting yield fine average droplet size as low as 0.74 µm. Meanwhile, when high biodiesel fraction was combined with low amplitude setting, the average droplet size increased dramatically by 80%. However, high amplitude setting could fix this and aid for slight further size refinement down to 0.54 µm which was the finest average droplet size.

Figure 4.18 shows the interaction between cycle and amplitude with respect to both ethanol and biodiesel middle setting. Shifting ethanol fraction up or down yield no difference to the outcome. The finest average droplet size that was obtained was 0.51 µm via low amplitude setting combines with high cycle setting. Maintain low amplitude setting while reducing the cycle setting causes the size to increase dramatically by 372%. High amplitude and high cycle setting yield a similar outcome; 0.63 µm which was 19.26% higher than the mentioned finest size obtained. This indicates that amplitude and cycle interaction are significantly important to take into account for obtaining desire average droplet size.
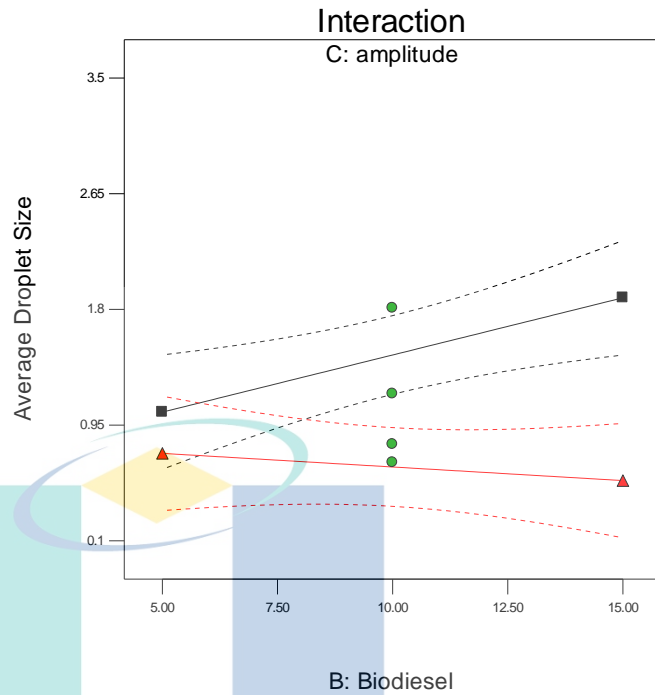
Figure 4.17   Interaction between amplitude and biodiesel with respect to the mid setting of cycle and ethanol content.
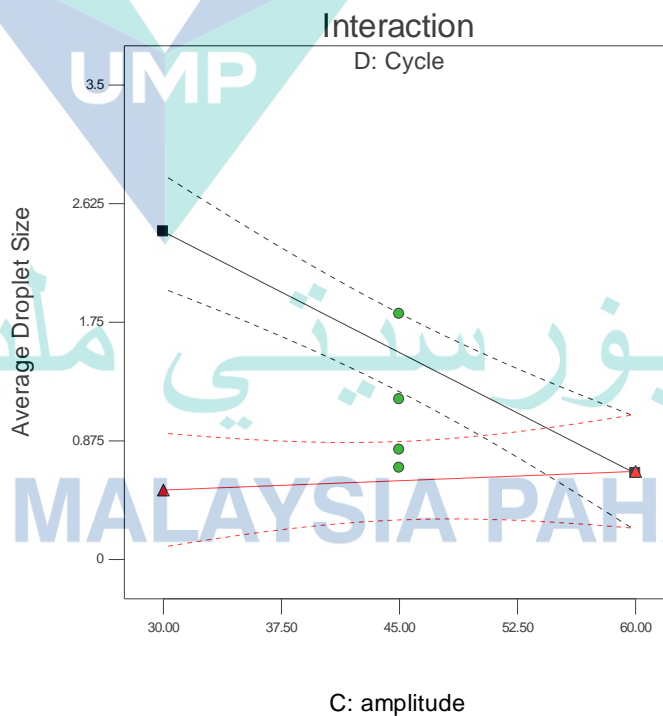
Figure 4.18   Interaction between cycle and amplitude with respect to mid ethanol and biodiesel content.

Figure 4.19 shows the interaction between amplitude and cycle setting with respect to low biodiesel setting combined with the middle range of ethanol content. The pattern is almost similar to the pattern in Figure 4.18 accept that no intersection was observed. Moreover, reducing biodiesel content suggest average droplet size improvement when low cycle setting was combined with low amplitude setting.
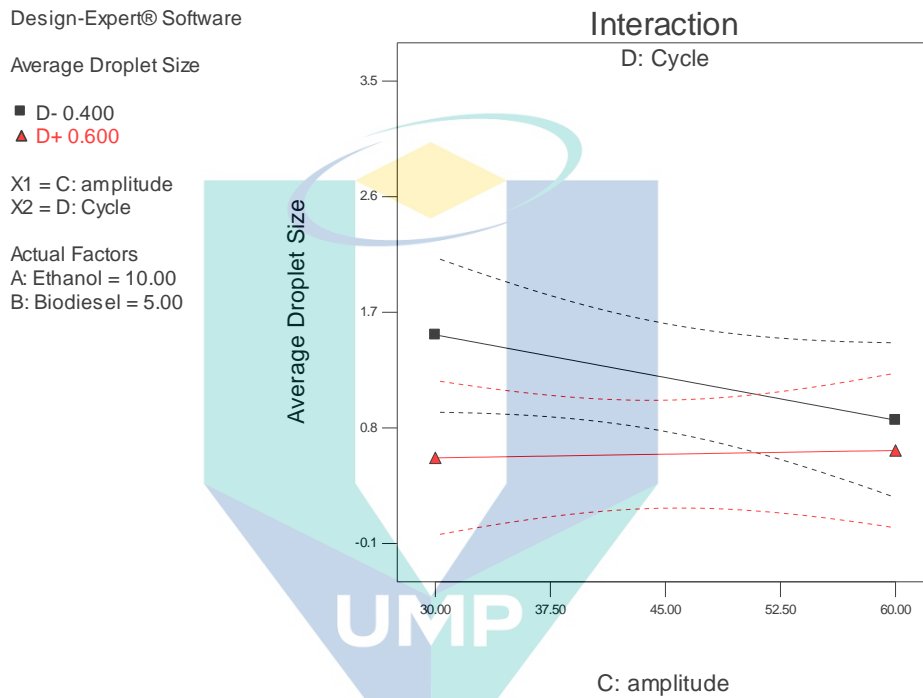
Figure 4.19   Interaction between amplitude and cycle setting with respect to low biodiesel setting and mid ethanol content.

Figure 4.20 shows the interaction between amplitude and cycle setting with respect to high biodiesel content. The intersection was observed when the amplitude was set to high yield opposite effect. The opposite effect, however, appeared to be minor. Figure 4.21 shows the interaction between amplitude and biodiesel with respect to the mid-range setting of the cycle while Figure 4.22 shows the interaction between amplitude and biodiesel with respect to low cycle setting. Increasing biodiesel content will have almost no effect on the increasing amplitude level. However, with a high percentage of biodiesel with low amplitude setting, the average droplet size increased. Meanwhile, with high cycle setting, the interaction is similar to any combination of amplitude or biodiesel percentage.
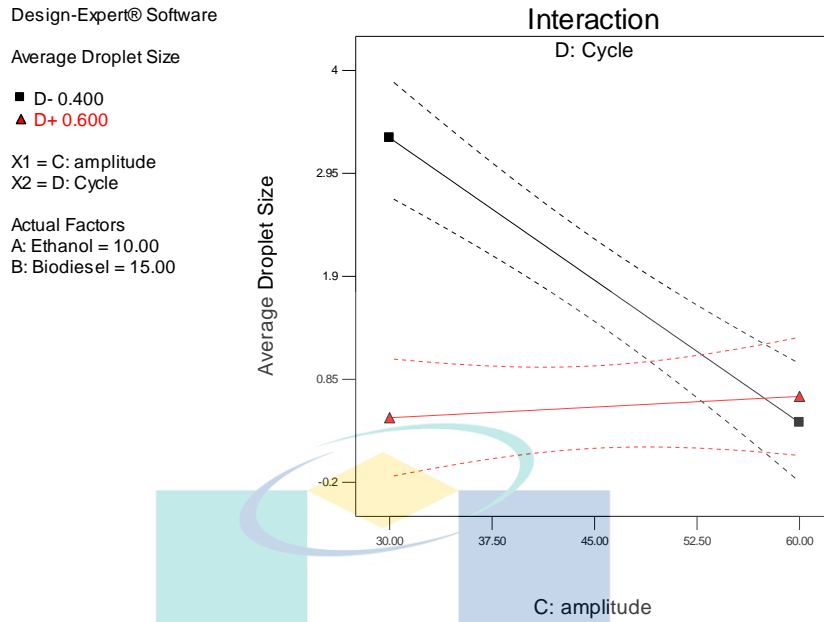
Figure 4.20   Interaction between amplitude and cycle setting with respect to high biodiesel and mid ethanol content.
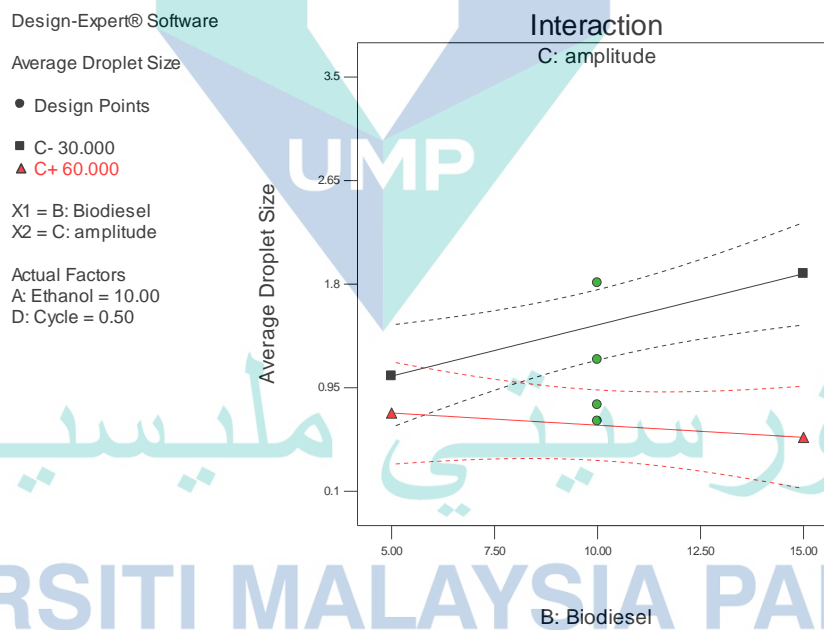
Figure 4.21   Interaction between amplitude and biodiesel with respect to the mid-range setting of the cycle on average droplet size.

Figure 4.23 shows the interaction between biodiesel and amplitude with respect to the high cycle setting. Regardless of high or low amplitude setting combined with either high or low biodiesel content yield similar results. In other words, the result suggests almost no significant difference either way. Figure 4.24 shows a cube presentation of

interaction between biodiesel, amplitude and cycle setting. The cube presentation offers numerical response values at each combination of three controls. Finally, Figure 4.25 shows a 3D representation of the interaction.
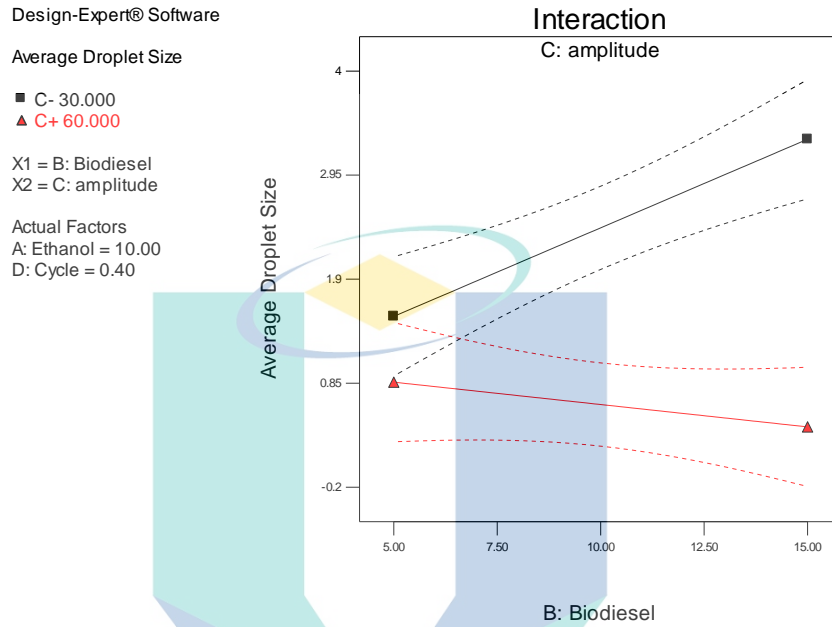
Figure 4.22   Interaction between biodiesel and amplitude with respect to low cycle setting on average droplet size.
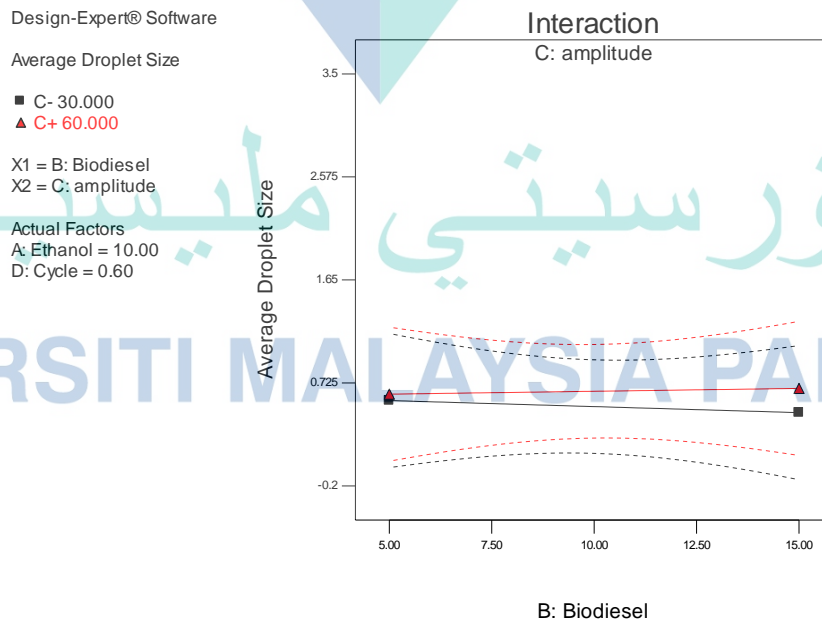
Figure 4.23   Interaction between biodiesel and amplitude with respect to high cycle setting on average droplet size.
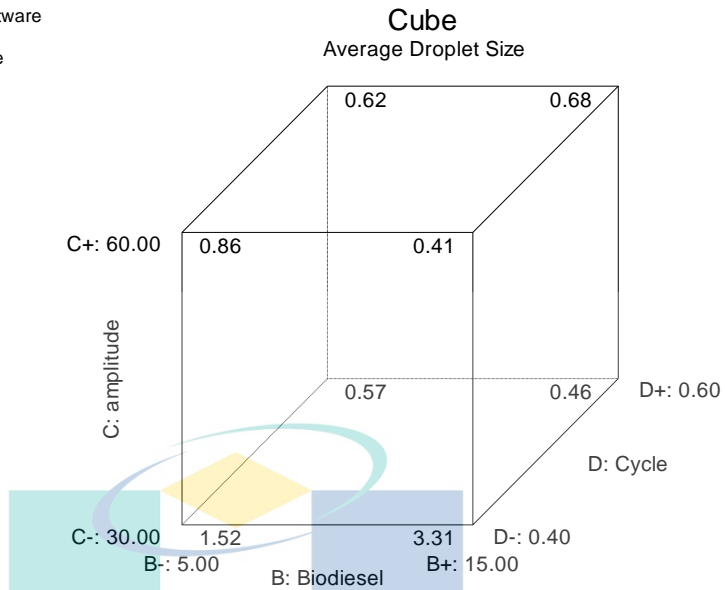
Figure 4.24   Cube presentation of control factors interaction (biodiesel, amplitude and cycle) with average droplet size
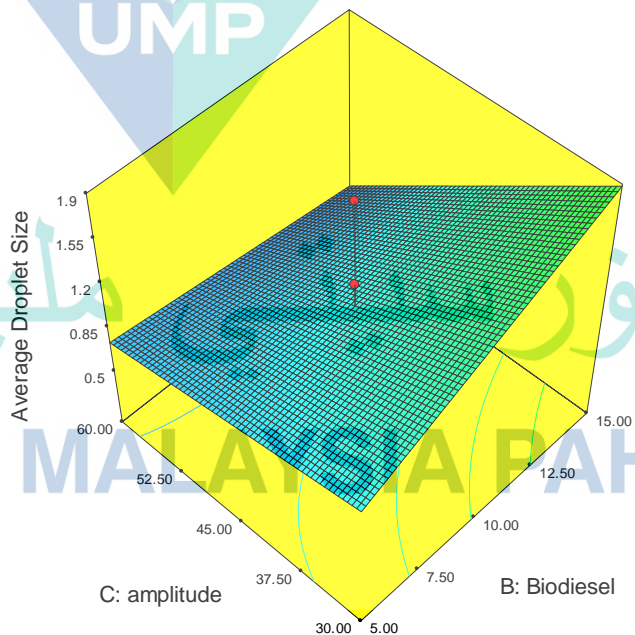
Figure 4.25   3D presentation of control factors interaction (biodiesel, amplitude and cycle) with average droplet size

Ultrasonic emulsification process introduced amplitude and cycle setting. It was evidenced that the amplitude range of setting may alter viscous and high surface tension effect of biodiesel content to the average droplet size. The interaction between amplitude and cycle setting on average droplet size suggests that despite high amplitude and high cycle setting applied to tri-fuel emulsions, a certain limit of outcome should be expected. The limit is altered with a high or low level of biodiesel content. The finding affects the understanding of the research problem in such a way, in order to obtain desired average droplet size, not only the amplitude and cycle setting effect but also biodiesel and ethanol response should be taken into consideration. The finding from objective 1 is important because it can be used as basis to alter the physicochemical properties of the prepared fuel correspond to the ultrasonic emulsification setting and mixing ratio. The information is important in order to acknowledge the significant effect of the control factors which can influence the decision on sample selection considering the physicochemical properties alteration. At the same time, it can be used to reduce the number of the sample that will be investigated for the subsequent objective.

4.3 Characterization of micro-explosion and spray of tri-fuel emulsion

In this section, fuel spray of three different tri-fuel emulsions was investigated for the micro-explosion phenomenon through the use of an optically accessible constant volume chamber and high-speed camera setup as discussed in Chapter 3. The result presentation is classified into two sections namely micro-explosion as secondary atomization characterization and the spray characterization. The micro-explosion as secondary atomization section is further discussed through presentation of the characteristics such as visual motion, droplet surface area change, centricity with minimum and maximum diameter change, axial distance. Furthermore, the spray characterization is presented through subsections of spray cone angle, spray spread on the axial direction and spray penetration.

4.3.1 Characterization of micro-explosion

Micro-explosion phenomenon can occur as high or low intensity with the effect of dynamic structure on a droplet within a relatively short and critical period. It can be seen that the micro-explosion phenomenon for all three samples was identical and have some common dynamic structure. A small scale micro-explosion known as puffing was

observed in great detail. This can be explained probably due to the governed effect by the balance between ethanol significant effect and biodiesel compensation attribute. Specifically, the surface tension and viscosity of tri-fuel emulsion were not as superior as diesel. The biodiesel ratio effect on surface tension was preventing the explosion to be a lot more severe. Micro-explosion observed in this study is classified under low-intensity type known as puffing due to high interfacial tension of biodiesel influence and consistent with the reported result on the previous study elsewhere (Qian et al., 2019).

Image processing such as threshold, noise reduction and edge detection plays an important role in distinguishing the effect of micro-explosion phenomenon on a droplet. Figure 4.26 shows selected zooming raw image sequence of puffing event after threshold and noise removal. The progression of droplet deformation can be seen occurs within a short period. A similar event was captured for all three samples except in pure diesel droplet. Micro-explosion was observed to occur in a variety of size and end up with similar deformity. The micro-explosion phenomenon found was under the low-intensity category known as puffing and in this case, the author classified the event as double-side puffing and single side puffing. The classification has not been documented in the previous literature.

Puffing could also occur as single side puffing. The one side effect of puffing is important to study because it can be considered as half the effect of double-side puffing as described in Figure 4.26. Figure 4.27 shows the sequence image of single side puffing evolution with various image processing technique. The puffing was observed to have a significant impact on the droplet during the spray injection. It was observed that the droplet was experiencing a shrinking episode before a unidirectional explosion was recorded. In consequence to the micro-explosion, a recoil effect could be clearly seen to the droplet as it was moving to the opposite direction relative to the explosion.

A particularly important sequence noted is where the size of the droplet decreased dramatically before the actual bursting event occurs. This is one of the behaviours that was observed before the actual eruption in all micro-explosion phenomenon for all three samples. The evolved shape from almost complete sphere shape to almost flat oval shape can be observed in all event of micro-explosion phenomenon recorded. That one moment in time is like all the mass of the droplet is compressed in before been burst out last in a very short amount of time. It was a closest in for a short period before break apart from

113

the inner core a little moment later. The probable explanation for the droplet diameter is dramatically changing before the explosion because of the boiling occurrence from the inside.
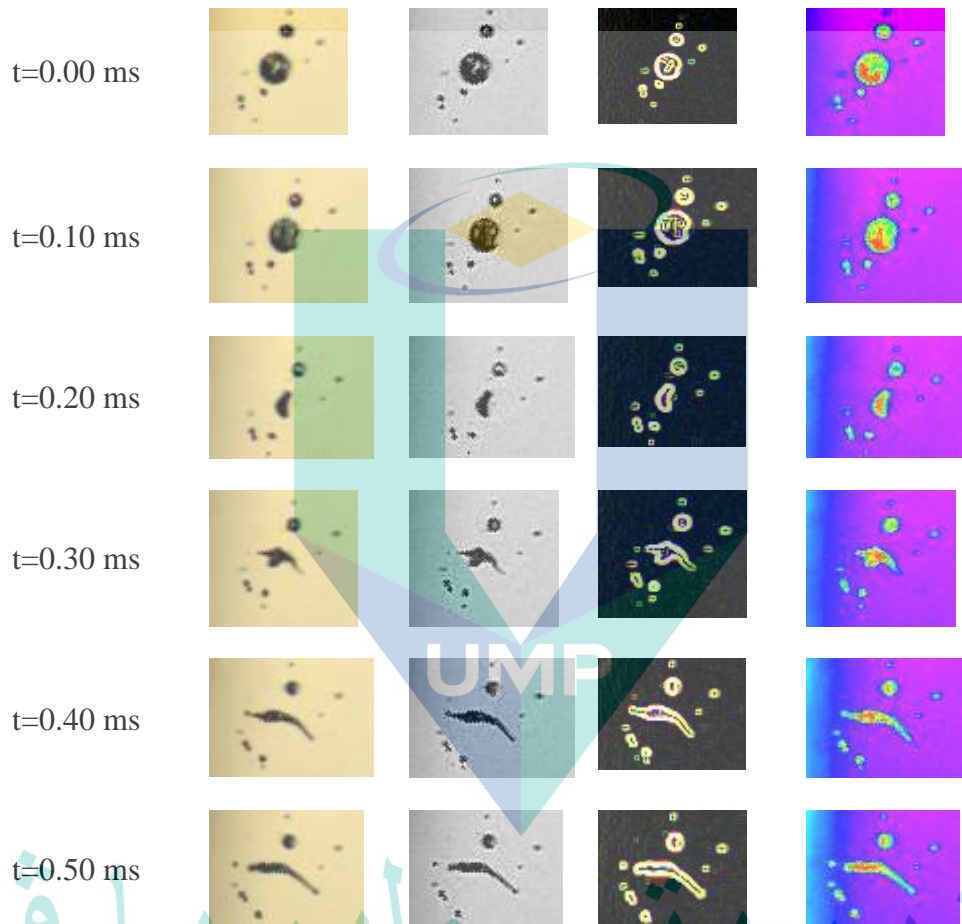
Figure 4.26   Micro-explosion phenomenon in the form of double side puffing from S20 presented as raw format, sharpening, edge detection and spectrum respectively

In view of the flat oval shape correspond to the final shape after the event, the structure deformation was observed affecting the adjacent droplet and ultimately it affecting the spray distribution. It can be seen that the almost flat oval shape maintaining its profile for the remaining time unless collide with other droplets nearby. The droplet deformed from spherical shape to oval. The evolution of droplet fragmentation and deformation due to the micro-explosion phenomenon explain this.

Direct evidence obtained that during the event, it was observed that droplet went through quick phase separation process before micro-explosion starts as stated in the

114

literature review section. This can be distinguished by observing some part of the droplet total dark and the other part with transparency appearance representing the alcohol part. Figure 4.28 support the discussion with the label part on the droplet with the transparent appearance that represents phase separation that occurs before the micro-explosion phenomenon initiate.
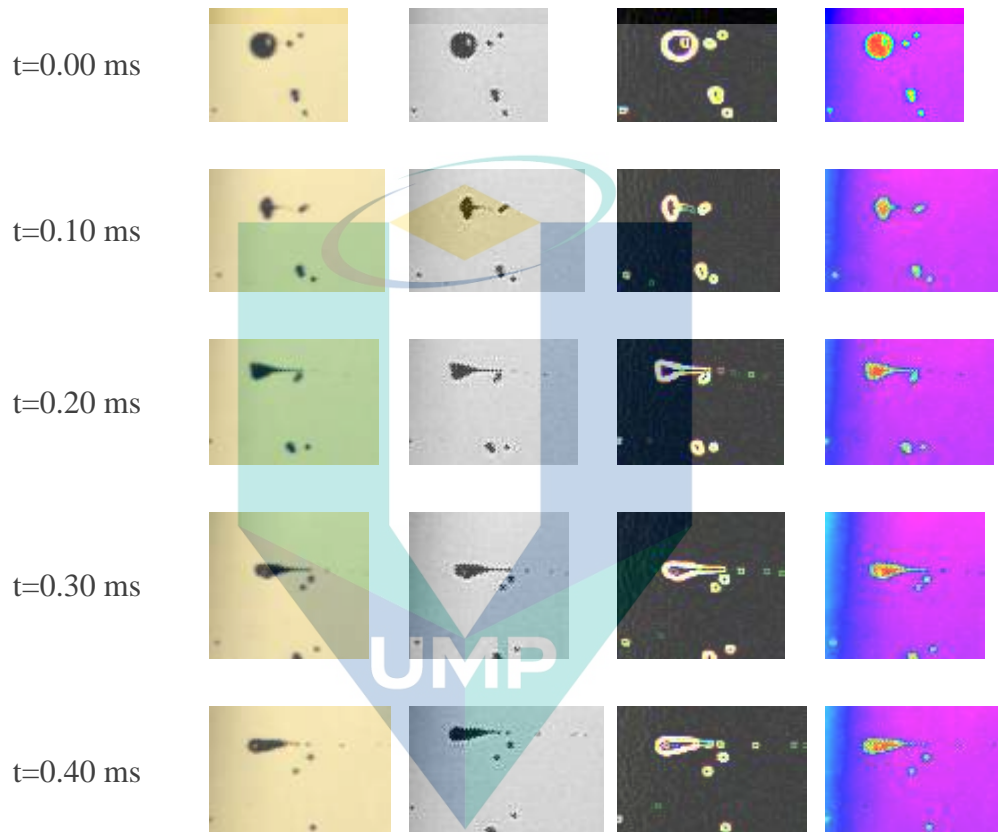
Figure 4.27   Micro-explosion phenomenon in the form of single side puffing from S20 presented as raw format, sharpening, edge detection and spectrum respectively

It was also observed that the micro-explosion phenomenon causes the droplet to vibrate and bounce a few times before shaping back to the original droplet. The vibration caused by the explosion initiates wavy condition to the original droplet as the droplet came back to its original shape. The vibrated droplet caused by the micro-explosion may or may not change the shape of the droplet. However, in all three samples observed, the effect of the vibration could not exceed the elastic limit of the droplet due to the high surface tension of biodiesel. Hence, the droplet returns to the original shape after multiple time shape transformation. Moreover, the shock wave was release by the micro-explosion observed in the study. The strength and force of the shockwave were not strong enough to affect the surrounding droplet in all direction. Although the blast of micro-explosion is

at micro-scale, the characteristics of the resulting shockwave are known similar to a large-scale explosion (Alvarado et al., 2012). The shockwave can be measured by the detection of vibration and frequency analysis techniques. The destruction is intended chaos at micro-scale, which disrupts the structure of the droplet and may affect the neighbouring droplets. Furthermore, the explosion promotes disorder, which creates mist droplets or at least spreads tiny pieces of droplets in all directions. The interruption is desirable since it promotes atomization for rapid combustion. The event complements the effort of the injector as a primary atomizer. The distinguishing feature of such disorder is what is known as secondary atomization.
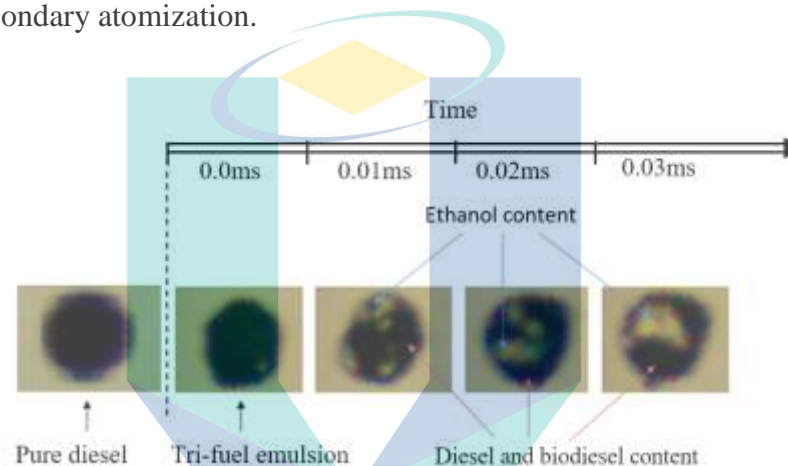
Figure 4.28   Droplet undergone phase separation phase before the micro-explosion phenomenon

Multiple minor puffing's events were observed to occur at the surface of the droplet in motion. But the occurrence can only be visible with image zoom-in mode. Apparently, the eruption was too small and has no effect on the other droplet nearby. In addition, the eruption has caused the birth of satellite droplets. Meanwhile, at the end of the spray shot under low velocity, micro-explosion phenomenon was observed to occur within the dilatational wave from the process of jet breakup in accordance to the basic theory of basic jet breakup describe by the Raleigh theory and extended by Weber that consider viscosity. Micro-explosion phenomenon was found integrated within the neck formation as a result of oscillation of jet from orifice nozzle.

Micro-explosion reduces the droplet size dramatically. In comparison with droplet undergo common deformation state, micro-explosion phenomenon deformed the droplet into smaller size or collision with other droplet surroundings. Furthermore, because the droplets were not at constant state and got affected by the velocity, the droplet collision occurs with other droplets. However, not all collision exercise observed turns out well. In

116

some cases, micro-explosion was seen as common breakup type as described in the theory of droplet atomization process known as shattering. The event of shattering the droplet was captured in Figure 4.29. Shattering is one of the interesting breakup modes that could possibly occur to a single spherical droplet after subject to relatively sudden impact. However, it was observed in this case, the micro-explosion phenomenon became the ground effect to the droplet undergone the process as a shattering process.

| t=0.00ms | t=0.02ms | t=0.04ms | t=0.06ms |
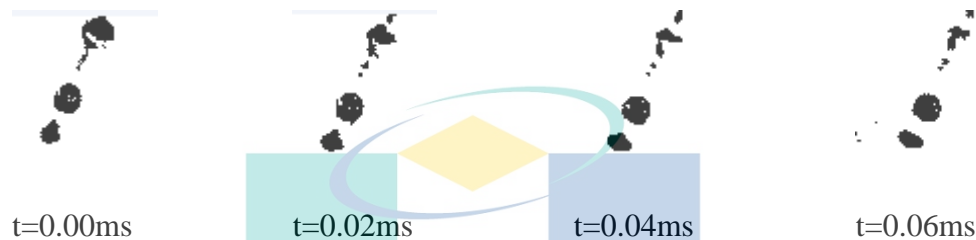
Figure 4.29   Micro-explosion as a shattering process

The micro-explosion phenomenon accelerates the droplet fragmentation process in addition to the influence of velocity caused by the injection pressure and evaporation process caused by the high temperature. This can be explained by referring to the value back to back alcohol and biodiesel with regards to surface tension. Agglomeration that was observed due to vigorous particle collision from the inside of droplet causes the dramatic shape change with time.

Micro-explosion under puffing category that was observed some of them have a common characteristics. They turn to change shape and got stretch to x-axis direction. Evidently, this causes droplet distance of axial x to dramatically increase. It is possible that this phenomenon is responsible for causing the spray shape to become wider and bigger distance on axial x of the spray apart from possible swirl and turbulence effect. Without collision, it was observed that individual droplet that undergone puffing either single side or double side category will return back to its original shape due to the strong surface tension caused by the influence of biodiesel ratio that exceeds the compensate ethanol effect.

The shape turns odd from common circle shape and burst. The burst reaches distance in the axial x-direction. Some turns to satellite droplet. Satellite droplet behaves like a common droplet. No shaking or boiling behaviour observed on satellite or baby droplet. The observation supports the definition of micro-explosion as coalescence

117

between droplet known as puffing and micro-explosion as sudden evaporation of inner component or bursting of boiling from inside the droplet.

4.3.1.1 Droplet Surface area change

The effect of the micro-explosion phenomenon on the droplet surface area is important to the study because exposing the maximum surface area of a droplet will enable fast vapour phase transformation. Figure 4.30 (a) shows the line graph which illustrates a plot comparison between droplet with and without micro-explosion in term of surface area change with time. It can be seen from the droplet that undergoes micro-explosion showed twice a sudden drop and increase, unlike droplet with no micro-explosion. The droplet surface area dropped dramatically from t=0.1 ms to t=0.25 ms for double side puffing. The sudden decrease of droplet surface area occurs just a moment before the micro-explosion phenomenon. This is followed by a gradual and continuous increment of the surface area up to 0.3 ms. The increment is expected due to the micro-explosion burst so long as there is no collision with any adjacent droplet takes place. Without any collision, it can be seen that the final result of the droplet surface area is still far below the original surface area compared to the surface area at the initial point before micro-explosion starts.

The directional of the affected area as the surface area gradually increase and will be presented as the axial deformation plot later. In comparison, without micro-explosion, droplet remains steady with no significant rise or fall pattern. Regardless of single or double side puffing, the micro-explosion initiated represented by concave up pattern in the graph.. In contrast, it is apparent that was not the case with the droplet with no micro-explosion. It was also observed from the common droplet behaviour that the evaporation rate is relatively small within such a short recording period. Figure 4.30 (b) is another micro-explosion event that demonstrates single side puffing with an almost similar pattern. The surface area of droplet undergone puffing decrease dramatically for 0.1 ms before increase significantly for a period of 0.3 ms. The droplet gets back to its normal behaviour after that similar to the droplet with no micro-explosion. To sum up, single side puffing effect on droplet surface area appeared to be similar with double side puffing with sudden and significant concave down pattern which opens up more chances for the evaporation process to concur.
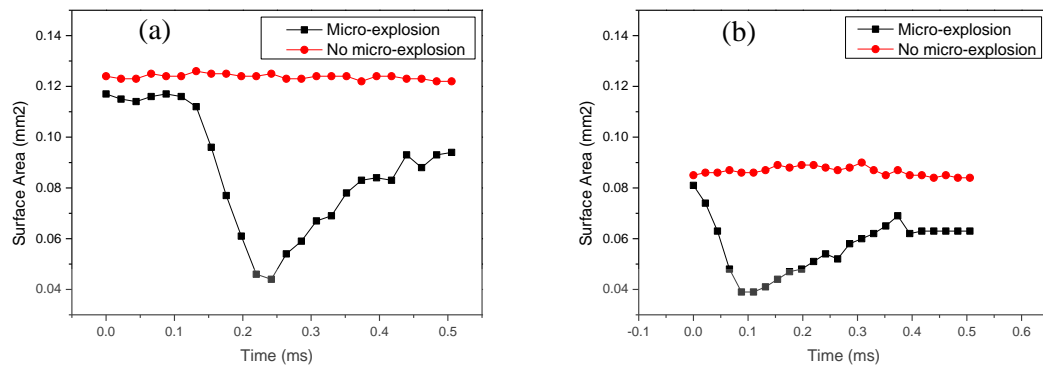
Figure 4.30   The surface area of droplet undergone (a) double side puffing and (b) single side puffing

The sudden surface area dropped was observed occurs at the initiation stage of the micro-explosion. Evidently, this is because of the initiation of the micro-explosion phenomenon. The finding is important because the surface area decrease of the droplet indicates that the overall atomization process could be improved. Overall, the concave pattern decreasing and increasing is the potential chance for the evaporation process to take place in between the frame. Furthermore, the evaporation rate is relatively small within such a short recording period as observed hence, micro-explosion phenomenon plays its role significantly. The condition of the fuel droplet surface area is determined by how strong is the surface tension. The decrease of droplet surface area may cause the temperature of the droplet to increase and facilitate the evaporation process. The evaporation can take place on the droplet surface. The rate of the evaporation based on the vapour diffusion from the droplet surface.

4.3.1.2   Centricity with Min and Max diameter change

Droplet centricity represents the spherical status of a droplet. The result is important because it demonstrates the effect of the micro-explosion phenomenon on a droplet in comparison with the droplet with no micro-explosion. Figure 4.31 (a) shows centricity of droplet undergone double side puffing in comparison with the droplet without micro-explosion. The value of the droplet centricity was reduced as the droplet going through the event. This indicates that the shape is losing its spherical shape dramatically within a short period. Figure 4.31 (b) provides information about droplet diameter at the minimum and maximum size in the event of double-side puffing. The information is complimenting in Figure 4.31 (a). Figure 4.31 (c) shows centricity of

droplet undergone single side puffing in comparison with the droplet without micro-explosion. The value of the droplet centricity was reduced as the droplet going through the event. Again, this indicates that the shape is losing its spherical shape dramatically within a short period. Figure 4.31 (d) shows droplet diameter at the minimum and maximum size in the event of single side puffing. It complements Figure 4.31 (c). The pattern looks similar to double-side puffing.
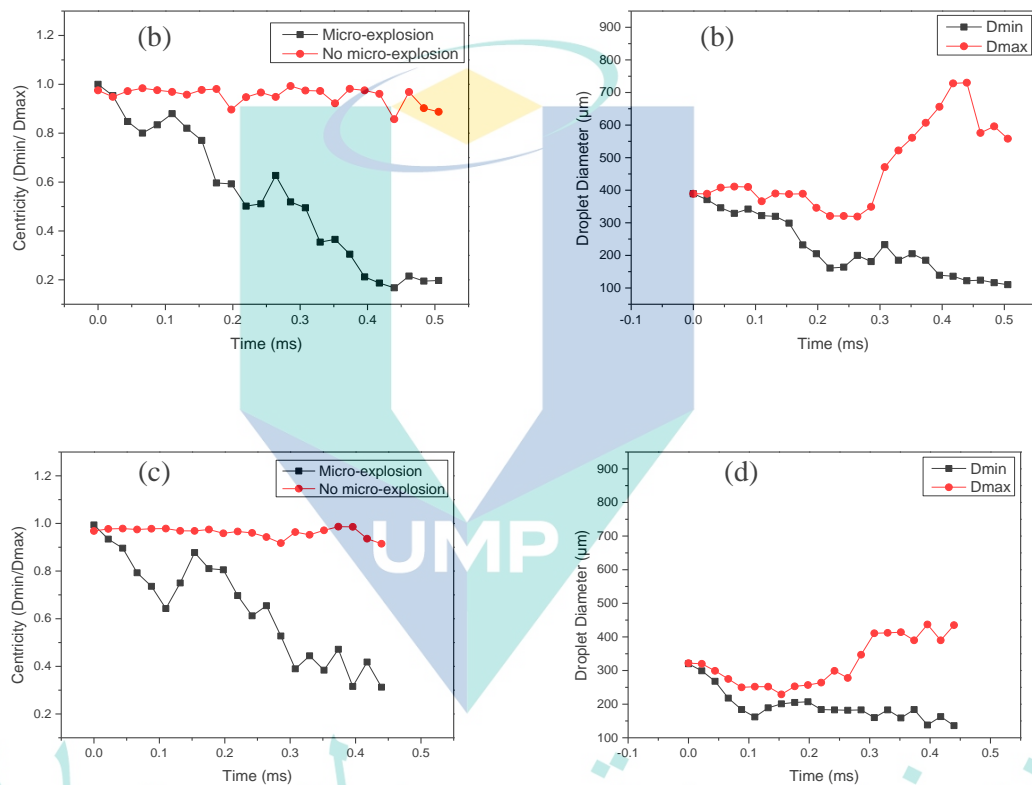
Figure 4.31   Centricity of droplet undergone double side puffing (a) with its droplet diameter (b) and centricity of droplet undergone single side puffing (c) with its droplet diameter (d)

The major finding is that the centricity of the droplet undergone micro-explosion phenomenon decrease significantly within a short period. Regardless of a single side or double side puffing, the centricity of both events shows a similar pattern. The meaning of the finding is that the micro-explosion phenomenon drastically changes the shape of the droplet from common spherical shape to irregular shape subject to the micro-explosion phenomenon. This is not the case with droplet with no micro-explosion behaviour. The finding is important because the sequence of puffing and micro-explosion phenomenon

actually affect droplet shape significantly within a short period which could be an advantage to allow the mixing of air and fuel to take place.

4.3.1.3   The axial distance on X and Y direction

The measured axial distance refers to the distance of the origin droplet and the satellite droplet location as a result of the bursting subject to axial direction X or Y. By analysing the axial distance result subject to the axial direction, one should be able to understand the impact of the phenomenon.

Figure 4.32 (a) shows the effect of double-side puffing on droplet bursting distance on axial x versus time in comparison to a selected droplet of almost similar size without micro-explosion phenomenon. Axial distance X decreased slightly before actual bursting and accelerate the increased of axial distance X. This was not the case with droplet with no micro-explosion behaviour.

Figure 4.32 (b) shows the effect of single-side puffing on droplet bursting distance on axial X versus time. The impact of the burst originated by the micro-explosion was illustrated by the dramatic increase of the axial distance X. For single side puffing, it was observed that the axial distance decreases slightly less than double side puffing at the beginning before accelerate to a positive value significantly after that.

Figure 4.32 (c) shows droplet bursting distance on axial-Y versus time. The droplet with a micro-explosion phenomenon experience a slight decrease in axial distance effect on axis Y in contrast to the droplet with not micro-explosion. The effect however temporary the droplet reshapes and get back to the axial distance original track. Droplet with no micro-explosion did not experience the axial distance change at all within that short period. Figure 4.32 (d) illustrates droplet bursting distance on axial Y with time due to puffing in comparison with axial distance Y for the droplet with no micro-explosion. Again, the axial distance Y decrease slightly in comparison with the droplet with no micro-explosion. However not as dramatically as axial distance X.

The key observation from this experiment is the droplet spreading dynamic causes by low-intensity micro-explosion phenomenon known as puffing. Regardless of single or double side puffing, the event promotes efficient atomization progression. Within a short period, the finding of micro-explosion impact on the axial distance X of droplet changes

121

significantly different than the droplet with no micro-explosion. The deformation and bursting outcome on axial distance X effect for a single or double side puffing produce a similar pattern. This is not the case with the effect on axial Y direction. Possibly the effect on axial Y direction yields concaves up pattern because of the surface tension effect as well as the momentum and gravity pull.
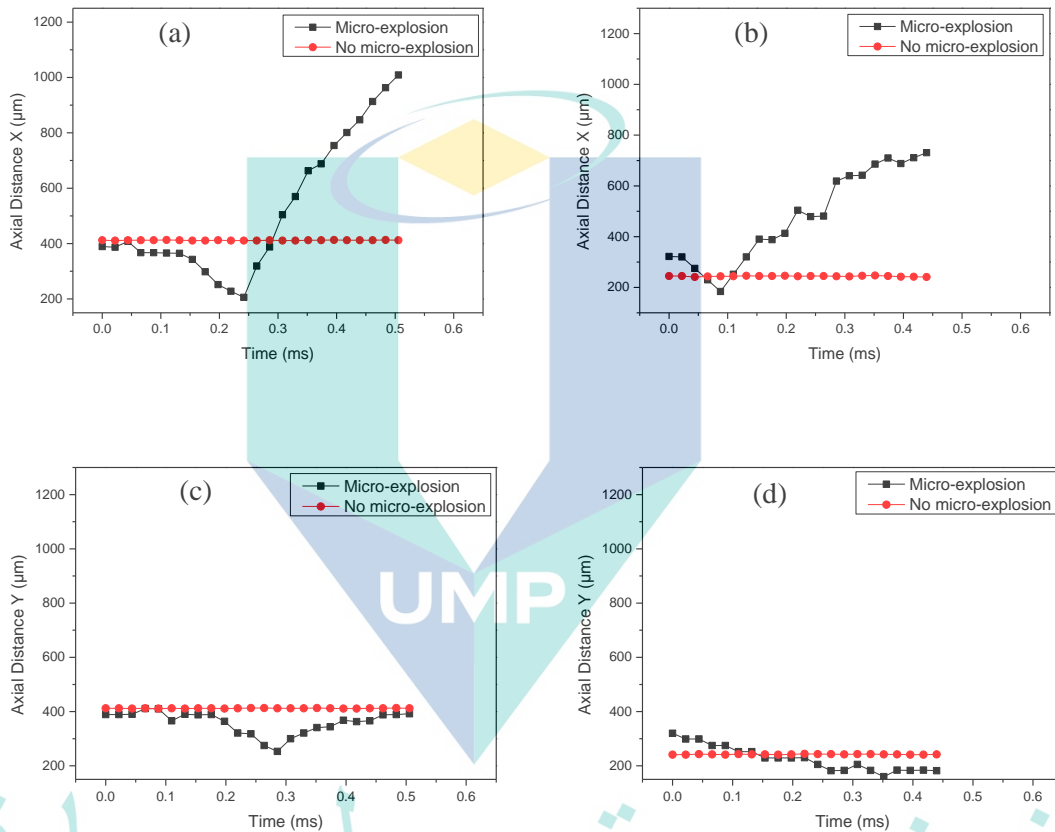
Figure 4.32   Axial distance X of droplet undergone (a) double side puffing and (b) single side puffing. Axial distance Y of droplet undergone (c) double side puffing and (d) single side puffing

Furthermore, the impact on axial Y direction which is in the same direction as spray penetration not as much as the axial distance X which is parallel to the spray spread. The meaning of the finding is that the micro-explosion phenomenon affects droplet axial distance X significantly and Y slightly. The event can be considered as a premonition to the spray characteristics which points out that the axial distance formation to the axial X direction and this may one of the explanation of why the spray axial distance increase. The result of the spray spread will be presented and discussed next.

122

4.3.2 Spray characteristics

Spray study is an effective way to understand the impact of the micro-explosion phenomenon macroscopically. A droplet can also be observed from the transient fuel spray as a group immersed in the continuous phase. Figure 4.33 shows the raw image sequence of S20 spray formation and with edge detection. S20 was chosen to demonstrate the spray characteristics in this section at a temperature of 650°C in the optical constant volume chamber. As evident from the figure, the spray loses its pattern and turn to mist a few centimetres from the injector nozzle. The micro-explosion phenomenon was expected to increase the spray spread at X-axis which will be revealed in the spray quantification such as spray cone angle, spray spread and spray penetration.

The edge detection method was found to be effective for the task to differentiate spray region for identification of primary and secondary atomization regime. The presence of the spray core was observed as well as visible voids within the spray. The liquid core was observed in the middle with the primary breakups. The presence of liquid core during initial injection and short liquid sheet at the end of the injection were observed. It was at this region where micro-explosion was located and presented in the previous section. The large irregular droplet created from primary atomization process breakup for the second time as spherical droplet and some of the droplet was visibly detected undergone micro-explosion phenomenon. Detail description of the finding has been presented in the previous section.

Figure 4.34 shows spray view in spectrum mode. With spectrum display, spray region located at the outskirt could be identified and characterized by fully dispersed droplet as a cloud. The cloud region is where the distribution droplet is expected to be very small with low velocity. The liquid film turns to droplet form with increasing distance from the nozzle. Visualization of the spray under spectrum mode helps not only to reveal the detailed structure of the spray but also to quantify the spray characteristics via method described in the previous section 3.5. The explanation of micro-explosion in the spray, can be more related in the interpretation of the spray characteristics through the spray spread, spray cone and spray penetration.

t=0 ms	
t=0.04 ms	
t=0.08 ms	
t=0.12 ms	
t=0.16 ms	
t=0.2 ms	
t=0.24 ms	
t=0.28 ms	
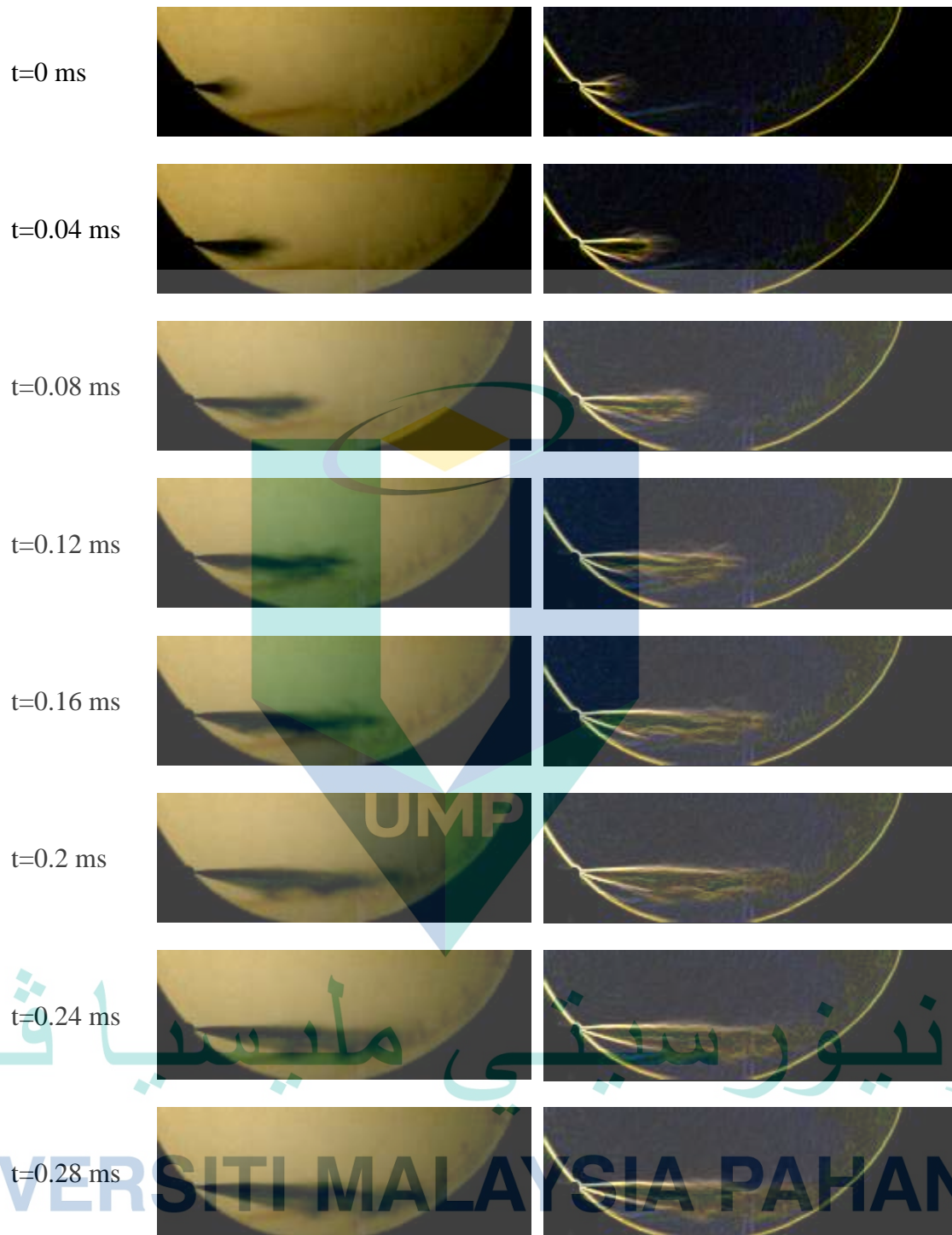
Figure 4.33   Raw Image sequence of typical spray behaviour of the emulsified fuel from S20 with edge detection at 650°C.

t=0.00ms   t=0.16ms
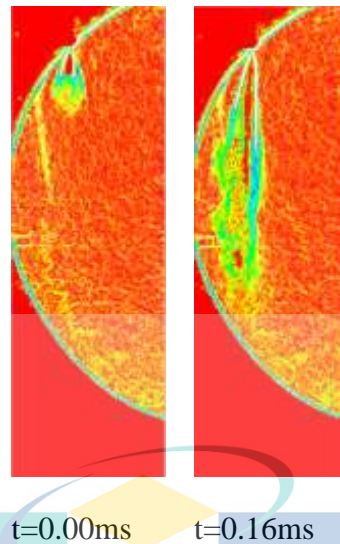
Figure 4.34   Extracted video sequence as the spectrum mode

4.3.2.1   Spray cone angle

As defined in the methodology section, the spray cone angle is important because it demonstrates the effect of the micro-explosion phenomenon on the fuel atomization process. It is widely known that wider spray cone angles are desirable because it means more coverage or dispersion of droplet in a group in the combustion chamber (Abdul Hamid, 2011). Figure 4.35 shows the spray cone angle at a temperature of 650°C. Overall, the spray cone angle of tri-fuel emulsions behaves competitively with diesel. The high temperature shows an effect on tri-fuel emulsion. At the initial stage of the injection, the spray cone angle of all tri-fuel emulsions was found higher than diesel. Incline value of the spray cone angle starts approximately at 0.2ms onward. With the increase of temperature, tri-fuel emulsion with micro-explosion phenomenon attribute improves in comparison to the status of the spray cone angle under room temperature.

The spray cone angle is one of the spray characteristics commonly presented to indicate spray improvement is achieved or not. The wider spray cone angle is typically suggested that the atomization process is satisfactorily achieved. On the other hand, reduction in the spray cone angle indicates the fuel spray atomization process is degrading for a specific reason. The finding from the spray cone angle suggests that tri-fuel emulsions improvement could be achieved and noticeable only at the beginning of the spray. Nevertheless, the spray cone angle is not the only approach available to examine fuel atomization performance. The radial distance is the other perspective that will be

presented and discussed next. The behaviour of the fuel spray is believed to directly have an impact on the combustion process. Although individual droplet may combust, spray as a form of mist typically combust as a group after the evaporation process. A similar pattern was found in the previous literature (Park, 2009). Furthermore, spray cone angle results is comparable to the recent study (Corral-Gómez, 2019).
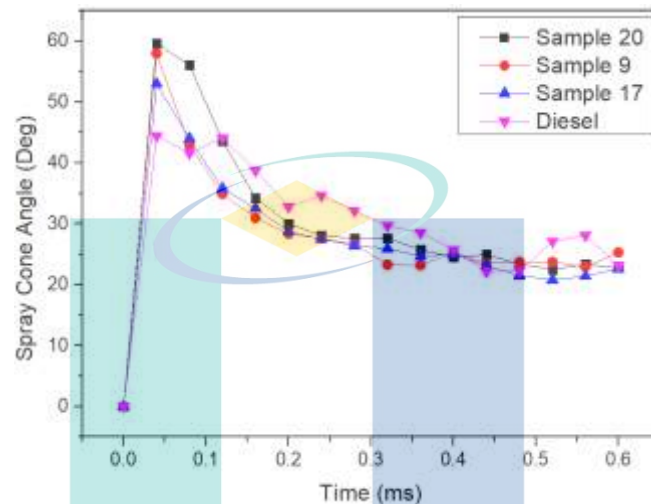
Figure 4.35   Spray cone angle under high temperature

4.3.2.2   Spray spread (the radial distance on Axis-X)

Apart from the spray cone angle, spray spread is another perspective of analysing the effect of micro-explosion phenomenon macroscopically. As defined in the methodology section, spray spread is a radial distance focusing on axial direction X. Figure 4.36 shows spray spread at axial X at 650°C temperature overtime. Overall, there was a significant improvement on the spray spread for all tri-fuel emulsions as compared to diesel. S20 lead at approximately 0.1 ms before competing by S9 at 0.25 ms. S17 appear to be in between the race. Diesel, on the other hand, starts with a low spread from the beginning of the injection. The spread rate decline at 0.4 ms before swirl up with increasing spread pattern 0.1 ms later.

Overall, there was a significant improvement on the spray spread for all tri-fuel emulsions as compared to diesel by 38.75% average enhancement. S20 lead with 40.72% average enhancement. S17 comes in second with 39.07% average enhancement leave S9 with 36.82% average enhancement. One of the explanations that cause significant spray spread improvement was puffing and micro-explosion phenomenon as observed in the

126

previous finding relative to the effect of micro-explosion phenomenon. The spread of satellite droplet as a cause of puffing inclined to spread to the X-axis direction parallel with the spray spread characteristics observed. The meaning of the finding is that low-intensity micro-explosion phenomenon or single and double side puffing caused the spray spread to increase exceeding diesel specifically at high temperature. The finding is important because despite only minor improvement was observed on the spray cone angle result, other perspectives such as spray spread or radial distance offer more positive sign and micro-explosion may have been part of the significant contributor.
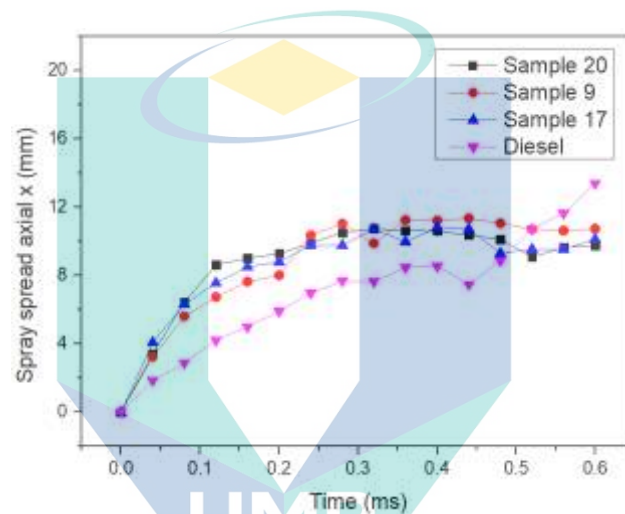
Figure 4.36   Spray spread at axial distance x under high temperature

4.3.2.3   Spray penetration

As defined in the methodological section, spray penetration is presented to acknowledge if there is any effect of micro-explosion phenomenon noticeable on the spray penetration. Spray penetration indicates the mass rate of the droplet in a group. With constant injection spray pressure, short spray penetration is expected which will be indicating fuel atomization improvement. High spray penetration, on the other hand, indicates viscous nous, heavy or large droplets. Figure 4.37 shows spray penetration of tri-fuel emulsions and diesel at high temperature. Unlike the spray penetration under room temperature, spray penetration under high temperature of tri-fuel emulsions was shorter, especially for S17 and S9. Spray penetration of diesel, on the other hand, appear shorter than tri-fuel emulsions under high temperature.

The result is consistent with other tri-fuel recent study (Corral-Gómez, 2019). From the spray penetration finding, a possible explanation for tri-fuel emulsions high

127

spray penetration in comparison to diesel could have been because of the effect of biodiesel ratio which tails the ethanol content on the physicochemical properties. As biodiesel increases the viscosity level, ethanol decreases it slightly to compete with diesel. The major finding is that the effect of puffing or low-intensity micro-explosion phenomenon could not overcome the effect of droplet component ratio influence. The meaning of the finding is that despite puffing or low-intensity micro-explosion phenomenon causes the spray spread on axial X distance while reducing the droplet size, spray penetration finding suggests that the accumulative droplet within the spray injection causing the momentum of the spray to increase. The result of the spray penetration is consistent with the previously presented finding of the micro-explosion effect on droplet bursting and deformed prone to the axial X more than axial Y. The result is also comparable to the recent study (Boggavarapu, 2019).
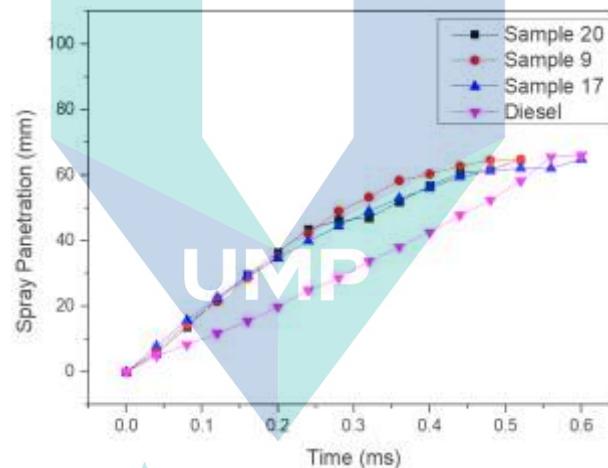
Figure 4.37   Spray penetration under high temperature

4.4   Combustion characteristics

In this section, combustion characteristics in term of combustion pressure, heat release rate, and ignition delay period under constant speed with various load were presented and compared with diesel.

4.4.1   Combustion pressure

The focus of the combustion pressure analysis is on the peak near the TDC. The combustion pressure that forces the piston down during the combustion stroke is where the engine power comes from. The combustion pressure indicates the progress of the

combustion. It was noticeable that as the load is increased, combustion peak pressure also increases. In addition, on first sight, it appears that wavy regularity after the peak pressure was detected and becoming more apparent for all samples including diesel indicating the engine experiencing knocking phenomenon. Figure 4.38 (a) shows plotted in-cylinder pressure of tri-fuel emulsions in comparison with a diesel under the no-load condition at constant speed 1800 r/min. Under the no-load condition, the in-cylinder pressure of S9 and S20 were the first two peaks to rise at 4° CA after the TDC. The in-cylinder peak pressure of S17 was observed to be the highest with 63 bar in comparison with the rest of tri-fuel emulsions including diesel at 6° CA after TDC. 1° CA after that, diesel came in as the last position with the lowest peak in-cylinder pressure with 59 bar.

Meanwhile, Figure 4.38 (b) shows plotted in-cylinder pressure of tri-fuel emulsions in comparison with a diesel under 50% load condition at constant speed 1800 r/min. S9 risen before diesel, however, both reach the peak at the same time at 5° after TDC. Diesel achieved the highest peak pressure; 70 bar among all with S20 with the lowest peak pressure; 66 bar. S17 was the last one to reach the peak pressure; 67 bar, slightly higher than S20 and almost similar peak pressure reading as S9; 67 bar. Figure 4.38 (c) shows plotted in-cylinder pressure of tri-fuel emulsions in comparison with a diesel under 100% load condition at constant speed 1800 r/min. S17 achieve the highest peak pressure; 76 bar, closely followed by S20 with 74 bar and diesel with 74 bar. S20 and diesel were the two first to rise and reach the peak pressure. The lowest peak pressure recorded was S9 with 72 bar.

The noticeable point of the minor wave observed after the peak pressure means the engine experience light knock phenomenon. The intensity of the knock was not that severe and was not characterized as a heavy knock considering the amplitude pressure frequency fluctuation detected was fairly low. It was inevitable as it was not only fuel factor could influence knocking but also the engine design. Since the wave can be detected even with diesel as a reference fuel, the author decided to disregard the engine sensitivity to such light knocking due to any possible fuel factor. The increase of the combustion pressure as the load is increased is the effect of heat expansion. The same volume with the increase in temperature which then causes the pressure to rise.

Figure 4.39 shows the simplify version of tri-fuel emulsions in-cylinder peak pressure compared to pure diesel at different load. At the end of the ignition delay period,

the pressure curve is separated from the compression curve. The uncontrolled combustion normally starts at that point. Onward, the sudden and rapid pressure rise are due to the continuous fuel supply. The delay period should affect the in-cylinder pressure because of the heterogeneous mixture.
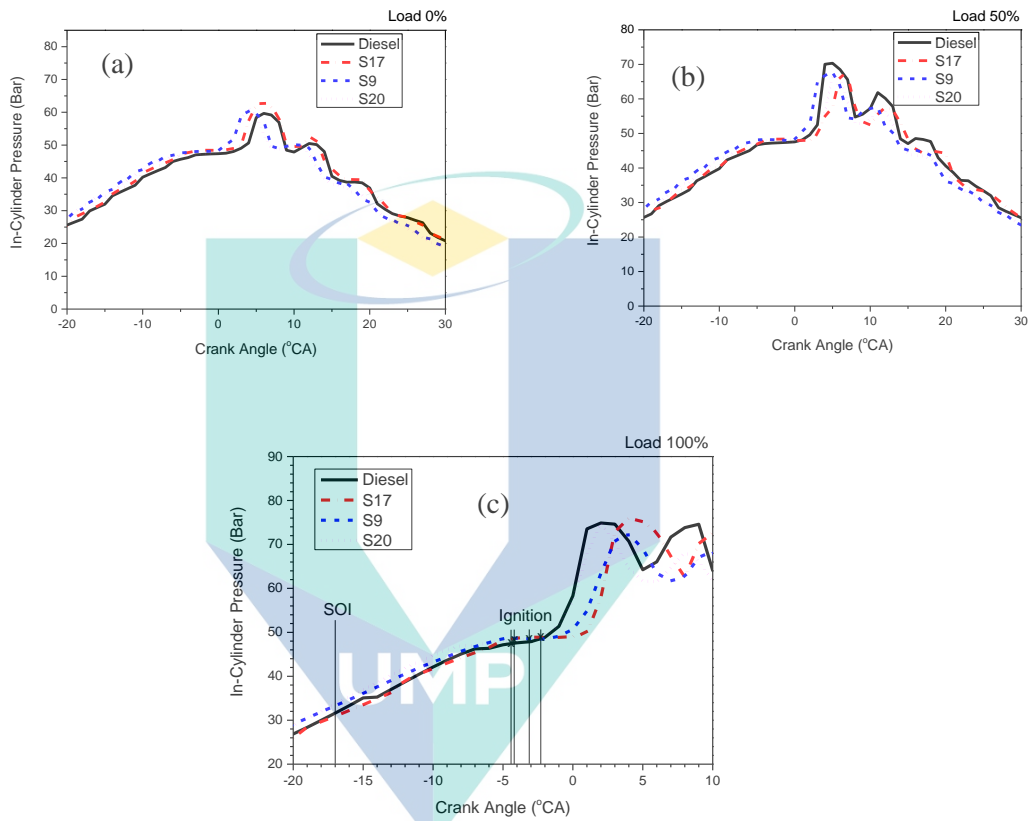
Figure 4.38　Combustion pressure from 0% load to 100% load
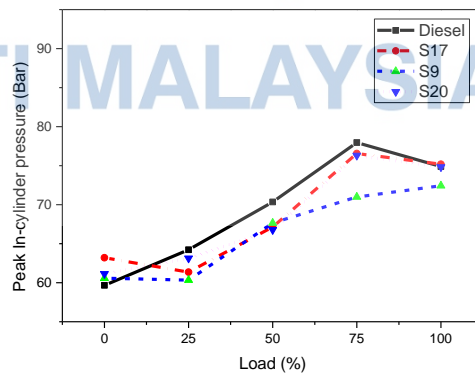
Figure 4.39　Peak combustion pressure of different loads

130

The increase in pressure depends on that ignition delay period. Late in combustion resultant in the increase of fuel quantity before the burning of fuel can take place. Such a condition affects the smooth running of the engine. The early rise of peak pressure due to short ignition delay while the late rise of peak pressure because of the long period of ignition delay. High or low peak pressure depends on the process of fuel rate burning with time. The best way is to look at the HRR plot as presented next.

4.4.2 Heat release rate

The rate of fuel burning is important because it determines the effectiveness of the combusted fuel in the CI engine. Ignition delay period can be obtained from the HRR plot. Figure 4.40 (a) shows the ignition delay period obtained from the HRR plot for no-load at a constant speed. From the point of injection starts till the start of the combustion, the HRR exhibit negative value as expected. The heat release change to positive value from negative value indicates the start of combustion. During the period of delay, S9 and S20 went low while S17 and diesel steadily slightly just below the positive line waiting for the moment to rise and combust. HRR S9 and S20, however, initiate the rise earlier than S17 and diesel.

Figure 4.40 (b) shows where the ignition starts for each sample. At slightly 2° BTDC, combustion starts for S20 and S9. Diesel and S17 start approximately 1° CA later. Tri-fuel emulsion came up with the shortest ignition delay period in comparison with diesel. Meanwhile, S20 starts ignited before S9, diesel and S17. With no load, peak HRR of S17 was observed to be the highest with 4,5276 J/CA^o in comparison with the rest of the samples including diesel. Diesel came in second place with3,9796 J/CA^o 13.77% lower than S17. The trend indicates that short ignition delay yield low HRR peak while long ignition delay yields high peak HRR.

Figure 4.40 (c) shows plotted HRR of tri-fuel emulsions in comparison with a diesel under 50% load condition at constant speed 1800 r/min while Figure 4.40 (d) shows detail that focuses on the point where the ignition starts for each sample with 50% load. S9 was the first to ignite before the rest of the fuels. However, S9 achieved the lowest rate of heat release with 5,2133 J/CA^o. Diesel starts to burn after S9 and achieved the highest HRR in comparison to the rest of tri-fuel emulsions with 6,1554 J/CA^o. S17 peak came in second place with 58321 J/CA^o before S20 with 5,4632 J/Ca^o.

Figure 4.40 (e) shows plotted HRR of tri-fuel emulsions in comparison with a diesel under 100% load condition at constant speed 1800 r/min while Figure 4.40 (f) shows detail to focus on the point where the ignition starts for each sample. S17 was the last to ignite. However, S17 achieved the highest HRR peak with 70564 J/CA°. Diesel was the first to ignite among all and gets the second-highest HRR peak with 62989 J/CA°, S20 ignited almost at the same period as diesel nonetheless obtain the lowest HRR peak with 56468 J/CA°. Overall, it was noticeable that as load increased, the peak of the HRR also increases.

During the ignition delay period, heat release curve exhibit negative value is due to fuel atomization and evaporation effect consistent with the previous study (Lakshminarayanan et al., 2010). The effect of the micro-explosion phenomenon can be seen with the period of ignition delay reduced with 0% load. The physical delay part where the result of fuel atomization and time is taken for the air-fuel to mix happening in the ignition delay period. Heat release during the combustion provides energy for the internal combustion engine. Combustion cannot immediately start after the injection of the fuel. There is a slight delay period that was observed before combustion could really start. It was between the start of injection and the start of detectable HRR rise. The period is commonly known as the ignition delay period.

As the fuel got injected, the fuel going through the physical delay period. Physical delay period means the mixing process takes place. In the mixing process, primary and secondary atomization plays a vital role to ensure the fuel could mix with air fast enough to allow the chemical reaction to take place. Fuel atomization is simply encouraging that mixing. The fuel changes the state from liquid to vapour form. The fuel cannot really proceed to chemical reaction process fast enough without the fuel change it states to vapour form and mix with air. It is vital for the fuel to be properly atomized before combustion can take place. The fuel has to be in vapour form fast enough so that combustion can take place.

If the ignition delay is very short, a short quantity of fuel will accumulate in liquid or vapour form in the combustion chamber. The relatively small amount of fuel will be accumulated in this case. Longer ignition delay period means a greater amount of fuel is accumulated in the chamber without burning. When burning starts, immediate burning will cause high range pressure and temperature rate than usual. This will cause an

unsmooth burning process and as a result engine knock become amplified and intense. The sudden rise of pressure can be seen due to sudden accumulated fuel combustion.
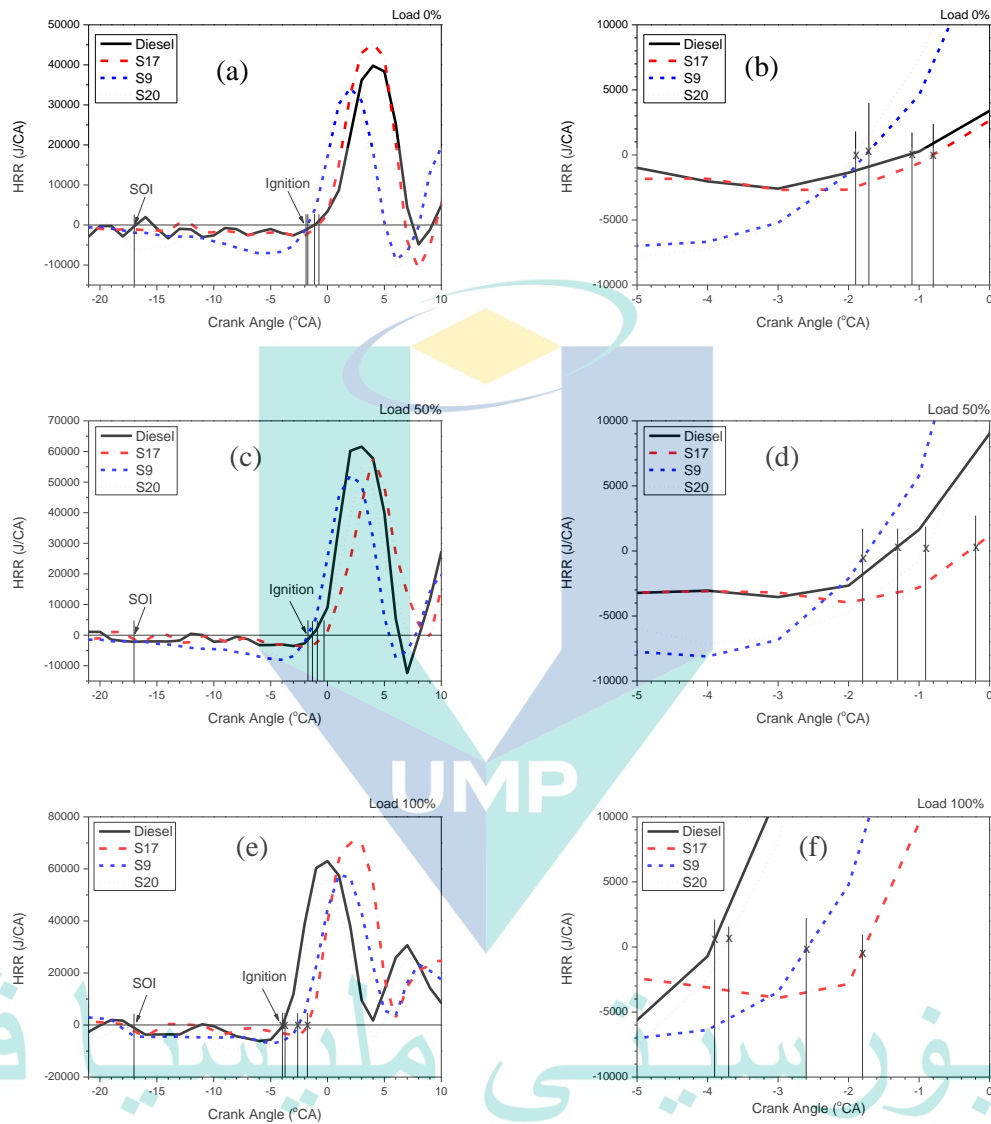
Figure 4.40   HRR with the point of ignition at (a), (b) 0% load, (c), (d) 50% load and (e), (f) 100% load

Diesel, on the other hand, should be expected on the rising trend all the way during the ignition delay period without disturbance. At all load, unlike diesel, tri-fuel emulsions should be expected with the trend of a slight decrease of in-cylinder temperature at the end of the ignition delay period because of the latent heat of evaporation effect. The latent heat of evaporation effect can come from the attribute of ethanol content from the tri-fuel emulsions consistent with the previous study (Hulwan, 2011; Mendes Guedes et al., 2018; S. A. Shahir, 2014) The cooling effect should reduce the in-cylinder temperature slightly before combustion starts. The droplet within the spray went through the change of states from liquid form to the gas phase and require a certain amount of energy. During the process, instead of temperature keeps on in hiking state, the temperature will not change and the heat goes directly into the process of change of state.

4.4.3 Ignition delay period

Ignition delay period derived from the HRR is important to the study. Figure 4.41 shows the ignition delay period of tri-fuel emulsions in comparison with a diesel under various load condition at constant speed 1800 r/min. Overall, with no load, the total period of ignition delay for tri-fuel emulsions appeared to be slightly lower than diesel. However, under different loads, tri-fuel emulsions behave a little differently. With load, tri-fuels require an additional period to ignite compared to diesel. At all load condition, S17 has the highest ignition delay period. Under the no-load condition, S9 and S20 appear to have shorter ignition delay period than diesel. As load is increased, the pattern indicates a reduction of the delay period. The shortest ignition delay period can be seen with 100% load.

The other part of the ignition delay is a chemical delay, which means the chemical reaction process. It is sometimes known as the interaction process or pre-flame period. Practically, a chemical delay period is more than a physical delay. However, at a high temperature, the physical delay is more than a chemical delay. As observed, the injection period is more than the ignition delay period. That means, more fuel is injected even after the ignition delay period ends. Not all droplet injected in the engine went through the ignition delay period. Only a few of the first injection has to go through the delay period. There is no time gap for each fuel that got injected after the ignition delay period ends.

134

The finding of the effect of load in shortening the ignition delay period is as expected. As load is increased, the pattern indicates a reduction of delay period probably due to the high temperature exceeding the norm and all the fuels only have limited period than usual to evaporate and ignite. At this stage, secondary atomization is less priority and the cooling effect is much needed. The result is parallel to other studies that highlight linearity approximation on the decrease of the delay period with the increasing load.

The percentage of ethanol content in tri-fuel emulsion slightly increase the ignition delay period was due to ethanol content consistent with the literature (Pradelle et al., 2019b; Tse, 2015). In addition, the estimated ethanol low-value cetane number could have led to low in-cylinder temperature and pressure build. Consequently, it is possible that it takes more time for overall tri-fuel emulsions to ignite. Recall from the literature review section, during the ignition delay period, because of the variance outcome of fuel atomization, evaporation and air-fuel mixing process, the possible variation of equivalence ratio either locally over lean or locally over rich mix is usually occurred. As a result, even with no load, the air-fuel ratio is increased (lean), as a result, low temperature, and ignition delay is expected to increase. On the other hand, with an increase in load, the air-fuel ratio is lower (rich), combustion temperature increase and ignition delay period reduced. The result is comparable to the recent study (Venu, 2019).
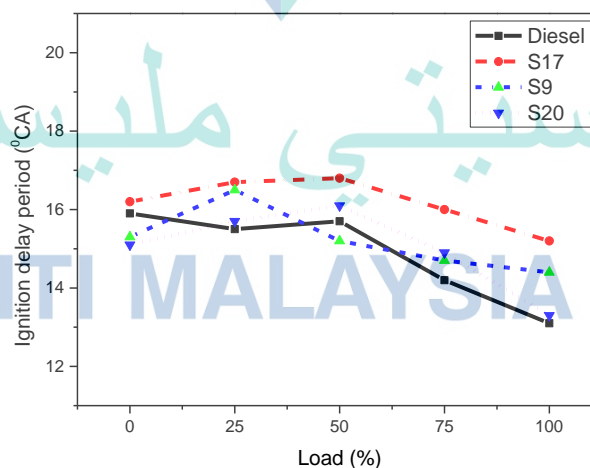
Figure 4.41   Ignition delay period of tri-fuel emulsion against diesel under various load condition

Overall, the research has accomplished all the objectives. Recapitulation, the results of the effect of the fuel preparation control factors on the selected physicochemical properties has given insight to the factors which is significant in considering the second objective. The results of the micro-explosion phenomenon manifestation on the spray droplets of tri-fuel emulsions from the second objective indicated reliability of the secondary atomization process which was not discovered before. Meanwhile, the third objective on the spray characteristics is a macroscopic perspective that are useful for interpretation of tri-fuel emulsions with micro-explosion phenomenon attribute. The discovery of the combustion characteristics in the end is hoped can be a thrust for tri-fuel emulsions realizational thought for practical consideration in the future. The research should not stop here but to proceed further to the next level.
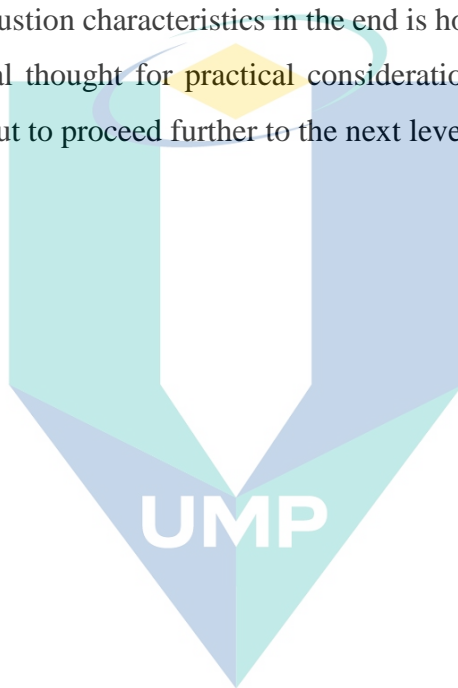
CHAPTER 5

CONCLUSION

5.1   Introduction

This chapter draws a conclusion which answers the research question. The first objective deal with the effect of specific control factor on the fuel characterization. Next objective considers the quantitative and photographic analysis of micro-explosion phenomenon effect on single droplet couple with macroscopic perspective via spray characteristic. Final objective proceeds with the sneak combustion characteristics and the engine emission outcome.

5.2   Conclusions

The first objective of the study was fully met. The effect of proportion ratio and ultrasonic emulsifying setting on the physicochemical properties of tri-fuel emulsion was synthesized. Statistical analysis was done to present the interaction between control factors related to agitation mechanisms such as amplitude and cycle as well as control factors related to formulation ratios such as percentage content of ethanol and biodiesel. It was found that the Interaction between control factors exist and affect the physicochemical properties of the tri-fuel emulsion prepared. Density, viscosity and surface tension are the significant properties relevant to the fuel atomization process. Furthermore, droplet quality before and after going through the fuel injection system that previously merely presumed to be identical have been compared. Morphology basis of tri-fuel emulsion droplet before and after the injection has been confirmed. The conclusion is made to justify meeting the first objective as follow:

i.   Percentage of ethanol content has a significant effect on tri-fuel emulsion physicochemical properties without any significant interaction with other control factors with the P-Value of 0.0023.

ii.   Ethanol influence to the change in density by 1.54%.

137

iii. Two control factor interaction, mainly ethanol and biodiesel were detected statistically on the viscosity reading with the P-value < 0.0001.

iv. Ethanol influence strongly the viscosity and the significant decrease of the viscosity due to the ethanol effect can be compensated by the biodiesel opposite effect.

v. Cycle setting plays a significant role to balance the magnitude of the interaction between biodiesel and ethanol effect on viscosity.

vi. Interaction between cycle setting and ethanol percentage to the decrease of surface tension was statistically significant with P-value 0.0383.

vii. High cycle setting deescalates the decrease of the surface tension as a result of the ethanol effect.

viii. Amplitude plays a significant role in manipulating biodiesel effect on the increase or decrease of the surface tension.

ix. When high biodiesel fraction was combined with low amplitude setting, the average droplet size increased dramatically by 80%. However, high amplitude setting could fix this and aid for slight further size refinement down to 0.54 µm which was the finest average droplet size.

x. The finest average droplet size that was obtained was 0.51 µm via low amplitude setting combines with high cycle setting. Maintaining a low amplitude setting while reducing the cycle setting causes the size to increase dramatically by 372%.

Based on the results of the first objective and the novelty discussed in chapter 2, samples S9, S17 and S20 are selected to conduct the study of objective 2, 3 and 4. In the second objective, the presence and sequence of micro-explosion phenomenon was investigated. The second objective was fully met as the impact of the micro-explosion was revealed and the image of droplet undergone micro-explosion phenomenon was located, processed and quantified. The specific diameter, centricity change, axial X and Y spread and the surface area change as a result of the micro-explosion phenomenon was exposed. Furthermore, the finding removed the positional ambiguity of the micro-explosion phenomenon possible occurrence in CI engine. The most important finding

138

from the second objective was the complexity of the breakup process caused by the micro-explosion phenomenon. The common structure of droplet gone through micro-explosion phenomenon that was previously unknown was revealed. The following conclusion was drawn pertaining to meeting the second objective of the research: -

i. Low-intensity category of micro-explosion phenomenon with a single side and double side puffing were observed.

ii. The micro-explosion observed in this study was classified under low-intensity type known as puffing.

iii. The micro-explosion phenomenon can accelerate the droplet fragmentation process in addition to the influence of velocity which was caused by the injection pressure and the high-temperature setting.

iv. Without collision, an individual droplet that undergone puffing either single side or double side category will return back to its original shape.

v. The spread of satellite droplet as a cause of puffing inclined to spread to the X-axis direction.

In the third objective, the effect of the micro-explosion phenomenon to the spray characteristics was assessed. High-pressure spray characteristics of tri-fuel emulsion under low and high temperature were compared namely spray cone angle, spray spread – axial distance and spray penetration. The information obtained from the second objective was acknowledged and the following conclusion was drawn to justify meeting the third objective of the research:

i. The spread of satellite droplet as a cause of puffing inclined to spread to the X-axis direction was parallel with the spray spread characteristics observed.

ii. There was a significant improvement on the spray spread for all tri-fuel emulsions as compared to diesel by 38.75% overall average enhancement.

iii. S20 lead with 40.72% average enhancement. S17 comes in second with 39.07% average enhancement leave S9 with 36.82% average enhancement.

139

In the fourth objective, the effect of the micro-explosion phenomenon to the tri-fuel emulsion combustion characteristics was evaluated. Result from single cylinder CI engine test, HRR and in-cylinder pressure were analysed. The following conclusion was drawn to justify the meeting of the fourth research objective:

i. During the ignition delay period, HRR curve exhibit negative value was due to atomization and evaporation effect.

ii. With 0% load, peak HRR of tri-fuel emulsion specifically S17 was the highest exceeding diesel by 13.77%.

iii. Another significant difference during the ignition delay period was that all tri-fuel emulsions cool down slightly before actual ignition as a result of latent heat of evaporation effect and it was not the case for diesel.

iv. With 0% load, in-cylinder pressure for all tri-fuel emulsions during the ignition delay period exceed diesel.

v. With 0% load, peak in-cylinder pressure for all tri-fuel emulsions exceeds diesel with S17 to be the highest, 63 bar.

5.3 Shortcoming and limitation

Obtain heat using the actual high compression method could have been the ideal method. However, in this experiment, the source of heat was coming from the heater. To imitate the heat source coming from the actual high compression is not feasible considering interference and the unfiltered factor which may distort the objective of the study. In addition, informative description of the micro-explosion phenomenon could not be exposed via such method due to limitation of space and visually inaccessible. Potentially, considering such an approach will require customized heat resistance optical glass, piston, connecting rod and other related apparatus with special heat treatment material. Thus, may concur high cost.

5.4 Recommendation and future direction

The recommendation work for future research are listed as follows: -

   i.   Bioethanol

  ii.   Performance and emission

 iii.   Use laser technology to track and quantify undetected micro-explosion in the highly populated droplet in the middle region of the spray.

 iv.   Study the event using wave signal analysis or known as acoustic system detection method.

  v.   There are still a few other factors that can be considered in future study. Include high pressure in the combustion chamber.

 vi.   Study the temperature change as a result of micro-explosion phenomenon subject to variation of fuel injection pressure using a highly sensitive thermocouple.

 vii.   Study the tri-fuel emulsion boiling nucleation initiation and from a chemistry point of view.

viii.   To uncover the distinction between physical delay and chemical reaction period of tri-fuel emulsion in the combustion stage.

 ix.   To Compare tri-fuel emulsion spray characteristics (without combustion) with combust flame behaviour.

  x.   To track the common spot of ignition commencement within the heterogeneous ignition charge of tri-fuel emulsion and analyse statistically the possible prediction of the repeatability occurrence spot.

REFERENCES

A. Ismael, M., Heikal, M., A. Aziz, A., Crua, C., El-Adawy, M., Nissar, Z., … Firmansyah. (2018). Investigation of Puffing and Micro-Explosion of Water-in-Diesel Emulsion Spray Using Shadow Imaging. *Energies*, *11*(9), 2281. https://doi.org/10.3390/en11092281

Abdul Hamid, A. H. (2011). Spray cone angle and air core diameter of hollow cone swirl rocket injector. *IIUM Engineering Journal*, *12*(3), 1–9. https://doi.org/10.31436/iiumej.v12i3.66

Abidin, M. I. I. Z., Raman, A. A. A., & Nor, M. I. M. (2013). Review on Measurement Techniques for Drop Size Distribution in a Stirred Vessel. *Industrial & Engineering Chemistry Research*, *52*(46), 16085–16094. https://doi.org/10.1021/ie401548z

Abu-Hamdeh, N. H., & Alnefaie, K. A. (2015). A comparative study of almond and palm oils as two bio-diesel fuels for diesel engine in terms of emissions and performance. *Fuel*, *150*(February), 318–324. https://doi.org/10.1016/j.fuel.2015.02.040

Adam, A., Inukai, N., Kidoguchi, Y., Miwa, K., & Miyashiro, S. (2007). A Study on Droplets Evaporation at Diesel Spray Boundary during Ignition Delay Period. *SAE Paper*, 1379–1389. https://doi.org/10.4271/2007-01-1893

Adam, A., Yatsufusa, T., Gomi, T., Irie, N., & Kidoguchi, Y. (2009). Analysis of Droplets Evaporation Process of Diesel Spray at Ignition Delay Period using Dual Nano-spark Shadowgraph Photography Method. *SAE Int. J. Engines*, *2*, 703–711. https://doi.org/10.4271/2009-32-0017

Afshar Ghotli, R., Abdul Aziz, A. R., & Ibrahim, S. (2017). Effect of Various Curved-Blade Impeller Geometries on Drop Size in a Liquid–Liquid Stirred Vessel. *Chemical Engineering Communications*, *204*(8), 884–896. https://doi.org/10.1080/00986445.2017.1325738

Agarwal, A. K., Gupta, T., Bothra, P., & Shukla, P. C. (2015). Emission profiling of diesel and gasoline cars at a city traffic junction. *Particuology*, *18*, 186–193. https://doi.org/10.1016/j.partic.2014.06.008

Ağbulut, Ü., Sarıdemir, S., & Albayrak, S. (2019). Experimental investigation of combustion, performance and emission characteristics of a diesel engine fuelled with diesel–biodiesel–alcohol blends. *Journal of the Brazilian Society of Mechanical Sciences and Engineering*, *41*(9), 389. https://doi.org/10.1007/s40430-019-1891-8

Ağbulut, Ü., Sarıdemir, S., & Karagöz, M. (2020). Experimental investigation of fusel oil (isoamyl alcohol) and diesel blends in a CI engine. *Fuel*, *267*(January), 117042. https://doi.org/10.1016/j.fuel.2020.117042

Al Basir, F., & Roy, P. K. (2015). Effects of Temperature and Stirring on Mass Transfer to Maximize Biodiesel Production from Jatropha curcas Oil: A Mathematical Study. *International Journal of Engineering Mathematics*, *2015*, 1–9. https://doi.org/10.1155/2015/278275

Ali, O. M., Mamat, R., Abdullah, N. R., & Abdullah, A. A. (2016). Analysis of blended fuel properties and engine performance with palm biodiesel–diesel blended fuel. *Renewable Energy*, *86*, 59–67. https://doi.org/10.1016/j.renene.2015.07.103

Alptekin, E. (2017). Emission, injection and combustion characteristics of biodiesel and oxygenated fuel blends in a common rail diesel engine. *Energy*, *119*, 44–52. https://doi.org/10.1016/j.energy.2016.12.069

Alvarado, J. L., & Nam, H. (2012). Experimental Investigation of Microexplosion Phenomena in Emulsified Vegetable Oil-Methanol Blends. *Volume 2: Heat Transfer Enhancement for Practical Applications; Fire and Combustion; Multi-Phase Systems; Heat Transfer in Electronic Equipment; Low Temperature Heat Transfer; Computational Heat Transfer*, 205–212. https://doi.org/10.1115/HT2012-58311

Anderson, M. J., Whitcomb, P. J., Kraber, S. L., & Adams, W. (2018). Stat-Ease Handbook for Experimenters (Version 11). *Stat-Ease,Inc.*

Annamalai, M., Dhinesh, B., Nanthagopal, K., SivaramaKrishnan, P., Isaac JoshuaRamesh Lalvani, J., Parthasarathy, M., & Annamalai, K. (2016). An assessment on performance, combustion and emission behavior of a diesel engine powered by ceria nanoparticle blended emulsified biofuel. *Energy Conversion and Management*, *123*, 372–380. https://doi.org/10.1016/j.enconman.2016.06.062

Anwar, M., Rasul, M., Ashwath, N., & Rahman, M. (2018). Optimisation of Second-Generation Biodiesel Production from Australian Native Stone Fruit Oil Using Response Surface Method. *Energies*, *11*(10), 2566. https://doi.org/10.3390/en11102566

Armas, O., Martínez-Martínez, S., & Mata, C. (2011). Effect of an ethanol–biodiesel–diesel blend on a common rail injection system. *Fuel Processing Technology*, *92*(11), 2145–2153. https://doi.org/10.1016/j.fuproc.2011.06.010

Atabani, A. E., Silitonga, A. S., Badruddin, I. A., Mahlia, T. M. I., Masjuki, H. H., & Mekhilef, S. (2012). A comprehensive review on biodiesel as an alternative energy resource and its characteristics. *Renewable and Sustainable Energy Reviews*, *16*(4), 2070–2093. https://doi.org/10.1016/j.rser.2012.01.003

Avulapati, M. M., Ganippa, L. C., Xia, J., & Megaritis, A. (2016). Puffing and micro-explosion of diesel–biodiesel–ethanol blends. *Fuel*, *166*, 59–66. https://doi.org/10.1016/j.fuel.2015.10.107

Avulapati, M. M., Megaritis, T., Xia, J., & Ganippa, L. (2019). Experimental understanding on the dynamics of micro-explosion and puffing in ternary emulsion droplets. *Fuel*, *239*(May 2018), 1284–1292. https://doi.org/10.1016/j.fuel.2018.11.112

Aydın, F., & Öğüt, H. (2017). Effects of using ethanol-biodiesel-diesel fuel in single cylinder diesel engine to engine performance and emissions. *Renewable Energy*, *103*, 688–694. https://doi.org/10.1016/j.renene.2016.10.083

Badock, C., Wirth, R., Fath, A., & Leipertz, A. (1999). Investigation of cavitation in real size diesel injection nozzles. *International Journal of Heat and Fluid Flow*, *20*(5), 538–544. https://doi.org/10.1016/S0142-727X(99)00043-0

Barabas, I., & Todoru, I.-A. (2011). Utilization of Biodiesel-Diesel-Ethanol Blends in CI Engine. In *Biodiesel- Quality, Emissions and By-Products* (p. 21). https://doi.org/10.5772/27137

Barabás, I., Todoruţ, A., & Băldean, D. (2010). Performance and emission characteristics of an CI engine fueled with diesel–biodiesel–bioethanol blends. *Fuel*, *89*(12), 3827–3832. https://doi.org/10.1016/j.fuel.2010.07.011

Barad, M. (2018). *Strategies and Techniques for Quality and Flexibility* (P. Janusz Kacprzyk, Polish Academy of Sciences, Systems Research Institute, Warsaw, ed.). https://doi.org/10.1007/978-3-319-68400-0

Bedford, F., Rutland, C., Dittrich, P., Raab, A., & Wirbeleit, F. (2000). Effects of Direct Water Injection on DI Diesel Engine Combustion. *SAE Paper*, *2000-01–29*, 1–10. https://doi.org/https://doi.org/2000-01-29

Bergthorson, J. M., & Thomson, M. J. (2015). A review of the combustion and emissions properties of advanced transportation biofuels and their impact on existing and future engines. *Renewable and Sustainable Energy Reviews*, *42*, 1393–1417. https://doi.org/10.1016/j.rser.2014.10.034

Bhattacharjee, S. (2016). DLS and zeta potential – What they are and what they are not? *Journal of Controlled Release*, *235*, 337–351. https://doi.org/10.1016/j.jconrel.2016.06.017

Bidita, B. S., Suraya, A. R., Shazed, M. A., Mohd Salleh, M. A., & Idris, A. (2014). Influence of Fuel Additive in the Formulation and Combustion Characteristics of Water-in-Diesel Nanoemulsion Fuel. *Energy & Fuels*, *28*(6), 4149–4161. https://doi.org/10.1021/ef5002259

Bidita, B. S., Suraya, A. R., Shazed, M. A., Salleh, M. A. M., & Idris, A. (2016). Preparation, characterization and engine performance of water in diesel nanoemulsions. *Journal of the Energy Institute*, *89*(3), 354–365. https://doi.org/10.1016/j.joei.2015.03.004

Boggavarapu, P., & Ravikrishna, R. V. (2019). Evaporating spray characteristics of a diesel-ethanol micro-emulsion. *Fuel*, *246*(October 2018), 104–107. https://doi.org/10.1016/j.fuel.2019.02.035

Botero, M. L., Huang, Y., Zhu, D. L., Molina, A., & Law, C. K. (2012). Synergistic combustion of droplets of ethanol, diesel and biodiesel mixtures. *Fuel*, *94*, 342–347. https://doi.org/10.1016/j.fuel.2011.10.049

Calam, A., Solmaz, H., Yılmaz, E., & İçingür, Y. (2019). Investigation of effect of compression ratio on combustion and exhaust emissions in A HCCI engine. *Energy*, *168*, 1208–1216. https://doi.org/10.1016/j.energy.2018.12.023

Califano, V., Calabria, R., & Massoli, P. (2014). Experimental evaluation of the effect of emulsion stability on micro-explosion phenomena for water-in-oil emulsions. *Fuel*, *117*(PART A), 87–94. https://doi.org/10.1016/j.fuel.2013.08.073

Caliskan, H., & Mori, K. (2017). Environmental, enviroeconomic and enhanced thermodynamic analyses of a diesel engine with diesel oxidation catalyst (DOC) and diesel particulate filter (DPF) after treatment systems. *Energy*, *128*, 128–144. https://doi.org/10.1016/j.energy.2017.04.014

Campos-Fernández, J., Arnal, J. M., Gómez, J., & Dorado, M. P. (2012). A comparison of performance of higher alcohols/diesel fuel blends in a diesel engine. *Applied Energy*, *95*, 267–275. https://doi.org/10.1016/j.apenergy.2012.02.051

Cheenkachorn, K., & Fungtammasan, B. (2010). An Investigation of Diesel-Ethanol-Biodiesel Blends for Diesel Engine: Part 1. Emulsion Stability and Fuel Properties. *Energy Sources, Part A: Recovery, Utilization, and Environmental Effects*, *32*(7), 637–644. https://doi.org/10.1080/15567030903059608

Chen, G.-B., Li, Y.-H., Lan, C.-H., Lin, H.-T., & Chao, Y.-C. (2017). Micro-explosion and burning characteristics of a single droplet of pyrolytic oil from castor seeds. *Applied Thermal Engineering*, *114*, 1053–1063. https://doi.org/10.1016/j.applthermaleng.2016.12.052

Chen, G., & Tao, D. (2005). An experimental study of stability of oil–water emulsion. *Fuel Processing Technology*, *86*(5), 499–508. https://doi.org/10.1016/j.fuproc.2004.03.010

Cho, P., Law, C. K., & Mizomoto, M. (1991). Effect of Pressure on the Micro-explosion of Water/Oil Emulsion Droplets Over a Hot Plate. *Journal of Heat Transfer*, *113*(1), 272–274. https://doi.org/10.1115/1.2910545

Corral-Gómez, L., Rubio-Gómez, G., Martínez-Martínez, S., & Sánchez-Cruz, F. A. (2019). Effect of diesel-biodiesel-ethanol blends on the spray macroscopic parameters in a common-rail diesel injection system. *Fuel*, *241*(December 2018), 876–883. https://doi.org/10.1016/j.fuel.2018.12.081

Costello, S., Attfield, M. D., Lubin, J. H., Neophytou, A. M., Blair, A., Brown, D. M., … Silverman, D. T. (2018). Ischemic Heart Disease Mortality and Diesel Exhaust and Respirable Dust Exposure in the Diesel Exhaust in Miners Study. *American Journal of Epidemiology*, *187*(12), 2623–2632. https://doi.org/10.1093/aje/kwy182

Datta, A., & Mandal, B. K. (2016). Impact of alcohol addition to diesel on the performance combustion and emissions of a compression ignition engine. *Applied Thermal Engineering*, *98*, 670–682. https://doi.org/10.1016/j.applthermaleng.2015.12.047

Datta, A., Palit, S., & Mandal, B. K. (2014). An experimental study on the performance and emission characteristics of a CI engine fuelled with Jatropha biodiesel and its blends with diesel. *Journal of Mechanical Science and Technology*, *28*(5), 1961–1966. https://doi.org/10.1007/s12206-014-0344-7

145

de França, H. H., da Silva, N. C., & Honorato, F. A. (2019). Evaluation of diesel exhaust fluid (DEF) using near-infrared spectroscopy and multivariate calibration. *Microchemical Journal*, *150*(August), 104155. https://doi.org/10.1016/j.microc.2019.104155

Dunmore, R. E., Hopkins, J. R., Lidster, R. T., Lee, J. D., Evans, M. J., Rickard, A. R., … Hamilton, J. F. (2015). Diesel-related hydrocarbons can dominate gas phase reactive carbon in megacities. *Atmospheric Chemistry and Physics*, *15*(17), 9983–9996. https://doi.org/10.5194/acp-15-9983-2015

Dürre, P. (2007). Biobutanol: An attractive biofuel. *Biotechnology Journal*, *2*(12), 1525–1534. https://doi.org/10.1002/biot.200700168

E, J., Zhao, X., Qiu, L., Wei, K., Zhang, Z., Deng, Y., … Liu, G. (2019). Experimental investigation on performance and economy characteristics of a diesel engine with variable nozzle turbocharger and its application in urban bus. *Energy Conversion and Management*, *193*(April), 149–161. https://doi.org/10.1016/j.enconman.2019.04.062

Ejim, C. E., Rahman, M. A., Amirfazli, A., & Fleck, B. A. (2010). Effects of liquid viscosity and surface tension on atomization in two-phase, gas/liquid fluid coker nozzles. *Fuel*, *89*(8), 1872–1882. https://doi.org/10.1016/j.fuel.2010.03.005

EL-Seesy, A. I., & Hassan, H. (2019). Combustion Characteristics of a Diesel Engine Fueled by Biodiesel-Diesel-N-Butanol Blend and Titanium Oxide Additives. *Energy Procedia*, *162*, 48–56. https://doi.org/10.1016/j.egypro.2019.04.006

Elsanusi, O. A., Roy, M. M., & Sidhu, M. S. (2017). Experimental Investigation on a Diesel Engine Fueled by Diesel-Biodiesel Blends and their Emulsions at Various Engine Operating Conditions. *Applied Energy*, *203*, 582–593. https://doi.org/10.1016/j.apenergy.2017.06.052

Fahd, M. E. A., Wenming, Y., Lee, P. S., Chou, S. K., & Yap, C. R. (2013). Experimental investigation of the performance and emission characteristics of direct injection diesel engine by water emulsion diesel under varying engine load condition. *Applied Energy*, *102*, 1042–1049. https://doi.org/10.1016/j.apenergy.2012.06.041

Farzad, R., Puttinger, S., Pirker, S., & Schneiderbauer, S. (2018). Investigation of droplet size distribution for liquid-liquid emulsions in Taylor-Couette flows. *Journal of Dispersion Science and Technology*, *39*(2), 250–258. https://doi.org/10.1080/01932691.2017.1312431

Fayyazbakhsh, A., & Pirouzfar, V. (2017). Comprehensive overview on diesel additives to reduce emissions, enhance fuel properties and improve engine performance. *Renewable and Sustainable Energy Reviews*, *74*(October 2016), 891–901. https://doi.org/10.1016/j.rser.2017.03.046

Fenouillot, F., Cassagnau, P., & Majesté, J.-C. (2009). Uneven distribution of nanoparticles in immiscible fluids: Morphology development in polymer blends. *Polymer*, *50*(6), 1333–1350. https://doi.org/10.1016/j.polymer.2008.12.029

Fernando, S., & Hanna, M. (2004). Development of a Novel Biofuel Blend Using Ethanol−Biodiesel−Diesel Microemulsions: EB-Diesel. *Energy & Fuels*, *18*(6), 1695–1703. https://doi.org/10.1021/ef049865e

Fischer, K., & Schmidt, M. (2016). Pitfalls and novel applications of particle sizing by dynamic light scattering. *Biomaterials*, *98*, 79–91. https://doi.org/10.1016/j.biomaterials.2016.05.003

Fu, G., Zhao, C., Liu, B., Zhang, F., Pang, S., & Li, Y. (2012). Investigation on the combustion characteristics of a diesel engine fueled with diesel–azides blends. *Applied Energy*, *91*(1), 98–102. https://doi.org/10.1016/j.apenergy.2011.09.003

Fu, W. B., Hou, L. Y., Wang, L., & Ma, F. H. (2002). A unified model for the micro-explosion of emulsified droplets of oil and water. *Fuel Processing Technology*, *79*(2), 107–119. https://doi.org/10.1016/S0378-3820(02)00106-6

Fu, W., Gong, J., & Hou, L. (2006). There is no micro-explosion in the diesel engines fueled with emulsified fuel. *Chinese Science Bulletin*, *51*(10), 1261–1265. https://doi.org/10.1007/s11434-006-1261-7

Gan, Y., Lim, Y. S., & Qiao, L. (2012). Combustion of nanofluid fuels with the addition of boron and iron particles at dilute and dense concentrations. *Combustion and Flame*, *159*(4), 1732–1740. https://doi.org/10.1016/j.combustflame.2011.12.008

Gautam, R., & Kumar, N. (2016). Effect of ethanol addition on the properties of Jatropha ethyl ester. *Energy Sources, Part A: Recovery, Utilization, and Environmental Effects*, *38*(23), 3464–3469. https://doi.org/10.1080/15567036.2016.1145766

Gehmlich, R. K., Mueller, C. J., Ruth, D. J., Nilsen, C. W., Skeen, S. A., & Manin, J. (2018). Using ducted fuel injection to attenuate or prevent soot formation in mixing-controlled combustion strategies for engine applications. *Applied Energy*, *226*(January), 1169–1186. https://doi.org/10.1016/j.apenergy.2018.05.078

Geng, P., Cao, E., Tan, Q., & Wei, L. (2017). Effects of alternative fuels on the combustion characteristics and emission products from diesel engines: A review. *Renewable and Sustainable Energy Reviews*, *71*(December), 523–534. https://doi.org/10.1016/j.rser.2016.12.080

Ghadikolaei, M. A. (2016). Effect of alcohol blend and fumigation on regulated and unregulated emissions of IC engines—A review. *Renewable and Sustainable Energy Reviews*, *57*, 1440–1495. https://doi.org/10.1016/j.rser.2015.12.128

Ghadikolaei, M. A., Cheung, C. S., & Yung, K. (2018). Study of combustion, performance and emissions of diesel engine fueled with diesel/biodiesel/alcohol blends having the same oxygen concentration. *Energy*, *157*, 258–269. https://doi.org/10.1016/j.energy.2018.05.164

Ghaedi, A., Shafaghat, R., Jahanian, O., & Motallebi Hasankola, S. S. (2020). Comparing the performance of a CI engine after replacing the mechanical injector with a common rail solenoid injector. *Journal of Thermal Analysis and Calorimetry*, *139*(4), 2475–2485. https://doi.org/10.1007/s10973-019-08760-1

Ghaemi, S., Rahimi, P., & Nobes, D. S. (2008). Measurement of Droplet Centricity and Velocity in the Spray Field of an Effervescent Atomizer. *14th Int Symposium on Applications of Laser Techniques to Fluid Mechanics*, (Rallison 1984), 7–10.

Ghodke, A., Gage, G., Madane, A., Shinare, A., & Naik, K. S. (2017). Improved Catalytic Convertor for CI Engine Emission Control System. *International Journal of Research in Advent Technology (IJRAT) Special Issue*, (14th & 15th February 2017), 1–5.

Ghojel, J. I., & Tran, X.-T. (2010). Ignition Characteristics of Diesel−Water Emulsion Sprays in a Constant-Volume Vessel: Effect of Injection Pressure and Water Content. *Energy & Fuels*, *24*(7), 3860–3866. https://doi.org/10.1021/ef1001875

Ghurri, A., Kim, J.-D., Kim, H. G., Jung, J.-Y., & Song, K.-K. (2012). The effect of injection pressure and fuel viscosity on the spray characteristics of biodiesel blends injected into an atmospheric chamber. *Journal of Mechanical Science and Technology*, *26*(9), 2941–2947. https://doi.org/10.1007/s12206-012-0703-1

Guo, Z. G., Wang, S. R., & Wang, X. Y. (2013). Emulsification of Bio-Oil Heavy Fraction with Diesel by Mechanical and Ultrasonic Technologies. *Applied Mechanics and Materials*, *316–317*, 1133–1137. https://doi.org/10.4028/www.scientific.net/AMM.316-317.1133

Guo, Z. G., Yin, Q. Q., & Wang, S. R. (2011). Bio-Oil Emulsion Fuels Production Using Power Ultrasound. *Advanced Materials Research*, *347–353*, 2709–2712. https://doi.org/10.4028/www.scientific.net/AMR.347-353.2709

H-Z.Sheng, Z-P.Zhang, C.-K. W. (1990). *Study of atomization and micro-explosion of water in diesel fuel emulsion droplets in spray with in a high temperature, high pressure bomb*.

Hagos, F. Y. (2006). *Fuelling a small capacity agricultural unmodified diesel engine with macro emulsified ethanol , diesel and jatropha derived biodiesel: performance & emission studies*. Retrieved from http://dspace.dtu.ac.in:8080/jspui/handle/repository/13538

Hagos, F. Y., Ali, O. M., Mamat, R., & Abdullah, A. A. (2017). Effect of emulsification and blending on the oxygenation and substitution of diesel fuel for compression ignition engine. *Renewable and Sustainable Energy Reviews*, *75*(August), 1281–1294. https://doi.org/10.1016/j.rser.2016.11.113

Hagos, F. Y., Aziz, A. R. A., & Tan, I. M. (2011). Water-in-diesel emulsion and its micro-explosion phenomenon-review. *2011 IEEE 3rd International Conference on Communication Software and Networks*, 314–318. https://doi.org/10.1109/ICCSN.2011.6014903

Han, K., Yang, B., Zhao, C., Fu, G., Ma, X., & Song, G. (2016). Experimental study on evaporation characteristics of ethanol–diesel blend fuel droplet. *Experimental Thermal and Fluid Science*, *70*, 381–388. https://doi.org/10.1016/j.expthermflusci.2015.10.001

HANSEN, A. (2005). Ethanol-diesel fuel blends - a review. *Bioresource Technology*, *96*(3), 277–285. https://doi.org/10.1016/j.biortech.2004.04.007

Harlow, F. H., & Shannon, J. P. (1967). Distortion of a Splashing Liquid Drop. *Science*, *157*(3788), 547–550. https://doi.org/10.1126/science.157.3788.547

Hasannuddin, A. K., Wira, J. Y., Sarah, S., Ahmad, M. I., Aizam, S. A., Aiman, M. A. B., … Azrin, M. A. (2016). Durability studies of single cylinder diesel engine running on emulsion fuel. *Energy*, *94*(x), 557–568. https://doi.org/10.1016/j.energy.2015.10.144

Hasannuddin, A. K., Wira, J. Y., Sarah, S., Wan Syaidatul Aqma, W. M. N., Abdul Hadi, A. R., Hirofumi, N., … Azrin, M. A. (2016). Performance, emissions and lubricant oil analysis of diesel engine running on emulsion fuel. *Energy Conversion and Management*, *117*, 548–557. https://doi.org/10.1016/j.enconman.2016.03.057

Hasannuddin, A. K., Yahya, W. J., Sarah, S., Ithnin, A. M., Syahrullail, S., Sugeng, D. A., … Ramlan, N. A. (2018). Performance, emissions and carbon deposit characteristics of diesel engine operating on emulsion fuel. *Energy*, *142*, 496–506. https://doi.org/10.1016/j.energy.2017.10.044

He, B.-Q. (2016). Advances in emission characteristics of diesel engines using different biodiesel fuels. *Renewable and Sustainable Energy Reviews*, *60*, 570–586. https://doi.org/10.1016/j.rser.2016.01.093

Hegab, A., La Rocca, A., & Shayler, P. (2017). Towards keeping diesel fuel supply and demand in balance: Dual-fuelling of diesel engines with natural gas. *Renewable and Sustainable Energy Reviews*, *70*(January), 666–697. https://doi.org/10.1016/j.rser.2016.11.249

Hielscher, T. (2005). Ultrasonic Production of Nano-Size Dispersions and Emulsions. *Ens*, (December), 14–16. https://doi.org/https://doi.org/arXiv:0708

Hoekman, S. K., & Robbins, C. (2012). Review of the effects of biodiesel on NOx emissions. *Fuel Processing Technology*, *96*, 237–249. https://doi.org/10.1016/j.fuproc.2011.12.036

Höök, M., & Tang, X. (2013). Depletion of fossil fuels and anthropogenic climate change—A review. *Energy Policy*, *52*, 797–809. https://doi.org/10.1016/j.enpol.2012.10.046

Hulwan, D. B., & Joshi, S. V. (2011). Performance, emission and combustion characteristic of a multicylinder DI diesel engine running on diesel–ethanol–biodiesel blends of high ethanol content. *Applied Energy*, *88*(12), 5042–5055. https://doi.org/10.1016/j.apenergy.2011.07.008

Hussan, M. J., Hassan, M. H., Kalam, M. A., & Memon, L. A. (2013). Tailoring key fuel properties of diesel–biodiesel–ethanol blends for diesel engine. *Journal of Cleaner Production*, *51*, 118–125. https://doi.org/10.1016/j.jclepro.2013.01.023

Ismael, M. A., Heikal, M. R., Rashid, A., Aziz, A., & Crua, C. (2016). An overview of experimental techniques of the investigation of water-diesel emulsion characteristics droplets micro-explosion. *ARPN Journal of Engineering and Applied Sciences*, *11*(20), 11975–11981.

Issariyakul, T., & Dalai, A. K. (2014). Biodiesel from vegetable oils. *Renewable and Sustainable Energy Reviews*, *31*, 446–471. https://doi.org/10.1016/j.rser.2013.11.001

Ithnin, A. M., Noge, H., Abdul Kadir, H., & Jazair, W. (2014). An overview of utilizing water-in-diesel emulsion fuel in diesel engine and its potential research study. *Journal of the Energy Institute*, *87*(4), 273–288. https://doi.org/10.1016/j.joei.2014.04.002

Jamrozik, A., Tutak, W., Pyrc, M., & Sobiepański, M. (2017). Effect of diesel-biodiesel-ethanol blend on combustion, performance, and emissions characteristics on a direct injection diesel engine. *Thermal Science*, *21*(1 Part B), 591–604. https://doi.org/10.2298/TSCI160913275J

Jeong, I., Lee, K. H., & Kim, J. (2008). Characteristics of auto-ignition and micro-explosion behavior of a single droplet of water-in-fuel. *Journal of Mechanical Science and Technology*, *22*(1), 148–156. https://doi.org/10.1007/s12206-007-1018-5

Jin, C., Pang, X., Zhang, X., Wu, S., Ma, M., Xiang, Y., … Liu, H. (2019). Effects of C3–C5 alcohols on solubility of alcohols/diesel blends. *Fuel*, *236*(September 2018), 65–74. https://doi.org/10.1016/j.fuel.2018.08.129

Jones, S. F., Evans, G. M., & Galvin, K. P. (1999). Bubble nucleation from gas cavities — a review. *Advances in Colloid and Interface Science*, *80*(1), 27–50. https://doi.org/10.1016/S0001-8686(98)00074-8

Joshi, R. M., & Pegg, M. J. (2007). Flow properties of biodiesel fuel blends at low temperatures. *Fuel*, *86*(1–2), 143–151. https://doi.org/10.1016/j.fuel.2006.06.005

Júnior, L. C. S. S., Ferreira, V. P., da Silva, J. A. M., Torres, E. A., & Pepe, I. M. (2018). Oxidized biodiesel as a cetane improver for diesel–biodiesel–ethanol mixtures in a vehicle engine. *Journal of the Brazilian Society of Mechanical Sciences and Engineering*, *40*(2), 79. https://doi.org/10.1007/s40430-018-1029-4

Juttulapa, M., Piriyaprasarth, S., Takeuchi, H., & Sriamornsak, P. (2017). Effect of high-pressure homogenization on stability of emulsions containing zein and pectin. *Asian Journal of Pharmaceutical Sciences*, *12*(1), 21–27. https://doi.org/10.1016/j.ajps.2016.09.004

Kadota, T., & Yamasaki, H. (2002). Recent advances in the combustion of water fuel emulsion. *Progress in Energy and Combustion Science*, *28*(5), 385–404. https://doi.org/10.1016/S0360-1285(02)00005-9

Kadota, Toshikazu, Tanaka, H., Segawa, D., Nakaya, S., & Yamasaki, H. (2007). Microexplosion of an emulsion droplet during Leidenfrost burning. *Proceedings of the Combustion Institute*, *31*(2), 2125–2131.

https://doi.org/10.1016/j.proci.2006.07.001

Karthe, M., Tamilarasan, M., Prasanna, S. C., & Manikandan, A. (2016). Experimental Investigation on Reduction of NO_X Emission Using Zeolite Coated Converter in CI Engine. *Applied Mechanics and Materials*, *854*, 72–77. https://doi.org/10.4028/www.scientific.net/AMM.854.72

Khan, M. Y., Abdul Karim, Z. A., Aziz, a. R. A., & Tan, I. M. (2014). Experimental Investigation of Microexplosion Occurrence in Water in Diesel Emulsion Droplets during the Leidenfrost Effect. *Energy & Fuels*, *28*(11), 7079–7084. https://doi.org/10.1021/ef501588z

Khoobbakht, G., Najafi, G., Karimi, M., & Akram, A. (2016). Optimization of operating factors and blended levels of diesel, biodiesel and ethanol fuels to minimize exhaust emissions of diesel engine using response surface methodology. *Applied Thermal Engineering*, *99*(2016), 1006–1017. https://doi.org/10.1016/j.applthermaleng.2015.12.143

Kim, Y., Han, E., & Sohn, S. (2017). Demand Forecasting for Heavy-Duty Diesel Engines Considering Emission Regulations. *Sustainability*, *9*(2), 166. https://doi.org/10.3390/su9020166

Klajn, F. F., Gurgacz, F., Lenz, A. M., Iacono, G. E. P., Souza, S. N. M. de, & Ferruzzi, Y. (2020). Comparison of the emissions and performance of ethanol-added diesel–biodiesel blends in a compression ignition engine with those of pure diesel. *Environmental Technology*, *41*(4), 511–520. https://doi.org/10.1080/09593330.2018.1504122

Klett, D. E., Afify, E. M., Srinivasan, K. K., & Jacobs, T. J. (2017). Energy Conversion. In D. Y. Goswami & F. Kreith (Eds.), *Energy Conversion, Second Edition*. https://doi.org/10.1201/9781315374192

Kraft, D. (2014). Particle Formation and Models in Internal Combustion Engines. *Como.Cheng.Cam.Ac.Uk*, (142). https://doi.org/ISSN 1473-4273

Krishna, S. M., Abdul Salam, P., Tongroon, M., & Chollacoop, N. (2019). Performance and emission assessment of optimally blended biodiesel-diesel-ethanol in diesel engine generator. *Applied Thermal Engineering*, *155*, 525–533. https://doi.org/10.1016/j.applthermaleng.2019.04.012

Kubota, N., & Sonobe, T. (1988). Combustion Mechanism of Azide Polymer. *Propellants, Explosives, Pyrotechnics*, *13*(6), 172–177. https://doi.org/10.1002/prep.19880130604

Kumar, N., Varun, & Chauhan, S. R. (2013). Performance and emission characteristics of biodiesel from different origins: A review. *Renewable and Sustainable Energy Reviews*, *21*, 633–658. https://doi.org/10.1016/j.rser.2013.01.006

Kwanchareon, P., Luengnaruemitchai, A., & Jai-In, S. (2007). Solubility of a diesel–biodiesel–ethanol blend, its fuel properties, and its emission characteristics from diesel engine. *Fuel*, *86*(7–8), 1053–1061. https://doi.org/10.1016/j.fuel.2006.09.034

Labeckas, G., Slavinskas, S., & Mažeika, M. (2014). The effect of ethanol–diesel–biodiesel blends on combustion, performance and emissions of a direct injection diesel engine. *Energy Conversion and Management*, *79*, 698–720. https://doi.org/10.1016/j.enconman.2013.12.064

Lakshminarayanan, P. A., & Aghav, Y. V. (2010). *Modelling Diesel Combustion*. https://doi.org/10.1007/978-90-481-3885-2

Lalvani, J. I. J., Parthasarathy, M., Dhinesh, B., & Annamalai, K. (2015). Experimental investigation of combustion, performance and emission characteristics of a modified piston. *Journal of Mechanical Science and Technology*, *29*(10), 4519–4525. https://doi.org/10.1007/s12206-015-0951-y

Lapuerta, M., Armas, O., & García-Contreras, R. (2009). Effect of Ethanol on Blending Stability and Diesel Engine Emissions. *Energy & Fuels*, *23*(9), 4343–4354. https://doi.org/10.1021/ef900448m

Lee, C. S., Park, S. W., & Kwon, S. Il. (2005). An Experimental Study on the Atomization and Combustion Characteristics of Biodiesel-Blended Fuels. *Energy & Fuels*, *19*(5), 2201–2208. https://doi.org/10.1021/ef050026h

Leopold, B. D., & Hutchins, M. (2016). Impact of wind energy on wildlife: Synthesis. *Human-Wildlife Interactions*, *10*(1), 81–82. https://doi.org/10.26077/srnd-8307

Li, D., Zhen, H., Xingcai, L., Wu-gao, Z., & Jian-guang, Y. (2005). Physico-chemical properties of ethanol–diesel blend fuel and its effect on performance and emissions of diesel engines. *Renewable Energy*, *30*(6), 967–976. https://doi.org/10.1016/j.renene.2004.07.010

LI, J., GUO, C., WANG, W. Bin, & WU, Z. J. (2011). Optimal Mixture Ratios of Biodiesel Ethanol Diesel for Diesel Engines. *Energy and Power Engineering*, *03*(05), 625–629. https://doi.org/10.4236/epe.2011.35078

Li, R., Wang, Z., Ni, P., Zhao, Y., Li, M., & Li, L. (2014). Effects of cetane number improvers on the performance of diesel engine fuelled with methanol/biodiesel blend. *Fuel*, *128*, 180–187. https://doi.org/10.1016/j.fuel.2014.03.011

Li, Y. H. (2011). Experimental Study on the Combustion Characteristics of Municipal Solid Waste. *Advanced Materials Research*, *204–210*(6), 1351–1356. https://doi.org/10.4028/www.scientific.net/AMR.204-210.1351

Li, Y., Weinstein, M., Caudle, M., Steeley, S., Grubert, G., & Punke, A. (2017). Catalyzed soot filters (CSF) with H 2 S control function for lean NO x trap (LNT) systems. *Catalysis Today*, *297*(3), 70–77. https://doi.org/10.1016/j.cattod.2016.12.043

Liang, Y., Shu, G., Wei, H., & Zhang, W. (2013). Effect of oxygen enriched combustion and water–diesel emulsion on the performance and emissions of turbocharged diesel engine. *Energy Conversion and Management*, *73*, 69–77. https://doi.org/10.1016/j.enconman.2013.04.023

Lightfoot, M. (2009). FUNDAMENTAL CLASSIFICATION OF ATOMIZATION PROCESSES. *Atomization and Sprays*, *19*(11), 1065–1104. https://doi.org/10.1615/AtomizSpr.v19.i11.50

Lin, C.-Y., & Chen, L.-W. (2006). Emulsification characteristics of three- and two-phase emulsions prepared by the ultrasonic emulsification method. *Fuel Processing Technology*, *87*(4), 309–317. https://doi.org/10.1016/j.fuproc.2005.08.014

Lin, Y.-S., & Lin, H.-P. (2010). Study on the spray characteristics of methyl esters from waste cooking oil at elevated temperature. *Renewable Energy*, *35*(9), 1900–1907. https://doi.org/10.1016/j.renene.2010.01.014

Liu, H., Hu, B., & Jin, C. (2016). Effects of different alcohols additives on solubility of hydrous ethanol/diesel fuel blends. *Fuel*, *184*, 440–448. https://doi.org/10.1016/j.fuel.2016.07.037

Liu, H., Lee, C., Huo, M., & Yao, M. (2011). Comparison of Ethanol and Butanol as Additives in Soybean Biodiesel Using a Constant Volume Combustion Chamber. *Energy & Fuels*, *25*(4), 1837–1846. https://doi.org/10.1021/ef200111g

Liu, Y, Cheng, W. L., Huo, M., Lee, C. F., & Li, J. (2010). Effects of Micro-Explosion on Butanol-Biodiesel-Diesel Spray and Combustion. *ILASS-Americas 22nd Annual Conference on Liquid Atomization and Spray Systems*, (May 2010), 1–8.

Liu, Yu, Li, J., & Jin, C. (2015). Fuel spray and combustion characteristics of butanol blends in a constant volume combustion chamber. *Energy Conversion and Management*, *105*, 1059–1069. https://doi.org/10.1016/j.enconman.2015.08.047

López, A. F., Cadrazco, M., Agudelo, A. F., Corredor, L. A., Vélez, J. A., & Agudelo, J. R. (2015). Impact of n-butanol and hydrous ethanol fumigation on the performance and pollutant emissions of an automotive diesel engine. *Fuel*, *153*, 483–491. https://doi.org/10.1016/j.fuel.2015.03.022

Mahmudul, H. M., Hagos, F. Y., Mamat, R., Abdullah, A. A., & Awad, O. I. (2016). Experimental investigation of the impact of using alcohol- biodiesel-diesel blending fuel on combustion of single cylinder CI engine. *IOP Conference Series: Materials Science and Engineering*, *160*, 012038. https://doi.org/10.1088/1757-899X/160/1/012038

Mahmudul, H. M., Hagos, F. Y., Mamat, R., Adam, A. A., Ishak, W. F. W., & Alenezi, R. (2017). Production, characterization and performance of biodiesel as an alternative fuel in diesel engines – A review. *Renewable and Sustainable Energy Reviews*, *72*(April 2016), 497–509. https://doi.org/10.1016/j.rser.2017.01.001

Mahmudul, H. M., Hagos, F. Y., Mukhtar N. A, M., Mamat, R., & Adam Abdullah, A. (2018). Effect of Alcohol on Diesel Engine Combustion Operating with Biodiesel-Diesel Blend at Idling Conditions. *IOP Conference Series: Materials Science and Engineering*, *318*(1), 012071. https://doi.org/10.1088/1757-899X/318/1/012071

Malvern instruments. (1999). Zetasizer HR 3000. *Biofutur*, *1999*(188), 54. https://doi.org/10.1016/S0294-3506(99)80105-7

Marinho, R., Horiuchi, L., & Pires, C. A. (2018). EFFECT OF STIRRING SPEED ON CONVERSION AND TIME TO PARTICLE STABILIZATION OF POLY (VINYL CHLORIDE) PRODUCED BY SUSPENSION POLYMERIZATION PROCESS AT THE BEGINNING OF REACTION. *Brazilian Journal of Chemical Engineering*, *35*(2), 631–640. https://doi.org/10.1590/0104-6632.20180352s20160453

Martins, F., Felgueiras, C., Smitkova, M., & Caetano, N. (2019). Analysis of Fossil Fuel Energy Consumption and Environmental Impacts in European Countries. *Energies*, *12*(6), 964. https://doi.org/10.3390/en12060964

Mashkour, M. A., & Mohammed, A. A. (2017). Impact of mixing speed & reaction time on the biodiesel production from sunflower oil. *Journal of the Association of Arab Universities for Basic and Applied Sciences*, *24*(January), 101–134.

Mat Yasin, M.H., Yusaf, T., Mamat, R., & Fitri Yusop, A. (2014). Characterization of a diesel engine operating with a small proportion of methanol as a fuel additive in biodiesel blend. *Applied Energy*, *114*, 865–873. https://doi.org/10.1016/j.apenergy.2013.06.012

Mat Yasin, Mohd Hafizil, Mamat, R., Najafi, G., Ali, O. M., Yusop, A. F., & Ali, M. H. (2017). Potentials of palm oil as new feedstock oil for a global alternative fuel: A review. *Renewable and Sustainable Energy Reviews*, *79*(February), 1034–1049. https://doi.org/10.1016/j.rser.2017.05.186

Mehta, R. N., Chakraborty, M., & Parikh, P. A. (2012). Comparative study of stability and properties of alcohol-diesel blends. *International Journal of Chemical Technology*, *19*(March), 134–139.

Mehta, R. N., Chakraborty, M., & Parikh, P. A. (2014). Nanofuels: Combustion, engine performance and emissions. *Fuel*, *120*, 91–97. https://doi.org/10.1016/j.fuel.2013.12.008

Mehta, R. N., More, U., Malek, N., Chakraborty, M., & Parikh, P. A. (2015). Study of stability and thermodynamic properties of water-in-diesel nanoemulsion fuels with nano-Al additive. *Applied Nanoscience*, *5*(8), 891–900. https://doi.org/10.1007/s13204-014-0385-3

Melo-Espinosa, E. A., Piloto-Rodríguez, R., Goyos-Pérez, L., Sierens, R., & Verhelst, S. (2015). Emulsification of animal fats and vegetable oils for their use as a diesel engine fuel: An overview. *Renewable and Sustainable Energy Reviews*, *47*, 623–633. https://doi.org/10.1016/j.rser.2015.03.091

Mendes Guedes, A. D., Leal Braga, S., & Pradelle, F. (2018). Performance and combustion characteristics of a compression ignition engine running on diesel-biodiesel-ethanol (DBE) blends – Part 2: Optimization of injection timing. *Fuel*, *225*(September 2017), 174–183. https://doi.org/10.1016/j.fuel.2018.02.120

Mofijur, M., Rasul, M. G., Hyde, J., Azad, A. K., Mamat, R., & Bhuiya, M. M. K. (2016). Role of biofuel and their binary (diesel–biodiesel) and ternary (ethanol–biodiesel–diesel) blends on internal combustion engines emission reduction. *Renewable and Sustainable Energy Reviews*, *53*(October 2015), 265–278.

https://doi.org/10.1016/j.rser.2015.08.046

Mohamed Shameer, P., Ramesh, K., Sakthivel, R., & Purnachandran, R. (2017). Effects of fuel injection parameters on emission characteristics of diesel engines operating on various biodiesel: A review. *Renewable and Sustainable Energy Reviews*, *67*(3), 1267–1281. https://doi.org/10.1016/j.rser.2016.09.117

Morganti, K., Almansour, M., Khan, A., Kalghatgi, G., & Przesmitzki, S. (2018). Leveraging the benefits of ethanol in advanced engine-fuel systems. *Energy Conversion and Management*, *157*(November 2017), 480–497. https://doi.org/10.1016/j.enconman.2017.11.086

Moussa, O., Tarlet, D., Massoli, P., & Bellettre, J. (2018). Parametric study of the micro-explosion occurrence of W/O emulsions. *International Journal of Thermal Sciences*, *133*(October 2017), 90–97. https://doi.org/10.1016/j.ijthermalsci.2018.07.016

Movahednejad, E., Ommi, F., & Hosseinalipour, S. M. (2010). Prediction of Droplet Size and Velocity Distribution in Droplet Formation Region of Liquid Spray. *Entropy*, *12*(6), 1484–1498. https://doi.org/10.3390/e12061484

Mueller, C. J., Nilsen, C. W., Ruth, D. J., Gehmlich, R. K., Pickett, L. M., & Skeen, S. A. (2017). Ducted fuel injection: A new approach for lowering soot emissions from direct-injection engines. *Applied Energy*, *204*, 206–220. https://doi.org/10.1016/j.apenergy.2017.07.001

Mura, E., Calabria, R., Califano, V., Massoli, P., & Bellettre, J. (2014). Emulsion droplet micro-explosion: Analysis of two experimental approaches. *Experimental Thermal and Fluid Science*, *56*, 69–74. https://doi.org/10.1016/j.expthermflusci.2013.11.020

Mura, E., Massoli, P., Josset, C., Loubar, K., & Bellettre, J. (2012). Study of the micro-explosion temperature of water in oil emulsion droplets during the Leidenfrost effect. *Experimental Thermal and Fluid Science*, *43*, 63–70. https://doi.org/10.1016/j.expthermflusci.2012.03.027

Nabi, M. N., Rasul, M. G., & Brown, R. J. (2020). Notable reductions in blow-by and particle emissions during cold and hot start operations from a turbocharged diesel engine using oxygenated fuels. *Fuel Processing Technology*, *203*(January), 106394. https://doi.org/10.1016/j.fuproc.2020.106394

Naylor, R. L., & Higgins, M. M. (2017). The political economy of biodiesel in an era of low oil prices. *Renewable and Sustainable Energy Reviews*, *77*(February), 695–705. https://doi.org/10.1016/j.rser.2017.04.026

Nazha, M. A. A., Rajakaruna, H., & Crookes, R. J. (1998). Soot and gaseous species formation in a water-in-liquid fuel emulsion spray—a mathematical approach. *Energy Conversion and Management*, *39*(16–18), 1981–1989. https://doi.org/10.1016/S0196-8904(98)00079-X

Nehring, R. (2009). Traversing the mountaintop: world fossil fuel production to 2050. *Philosophical Transactions of the Royal Society B: Biological Sciences*, *364*(1532), 3067–3079. https://doi.org/10.1098/rstb.2009.0170

Noorollahi, Y., Azadbakht, M., & Ghobadian, B. (2018). The effect of different diesterol (diesel–biodiesel–ethanol) blends on small air-cooled diesel engine performance and its exhaust gases. *Energy*, *142*, 196–200. https://doi.org/10.1016/j.energy.2017.10.024

Nour, M., Kosaka, H., Bady, M., Sato, S., & Abdel-Rahman, A. K. (2017). Combustion and emission characteristics of DI diesel engine fuelled by ethanol injected into the exhaust manifold. *Fuel Processing Technology*, *164*, 33–50. https://doi.org/10.1016/j.fuproc.2017.04.018

Ocampo-Barrera, R., Villasenor, R., & Diego-Marin, A. (2001). An experimental study of the effect of water content on combustion of heavy fuel oil/water emulsion droplets. *Combustion and Flame*, *126*(4), 1845–1855. https://doi.org/10.1016/S0010-2180(01)00295-4

Pachiannan, T., Zhong, W., Rajkumar, S., He, Z., Leng, X., & Wang, Q. (2019). A literature review of fuel effects on performance and emission characteristics of low-temperature combustion strategies. *Applied Energy*, *251*(301), 113380. https://doi.org/10.1016/j.apenergy.2019.113380

Palash, S. M., Masjuki, H. H., Kalam, M. A., Masum, B. M., Sanjid, A., & Abedin, M. J. (2013). State of the art of NOx mitigation technologies and their effect on the performance and emission characteristics of biodiesel-fueled Compression Ignition engines. *Energy Conversion and Management*, *76*, 400–420. https://doi.org/10.1016/j.enconman.2013.07.059

Park, S. H., Kim, S. H., & Lee, C. S. (2009). Mixing Stability and Spray Behavior Characteristics of Diesel−Ethanol−Methyl Ester Blended Fuels in a Common-Rail Diesel Injection System. *Energy & Fuels*, *23*(10), 5228–5235. https://doi.org/10.1021/ef9004847

Park, S. H., & Lee, C. S. (2014). Applicability of dimethyl ether (DME) in a compression ignition engine as an alternative fuel. *Energy Conversion and Management*, *86*, 848–863. https://doi.org/10.1016/j.enconman.2014.06.051

Park, S. H., Suh, H. K., & Lee, C. S. (2010). Nozzle flow and atomization characteristics of ethanol blended biodiesel fuel. *Renewable Energy*, *35*(1), 144–150. https://doi.org/10.1016/j.renene.2009.06.012

Pasel, J., Samsun, R. C., Meißner, J., Tschauder, A., & Peters, R. (2020). Recent advances in diesel autothermal reformer design. *International Journal of Hydrogen Energy*, *45*(3), 2279–2288. https://doi.org/10.1016/j.ijhydene.2019.11.137

Patil, V., Navale, L. G., & Talib, M. (2017). Effect of Silica Gel based Diesel Particulate Filter on a C.I. engine. *Materials Today: Proceedings*, *4*(8), 7680–7685. https://doi.org/10.1016/j.matpr.2017.07.102

Paul, A., Panua, R., & Debroy, D. (2017). An experimental study of combustion, performance, exergy and emission characteristics of a CI engine fueled by Diesel-ethanol-biodiesel blends. *Energy*, *141*, 839–852. https://doi.org/10.1016/j.energy.2017.09.137

Pereira, G. C. Q., Braz, D. S., Hamaguchi, M., Ezeji, T. C., Maciel Filho, R., & Mariano, A. P. (2018). Process design and economics of a flexible ethanol-butanol plant annexed to a eucalyptus kraft pulp mill. *Bioresource Technology*, *250*(September 2017), 345–354. https://doi.org/10.1016/j.biortech.2017.11.022

Pradelle, F., Leal Braga, S., Fonseca de Aguiar Martins, A. R., Turkovics, F., & Nohra Chaar Pradelle, R. (2019a). Experimental assessment of some key physicochemical properties of diesel-biodiesel-ethanol (DBE) blends for use in compression ignition engines. *Fuel*, *248*(March), 241–253. https://doi.org/10.1016/j.fuel.2019.03.087

Pradelle, F., Leal Braga, S., Fonseca de Aguiar Martins, A. R., Turkovics, F., & Nohra Chaar Pradelle, R. (2019b). Performance and combustion characteristics of a compression ignition engine running on diesel-biodiesel-ethanol (DBE) blends – Potential as diesel fuel substitute on an Euro III engine. *Renewable Energy*, *136*, 586–598. https://doi.org/10.1016/j.renene.2019.01.025

Praveena, V., & Martin, M. L. J. (2018). A review on various after treatment techniques to reduce NOx emissions in a CI engine. *Journal of the Energy Institute*, *91*(5), 704–720. https://doi.org/10.1016/j.joei.2017.05.010

Qi, D. H., Chen, H., Geng, L. M., Bian, Y. Z., & Ren, X. C. (2010). Performance and combustion characteristics of biodiesel–diesel–methanol blend fuelled engine. *Applied Energy*, *87*(5), 1679–1686. https://doi.org/10.1016/j.apenergy.2009.10.016

Qian, Y., Zhao, P., Tao, C., Meng, S., Wei, J., & Cheng, X. (2019). Experimental study on evaporation characteristics of lubricating oil/gasoline blended droplet. *Experimental Thermal and Fluid Science*, *103*(193), 99–107. https://doi.org/10.1016/j.expthermflusci.2019.01.010

Rahman, M., Rasul, M., & Hassan, N. (2017). Study on the Tribological Characteristics of Australian Native First Generation and Second Generation Biodiesel Fuel. *Energies*, *10*(1), 55. https://doi.org/10.3390/en10010055

Rahman, S. M. A., Masjuki, H. H., Kalam, M. A., Abedin, M. J., Sanjid, A., & Rahman, M. M. (2014). Assessing idling effects on a compression ignition engine fueled with Jatropha and Palm biodiesel blends. *Renewable Energy*, *68*(x), 644–650. https://doi.org/10.1016/j.renene.2014.02.050

Rajesh, K., & D.B, G. (2019). Assessment of ethanol as fuel additive to diesel-biodiesel blends on emission characteristics in CI engine. *International Journal of Advanced Technology and Engineering Exploration*, *6*(52), 61–70. https://doi.org/10.19101/IJATEE.2019.650012

Rajesh, S., Kulkarni, B. M., Banapurmath, N. R., & Kumarappa, S. (2011). An Experimental Study on performance and emission characteristics of multi cylinder CRDI diesel engine fueled with Ethanol, Acid oil based Biodiesel and Diesel blends. *International Journal of Current Engineering and Technology*, *7*(1), 256–265. https://doi.org/10.14741/Ijcet/22774106/7.1.2017.40

Rajesh, S., Kulkarni, B. M., Banapurmath, N. R., & Kumarappa, S. (2018). Effect of injection parameters on performance and emission characteristics of a CRDi diesel engine fuelled with acid oil biodiesel–ethanol blended fuels. *Biofuels*, *9*(3), 353–

367. https://doi.org/10.1080/17597269.2016.1271628

Rakopoulos, D. C., Rakopoulos, C. D., Papagiannakis, R. G., & Kyritsis, D. C. (2011). Combustion heat release analysis of ethanol or n-butanol diesel fuel blends in heavy-duty DI diesel engine. *Fuel*, *90*(5), 1855–1867. https://doi.org/10.1016/j.fuel.2010.12.003

Ramkumar, S., & Kirubakaran, V. (2016). Biodiesel from vegetable oil as alternate fuel for C.I engine and feasibility study of thermal cracking: A critical review. *Energy Conversion and Management*, *118*, 155–169. https://doi.org/10.1016/j.enconman.2016.03.071

Rao, D. C. K., Karmakar, S., & Som, S. K. (2017). Puffing and Micro-Explosion Behavior in Combustion of Butanol/Jet A-1 and Acetone-Butanol-Ethanol (A-B-E)/Jet A-1 Fuel Droplets. *Combustion Science and Technology*, *189*(10), 1796–1812. https://doi.org/10.1080/00102202.2017.1333502

Rao, D. C. K., Syam, S., Karmakar, S., & Joarder, R. (2017). Experimental investigations on nucleation, bubble growth, and micro-explosion characteristics during the combustion of ethanol/Jet A-1 fuel droplets. *Experimental Thermal and Fluid Science*, *89*, 284–294. https://doi.org/10.1016/j.expthermflusci.2017.08.025

Rashedul, H. K., Masjuki, H. H., Kalam, M. A., Ashraful, A. M., Ashrafur Rahman, S. M., & Shahir, S. A. (2014). The effect of additives on properties, performance and emission of biodiesel fuelled compression ignition engine. *Energy Conversion and Management*, *88*, 348–364. https://doi.org/10.1016/j.enconman.2014.08.034

Ravi Kumar, M. (2017). An Experimental Investigation on NOx Emission Reduction and Performance Evaluation of CI Engine using EGR System. *International Journal of Engineering Research And Advanced Technology*, *3*(7), 1–17. https://doi.org/https://doi.org/10.7324/

Reitz, R. D., & Duraisamy, G. (2015). Review of high efficiency and clean reactivity controlled compression ignition (RCCI) combustion in internal combustion engines. *Progress in Energy and Combustion Science*, *46*, 12–71. https://doi.org/10.1016/j.pecs.2014.05.003

Rhim, J., & No, S. (2001). Breakup Length of Conical Emulsion Sheet Discharged By Pressure-Swirl Atomizer. *International Journal*, *2*(3), 103–107.

Rulli, M. C., Casirati, S., Dell'Angelo, J., Davis, K. F., Passera, C., & D'Odorico, P. (2019). Interdependencies and telecoupling of oil palm expansion at the expense of Indonesian rainforest. *Renewable and Sustainable Energy Reviews*, *105*(February), 499–512. https://doi.org/10.1016/j.rser.2018.12.050

S. Fernando, & M. Hanna. (2005). Phase behaviour of the ethanol-biodiesel-diesel micro-emulsion system. *Transactions of the ASAE*, *48*(3), 903–908. https://doi.org/10.13031/2013.18494

Sadhik Basha, J., & Anand, R. B. (2011). Role of nanoadditive blended biodiesel emulsion fuel on the working characteristics of a diesel engine. *Journal of Renewable and Sustainable Energy*, *3*(2), 023106.

https://doi.org/10.1063/1.3575169

Sadhik Basha, J., & Anand, R. B. (2014). Performance, emission and combustion characteristics of a diesel engine using Carbon Nanotubes blended Jatropha Methyl Ester Emulsions. *Alexandria Engineering Journal*, *53*(2), 259–273. https://doi.org/10.1016/j.aej.2014.04.001

Sales, R. S., & Support, A. (2014). Dynamic Light Scattering Training Achieving reliable nano particle sizing. *Dynamic Light Scattering Training: Achieving Reliable Nano Particle Sizing (Online)*, *Accessed 2*, Available from: http://149.171.168.221/partcat/wp-.

Salvador, F. J., De la Morena, J., Martínez-López, J., & Jaramillo, D. (2017). Assessment of compressibility effects on internal nozzle flow in diesel injectors at very high injection pressures. *Energy Conversion and Management*, *132*, 221–230. https://doi.org/10.1016/j.enconman.2016.11.032

Santini, E. R., Gosala, D. B., & Shaver, G. M. (2016). Effects of Internal EGR on Modern Diesel Engines Internal Equipped with VVA at Idle. *The Summer Undergraduate Research Fellowship (SURF) Symposium*, (4 August 2016), 1–5.

Sarkar, A., & Saha, U. K. (2018). Impact of Intake Charge Preheating on a Biogas Run Dual Fuel Diesel Engine Using Ternary Blends of Diesel-Biodiesel-Ethanol. *Journal of Energy Engineering*, *144*(3), 04018031. https://doi.org/10.1061/(ASCE)EY.1943-7897.0000548

Schaschke, C., Fletcher, I., & Glen, N. (2013). Density and Viscosity Measurement of Diesel Fuels at Combined High Pressure and Elevated Temperature. *Processes*, *1*(2), 30–48. https://doi.org/10.3390/pr1020030

Seifi, M. R., Hassan-Beygi, S. R., Ghobadian, B., Desideri, U., & Antonelli, M. (2016). Experimental investigation of a diesel engine power, torque and noise emission using water–diesel emulsions. *Fuel*, *166*(November), 392–399. https://doi.org/10.1016/j.fuel.2015.10.122

Sendzikiene, E., Makareviciene, V., & Janulis, P. (2006). Influence of fuel oxygen content on diesel engine exhaust emissions. *Renewable Energy*, *31*(15), 2505–2512. https://doi.org/10.1016/j.renene.2005.11.010

Sener, R., Yangaz, M. U., & Gul, M. Z. (2020). Effects of injection strategy and combustion chamber modification on a single-cylinder diesel engine. *Fuel*, *266*(September 2019), 117122. https://doi.org/10.1016/j.fuel.2020.117122

Senthil Kumar, M., & Jaikumar, M. (2014). A comprehensive study on performance, emission and combustion behavior of a compression ignition engine fuelled with WCO (waste cooking oil) emulsion as fuel. *Journal of the Energy Institute*, *87*(3), 263–271. https://doi.org/10.1016/j.joei.2014.03.001

Shaddix, C. R., & Tennison, P. J. (1998). Effects of char content and simple additives on biomass pyrolysis oil droplet combustion. *Symposium (International) on Combustion*, *27*(2), 1907–1914. https://doi.org/10.1016/S0082-0784(98)80034-9

Shahid, E., & Jamal, Y. (2011). Performance evaluation of a diesel engine using biodiesel. *Pak. J. Engg. & Appl. Sci. Vol*, *9*, 68–75. Retrieved from http://www.uet.edu.pk/export/sites/UETWebPortal/research/researchinfo/9-RJ-JULY-2011/9-Art-9.pdf

Shahid, E. M., & Jamal, Y. (2011). Production of biodiesel: A technical review. *Renewable and Sustainable Energy Reviews*, *15*(9), 4732–4745. https://doi.org/10.1016/j.rser.2011.07.079

Shahir, S. A., Masjuki, H. H., Kalam, M. A., Imran, A., Fattah, I. M. R., & Sanjid, A. (2014). Feasibility of diesel–biodiesel–ethanol/bioethanol blend as existing CI engine fuel: An assessment of properties, material compatibility, safety and combustion. *Renewable and Sustainable Energy Reviews*, *32*, 379–395. https://doi.org/10.1016/j.rser.2014.01.029

Shahir, V. K., Jawahar, C. P., & Suresh, P. R. (2015). Comparative study of diesel and biodiesel on CI engine with emphasis to emissions—A review. *Renewable and Sustainable Energy Reviews*, *45*, 686–697. https://doi.org/10.1016/j.rser.2015.02.042

Sharanappa, P., & Navindgi, M. C. (2017). Physico-chemical properties of diesel-biodiesel-ethanol blends. *International Journal of Scientific & Engineering Research*, *8*(2), 506–510.

Sheng, H. Z., Chen, L., Zhang, Z. P., Wu, C. K., An, C., & Cheng, C. Q. (1994). The droplet group microexplosions in water-in-oil emulsion sprays and their effects on diesel engine combustion. *Symposium (International) on Combustion*, *25*(1), 175–181. https://doi.org/10.1016/S0082-0784(06)80642-9

Shi, X., Yu, Y., He, H., Shuai, S., Wang, J., & Li, R. (2005). Emission characteristics using methyl soyate-ethanol-diesel fuel blends on a diesel engine. *Fuel*, *84*(12), 1543–1549. https://doi.org/10.1016/j.fuel.2005.03.001

Shudo, T., Nakajima, T., & Hiraga, K. (2009). Simultaneous reduction in cloud point, smoke, and NO x emissions by blending bioethanol into biodiesel fuels and exhaust gas recirculation. *International Journal of Engine Research*, *10*(1), 15–26. https://doi.org/10.1243/14680874JER01908

Singh, G., Singh, A. P., & Agarwal, A. K. (2014). Experimental investigations of combustion, performance and emission characterization of biodiesel fuelled HCCI engine using external mixture formation technique. *Sustainable Energy Technologies and Assessments*, *6*, 116–128. https://doi.org/10.1016/j.seta.2014.01.002

Song, H., Quinton, K., Peng, Z., Zhao, H., & Ladommatos, N. (2016). Effects of Oxygen Content of Fuels on Combustion and Emissions of Diesel Engines. *Energies*, *9*(1), 28. https://doi.org/10.3390/en9010028

Sorate, K. A., & Bhale, P. V. (2015). Biodiesel properties and automotive system compatibility issues. *Renewable and Sustainable Energy Reviews*, *41*, 777–798. https://doi.org/10.1016/j.rser.2014.08.079

Srinivasnaik, M., Sudhakar, T. V. V, Balunaik, B., & SomiReddy, A. (2015). Alcohols as Alternative Fuels for Diesel Engines: A Review. *International Journal of Applied Science and Technology*, *3*(Vi), 1–8.

Subramanian, K. A. (2011). A comparison of water–diesel emulsion and timed injection of water into the intake manifold of a diesel engine for simultaneous control of NO and smoke emissions. *Energy Conversion and Management*, *52*(2), 849–857. https://doi.org/10.1016/j.enconman.2010.08.010

Suhaimi, H., Adam, A., Mrwan, A. G., Abdullah, Z., Othman, M. F., Kamaruzzaman, M. K., & Hagos, F. Y. (2018). Analysis of combustion characteristics, engine performances and emissions of long-chain alcohol-diesel fuel blends. *Fuel*, *220*(February), 682–691. https://doi.org/10.1016/j.fuel.2018.02.019

Tan, Y. H., Abdullah, M. O., Nolasco-Hipolito, C., Zauzi, N. S. A., & Abdullah, G. W. (2017). Engine performance and emissions characteristics of a diesel engine fueled with diesel-biodiesel-bioethanol emulsions. *Energy Conversion and Management*, *132*(January), 54–64. https://doi.org/10.1016/j.enconman.2016.11.013

Tanaka, H., Kadota, T., Segawa, D., Nakaya, S., & Yamasaki, H. (2006). Effect of Ambient Pressure on Micro-Explosion of an Emulsion Droplet Evaporating on a Hot Surface. *JSME International Journal Series B*, *49*(4), 1345–1350. https://doi.org/10.1299/jsmeb.49.1345

Tang, C., Feng, Z., Zhan, C., Ma, W., & Huang, Z. (2017). Experimental study on the effect of injector nozzle K factor on the spray characteristics in a constant volume chamber: Near nozzle spray initiation, the macroscopic and the droplet statistics. *Fuel*, *202*, 583–594. https://doi.org/10.1016/j.fuel.2017.04.078

Thangavelu, S. K., Ahmed, A. S., & Ani, F. N. (2016). Impact of metals on corrosive behavior of biodiesel–diesel–ethanol (BDE) alternative fuel. *Renewable Energy*, *94*, 1–9. https://doi.org/10.1016/j.renene.2016.03.015

Tran, Q. M. (2019). Projection of fossil fuel demands in Vietnam to 2050 and climate change implications. *Asia & the Pacific Policy Studies*, *6*(2), 208–221. https://doi.org/10.1002/app5.274

Trindade, W. R. da S., & Santos, R. G. dos. (2017). Review on the characteristics of butanol, its production and use as fuel in internal combustion engines. *Renewable and Sustainable Energy Reviews*, *69*(November 2016), 642–651. https://doi.org/10.1016/j.rser.2016.11.213

Trizano-Hermosilla, I., & Alvarado, J. M. (2016). Best Alternatives to Cronbach's Alpha Reliability in Realistic Conditions: Congeneric and Asymmetrical Measurements. *Frontiers in Psychology*, *7*. Retrieved from www.statease.com

Tse, H., Leung, C. W., & Cheung, C. S. (2015). Investigation on the combustion characteristics and particulate emissions from a diesel engine fueled with diesel-biodiesel-ethanol blends. *Energy*, *83*(February), 343–350. https://doi.org/10.1016/j.energy.2015.02.030

Tutak, W. (2014). Bioethanol E85 as a fuel for dual fuel diesel engine. *Energy Conversion and Management*, *86*, 39–48. https://doi.org/10.1016/j.enconman.2014.05.016

Tutak, W., Lukács, K., Szwaja, S., & Bereczky, Á. (2015). Alcohol–diesel fuel combustion in the compression ignition engine. *Fuel*, *154*(April), 196–206. https://doi.org/10.1016/j.fuel.2015.03.071

Unglert, M., Bockey, D., Bofinger, C., Buchholz, B., Fisch, G., Luther, R., … Krahl, J. (2020). Action areas and the need for research in biofuels. *Fuel*, *268*(January), 117227. https://doi.org/10.1016/j.fuel.2020.117227

van Hoeve, W., Gekle, S., Snoeijer, J. H., Versluis, M., Brenner, M. P., & Lohse, D. (2010). Breakup of diminutive Rayleigh jets. *Physics of Fluids*, *22*(12), 122003. https://doi.org/10.1063/1.3524533

Vellaiyan, S., & Amirthagadeswaran, K. S. (2016). The role of water-in-diesel emulsion and its additives on diesel engine performance and emission levels: A retrospective review. *Alexandria Engineering Journal*, *55*(3), 2463–2472. https://doi.org/10.1016/j.aej.2016.07.021

Venu, H. (2019). An experimental assessment on the influence of fuel-borne additives on ternary fuel (diesel–biodiesel–ethanol) blends operated in a single cylinder diesel engine. *Environmental Science and Pollution Research*, *26*(14), 14660–14672. https://doi.org/10.1007/s11356-019-04739-5

Venu, H., & Dinesh Babu, M. (2018). Improvement of ternary fuel combustion with various injection pressure strategies in a toroidal re-entrant combustion chamber. *Environmental Science and Pollution Research*, *25*(32), 32024–32043. https://doi.org/10.1007/s11356-018-3174-9

Venu, H., & Madhavan, V. (2017). Influence of diethyl ether (DEE) addition in ethanol-biodiesel-diesel (EBD) and methanol-biodiesel-diesel (MBD) blends in a diesel engine. *Fuel*, *189*, 377–390. https://doi.org/10.1016/j.fuel.2016.10.101

Vinet, L., & Zhedanov, A. (2010). A "missing" family of classical orthogonal polynomials. *Journal of Physics A: Mathematical and Theoretical*, *44*(8), 085201. https://doi.org/10.1088/1751-8113/44/8/085201

Wan Ghazali, W. N. M., Mamat, R., Masjuki, H. H., & Najafi, G. (2015). Effects of biodiesel from different feedstocks on engine performance and emissions: A review. *Renewable and Sustainable Energy Reviews*, *51*, 585–602. https://doi.org/10.1016/j.rser.2015.06.031

Wang, C. H., & Law, C. K. (1985). Microexplosion of fuel droplets under high pressure. *Combustion and Flame*, *59*(1), 53–62. https://doi.org/10.1016/0010-2180(85)90057-4

Wang, W., Cheng, W., Duan, J., Wang, P., & Gong, J. (2014). Discussion on the influence of stirring speed on drop size prediction in an oil-water stirring tank using population balance models. *Asia-Pacific Journal of Chemical Engineering*, *9*(2), 309–315. https://doi.org/10.1002/apj.1766

Watanabe, H., Harada, T., Hoshino, K., Matsushita, Y., Aoki, H., & Miura, T. (2008). An experimental investigation of the characteristics of the secondary atomization and spray combustion for emulsified fuel. *Journal of Chemical Engineering of Japan*, *41*(12), 1110–1118. https://doi.org/10.1252/jcej.08we144

Watanabe, H., & Okazaki, K. (2013). Visualization of secondary atomization in emulsified-fuel spray flow by shadow imaging. *Proceedings of the Combustion Institute*, *34*(1), 1651–1658. https://doi.org/10.1016/j.proci.2012.07.005

Watanabe, H., Suzuki, Y., Harada, T., Matsushita, Y., Aoki, H., & Miura, T. (2010). An experimental investigation of the breakup characteristics of secondary atomization of emulsified fuel droplet. *Energy*, *35*(2), 806–813. https://doi.org/10.1016/j.energy.2009.08.021

Whitcomb, P. J. (2004). *RSM Simplified*. https://doi.org/10.4324/9781482293777

Wilman, E. A. (2019). Market Redirection Leakage in the Palm Oil Market. *Ecological Economics*, *159*(February), 226–234. https://doi.org/10.1016/j.ecolecon.2019.01.014

Wu, D., Wang, W., Sheng, H., & Yao, J. (2012). Microexplosion of Three-Phase Diesel-Methanol-Water Emulsion Spray. *Asian Journal of Chemistry*, *24*(5), 2100–2106.

Wu, H., Nithyanandan, K., Zhang, J., Lin, Y., Lee, T. H., Lee, C. F., & Zhang, C. (2015). Impacts of Acetone–Butanol–Ethanol (ABE) ratio on spray and combustion characteristics of ABE–diesel blends. *Applied Energy*, *149*, 367–378. https://doi.org/10.1016/j.apenergy.2014.11.053

Yahaya Khan, M., Abdul Karim, Z. A., Aziz, A. R. A., Heikal, M. R., & Crua, C. (2017). Puffing and Microexplosion Behavior of Water in Pure Diesel Emulsion Droplets During Leidenfrost Effect. *Combustion Science and Technology*, *189*(7), 1186–1197. https://doi.org/10.1080/00102202.2016.1275593

Yang, W. M., An, H., Chou, S. K., Chua, K. J., Mohan, B., Sivasankaralingam, V., … Li, J. (2013). Impact of emulsion fuel with nano-organic additives on the performance of diesel engine. *Applied Energy*, *112*, 1206–1212. https://doi.org/10.1016/j.apenergy.2013.02.027

Yatsufusa, T., Kumura, T., Nakagawa, Y., & Kidoguchi, Y. (2009). Advantage of Using Water-Emulsified Fuel on Combustion and Emission Characteristics. *Proceedings of the European Combustion Meeting 2009*, 1–6.

Yilmaz, N. (2012). Comparative analysis of biodiesel–ethanol–diesel and biodiesel–methanol–diesel blends in a diesel engine. *Energy*, *40*(1), 210–213. https://doi.org/10.1016/j.energy.2012.01.079

Yilmaz, N., & Atmanli, A. (2017). Experimental assessment of a diesel engine fueled with diesel-biodiesel-1-pentanol blends. *Fuel*, *191*, 190–197. https://doi.org/10.1016/j.fuel.2016.11.065

Yuan, W., Hansen, A., & Zhang, Q. (2005). Vapor pressure and normal boiling point predictions for pure methyl esters and biodiesel fuels. *Fuel*, *84*(7–8), 943–950. https://doi.org/10.1016/j.fuel.2005.01.007

Yusri, I. M., Mamat, R., Azmi, W. H., Omar, A. I., Obed, M. A., & Shaiful, A. I. M. (2017). Application of response surface methodology in optimization of performance and exhaust emissions of secondary butyl alcohol-gasoline blends in SI engine. *Energy Conversion and Management*, *133*, 178–195. https://doi.org/10.1016/j.enconman.2016.12.001

Zeng, Y., & Lee, C. (2001). Modeling of micro-explosion for multicomponent droplets. *11th International Multidimensional Engine Modeling User's Group Meeting Agenda*, 1–6.

Zeng, Y., & Lee, C. F. (2007). Modeling droplet breakup processes under micro-explosion conditions. *Proceedings of the Combustion Institute*, *31*(2), 2185–2193. https://doi.org/10.1016/j.proci.2006.07.237

Zhan, C., Feng, Z., Ma, W., Zhang, M., Tang, C., & Huang, Z. (2018). Experimental investigation on effect of ethanol and di-ethyl ether addition on the spray characteristics of diesel/biodiesel blends under high injection pressure. *Fuel*, *218*(January), 1–11. https://doi.org/10.1016/j.fuel.2017.12.038

Zheng, Z., Wang, X., Zhong, X., Hu, B., Liu, H., & Yao, M. (2016). Experimental study on the combustion and emissions fueling biodiesel/n-butanol, biodiesel/ethanol and biodiesel/2,5-dimethylfuran on a diesel engine. *Energy*, *115*, 539–549. https://doi.org/10.1016/j.energy.2016.09.054

Zöldy, M. (2011). ETHANOL–BIODIESEL–DIESEL BLENDS AS A DIESEL EXTENDER OPTION ON COMPRESSION IGNITION ENGINES. *TRANSPORT*, *26*(3), 303–309. https://doi.org/10.3846/16484142.2011.623824

Zverlov, V. V., Berezina, O., Velikodvorskaya, G. A., & Schwarz, W. H. (2006). Bacterial acetone and butanol production by industrial fermentation in the Soviet Union: use of hydrolyzed agricultural waste for biorefinery. *Applied Microbiology and Biotechnology*, *71*(5), 587–597. https://doi.org/10.1007/s00253-006-0445-z

APPENDICES

165
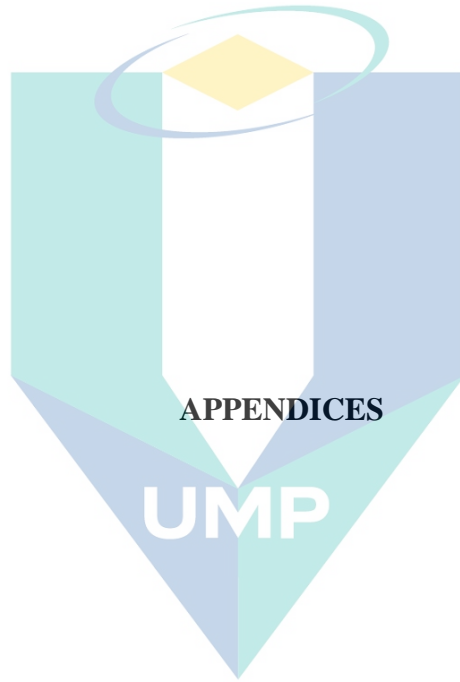
APPENDIX A

PHYSICOCHEMICAL PROPERTIES OF DIESEL, BIODIESEL, ALCOHOL AND TRI-FUEL FOR THE LITERATURE REVIEW SECTION

Table A1.1   Physicochemical properties of diesel

Properties	Diesel
Density (g/m^3)	0.81-0.87
Viscosity (cSt)	1.9-4.3
Flashpoint ($^{\circ}$C)	50-96
Cetane number	20.1-55
Boiling point ($^{\circ}$C)	177.8-360
Surface tension (mN/m)	23.0-29.0
Oxygen content (%wt)	0
Heat of vaporization (kJ/kg)	250-290
Calorific Value (MJ/kg)	42.5-45.8
Autoignition temp ($^{\circ}$C)	250-316
Latent Heat of evaporation (kJ/kg)	250-260

Table A2.1   Comparison of alcohol physicochemical properties

Properties	Ethanol	Butanol	Methanol	Propanol	Pentanol
Density (g/cm^3)	0.76-0.8	0.81	0.76-0.79	0.80	0.81-0.85
Viscosity (cSt)	0.95-1.4	1.8-3.64	0.44-0.59	2.8	2.83-2.89
Flashpoint (^{o}C)	12.7-55	29-35	11-78	-	49
Cetane no	5-11	15-25	5-6	15	20-24.3
Boiling point (^{o}C)	77-78.40	116.85-117.4	64.5	-	-
Surface tension (mN/m)	19.19-25.0	24-29	-	-	-
Oxygen Content (%wt)	34.7-35.0	21.6	49.9-50.0	-	-
Heat of vaporization (KJ/kg)	836-846	585-592	1100	-	308
Calorific Value (MJ/kg)	26.4-28.18	33-37.3	19.7	30.6	35
Autoignition temp (^{o}C)	365-423	-	464-470	-	-
Latent heat of evaporation (kJ/kg)	780-922	585	1109-1178	779	-

Table A3.1   Physicochemical properties of biodiesel

Properties	Biodiesel
Density (g/m^3)	0.85-0.92
Viscosity (cSt)	4-7
Flashpoint (^{o}C)	97-217
Cetane number	47-70
Boiling point (^{o}C)	300-366
Surface tension (mN/m)	25.0-38.6
Oxygen content (%wt)	10-11.2
Heat of vaporization (kJ/kg)	300-320.2
Calorific Value (MJ/kg)	35.86-44.6
Autoignition temp (^{o}C)	342-363
Latent Heat of evaporation (kJ/kg)	200-240

Table A4.1   Physicochemical properties of tri-fuel

Biodiesel	Ethanol	Density (g/m3)	Viscosity (cSt)	Flash point (oC)	Cetane number	Surface tension (mN/m)	Calorific Value (MJ/kg)
0	0	0.81-0.87	1.9-4.3	50-96	20.1-55	23.0-29.0	42.5-45.8
5	5	0.83-0.84	2.40-4.20	17.5-80.0	47.30-56.26	30.79	41.7-48.48
10	5	0.82-0.85	2.41-4.30	14-115	47.70-56.20	27.00-34.62	41-48.15
15	5	0.83-0.85	2.52-3.70	16.00-73.28	48.60-56.32	34.66	41.41-43.8
20	5	0.83-0.85	2.52-3.04	18-40	45.00-53.7	27.80-32.86	40.9-42
25	5	0.85	2.75	15-18	51.68-52.00	34.83	41.12
30	5	0.84	2.63				
35	5	0.85	3.40	94.71	51.25		
40	5	0.84	3.47			28.03	
45	5	0.86	4.80				
50	5	0.83	4.90	45	52.38		42.1
5	10	0.81-0.83	2.70-4.00	13.5-85.0	46.67	22-30	41-47.56

10	10	0.82-0.85	2.2-4.00	15-90	46.00-53.60	24.00	35-45.9
15	10	0.82-0.84	2.37-3.10	76.16	49.24-49.41	25.00-30.66	34-40.66
20	10	0.82-0.85	2.40-3.60	16-60	43.00-50.40	31.77	40.52-43.17
25	10	0.83	2.88				
30	10	0.82-0.84	2.04-2.63	18.5	40.50-47.30	27.15	39.1
40	10	0.83-0.85	2.60-4.20	19.0-97.5	47.20-49.58		38.7
45	10						
50	10	0.83	4.30	38	50.62		40.25
5	15	0.81-0.85	1.80-3.80	13-90	45.1-51		46.59
10	15	0.81-0.82	2.40-3.80	65-70		23.00	34-44.76
25	15	0.84	3.07	83.12	47.67		
30	15	0.84	3.23	87.91	46.48		
35	15	0.84	3.80				
50	15	0.82-0.83	3.42-3.78	24-30	45-48		37.6-39.1
5	20	0.81	3.00			30.00	
10	20	0.78-0.83	2.38-3.60	14	50.00		39.9-42.66
15	20	0.80-0.83	2.54-2.62	69.97	43.62		
30	20	0.84	2.14-3.40	15	47.20	23.10	37.8
10	25	0.77-0.78	2.20-3.50				41.02-41.92
25	25	0.83-0.84	2.80-3.00	77.21	43.05		
5	30	0.81	2.90			28.50	
20	30	0.82-0.83	2.40-2.90	12.5	50.00		38.96
15	35	0.81	2.80				
10	40	0.80-0.82	2.00-2.40	12	41.00		36.33

SUMMARY OF TRI-FUEL STUDIES ON COMBUSTION, PERFORMANCE AND EMISSION FOR THE LITERATURE REVIEW SECTION

Table B1.1   Summary of tri-fuel studies on combustion, performance and emission

Alcohol	%	Biodiesel feedstock	%	Speed (RPM)	ID Period	HRR	C/pressure	BSFC	Torque	Power	BTE	NOx	THC	PM	CO
Ethanol	3-4	Soybean	12-16	1100-3600	-	-	-	↕	-	-	-	↑	↑	↓	↕
Ethanol	5	Soybean	20	1200-2800	-	-	-	-	-	-	-	↑	↕	↓	↕
Ethanol	5	Soybean	20	1200-2800	-	-	-	↑	-	-	-	↑	↓	↓	↕
Bio-ethanol	2-4	Unknown	2-8	-	-	-	-	-	-	-	-	↓	↓	↓	↓
Ethanol	2-65	Rapeseed	29-77	1200-2000	-	-	-	-	-	-	-	-	-	-	-
Ethanol	5-15	Palm oil	5-15	-	-	-	-	-	-	-	-	↑	↓	-	↓
Ethanol	5	mono	20	1200-2800	-	-	-	-	-	-	-	-	-	-	-
Ethanol	5	Soybean	20	744-2150	-	-	-	-	-	-	-	↑	↓	-	↓
Ethanol	7.7	Soybean	30	1410-2126	-	-	-	↑	-	-	↕	↓	↕	↓	-

Alcohol		Feedstock													
Ethanol	15-18	Soybean, Castor, Residual	2-5	1800-200	-	-	-	↕	-	-	-	↓	-	-	↑
Ethanol	5	Palm oil	11	1500-3500	-	-	-	-	-	↓	-	↕	↕	↓	↓
Methanol	5-10	Soybean	43.2-47.5	1300-2100	↓	↑	↑	-	↕	↕	-	↕	↑	-	↓
Ethanol	5-10	Rape oil	10-25	-	-	-	-	-	↑	-	-	↓	↑	↓	-	↓
Butanol	5-10	Soybean	10-15	-	-	-	-	-	-	-	-	-	-	-	-
Ethanol	20-40	Jatropha	10-20	1200-1600	↑	↑	↕	↑	↓	-	-	↑	-	↓	↑
Ethanol	2-4	Rapeseed	4-8	1000-4000	-	-	-	↕	-	-	-	-	-	-	-
Ethanol	2-5	Soybean	20	-	-	-	-	-	-	-	-	↓	↑	↑	↑
Ethanol	5	Rapeseed	10-25	-	-	-	-	↑	↓	↓	↓	↑	↓	↓	↓
Ethanol, methanol	10-20	Used Cooking oil	40-45	-	-	-	-	↑	-	-	-	↕	↑	-	↑
Ethanol	10	Soybean	30	-	-	-	-	-	-	-	-	-	-	↑	-
Methanol	5	Palm oil	20	1500-3500	↓	↑	↕	↑	-	↓	↑	↑	-	-	↓
Butanol	5-15	Palm oil	20	-	-	-	-	↑	-	-	↑	-	-	↓	-
Ethanol	3-25	Used cooking oil	37.5-48.5	-	-	-	-	-	-	-	-	↓	↑	-	↑
Ethanol	5-20	Waste cooking oil	15	1800	↓	↓	↓	-	-	-	-	↓	-	↓	-

Alcohol		Oil													
Butanol	10-20	Waste Cooking oil	40-45	1500	↑	↑	↓	↑	-	-	↓	-	-	-	↑
Butanol	20	Palm oil	5	1200-2400	↑	↑	↓	-	-	-	-	-	-	-	-
Pentanol	10-20	Vegetable oil	10-20	1200-2400	↑	↓	↓	↓	-	↑	↑	↑	↓	↓	↓
Butanol	20	Palm oil	5	1200-2400	-	-	-	↑	↓	↓	↓	↓	-	-	↓
Pentanol	5-10	Palm oil	10-20	1200-2400	-	-	-	↕	-	↑	-	↑	↓	↓	↓
Ethanol, methanol	20	Jatropha	40	-	↕	↕	↕	↑	-	↑	-	↑	↑	↓	↕
Ethanol	2-12	Acid oil	60	-	-	-	-	-	-	-	↓	↓	↑	↑	↑
Ethanol	4-16	Acid oil	50	1200-1800	-	-	↑	-	-	-	↓	↓	↑	-	↑
Pentanol	5-20	Waste oil	20	2000	-	-	-	↑	-	-	↓	↑	↑	-	↑
Ethanol, methanol	15	Palm stearin	15	1500	↑	↑	↓	↑	-	-	↑	↓	-	↓	↕
Ethanol	5-50	Rapeseed	20	1500	↑	↕	↕	↑	-	-	↕	↕	↕	-	↕
Ethanol	5-15	Waste cooking oil	5-15	1600-2400	-	-	-	↑	↓	↓	↓	↓	-	-	↓
Ethanol	5-20	Pongamia piñata	50	1500	-	↕	↕	↓	-	-	↑	-	↓	↓	-
Ethanol	10	Cottonseed	30	1500	-	-	-	↓	-	-	↑	-	-	↓	-
Butanol	5	Palm oil	5	1000-1500	-	-	-	↓	↓	↓	-	↑	-	-	↓

Ethanol	2.5-5	Safflower	2.5-5	1000-2400	-	-	-	↕	↕	↕	-	↑	↑	-	↕
Butanol, Ethanol	20	Palm oil	5-20	1200	↓	↑	↑	-	-	-	-	-	-	-	-
Ethanol	15-20	Waste cooking oil	15-20	1800	-	-	-	↑	-	-	↕	↓	↑	↓	↑
Ethanol	5-20	beef tallow + soybean	7-15	1500-2100	-	-	-	-	-	-	-	-	-	-	-
Ethanol	1-3	Waste cooking oil	2-6	1700-2900	-	-	-	↑	↑	↑	-	↕	↓	-	↓
Ethanol	5-10	Jatropha	15-20	1500	↑	↓	↓	↑	-	-	↓	↓	↑	-	↑
Ethanol	2-6	soybean and yellow grease	5-35	1400-3450	-	-	-	-	↓	↓	-	↓	↑	↓	↓
Ethanol	10	Jatropha	20	1500	↕	↑	↑	↓	-	-	↕	↑	↓	↓	↓
Ethanol	15-30	Fatty acid	14-17	1500-2500	↑	↕	-	↑	-	-	↑	↓	↑	↓	↑
Ethanol	5-20	Soybean	15	1500-2100	↑	-	↓	↑	↓	-	-	-	-	-	-
Ethanol	5	Unknown	10-15	1200-3200	-	-	-	↓	-	↑	↑	↑	-	-	↓
Ethanol	15	Waste cooking oil	5	1400-2200	-	-	↑	-	-	↑	↓	↑	↓	↑	
Ethanol	5-10	Palm oil	3-10	1400-3200	-	↑	↓	↑	↓	↓	-	↑	-	-	-

| Ethanol | 10 | Jatropha | 20 | 1800-2800 | ↓ | ↓ | ↓ | - | - | - | ↓ | ↑ | ↓ | ↓ | ↓ |
| Ethanol | 5-10 | Palm oil | 17-49 | 1600 | - | - | - | ↑ | - | - | ↓ | ↑ | - | - | ↑ |

Remark:

↕ no change in property compared to base fuel (diesel).

↑ increase in property compared to base fuel (diesel).

↓ decrease in property compared to base fuel (diesel).

**THE EXPERIMENTAL AND PREDICTIVE PLOT OF CONTROL FACTOR
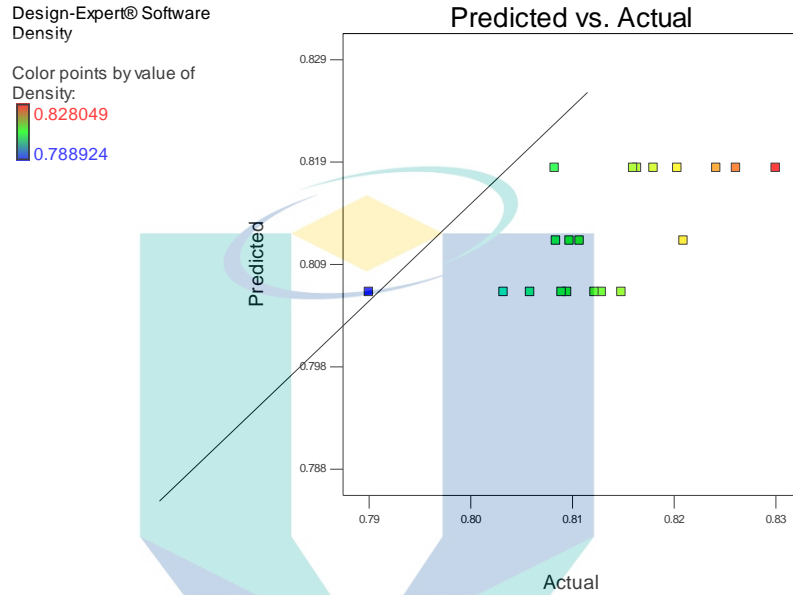ON DENSITY, VISCOSITY, SURFACE TENSION AND AVERAGE DROPLET
SIZE**

Figure C2.1   The experimental and predictive plot effect of control factor on density (g/m^3)
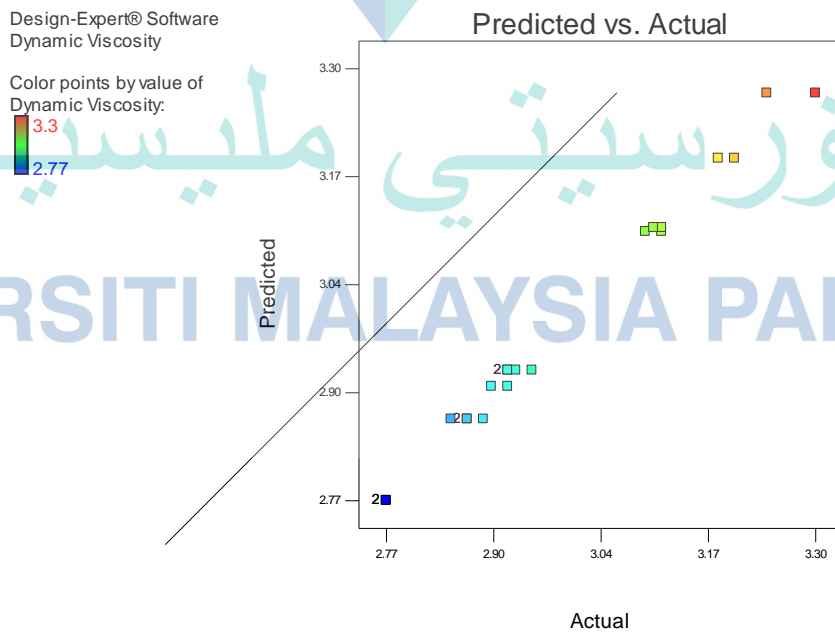
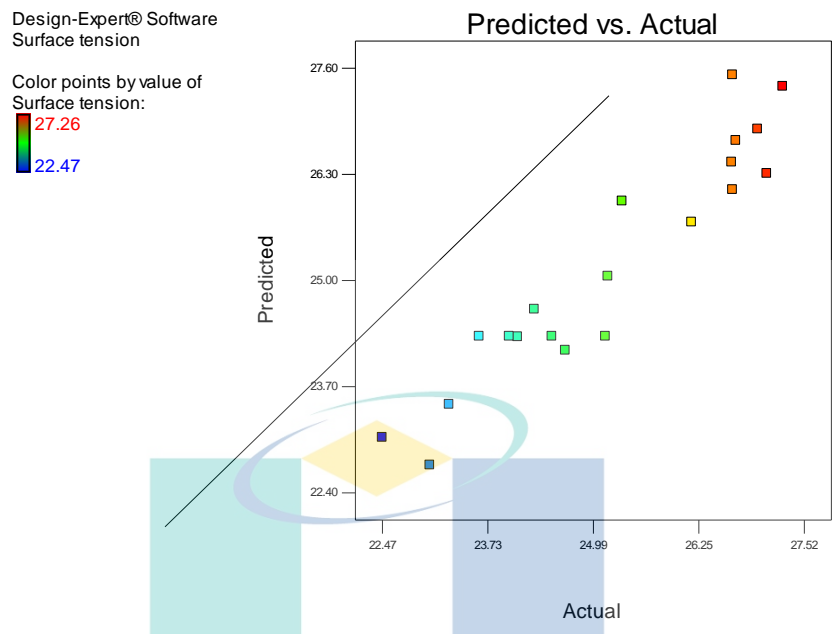Figure C2.2   The experimental and predictive plot effect of control factor on viscosity at $40^{o}C$ (cP)

Figure C2.3   The experimental and predictive plot effect of control factor on surface tension (mN/m)
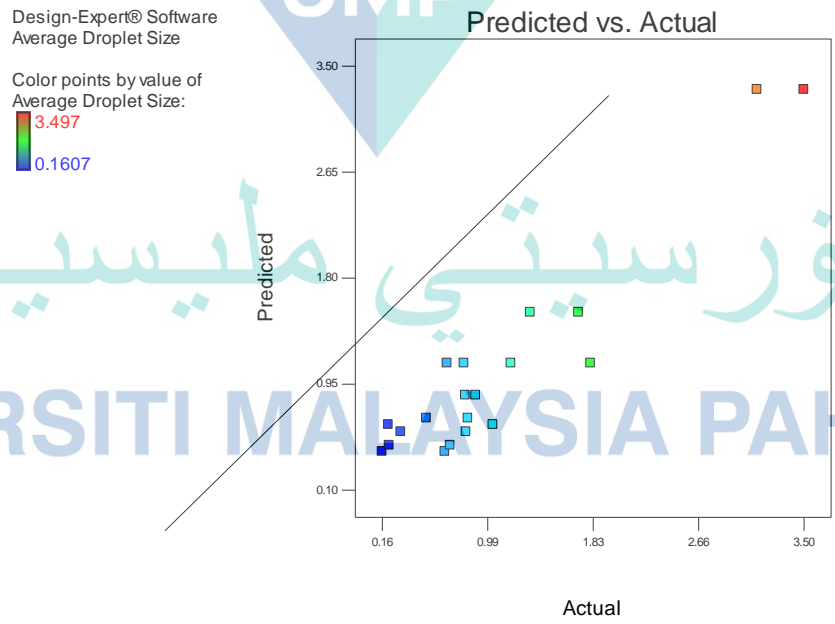

Figure C2.4   The experimental and predictive plot of the average droplet size

APPENDIX D

LIST OF PUBLICATION

M. Mukhtar N. A, Abd Rashid Abd Aziz, A Rashid, Ftwi Yohaness Hagos, M. Mat Noor, K Kadirgama, R Mamat, The influence of formulation ratio and emulsifying settings on tri-fuel (diesel-ethanol-biodiesel) emulsions properties, Energies 12 (9), January, 2019

M. Mukhtar N. A., Ftwi Yohaness Hagos, Rizalman Mamat, A. Adam Abdullah, Abd Rashid Abd Aziz, Tri-fuel emulsion with secondary atomization attributes for greener compression ignition engine - A critical review, Renewable and Sustainable Energy Review, Volume 111, P490-506 May, 2019.

M. Nazrul HM. Bahrudin, M. Mukhtar N. A, Ftwi Yohaness Hagos, Rizalman Mamat, A Adam Abdullah, ZAA Karim, Comparison between tri-fuel emulsion (diesel-ethanol-biodiesel) with and without surfactant, AIP Conference Proceedings 2059 (1), 020056, November, 2019

H. M. Mahmudul, Ftwi Yohaness Hagos, M. Mukhtar N. A, Rizalman Mamat, A Adam Abdullah, Effect of Alcohol on Diesel Engine Combustion Operating with Biodiesel-Diesel Blend at Idling Conditions, IOP Conference Series: Materials Science and Engineering 318 (1), 012071, March, 2018

K. H. Lee, M. Mukhtar N. A, Ftwi Yohaness Hagos, M. Mat Noor, A study of the stabilities, microstructures and fuel characteristics of tri-fuel (diesel-biodiesel-ethanol) using various fuel preparation methods, IOP Conference Series: Materials Science and Engineering 257 (1), 012077, October, 2017

M. H. Low, M. Mukhtar N. A, Ftwi Yohaness Hagos, M. Mat Noor, Tri-fuel (diesel-biodiesel-ethanol) emulsion characterization, stability and the corrosion effect, IOP Conference Series: Materials Science and Engineering 257 (1), 012082, October, 2017

LIST OF COMPETITION AND AWARD

Silver medal research category, 30th International Invention, Innovation and Technology Exhibition (ITEX), 2019

Gold medal research category, Creation, Innovation, Technology and Research Exposition (CITREX), 2019

Gold medal research category, 29th International Invention, Innovation and Technology Exhibition (ITEX), 2018

Gold medal research category, Creation, Innovation, Technology and Research Exposition (CITREX), 2018

Bronze medal research category, International Conference and Exposition on Inventions by Institutions of Higher Learning (PECIPTA), 2017

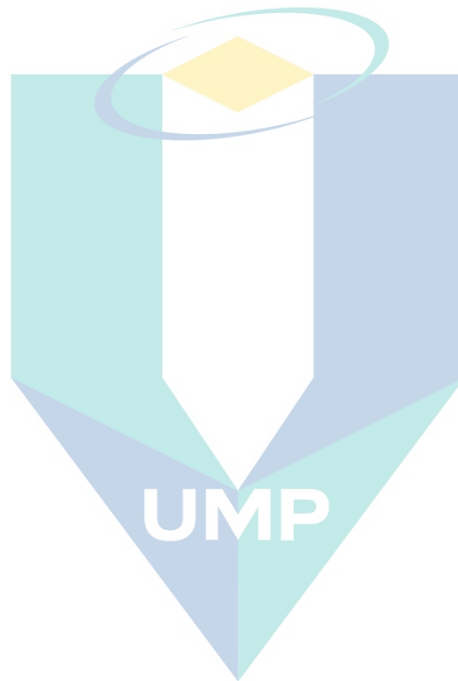Gold medal research category, Creation, Innovation, Technology and Research Exposition (CITREX), 2017

LIST OF PENDING PATENT

Method of Identifying emulsifier parameters on the stability and preparing stabilized emulsified Tri-fuel emulsion